UNIVERSITÀ DEGLI STUDI DI PALERMO
Dottorato di Ricerca in Scienze Agrarie, Forestali e Ambientali (SAFA)
Dipartimento di Scienze Agrarie e Forestali (SAF)
Settore Scientifico Disciplinare "AGR/08 Idraulica Agraria e Sistemazioni Idraulico-Forestali"

INFLUENCE OF SOIL SURFACE SEALING AND HYDROPHOBICITY ON WATER INFILTRATION

IL DOTTORE
Dr. Vincenzo Alagna

IL COORDINATORE
Prof. Vincenzo Bagarello

IL TUTOR
Prof. Massimo Iovino

IL CO-TUTOR
Prof. Giuseppe Giordano

CICLO XXIX
ANNO CONSEGUIMENTO TITOLO 2017

ACKNOWLEDGEMENTS

First of all, I want to thank my advisor Prof. Massimo Iovino for the efforts that he has made to guide me during entire doctoral studies. My deep gratitude and appreciation also for his support, inspiration, and encouragement in this hard period.

Also many thanks to the Professors Vincenzo Bagarello, Giuseppe Provenzano and Giuseppe Giordano for their helpful advice.

I should like to thank the Spanish supervisor Prof. Jorge Mataix-Solera for taking me in field in the hottest ever summer (40 °C and more) during which we risked a sunburn and for the beer at midday in each sampling days.

A huge thanks goes out to my colleagues and friends Simone Di Prima, Giovanni Rallo and Dario Autovino, I wish them a bright future in the research.

I would like to thank my brother Claudio, and my parents for allowing me to study despite some economic difficulties.

Last, but not least, the department mates over the past three years: Mirko Castellini, Houba Ghazouani, Amro Negm, Marìa Amparo Martìnez Gimeno (called Amparetto because so long), Roberta Calvo, Adele Amico Roxas and Emilio Badalamenti.

My thanks also go to my friends, I.D., M.S., G.R., N.V., M.M., B.S.

Each of them has left a mark in my life and for this, I offer my very sincere thanks to everyone.

TABLE OF CONTENTS

General introduction

1.1. Problem definitions

Infiltration is the physical process involving downward movement of water through the boundary surface where the atmosphere interfaces with the soil. The phenomenon has many important implications on partition of rainfall between infiltration and runoff, profile recharge rate and solute transport. Furthermore, the unimpeded flow of water down through the soil is essential to agricultural production. Infiltration of rainfall or irrigation water influences the overall unsaturated redistribution process that results in soil moisture availability for plant transpiration, evaporation processes, chemical transport, and groundwater recharge. The infiltration rate is determined by soil surface characteristics including initial water content, storage capacity, and transmission properties of the soil. Water transfer is related to porosity and permeability of the soil profile. Typically, the soil transmission properties depend on the soil texture and structure, but are also influenced by vegetation types and cover, and organic matter content and quality. Finally, actual infiltration rate is conditioned by rainfall intensity. All these aspects play a role in controlling the infiltration rate but obviously each one (with a different way and weight) acts differently. Among all, the major weight is represented by initial soil water content, indeed the infiltration rate decreases with the increase of soil moisture until it reaches a steady state condition.

Soil hydraulic characterization generally is conducted under the hypothesis that the porous medium is rigid, homogeneous, isotropic and uniformly unsaturated (e.g., Reynolds and Elrick, 1990; Lassabatère et al., 2006). Conventionally, in these idealized porous media it has been assumed that water infiltration follows the model proposed by Philip (1957). However, this is an approximate way to represent field soils (Reynolds and Elrick, 2002), and it is practically impossible to verify these assumptions under field conditions (Verbist et al., 2010).

Agricultural soils of arid and semi-arid regions, in which an extensive robbery agriculture is conducted, are often characterized by insufficient organic matter contents. These soils are often unstructured and also characterized by high clay levels. When protective cover crops, mulches or crop residues are lacking, large portions of these soils with fine texture as a consequence of low organic matter content are exposed to the impact of raindrops. Individual soil particles can be detached from soil clods due to raindrops kinetic energy. These particles can clog surface pores and form many thin, rather impermeable layers of sediment at the surface, referred to as surface crusts. Surface crusts can range from a few millimeters to 1 cm

or more and they are usually made up of sandy or silty particles. Surface crusts hinder infiltration of rainwater into the profile, with the consequence that runoff increases. Breaking down of soil aggregates into smaller particles depends on the stability of soil aggregates, which is largely controlled by organic matter content. Organic matter content may also affect the pore-size distribution of the soil through soil structure development, which finally influences hydraulic conductivity. Numerous studies have linked organic carbon levels with aggregate stability, infiltration and soil strength, showing that a decrease in organic carbon content is often associated with degradation of soil physical conditions (e.g. Lado et al., 2004; Whitbread, 1995; Rawls et al., 2005). Soil aggregation and aggregate stability are the main factors affecting the susceptibility of soil to raindrop impact and consequently surface sealing and soil erosion.

Despite the lack of organic matter triggers aggregates breakdown thus resulting in surface crust development its excess in specific situations can give rise to soil water repellency (SWR) or hydrophobicity. This is a well-known occurrence in forest soils where the coating of mineral soil particles with hydrophobic organic compounds reduces or prevents water infiltration into the soil. Different forest species lead to a diversification of the organic matter and organic compounds accumulated in the organic horizon. However, high degree of water repellency was generally associated to evergreen trees and, in particular, to conifer trees like the family Pinaceae (e.g. Lichner et al., 2013) or some species of Eucalyptus which have considerable amount of resins, waxes or aromatic oils in the tissues (Doerr et al., 2000).

As consequence of soil water repellency matrix flux is reduced and infiltration fluxes concentrate in limited areas of the soil profile determining irregular wetting front and "fingered" flow that result in increased risk of groundwater contamination by leaching of soluble nutrients or pollutants. Overall, as consequence of soil water repellency, runoff and erosion can increase.

It was argued that hydrophobicity depends on the quality rather than the quantity of soil organic matter as well as on soil water content. The composition of organic matter varies considerably among different soil types and vegetation. Generally, the organic matter of forest soils is characterized by high fulvic acid content, while that of grassland soils is high in humic acids (Stevenson, 1985). Several authors showed that different type/quality/quantity of organic matter has different effect on soil hydraulic properties (e.g. Nemes et al., 2005; Wang et al., 2009; Lado et al., 2004). It was showed that the amphiphilic compounds contained in the organic matter are hydrophilic when wet, but below a critical moisture threshold, their hydrophilic ends are bond strongly with one another and the soil particles, while hydrophobic

ends are oriented towards the free space inducing water repellency (Ma'shum and Farmer, 1985; Tschapek, 1984). Severe water repellency is therefore expected following prolonged dry, warm summers that are typical of Mediterranean region with a transition from water repellent (hydrophobic) to wettable (hydrophilic) conditions during the autumn/winter months (Buczko et al., 2005; Lichner et al., 2013; Rodríguez-Alleres et al., 2007).

From these considerations it can be concluded that organic matter in soil indirectly influence water infiltration. Its excess is responsible of soil water repellency whereas its lacking reduces aggregate stability thus determining surface seals or crusts. In both cases, a decrease in water infiltration rate is observed and water infiltration does not follow the classic infiltration models proposed by Philip (1957).

Numerous laboratory and field methods have been proposed to determine the soil hydraulic properties, i.e. the water retention curve and the hydraulic conductivity function. The soil water retention curve describes the relation between volumetric soil water content, θ (L^3L^{-3}), and soil water pressure head, h (L). This characteristic represents the soil ability to store or release water and, typically, is designed as a non-linear S-shaped curve. The soil hydraulic conductivity function describes the relation between soil hydraulic conductivity, K ($L\ T^{-1}$) and θ or h. In turn, the soil hydraulic conductivity, K, is a measure of the soil capability to transmit water when submitted to a hydraulic gradient. It depends not only on the pore network which is implicitly affected by soil structure, but also on the soil water content. In particular, hydraulic conductivity decreases rapidly at decreasing the soil water content.

Laboratory and field methods are different by explored soil volume and analytical procedures used to estimate the hydraulic properties. Laboratory methods allow performing the experiments under controlled conditions and achieving accurate measurement of flow processes with reference to the sample examined. Measurements are also replicable but are often time consuming and require expensive equipment. Furthermore, they are performed on relatively small samples detached from soil profile and, as a result, their representativeness under field conditions are questionable. Laboratory methods are always applicable on homogeneous porous media, but they cannot be performed on crusted or water repellent soils. The crust is generally a few millimeters thick and is very difficult to sample as it often disintegrates under external forces. On the other side, the water repellency is altered when the soil is scrubbed. Whereby, use of field method is mandatory for hydraulic characterization of crusted or hydrophobic soils in order to accurately account for the effects of these two phenomena and evaluate the influence that they have on the infiltration process.

Field techniques are more representative than the laboratory ones because have the advantage of estimating water infiltration processes straight in situ, minimizing the disturbance of the sampled soil volume which maintains its functional connection with the surrounding soil (Bouma, 1982). When field methods are applied, the environmental conditions may prove more difficult to control but the information obtained from these field-based methods allows to better understanding the hydrological processes.

Over the last couple of decades, several field infiltrometer techniques have been developed for soil hydraulic characterization (Reynolds and Elrick, 1990; Reynolds et al. 2002; Bagarello et al., 2004; Nimmo et al., 2009; Lassabatère et al., 2006; Perroux and White, 1988). These techniques differ from one to another by the way of their implementation but they are reliable, easy to conduct and generally rapid. However, the knowledge of their peculiarities is essential because any existing infiltration techniques cannot be used in every condition. The choice of the most appropriate measuring method should be addressed according to the aimed objective or depending on the phenomenon to be quantified.

Depending on the specific devices used for the measurements the infiltration methods can be divided in ponded and tension infiltration techniques. These methods are engineered to measure water infiltration and characterize soil hydraulic properties. Water infiltration experiments typically consists of monitoring the cumulative volume of infiltrating water, I (L), into the porous media against the time, t (T).

Ponded infiltration techniques allow measurement of one-dimensional or three-dimensional infiltration, under a constant or falling head, through a circular area confined by a ring inserted to a small depth into the soil. Ponded infiltration techniques include the pressure infiltrometer (PI) (Reynolds and Elrick, 1990), the double- or concentric-ring infiltrometer (DRI) (Reynolds et al. 2002), the simplified falling head (SFH) technique (Bagarello et al., 2004), the bottomless bucket (BB) method (Nimmo et al., 2009).

The tension infiltration techniques use a tension infiltrometer or disk infiltrometer (Perroux and White, 1988). Water is supplied to the soil under suction by a porous plate or disk connected to a water reservoir while a Mariotte-type bubble tower allows to impose different pressure head values at the soil surface. Tension infiltrometer allows measurement of the soil hydraulic conductivity, K, and the soil sorptivity, S (L $T^{-1/2}$), at the imposed pressure heads avoiding the influence of macroporosity. According to Philip (1957), sorptivity is the ability of the soil to absorb water in the absence of gravity.

Infiltration experiments can be used in conjunction to other soil physical properties to estimate the unsaturated soil hydraulic properties. The BEST procedure (Beerkan Estimation

of Soil Transfer parameters) (Lassabatère et al., 2006) has received a wide interest in the last ten years. This method allows the simultaneous characterization of water retention and hydraulic conductivity curves on the basis of the particle-size distribution (PSD), the initial and final soil water contents and a ponded infiltration experiment. To keep the infiltration experiment as simple as possible the so-called Berkan technique is applied i.e. a three-dimensional (3D) field infiltration experiment at ideally zero pressure head. A known but small volume of water is poured into the cylinder allowing establishment of an almost constant hydraulic head on the soil surface. When the first volume of water has infiltrated the time is recorded and an identical amount of water is added. The procedure is repeated 8-15 times and the cumulative infiltration expressed as function of time. The analytical model by Haverkamp et al. (1994) is then fitted to the experimental cumulative infiltration data to obtain the structure dependent parameters K_s (L T^{-1}) and S. Then the soil hydraulic characteristic curves are estimated using a scale parameter derived from K_s and S and shape parameters, which are texture dependent, from particle-size analysis.

Despite BEST is very attractive, inexpensive and easy to apply only a few comparisons with S and K_s data collected by other techniques can be found in the literature. Therefore, there is the need to compare the BEST method with other infiltration techniques.

The BEST method and, more in general, the ponded infiltration methods, are not indicated for hydrophobic soils because the macropore network may be activated thus hindering the effects of hydrophobicity. Therefore, tension infiltrometer methods which avoid the influence of macroporosity are preferred to ponded ones (Wang et al., 2000; Letey, 2001).

Assessing the negative effects of soil water repellency and surface sealing is crucial for hydrological processes occurring in arid and semi-arid Mediterranean regions. In fact, the reduced infiltration may result in lower water availability for crops. The problem is enhanced by the circumstance that rainfall is highly variable among years, and during the year, between wet and dry seasons, but also during a single rainfall event. Furthermore, in the Mediterranean climate, rainfall events are frequently characterized by high intensity, thus increasing the risk of flooding and soil erosion, especially when soils are crusted or water repellent.

Infiltrometer experiments can be a valuable tool to assess the hydrological impact of soil water repellency and surface crust, also with the aim to comprehend how these phenomena can affect soil hydraulic properties.

1.2. Objectives

The main aim of the thesis was to estimate how water infiltration processes are affected by the occurrence of crusting and hydrophobicity in Mediterranean area. Both the phenomena have effects on the hydrological behavior of the ecosystems. The use of infiltration measurements allows to gain more insights about the relation between these phenomena and the soil hydraulic properties. In particular, for hydraulic characterization of crusted soils, a simplified method, a simple approach using extemporaneous measurements, as well as indirect methods alternative to the most known procedures, are proposed. With reference to the measurements of water repellency, new indices based on infiltration experiments carried out with a minidisk infiltrometer (MDI) are proposed and validated as an alternative to traditional droplet tests. Moreover, the effects of water content and leaching of organic compounds between the uppermost soil layers are also investigated.

1.3. Thesis outline

The thesis is divided into i) part A, dealing with field infiltration experiments to estimate the soil hydraulic properties, ii) part B, dealing with measurements of water infiltration on crusted soils to determine their hydrodynamic properties, and iii) part C, dealing with infiltration measurements carried out on hydrophobic soils. For each parts, the introductive chapters (A.1, B.1 and C.1) concern the state of art. Afterwards, for each part, the papers published or submitted for publication in international referred journals are presented dealing with the results of the experimental investigations conducted during the PhD activity. A total of eight papers (one for part A, three for part B and four for part C) are included.

The manuscript of part A *"Determining hydraulic properties of a loam soil by alternative infiltrometer techniques"* (chapter A.2) was published on *Hydrological Processes* in 2015. This chapter provides a comparison between several infiltrometer techniques for soil hydraulic characterization.

The first manuscript of part B*"A simple field method to measure the hydrodynamic properties of soil surface crust"* (chapter B.2) was presented at the *"10th AIIA Conference: AIIA13 – Horizons in agricultural, forestry and biosystems engineering"* in 2013 and published, in a special issues of *Journal of Agricultural Engineering.* This paper proposes a simple method to determine the hydraulic resistance of the surface crust by using a combination of a tension infiltration experiment conducted at the crust surface, and a ponded infiltration test conducted onto underlying soil after removing the crust. The manuscript *"Estimating hydraulic conductivity of a sealed loamy soil from Beerkan experiments in a*

Mediterranean vineyard" (chapter B.3) was submitted to *Soil* in 2016. The paper deals whit the applicability of the BEST method to determine hydraulic conductivity of sealed and un-sealed soils developed along and between vineyard rows. The manuscript *"Testing infiltration run effects on the estimated water transmission properties of a sandy-loam soil"* (chapter B.4) was published on *Geoderma* in 2016. It explores the effect of the height of water application and of initial soil water content on both soil saturated hydraulic conductivity and sorptivity determined by BEST procedure.

The first manuscript of part C, entitled *"Investigation on soil water repellency in a Mediterranean managed pine woodland"* (chapter C.2), was presented at the conference *"Biografia di un'idea: l'insegnamento di Salvatore Puglisi e l'attualità delle Sistemazioni Idraulico-Forestali"* held in 2016 and published on *Quaderni di Idronomia Montana*. The manuscript investigates soil water repellency in a Mediterranean managed pine woodland. At this aim, different indices derived by both traditional tests and infiltration experiments carried out with the minidisk infiltrometer (MDI) were applied. The vertical evolution of SWR in the upper part of two soil profiles was investigated in two Mediterranean pine woodlands. The manuscript *"Application of minidisk infiltrometer to estimate water repellency in Mediterranean pine forest soils"* (chapter C.3), that has been accepted by *Journal of Hydrology and Hydromechanics* in 2016, extends the investigation on SWR to a pine forest in Spain with new infiltration experiments conducted during the PhD activity. An original contribution of the study was to propose and to test alternative SWR indices, obtained from MDI experiments carried out only with water. The manuscript *"Alternative analysis of transient infiltration experiment to estimate soil water repellency"* (chapter C.4) was submitted to *Hydrological Processes* in 2016. The manuscript assesses the effects of water and ethanol estimates of sorptivity on the calculation of the classical repellency index proposed by Tilleman et al. (1989). A new repellency index based on the ratio between the slopes of the linearized data collected from wettable and hydrophobic stages in a single water infiltration experiment was also proposed. The manuscript *"Impact of reforestations with exotic and native species on water repellency of forest soils"* (chapter C.5) investigates, by using the traditional droplet tests, the effects of initial soil water contents on hydrophobicity of four Sicilian forest soils under both exotic and native species.

In the final chapter the main conclusions of the thesis are summarized.

References

Bagarello, V., Iovino, M., Elrick, D. 2004. A simplified falling head technique for rapid determination of field-saturated hydraulic conductivity. Soil Science Society of America Journal, 68: 66-73.

Bouma, J. 1982. Measuring the hydraulic conductivity of soil horizons with continuous macropores. Soil Science Society of America Journal, 46: 438-441.

Buczko, U., Bens, O., Hüttl, R.F. 2005. Variability of soil water repellency in sandy forest soils with different stand structure under Scots pine (Pinus sylvestris) and beech (Fagus sylvatica). Geoderma, 126(3–4): 317–336.

Doerr, S.H., Shakesby, R.A., Walsh, R.P.D. 2000. Soil water repellency: its causes, characteristics and hydro-geomorphological significance. Earth-Science Reviews, 51(1–4): 33–65.

Hallett, P.D. 2007. An introduction to soil water repellency. In: Proc. 8th Internat. Symp. Adjuvants for Agrochem. (ISAA2007), Internat. Soc. Agrichem. Adjuvants (ISAA).

Haverkamp, R., Ross, P.J., Smettem, K.R.J., Parlange, J.Y. 1994. Threedimensional analysis of infiltration from the disc infiltrometer. 2. Physically based infiltration equation. Water Resources Research, 30: 2931-2935.

Lado, M., Paz, A., Ben-Hur, M. 2004. Organic matter and aggregate-size interactions in saturated hydraulic conductivity. Soil Sci. Soc. Am. J., 68: 234–242.

Lassabatère, L., Angulo-Jaramillo, R., Soria Ugalde, J.M., Cuenca, R., Braud, I., Haverkamp, R. 2006. Beerkan estimation of soil transfer parameters through infiltration experiments – BEST. Soil Science Society of America Journal, 70: 521 -532

Letey, J. 2001. Causes and consequences of fire-induced soil water repellency. Hydrological Processes, 15: 2867-2875.

Lichner, L., Capuliak, J., Zhukova, N., Holko, L., Czachor, H., Kollar, J. 2013. Pines influence hydrophysical parameters and water flow in a sandy soil. Biologia, 68(6): 1104–1108.

Ma'shum, M., Farmer, V. 1985. Origin and assessment of water repellency of a sandy South Australian soil. Soil Research, 23(4): 623–626.

Nemes, A., Rawls, W.J., Pachepsky, Y.A. 2005. Influence of organic matter on the estimation of saturated hydraulic conductivity. Soil Science Society of America Journal, 69(4): 1330-1337.

Nimmo, J.R., Schmidt, K.M., Perkins, K.S., Stock, J.D. 2009. Rapid measurement of field-saturated hydraulic conductivity for areal characterization. Vadose Zone Journal, 8: 142-149.

Perroux, K.M., White, I. 1988. Designs for disc permeameters. Soil Science Society of America Journal, 52: 1205–1215.

Philip, J.R. 1957. The theory of infiltration, 1, The infiltration equation and its solution. Soil Science, 83: 345–357

Rawls, W.J., Nemes, A., Pachepsky, Ya.A. 2005. Effect of soil organic matter on soil hydraulic properties. p. 95–114. In Ya.A. Pachepsky and W.J. Rawls (ed.) Development of pedotransfer functions in soil hydrology. Elsevier, Amsterdam-New York.

Reynolds, W.D., Elrick, D.E. 1990. Ponded infiltration from a single ring: I. Analysis of steady flow. Soil Science Society of America Journal, 54: 1233-1241.

Reynolds, W.D., Elrick, D.E. 2002. 3.4.3.2.b Pressure infiltrometer. p. 826–836. In: J.H. Dane and G.C. Topp (Eds.). Methods of Soil Analysis, Physical Methods, Part 4, 3rd edition. Soil Sci. Soc. Am, Madison, WI.

Reynolds, W.D., Elrick, D.E., Youngs, E.G. 2002. 3.4.3.2.a Single-ring and double- or concentric-ring infiltrometers. In J. H. Dane, & G. C. Topp (Co-Eds.), Methods of soil analysis, Part 4, Physical methods (Number 5 in the Soil Science Society of America

book series, pp. 821–826). Madison: Soil Science Society of America, Inc Richrds, L., 1931. Capillary conduction of liquids through porous medium. Physics, 1: 318–333.

Rodríguez-Alleres, M., Benito, E., de Blas, E. 2007. Extent and persistence of water repellency in north-western Spanish soils. Hydrol. Process, 21(17): 2291–2299.

Stevenson, F.J. 1985. Geochemistry. In: Humic substances in soil, sediment, and water: geochemistry, isolation and characterization. (ed. Aiken, G.R., McKnight, D. M., Wershaw, R. L., MacCarthy, P.), pp. 13-52. John Wiley & Sons, New York.

Tillman, R.W., Scotter, D.R., Wallis, M.G., Clothier, B.E. 1989. Water-repellency and its measurement by using intrinsic sorptivity. Australian Journal of Soil Research, 27: 637-644.

Tschapek, M. 1984. Criteria for Determining the hydrophilicity-hydrophobicity of Soils. Zeitschrift für Pflanzenernährung und Bodenkunde, 147(2): 137–149.

Verbist, K., Torfs, S., Cornelis, W.M., Oyarzún, R., Soto, G., Gabriels, D. 2010. Comparison of single- and double-ring infiltrometer methods on stony soils. Vadose Zone Journal, 9: 462-475.

Wang, Z., Wu, Q.J., Wu, L., Ritsema, C.J., Dekker, L.W., Feyen, J. 2000. Effects of soil water repellency on infiltration rate and flow instability. Journal of Hydrology, 231-232: 265-276.

Wang, T., Wedin, D., Zlotnik, V.A. 2009. Field evidence of a negative correlation between saturated hydraulic conductivity and soil carbon in a sandy soil. Water resources research, 45(7).

Whitbread, A.M. 1995. Soil organic matter: its fractionation and role in soil structure. Soil Organic Matter Management for Sustainable Agriculture'.(Eds RDB Lefroy, GJ Blair, ET Craswell) ACIAR Proceedings, 56: 124-130.

Part A: Field infiltration experiments for soil hydraulic characterization

A.1 Infiltrometer devices

A.1.1. Minidisk infiltrometer (MDI)

The MDI (Decagon Device Inc. 2014) is a miniaturized tension infiltromenter (TI) that allows field measurement of soil hydrodynamic parameters (hydraulic conductivity, K (L T^{-1}), and sorptivity, S (L $T^{-1/2}$)), corresponding to near-saturated conditions. The apparatus is simple, inexpensive, portable, readily useable and it requires only a volume of 135 mL of water to operate. The device consists of a transparent polycarbonate tube, having a diameter of 31 mm and a length of 327 mm, and it is partitioned into two chambers by a rubber septum (Figure 1). The upper, or bubble, chamber controls the pressure head by means of a suction control tube. The lower chamber, or reservoir, is designed like a graduated cylinder with volume shown in mL. It contains about 90 mL of water that infiltrates into the soil, at the selected pressure head, h_0, through a porous sintered stainless steel disk (45 mm diameter and 3 mm thick) situated at the bottom of the infiltrometer that does not allow water to leak in open air. A layer of contact material is frequently placed under the infiltrometer to ensure good hydraulic connection between the disk and the soil. The adjustable suction control tube allows to apply on the soil surface pressure heads from -0.5 to -7 cm that are equal to the difference between the water level and the bottom of the suction control tube, z_b (L), within the bubble chamber. Once the MDI is placed on a soil surface, the rise of the first bubble of air into the reservoir indicates the beginning of the infiltration run. After a transient phase, during which the infiltration rate, i (L T^{-1}), decreases, water flow approaches a steady-state condition characterized by a constant value of steady state infiltration rate, i_s (L T^{-1}). The rate of water flow out of the MDI, can be monitored by reading the water level at the graduated scale of the reservoir. Time between

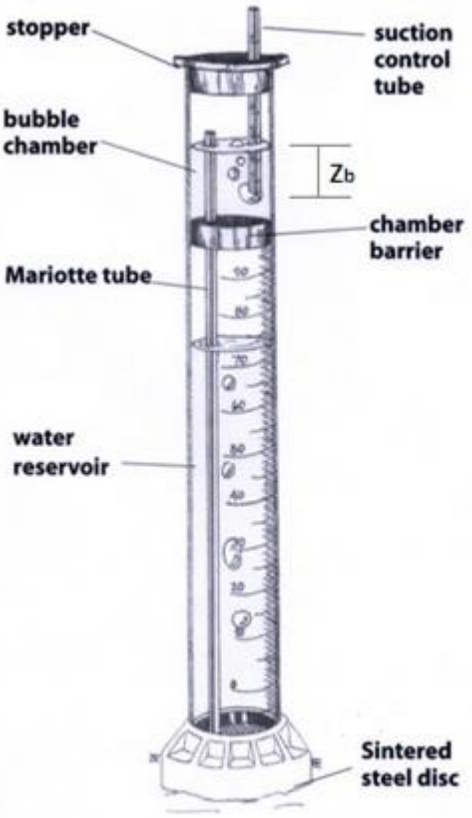

Fig. 1 Scheme of minidisk infiltrometer

two consecutive readings of the water level should be small enough especially at the beginning of the run.

A.1.2. Single ring Beerkan infiltrometer

The Beerkan infiltration experiment uses a simple annular ring with a radius of 75 mm in order to perform a ponded infiltration experiment. The surface vegetation is removed while the roots remain in situ in order to avoid soil disturbance (Lassabatère et al., 2006). Then, the cylinder is inserted to a depth of about 0.01 m to avoid lateral loss of the ponded water.

Fig. 2 Beerkan experiment: (a) removal surface vegetation, (b) ring inserted into the soil, (c) closing soil volume to inner wall sampler, (d) know water volume puring

A known volume of water (usually 150 mL) is poured in the cylinder at the start of the measurement and the elapsed time during infiltration is measured. When the amount of water has completely infiltrated, an identical amount of water is poured into the cylinder, and the time needed for the water to infiltrate is logged. The procedure is repeated for a series of about 8 to 15 known volumes of water and the corresponding infiltration time is recorded thus deducing an experimental cumulative infiltration, I (L), vs. time, t (T), relationship including a total of N_{tot} discrete points. The method also include of an indisturbed soil sample close to the infiltration site to estimate soil bulk density, ρ_b (M L^{-3}), and volumetric soil water content θ_i (L^3 L^{-3}). At the end of the experiment, the saturated soil is sampled to determine the saturated gravimetric water content and thus the saturated volumetric water content, θ_s (L^3L^{-3}), from ρ_b and the gravimetric water content. However, θ_s can alternatively be approximated by total soil porosity, determined from ρ_b (Mubarak et al., 2009). A soil sample is also collected for particle-size analysis.

A.1.3. Theory

During the last two decades, it has been intensively used the transient phase of the infiltration process out of a disk source for the determination of soil hydraulic properties (Angulo-

Jaramillo et al., 2016). The analysis based on transient three-dimensional flow offers several advantages over the classic methods based on the Wooding's steady flow equation (Angulo-Jaramillo et al., 2000). Indeed, this procedure of analysis involves shorter experiments, thus allowing to increase the number of replicates runs that is particularly effective when investigating the spatial variability of soil hydraulic properties. Furthermore, it samples a smaller soil volume, which makes the hypotheses of soil homogeneity and initial uniform water content more realistic. Finally, it allows to overcome the uncertainties related to the effective achievement of the steady infiltration flow (Hussen and Warrick, 1993a,b; Quadri et al., 1994; Vandervaere et al., 1997; 2000a). Transient flow models have been applied to analyze both ponded and tension infiltration experiments (e.g. Lassabatère et al., 2006, 2010; Yilmaz et al., 2010; Xu et al., 2012; Bagarello et al., 2007, 2014; Vandervaere et al., 1997, 2000a, 2002; Reynolds and Zebchuk, 1996; Reynolds, 2006, 2008; Reynolds et al., 2000; Angulo-Jaramillo et al., 2000; Vandervaere, 2002) but application to disk infiltrometers are by far the most numerous (Vandervaere et al., 1997; Reynolds, 2006, 2008; Angulo-Jaramillo et al., 2000; Vandervaere et al., 1997; Vandervaere, 2002).

The most common analytical models are described by equations formally identical to the Philip's (1957) one-dimensional infiltration model:

$$I = C_1\sqrt{t} + C_2 t \tag{1}$$

where I (L) is the cumulative infiltration, t (T) is the time and C_1 (L $T^{-1/2}$) and C_2 (L T^{-1}) are coefficients that differ according to the considered model.

Haverkamp et al. (1994) proposed a physically based three-dimensional infiltration equation, from a disk source, valid for short to medium times in which the coefficients C_1 and C_2 are defined as:

$$C_1 = S_0 \tag{2}$$

$$C_2 = \frac{2-\beta}{3}K_0 + \frac{\gamma S_0^2}{r(\theta_0 - \theta_i)} \tag{3}$$

where S_0 (L $T^{-1/2}$) is the soil sorptivity corresponding to the imposed pressure head, h_0 (L), β is a parameter depending on the capillary diffusivity function that lies in the interval [0, 1], K_0 (L T^{-1}) is the soil hydraulic conductivity corresponding to h_0, γ is a constant approximately

equal to 0.75, θ_0 (L^3L^{-3}) is the volumetric soil water content corresponding to h_0 and θ_i (L^3L^{-3}) is the initial soil water content. Substituting Eqs. (2) and (3) into Eq. (1) yields:

$$I = S_0\sqrt{t} + \left[\frac{2-\beta}{3}K_0 + \frac{\gamma S_0^2}{r(\theta_0 - \theta_i)}\right]t \tag{4}$$

The first term of right side of Eq. (4) takes into account the vertical capillary flow that dominates infiltration during its early stage. The second term accounts for the gravity-driven vertical flow and the third one represents the lateral capillary component flow that, as shown by Smettem et al. (1994), is linear with time.

According to Haverkamp et al. (1994), Eq. (4) can adequately describe the axisymmetric three-dimensional flow from the disk of a MDI for times smaller than the characteristic time scale, t_{grav} (T) (Philip, 1969):

$$t_{grav} = \left(\frac{S_0}{K_0}\right)^2 \tag{5}$$

The coefficients C_1 and C_2 can be estimated by fitting Eq. (1) to the experimental I vs. t data pairs. According to Vandervaere et al. (2000a), the commonly applied non-linear techniques do not allow to clearly verify the applicability of the Eq. (1), as it is almost impossible to detect any discontinuity in the infiltration process. However, adequacy of Eq. (1) can be checked if the data are linearized by dividing both sides of Eq. (1) by $\sqrt{t}$ thus giving:

$$\frac{I}{\sqrt{t}} = C_1 + C_2\sqrt{t} \tag{8}$$

In this form, called Cumulative Linearization, CL, method, C_1 corresponds to the intercept and C_2 to the slope of the regression line between $I/\sqrt{t}$ and $\sqrt{t}$.

When the hydraulic contact between the disk and the soil is ensured by a layer of contact material, the usability of Eq. (8) is compromised by the water initially stored in this additional layer during the early stages of infiltration. In this case, according to Vandervaere et al. (2000a), the applicability of Eq. (1) and the estimation of coefficients C_1 and C_2 can be carried out by differentiating the cumulative infiltration data with respect to the square root of time (Differentiated Linearization, DL, method):

$$\frac{dI}{d\sqrt{t}} = C_1 + 2C_2\sqrt{t} \quad (9)$$

If the model (Eq. 1) adequately describes the infiltration process, the $dI/d\sqrt{t}$ vs. $\sqrt{t}$ data points are arranged in a straight line. Coefficient C_1 is equal to the intercept whereas coefficient C_2 is equal to half the slope of the regression line. The influence of the contact material can be easily detected as signalled by number of data points, in the first stage of the run, showing a decreasing trend that deviates from the monotonically increasing linear behaviour. These measurements should be excluded in order to obtain unbiased values of C_1 and C_2 (Vandervaere et al., 2000a). Obviously Eq. (9) can also be applied in absence of a contact material layer between porous disk and the soil surface. In this case, if Eq. (1) correctly describes the infiltration process CL and DL methods should give similar results. According to Vandervaere et al. (2000a), using linearization in the form of Eq. (8) or (9) allow estimates of soil sorptivity potentially more accurate than those obtained from the slope of the Philip's (1957) one-dimensional horizontal infiltration equation:

$$I = S_0\sqrt{t} \quad (10)$$

In fact, with this approach the effects of gravity and lateral expansion at the hedge of the wetting bulb are neglected (Smettem et al., 1995), thus resulting in an overestimation of S_0 by an amount that depends on the chosen time interval for the regression I vs. $\sqrt{t}$ (Bonnel and Williams, 1986).

The three-dimensional transient infiltration model by Haverkamp et al. (1994) has been applied to a single ring Beerkan experiment with the aim to outline a procedure for the simultaneous determination of both the water retention curve, *h(θ)*, and the hydraulic conductivity function, *K(θ)* (Lassabatère et al., 2006). The procedure called, BEST (Beerkan Estimation of Soil Transfer parameter) focuses specifically on the van Genuchten (1980) relationship for the water retention curve with the Burdine (1953) condition and the Brooks and Corey (1964) relationship for hydraulic conductivity (Angulo-Jaramillo et al., 2016):

$$\frac{\theta - \theta_r}{\theta_s - \theta_r} = \left[1 + \left(\frac{h}{h_g}\right)^n\right]^{-m} \quad (9)$$

$$m = 1 - \frac{2}{n} \tag{10}$$

$$\frac{K(\theta)}{K_s} = \left(\frac{\theta - \theta_r}{\theta_s - \theta_r} \right)^{\eta} \tag{11}$$

$$\eta = \frac{2}{m \times n} + 2 + p \tag{12}$$

where θ (L^3L^{-3}) is the volumetric soil water content, h (L) is the soil water pressure head, K (L T^{-1}) is the soil hydraulic conductivity, n, m and η are shape parameters linked to the soil textural properties, p is a tortuosity parameter, and h_g (L), representing the inflection point of the water retention curve, θ_s (L^3L^{-3}, field-saturated soil water content), θ_r (L^3L^{-3}, residual soil water content) and K_s (L T^{-1}, field-saturated soil hydraulic conductivity) are scale parameters related to soil structure. In BEST, θ_r is assumed to be zero (Lassabatère et al., 2006).

For the estimation of soil hydraulic properties BEST method requires soil particle-size distribution (PSD) and bulk density (ρ_b, L^3L^{-3}), and makes use of Beerkan infiltration data with known initial and final soil water contents. Firstly, BEST estimates shape parameters on the basis of particle size analysis and soil porosity determination. More specifically, estimation of n is based on the soil particle size distribution (PSD), which is modeled as:

$$P(D) = \left[1 + \left(\frac{D_g}{D} \right)^N \right]^{-M} \tag{13}$$

where $P(D)$ is the fraction by mass of particles having a diameter below the specific value D (L), D_g (L) is a scale parameter, N and M=1-2/N are shape factors.

Fitting Eq. (13) to the measured PSD allows to calculate the shape index for PSD, p_M:

$$p_M = \frac{MN}{1 + M} \tag{14}$$

The m parameter of Eq. (9) is derived from the water retention shape index, p_m, as:

$$m = \frac{1}{p_m} \left(\sqrt{1 + p_m^2} - 1 \right) \tag{15}$$

where:

$$p_m = p_M (1+\kappa)^{-1} \tag{16}$$

and κ is a coefficient defined as:

$$\kappa = \frac{2s-1}{2s(1-s)} \tag{17}$$

where the fractal dimension of the media, *s*, varying from 0.5 to 1 (Minasny and McBratney, 2007), is defined as:

$$(1-f)^s + f^{2s} = 1 \tag{18}$$

in which f (L^3L^{-3}) is the soil porosity, that can be obtained from the soil bulk density, ρ_b. Parameters n and η can be calculated by Eqs. (10) and (12), respectively.

Minasny and McBratney (2007) using percentage of sand, sa (USDA classification), and clay, cl, contents, proposed an alternative way to estimate the n parameter used in the BEST procedure:

$$n = 2.18 + 0.11[48.087 - 44.954\ S(x_1) - 1.023\ S(x_2) - 3.896\ S(x_3)] \tag{19a}$$

where

$$x_1 = 24.547 - 0.238\ sa - 0.082\ cl \tag{19b}$$

$$x_2 = -3.569 + 0.081\ sa \tag{19c}$$

$$x_3 = 0.694 - 0.024\ sa + 0.048\ cl \tag{19d}$$

$$S(x) = \frac{1}{1+exp(-x)} \tag{19e}$$

Once the shape parameters of Eqs. (9) to (11) are estimated, the scale parameters h_g (L) and K_s (L T^{-1}) are obtained from a Beerkan infiltration experiment at zero pressure head (Lassabatère et al., 2006).

For an infiltration experiment with zero water pressure on a circular surface of radius, r (L), above a uniform soil with a uniform water content, θ_i, the three-dimensional cumulative infiltration, I (L), and the infiltration rate, i (L T^{-1}), can be approached by the following

explicit transient [Eqs.(20a) and (20b)] and steady-state [Eqs.(20c) and (20d)] expressions proposed by Haverkamp et al. (1994):

$$I(t) = S\sqrt{t} + \left(A\,S^2 + B\,K_s\right)t \tag{20a}$$

$$i(t) = \frac{S}{2\sqrt{t}} + \left(A\,S^2 + B\,K_s\right) \tag{20b}$$

$$I_s(t) = \left(A\,S^2 + K_s\right)t + C\frac{S^2}{K_s} \tag{20c}$$

$$i_s(t) = A\,S^2 + K_s \tag{20d}$$

where t (T) is the time and A (L^{-1}), B and C are constants that can be defined for the specific case of a Brooks and Corey (1964) (Eq. 11) relationship as:

$$A = \frac{\gamma}{r\left(\theta_s - \theta_i\right)} \tag{21a}$$

$$B = \frac{2-\beta}{3}\left[1 - \left(\frac{\theta_i}{\theta_s}\right)^{\eta}\right] + \left(\frac{\theta_i}{\theta_s}\right)^{\eta} \tag{21b}$$

$$C = \frac{1}{2(1-\beta)\left[1 - \left(\frac{\theta_i}{\theta_s}\right)^{\eta}\right]}\,ln\left(\frac{1}{\beta}\right) \tag{21c}$$

where β and γ are coefficients that are commonly set at 0.6 and 0.75, respectively, for $\theta_i < 0.25\,\theta_s$ (Smettem et al., 1994; Haverkamp et al., 1994).

The experimental steady-state infiltration rate, i_s^{exp} ($L\,T^{-1}$), is obtained from the last points of the infiltration curve, when water infiltration stabilizes:

$$i_s^{exp} = slope_{\,i=(N_{tot}-N_{end})\rightarrow N_{tot}}^{\,(t_i,I_i)} \tag{22}$$

where N_{tot} is the total number of discrete points (t_i, I_i) which describe the experimental cumulative infiltration curve, and N_{end}, is the number of points considered for the linear regression that define the steady-state condition.

In the BEST procedure, soil sorptivity is expressed as a function of the scale parameters and initial and final water contents using the approximation by Parlange (1975):

$$S^2(\theta_i,\theta_s) = -c_p(n,m,\eta)\theta_s K_s h_g\left(1-\frac{\theta_i}{\theta_s}\right)\left[1-\left(\frac{\theta_i}{\theta_s}\right)^{\eta}\right] \tag{23}$$

where

$$c_p(n,m,\eta) = \Gamma\left(1+\frac{1}{n}\right)\left\{\frac{\Gamma\left(m\eta-\frac{1}{n}\right)}{\Gamma(m\eta)}+\frac{\Gamma\left(m\eta+m-\frac{1}{n}\right)}{\Gamma(m\eta+m)}\right\} \tag{24}$$

where Γ stands for the gamma function.

The scale parameter, h_g, is derived from the concomitant estimation of K_s and S through fitting the infiltration model defined by Eqs. (20) onto the experimental cumulative infiltration and estimated by the following relation obtained from Eq. (23):

$$h_g = -\frac{S^2(\theta_i,\theta_s)}{c_p(n,m,\eta)(\theta_s-\theta_i)\left[1-\left(\frac{\theta_i}{\theta_s}\right)^{\eta}\right]K_s} \tag{25}$$

For the derivation of K_s and S, three different BEST algorithms were proposed i) slope, ii) intercept and iii) steady that differ only by the way Eq. (20a) is fitted to experimental infiltration data.

a) <u>BEST-Slope</u>

The original BEST-Slope algorithm (Lassabatere et al., 2006) considers Eq. (20a) for modelling the transient cumulative infiltration data. Expressing soil hydraulic conductivity as a function of sorptivity and experimental steady-state infiltration rate, i_s^{exp}, Eq. (20) leads to:

$$K_s = i_s^{exp} - A\,S^2 \tag{26}$$

and substituting in Eq. (20d):

$$I(t) = S\sqrt{t} + \left[A(1-B)S^2 + B\,i_s^{exp}\right]t \tag{27}$$

where, i_s^{exp} is estimated as the slope of the regression line fitted to the last data points describing steady-state conditions on the I vs. t plot. Sorptivity, S, is estimated by fitting Eq. (27) to the experimental data. Establishing a constraint like Eq. (27) between the estimator for sorptivity and the one for saturated hydraulic conductivity and inverting cumulative infiltration data through optimizing only sorptivity avoids parameter non-uniqueness and increases the robustness of the inverse procedure (Lassabatere et al., 2013). The fit is performed by minimizing the classical objective function for cumulative infiltration:

$$f\left(S,K_s,k\right)=\sum_{i=1}^{k}\left[I_i^{exp}-I\left(t_i\right)\right]^2 \tag{28}$$

where k is the number of data points considered for the transient state, I^{exp} and I are respectively the measured and the estimated cumulative infiltration using Eq. (27). Once S is estimated, K_s is calculated by Eq. (26).

As the infiltration model is valid only for transient condition, the fit may not be valid for large values of k. Therefore, BEST fits data for a minimum of five points to a maximum of N_{tot} points, representing the whole dataset. For each data subset containing the first k points, corresponding to a duration of the experiment equal to t_k, S and K_s are estimated and the time, t_{max} (T), defined as the maximum time for which the transient expression can be considered valid, is determined:

$$t_{max}=\frac{1}{4\left(1-B\right)^2}\left(\frac{S}{K_s}\right)^2 \tag{29}$$

where $(S/K_s)^2$ corresponds to the gravity time defined by Philip (1969). Then, the maximum time $t_{max,k}$ is compared with the maximum time of the experimental dataset used for the fit, i.e. t_k. The values of S and K_s are not considered valid unless $t_k \leq t_{max,k}$. Among all values of S and K_s that fulfill this condition, the S and K_s values corresponding to the largest k (k_{max}) are retained since they are considered more precise.

b) <u>BEST-Intercept</u>

Yilmaz et al. (2010) stated that BEST-slope may lead to erroneous estimates of K_s, especially when $i_s \approx AS^2$. Under such conditions, attempting to estimate K_s by Eq. (26) appears to be inappropriate. More specifically, when the estimated AS^2 value exceeds the measured infiltration rate at the end of the experiment, the values obtained for K_s are negative. To overcame this inconvenient, Yilmaz et al. (2010) proposed the BEST-intercept algorithm in

which the constraint between S and K_s is defined by using the intercept of the asymptotic expansion in Eq. (20c):

$$b_s^{exp} \approx C\frac{S^2}{K_s} \tag{30}$$

Therefore, b_s^{exp} is estimated by linear regression analysis of the data describing steady-state conditions on the I vs. t plot, and the following relationship is applied to estimate K_s:

$$K_s = C\frac{S^2}{b_s^{exp}} \tag{31}$$

In this way, the division operator is used rather than the subtraction operator and, thereby, obtaining negative values for the estimated K_s is avoided. Combining Eqs. (20a) and (31) yields the following relationship to fit onto the transient phase of the experimental cumulative infiltration curve:

$$I(t) = S\sqrt{t} + \left[A + \frac{BC}{b_s^{exp}}\right]S^2 t \tag{32}$$

Eq. (32), that is alternative to Eq. (27), is applied to determine S following the same steps described for BEST-slope, also in this case must be sought the time validity of the transient infiltration model through the calculation of t_{max}. The estimated sorptivity is then used to calculate K_s by Eq. (31).

c) <u>BEST-Steady</u>

Bagarello et al. (2014) proposed an alternative algorithm, named BEST-Steady, that makes use of the intercept (b_s^{exp}) and the slope (i_s^{exp}) of the straight line fitted to the data describing the steady-state condition of the infiltration experiment. Combining Eqs. (26) and (31) yields:

$$i_s^{\exp} = AS^2 + C\frac{S^2}{b_s^{\exp}} \tag{33}$$

and hence S can be calculated as:

$$S = \sqrt{\frac{i_s^{exp}}{A + \frac{C}{b_s^{exp}}}} \tag{34}$$

Then, K_s can be estimated using either Eq. (26) or (31). BEST-Steady does not make any direct use of the data describing the transient state. However, monitoring this stage is necessary to establish when a steady-state condition begins (estimating i_s^{exp}) and how much water infiltrates the soil before reaching this condition (estimating b_s^{exp}) (Angulo-Jaramillo et al., 2016).

The adequacy of the transient infiltration model (Eqs. 20) to fit the experimental data can be quantified by the relative error, E_r, according the following relationship proposed by Lassabatère et al. (2006):

$$E_r = \sqrt{\frac{\sum_{i=1}^{k}\left[I^{\exp}(t_i) - I(t_i)\right]^2}{\sum_{i=1}^{k}\left[I^{\exp}(t_i)\right]^2}} \tag{35}$$

According to these authors a $E_r \leq 5.5\%$ denotes an acceptable error for transient cumulative infiltration.

References

Angulo-Jaramillo R., Bagarello V., Iovino M., Lassabatere L. 2016. Infiltration measurements for soil hydraulic characterization. Springer: Switzerland.

Angulo-Jaramillo R., Vandervaere J.P., Roulier S., Thony J.L., Gaudet J.P., Vauclin M. 2000. Field measurement of soil surface hydraulic properties by disc and ring infiltrometers. A review and recent developments. Soil & Tillage Research, 55:1-29.

Bagarello V., Castellini M., Iovino M. 2007. Comparison of unconfined and confined unsaturated hydraulic conductivity. Geoderma, 137:394-400.

Bagarello V., Di Prima S., Iovino M. 2014. Comparing alternative algorithms to analyze the beerkan infiltration experiment. Soil Science Society of America Journal, 78(3):724-736, doi:10.2136/sssaj2013.06.0231.

Bonnell M., Williams J. 1986. The two parameters of the Philip infiltration equation. Their properties and spatial and temporal heterogeneity in a red earth of tropical semi-arid Queensland. Journal of Hydrology, 87:9-31.

Brooks R.H., Corey C.T. 1964. Hydraulic properties of porous media. Hydrol. Paper 3, Colorado State University, Fort Collins.

Burdine N.T. 1953. Relative permeability calculation from pore size distribution data. Petr. Trans. Am. Inst. Min. Metall. Eng., 198:71-77.

Decagon Devices Inc. 2014. Mini disk infiltrometer user's manual, version September 10, 2014. 2365 NE Hopkins Court, Pullman, WA 99163.

Haverkamp R. Ross P.J., Smettem K.R.J., Parlange J.Y. 1994. Three-dimensional analysis of infiltration from the disc infiltrometer. 2. Physically based infiltration equation. Water Resources Research, 30:2931-2935.

Haverkamp R., Leij F.J., Fuentes C., Sciortino A., Ross P.J. 2005. Soil water retention: I. Introduction of a shape index. Soil Science Society of America Journal 69:1881–1890.

Hussen A.A., Warrick A.W. 1993a. Algebraic models for disc tension permeameters. Water Resources Research, 29(8):2779-2786.

Hussen A.A., Warrick A.W. 1993b. Alternative analyses of hydraulic data from disc tension infiltrometers. Water Resources Research, 29(12):4103-4108.

Lassabatère L., Angulo-Jaramillo R., Soria Ugalde J.M., Cuenca R., Braud I., Haverkamp R. 2006. Beerkan estimation of soil transfer parameters through infiltration experiments – BEST. Soil Science Society of America Journal, 70:521-532.

Lassabatère L., Angulo-Jaramillo R., Soria Ugalde J.M., Cuenca R., Braud I., Haverkamp R. 2006. Beerkan estimation of soil transfer parameters through infiltration experiments – BEST. Soil Science Society of America Journal, 70:521-532.

Lassabatère L., Angulo-Jaramillo R., Goutaland D., Letellier L., Gaudet J.P., Winiarski T., Delolme C. 2010. Effect of settlement of sediments on water infiltration in two urban infiltration basins. Geoderma, 156:316-325.

Lassabatere L., Pu J., Bonakdari H., Joannis C., and Larrarte F.2013. Velocity Distribution in Open Channel Flows: Analytical Approach for the Outer Region. J. Hydraul. Eng., 139: 37-43.

Minasny B., McBratney A.B. 2007. Estimating the water retention shape parameter from sand and clay content. Soil Science Society of America Journal, 71:1105-1110.

Mubarak I., Mailhol J.C., Angulo-Jaramillo R., Bouarfa S., Ruelle P. 2009. Effect of temporal variability in soil hydraulic properties on simulated water transfer under high-frequency drip irrigation. Agricultural Water Management, 96:1547-1559.

Parlange J.-Y. 1975. On solving the flow equation in unsaturated soils by optimization: Horizontal infiltration. Soil Science Society of America Journal, 39:415–418.

Philip J.R. 1957. The theory of infiltration: 4. Sorptivity and algebraic infiltration equations. Soil Science, 84:257-264.

Philip J.R. 1957. The theory of infiltration: 4. Sorptivity and algebraic infiltration equations. Soil Science, 84:257-264.

Philip J.R. 1969. Theory of infiltration. Advances in Hydroscience, 5:215-296.

Quadri M.B., Clothier B.E., Angulo-Jaramillo R., Vauclin M., Green S.R. 1994. Axisymmetric transport of water and solute underneath a disk permeameter: experiments and numerical model. Soil Science Society of America Journal, 58:696-703.

Reynolds W.D. 2006. Tension infiltrometer measurements: implications of pressure head offset due to contact sand. Vadose Zone Journal, 5:1287-1292.

Reynolds, W.D. 2008. Chapter 82.Unsaturated hydraulic properties: field tension infiltrometer. p.1107-1127. In M.R.Carter and E.G.Gregorich (eds.), Soil Sampling and Methods of Analysis, 2nd edition, Canadian Society of Soil Science, CRC Press, Boca Raton, FL, USA.

Reynolds W.D., Zebchuk W.D. 1996. Use of contact material in tension infiltrometer measurements. Soil Technology, 9:141-159.

Reynolds W.D., Bowman B.T., Brunke R.R., Drury C.F., Tan C.S. 2000. Comparison of tension infiltrometer, pressure infiltrometer, and soil core estimates of saturated hydraulic conductivity. Soil Science Society of America Journal, 64:478–484.

Smettem K.R.J., Parlange J.Y., Ross J.P., Haverkamp R. 1994. Three-dimensional analysis of infiltration from disc infiltrometer. 1. A capillary-based theory. Water Resources Research, 30:2925-2929.

Smettem K.R.J., Ross P.J., Haverkamp R., Parlange J.Y. 1995. Three-dimensional analysis of infiltration from the disk infiltrometer. 3. Parameter estimation using a double-disk tension infiltrometer. Water Resources Research, 31(10):2491-2495.

Smiles D.E., Knight J.H. 1976. A note on the use of the Philip infiltration equation. Australian Journal of Soil Research, 14:103-108.

van Genuchten M.Th. 1980. A closed-form equation for predicting the hydraulic conductivity of unsaturated soils. Soil Science Society of America Journal, 44:892-898.

Vandervaere J.P. 2002. 3.5.4.1. Early time observations. p.889-894. In J.H.Dane and G.C.Topp (co-eds.), Methods of Soil Analysis, Part 4 – Physical Methods, Number 5 in the Soil Science Society of America Book Series, Soil Science Society of America Inc., Madison, WI, USA.

Vandervaere J.P., Peugeot C., Vauclin M., Angulo-Jaramillo R., Lebel T. 1997. Estimating hydraulic conductivity of crusted soils using disc infiltrometers and minitensiometers. Journal of Hydrology, 188-189:209-223.

Vandervaere J.-P., Vauclin M., Elrick D.E. 2000a. Transient flow from tension infiltrometers: I. The two-parameter equation. Soil Science Society of America Journal, 64:1263-1272.

Vandervaere J.-P., Vauclin M., Elrick D.E. 2000b. Transient flow from tension infiltrometers: II. Four methods to determine sorptivity and conductivity. Soil Science Society of America Journal, 64:1272-1284.

Yilmaz D., Lassabatère L., Angulo-Jaramillo R., Deneele D., Legret M. 2010. Hydrodynamic characterization of basic oxygen furnace slag through an adapted BEST method. Vadose Zone Journal, 9:1-10.

Xu X., Lewis C., Liu W., Albertson J.D., Kiely G. 2012. Analysis of single-ring infiltrometer data for soil hydraulic properties estimation: comparison of BEST and Wu methods. Agricultural Water Management, 107:34-41.

A.2. Determining hydraulic properties of a loam soil by alternative infiltrometer techniques*

V. Alagna*, V. Bagarello, S. Di Prima, M. Iovino

Dipartimento di Scienze Agrarie e Forestali, Università degli Studi di Palermo, Viale delle Scienze, 90128, Palermo, Italy.
*Corresponding Author: Vincenzo Alagna, tel.: 09123897065; fax: 091484035; e-mail: vincenzo.alagna01@unipa.it.

Abstract

Testing infiltrometer techniques to determine soil hydraulic properties is necessary for specific soils. For a loam soil, the water retention and hydraulic conductivity predicted by the BEST (Beerkan Estimation of Soil Transfer parameters) procedure of soil hydraulic characterization was compared with data collected by more standard laboratory and field techniques. Six infiltrometer techniques were also compared in terms of saturated soil hydraulic conductivity, K_s. BEST yielded water retention values statistically similar to those obtained in the laboratory and K_s values practically coinciding with those determined in the field with the pressure infiltrometer (PI). The unsaturated soil hydraulic conductivity measured with the tension infiltrometer (TI) was reproduced satisfactorily by BEST only close to saturation. BEST, the PI, one-potential experiments with both the TI and the mini disk infiltrometer (MDI), the simplified falling head (SFH) technique and the bottomless bucket (BB) method yielded statistically similar estimates of K_s, differing at the most by a factor of three. Smaller values were obtained with longer and more soil-disturbing infiltration runs. Any of the tested infiltration techniques appears usable to obtain the order of magnitude of K_s at the field site but the BEST, BB and PI data appear more appropriate to characterize the soil at some stage during a rainfall event. Additional investigations on both similar and different soils would allow development of more general procedures to apply infiltrometer techniques for soil hydraulic characterization.

Keywords: BEST (Beerkan Estimation of Soil Transfer parameters) procedure; Soil water retention; Soil hydraulic conductivity; Infiltrometer technique.

* This is the peer reviewed version of the article and it may be used for non-commercial purposes in accordance with Wiley Terms and Conditions for Self-Archiving. When citing, please refer to:Alagna, V., Bagarello, V., Di Prima, S., Iovino, M. (2016). Determining hydraulic properties of a loam soil by alternative infiltrometer techniques. Hydrol. Process, 30, 263–275

A.2.1. Introduction

The soil hydraulic properties are key information for understanding and simulating the hydrological processes (Assouline and Mualem, 2002; Wainwright and Parsons, 2002). Loam soils are particularly important to be characterized properly because they generally exhibit a good balance between large and small pores. Therefore, they have high economic interest since movement of water and air is easy and water retention is adequate (Hillel, 1998). Field infiltrometer techniques are becoming very popular for soil hydraulic characterization because the experiments are relatively easy, rapid and inexpensive.

Infiltrometer data are generally analyzed by assuming that the sampled porous medium is rigid, homogeneous, isotropic and uniformly unsaturated before the run (e.g., Reynolds and Elrick, 1990; Lassabatère et al., 2006). However, this is an approximate way to represent field soils (Reynolds and Elrick, 2002), and it is practically impossible to verify these assumptions under field conditions (Verbist et al., 2010). In addition, soil hydraulic properties generally exhibit a dynamic nature and even water application during the infiltrometer run can influence the measured infiltration rates (e.g., Bagarello et al., 2014b; Verbist et al., 2010) since flow is dominated by unstable structural macropores (Jarvis et al., 2013). Therefore, a given infiltrometer method cannot be suggested for general use and improving our knowledge of the potential of these methods is advisable for practical purposes.

Lassabatère et al. (2006) proposed the Beerkan Estimation of Soil Transfer parameters (BEST) procedure to estimate the soil water retention and hydraulic conductivity curves. Due to its simplicity and the physical soundness of the employed relationships and procedures, BEST is receiving increasing attention by the scientific community to tackle specific problems (Mubarak et al., 2009a,b, 2010; Lassabatère et al., 2010; Gonzalez-Sosa et al., 2010; Yilmaz et al., 2010; Bagarello et al., 2011) and to test and possibly improve or simplify specific experimental and analytical procedures (Minasny and McBratney, 2007; Bagarello et al., 2009, 2011, 2014c; Yilmaz et al., 2010; Xu et al., 2012; Bagarello and Iovino, 2012; Nasta et al., 2012). However, only a few comparisons of the predicted soil properties with data collected by other experimental methods can still be found in the literature (Yilmaz et al., 2010; Aiello et al., 2014; Bagarello et al., 2014a). The signs of a promising ability of the BEST procedure to yield a reasonably reliable soil hydraulic characterization can be found but these signs are not enough to suggest conclusions of general validity.

Among the soil hydraulic properties, saturated hydraulic conductivity, K_s, is particularly important since it controls many soil hydrological processes such as infiltration.

Given that K_s depends strongly on soil structure, many measurements have to be repeated over time to characterize its spatial and temporal variability (Lauren et al., 1988; Logsdon and Jaynes, 1996; Prieksat et al., 1994).Especially for structured soils, K_s should be measured directly in the field to minimize disturbance of the sampled soil and to maintain its functional connection with the surrounding soil (Bouma, 1982). Many methods have been developed over time for measurement of K_s but different methods often yield substantially dissimilar K_s values since this parameter is extremely sensitive to sample size, flow geometry, sample collection procedures and various soil physical-hydrological characteristics (Reynolds et al., 2000). Comparing methodologically similar techniques can help to better establish what happens when a measurement of K_s is carried out because, in this case, factors determining the relative performances of alternative techniques can be determined with more confidence. Comparison among methods allows to better establish what kind of information is contained in a measurement of K_s carried out with a particular method.

Infiltration experiments into an initially unsaturated soil through a circular source of a generally small diameter have become very common to determine K_s in the field and a wide variety of methods and calculation techniques are now available. For example, K_s can be determined with BEST, the pressure infiltrometer (PI) (Reynolds and Elrick, 1990), the simplified falling head (SFH) technique (Bagarello et al., 2004), the tension infiltrometer (TI) (Perroux and White, 1988; Ankeny et al., 1991), the mini disk infiltrometer (MDI) (Dohnal et al., 2010), and the bottomless bucket (BB) method (Nimmo et al., 2009).

Much is known about these methods. The PI is one of the most frequently applied infiltrometer methods (e.g., Angulo-Jaramillo et al., 2000; Bagarello et al., 2000; Mertens et al., 2002; Vauclin et al., 1994) and comparisons between this and other methods have been carried out (e.g., Reynolds et al., 2000; Verbist et al., 2009, 2013; Bagarello et al., 2013b), allowing for example to conclude that the PI data could be uncertain in cracking clay loam soils and that some soil disturbance can occur with particular devices and applicative procedures. The SFH technique is less applied than the PI technique although these two techniques should be expected to yield similar results in relatively rigid porous media (Bagarello et al., 2013b). Recently, the TI method was found to be a good candidate to become a reference method for determining the saturated hydraulic conductivity of stony soils among other alternative methods (Verbist et al., 2013).

However, there are also poorly understood issues. For example, the usability, for K_s determination, of a device developed for measuring unsaturated soil hydraulic conductivity is still uncertain. Comparing the TI with other infiltrometer devices specifically developed for

determination of K_s may help to address this issue. A reason of particular interest for this type of investigation is that the TI allows to minimize soil surface disturbance during the run, that can influence the measured conductivity (e.g. Bagarello et al., 2014b). Another point deserving developments is the usability of the MDI, that is a particular type of TI. The former device samples an appreciably smaller surface than the latter one and it is well known that determination of soil hydraulic conductivity at or close to saturation is strongly affected by the soil volume or the area sampled by an individual measurement (e.g., Lauren et al., 1988; Vepraskas and Williams, 1995; Lai and Ren, 2007). However, the relative performances of these two devices for a measurement of soil hydraulic conductivity are still unknown. Developing this issue is necessary also because there are examples in the literature that combine a measurement of K_s carried out with a relatively large ring with a measurement of conductivity very close to saturation (i.e., more or less the saturated hydraulic conductivity of the soil matrix) carried out with the MDI (Gonzalez-Sosa et al., 2010). In other terms, it should be established if the TI and the MDI yield similar results when they are applied with the same established pressure head, especially at or close to saturation. The performances of BEST in comparison with other infiltrometer methods to determine K_s are still largely unknown since only a few investigations have been carried out. A reason of interest for a comparison including the BB method is that it has so far received little field testing or comparison with other methods.

The general objective of this investigation was to assess usability of infiltrometer techniques for determining the soil hydraulic properties of a loam soil. In particular, the soil hydraulic properties predicted by the BEST procedure were compared with independent measurements of these properties. Six infiltration techniques to determine the saturated soil hydraulic conductivity were then compared.

A.2.2. Materials and methods

Field site and experimental procedures

The study site is located at the Department of Agricultural and Forestry Sciences of the Palermo University (13°21’6” E, 38°6’25” N) in western Sicily, Italy. The climate of the area is semi-arid Mediterranean, with a mean annual air temperature of 18.3°C and an annual rainfall of 855 mm in the period 1971-2000. The area, with a spontaneous, sparse herbaceous vegetation, is rectangular, nearly flat, and extends for approximately 150 m^2.

The following six infiltrometer methods were applied in this investigation to characterize the soil: Beerkan Estimation of Soil Transfer parameters (BEST) procedure,

single-ring pressure infiltrometer (PI), tension infiltrometer (TI), mini disk infiltrometer (MDI), simplified falling head technique, and bottomless bucket (BB) method. All these methods make use of a circular source to establish an infiltration process into an initially unsaturated porous medium but they differ by many aspects including measured soil hydraulic properties, boundary conditions on the infiltration surface, flow field characteristics, stage of the infiltration process used for the analysis, field equipment and difficulty of the experiment.

In particular, a complete soil hydraulic characterization can be obtained with BEST, the saturated soil hydraulic conductivity, K_s, and an estimate of the soil hydraulic conductivity function is given by the PI, and hydraulic conductivity, K, points at saturation or near saturation are obtained with the other techniques.

Boundary conditions vary between positive (PI) and negative but close to zero (TI, MDI) pressure heads on the infiltration surface and between constant (PI, TI, MDI) and variable (BEST, SFH, BB) water pressure heads during the run. Therefore, different factors, including changes in soil structure upon wetting, hydraulic contact between the device and the sampled soil and air entrapment, can influence the relative performances of the tested methods.

All methods except the SFH technique establish a three-dimensional flow field. One-dimensional flow required by the SFH technique implies a relatively deep insertion of the ring into the soil and hence the risk of compaction or shattering of the sampled soil volume with this technique. Moreover, soil's anisotropy could determine differences between the K_s values obtained with the SFH and the other methods, although ring infiltrometers are essentially expected to measure vertical soil water transmission parameters since rings establish downward flow (Reynolds and Elrick, 2005).

Steady infiltration data are used with the PI, TI (multi-potential experiment) and BB methods. The initial stage of the infiltration process is considered by the SFH technique and the information collected during both the transient and the steady-state stage of the run is used with the BEST, TI (one-potential) and MDI methods. Different durations of the field run are expected to determine different soil alteration phenomena (e.g., weakening of particle bonds) during the method's application. Possible uncertainties in the attainment of steady flow conditions during the run cannot be excluded, and they could affect the results obtained with some of the tested methods.

Finally, minimum experimental equipment and simple field runs are required for some methods (BEST, SFH, BB) whereas specific devices and more complicated runs are necessary with other methods (PI, TI, MDI). With some devices, the experiment can be expected to be

particularly accurate. For example, with the TI, the pressure head to be established on the infiltration surface can accurately be calibrated in the laboratory. However, more complicated devices and/or runs also imply more opportunities for errors or uncertainties of experimental nature.

Soil sampling and field experiments were carried out during the months from May to early October in 2013. The choice of the exact dates of the sampling campaign was made taking into account the opportunity to sample a soil with similar antecedent soil water content and bulk density conditions. At this aim, the gravimetric soil water content, w (g g^{-1}), and the dry soil bulk density, ρ_b (Mg m^{-3}), were checked periodically during the experimental period. In particular, a total of 36 undisturbed soil cores (0.05 m in height by 0.05 m in diameter) were collected at the 0 to 0.05 m and 0.05 to 0.10 m depths. These cores were used to determine ρ_b and w, and hence the soil water content at the beginning of an infiltration experiment, θ_i (m^3m^{-3}), and the soil porosity, ϕ (m^3m^{-3}), assuming a soil particle density of 2.65 Mg m^{-3}. Other 20 disturbed soil samples were collected during the sampling period for determining w. All samples were taken at randomly selected points and the same criterion was applied for all infiltrometer techniques.

Ten disturbed soil samples (0-0.10 m depth) were used to determine the particle size distribution (PSD), using conventional methods (Gee and Bauder, 1986). Fine size fractions were determined by the hydrometer method, whereas the coarse fractions were obtained by mechanical dry sieving. The clay (*cl*), silt (*si*), and sand (*sa*) percentages were determined according to the USDA standards (Gee and Bauder, 1986).

Following Dane and Hopmans (2002), the water retention curve at high pressure heads ($h \geq$ -1.5 m) was determined by hanging water columns on soil cores collected in stainless steel cylinders (inner diameter = 0.08 m, height = 0.05 m) at ten points. Given that soil water retention at low pressure heads is mostly influenced by adsorptive forces, repacked soil samples and the pressure plate apparatus were used for $h \leq$ -3 m. In particular, for each sampling point, the dried soil from the undisturbed core was crushed and sieved at 2 mm, and then it was packed into rings having an inside diameter of 0.05 m and a height of 0.01 m. Two replicated samples were used for each sampling point and applied pressure head. Volumetric water retention data were obtained for h values of -0.05, -0.1, -0.2, -0.4, -0.7, -1.2, -3.37, -10.2, -30.6 and -153.0 m.

Ten infiltration runs of the BEST (Lassabatère et al., 2006) type were carried out using a ring with an inner diameter of 0.15 m, inserted to a depth of about 0.01 m, and individual water volumes of 150 mL. An experimental cumulative infiltration, I (L), vs. time, t (L),

relationship including N_{tot} discrete points, N_{tot} being the number of collected (t, I) data points ($9 \leq N_{tot} \leq 20$, depending on the run; mean = 14), was then deduced.

Ten single-ring pressure infiltrometer (PI) tests were conducted using a device similar to the one by Ciollaro and Lamaddalena (1998). A ring with an inner diameter of 0.15 m was inserted to a depth d = 0.12 m. Water was carefully poured on the soil surface to a small depth before opening the infiltrometer reservoir. A constant depth of ponding, H_1 = 0.053 m, was established on the soil surface, and flow rate was monitored until attainment of quasi steady-state conditions. A constant depth of ponding, H_2 = 0.11 m, was then established, and flow rate was monitored until another quasi steady-state condition was detected. Apparent steady-state flow rates (Q_{s1} and Q_{s2}) corresponding to the two applied H levels (H_1 and H_2, respectively) were estimated from the flow rate versus time plot.

A tension infiltrometer (TI) with a 0.24 m diameter base plate unit and a separated water supply unit was used. A 10 mm thick layer of contact material (Reynolds and Zebchuk, 1996; Bagarello et al., 2001; Reynolds, 2006) was placed over the surface and the pressure head offset determined by the contact material layer was considered in establishing the pressure head on the TI membrane (Reynolds, 2006). Ten multi-potential experiments were carried out applying an ascending sequence of pressure heads, h_0 (L), at the soil surface (-120, -60, -30, and -10 mm), to exclude the effects of hysteresis on the measured soil hydraulic conductivity (Reynolds and Elrick, 1991; Bagarello et al., 2005, 2007). The apparent steady-state infiltration rate was determined for each applied pressure head.

One-potential (h_0 = 0) TI runs were carried out at other ten sampling points, and twenty one-potential (h_0 = 0) experiments were carried out with the mini disk infiltrometer (MDI) (Madsen and Chandler, 2007; Dohnal et al., 2010). More runs were carried out with the MDI than with all other techniques since the former device samples a small area (approximately 15 cm^2).

Ten points were sampled to determine K_s by the simplified falling head (SFH) technique (Bagarello et al., 2004) using 0.15 m diameter rings inserted to a depth of 0.12 m. Undisturbed soil cores collected two or three days before the SFH test allowed to estimate the soil water content at the time of sampling, θ_i (m^3m^{-3}), that was used, with the estimated porosity, to determine the volume of water to be applied for the one-dimensional infiltration test. The initial depth of ponding for the SFH runs was 40 mm. The time, t_a (T), from the application of water to the instant at which the surface area was no longer covered by water was measured.

Finally, ten infiltration runs of the bottomless bucket (BB) type were carried out (Nimmo et al., 2009). A 0.15 m inner diameter ring was inserted into the soil to a depth of about 0.05 m. Water was poured on the confined infiltration surface to establish an initial depth of water of 0.1 m. The time from this application to the instant at which the surface area was covered by 0.02 m of water was measured and another volume of water was poured immediately into the ring to re-establish a ponded depth of water of 0.1 m. This procedure was repeated until the rate of decline of the falling head was nearly constant. Five to ten volumes of water were used, depending on the sampling point.

Calculation of soil hydraulic properties

The BEST procedure (Lassabatère et al., 2006) was applied to determine the parameters of the van Genuchten (1980) relationship for the water retention curve with the Burdine (1953) condition and the Brooks and Corey (1964) relationship for hydraulic conductivity. The Beerkan infiltration run was analyzed by the BEST-slope (Lassabatère et al., 2006), BEST-intercept (Yilmaz et al., 2010) and BEST-steady (Bagarello et al., 2014c) algorithms. Taking into account the small size of the sampled area and the random sampling for textural characterization, a representative PSD was obtained by averaging the ten individual PSDs. A mean value of both the antecedent soil water content, θ_i, and the dry soil bulk density, ρ_b, was similarly used to apply BEST. Therefore, the field site was assumed to be homogeneous in terms of PSD, θ_i, ρ_b, and hence estimated soil porosity, ϕ, but a location-dependent water retention curve and hydraulic conductivity function were obtained (Bagarello et al., 2014a).

The two-level PI runs were analyzed with the Two-Ponding-Depth (TPD) approach by Reynolds and Elrick (1990) to obtain an estimate of both K_s and the so-called α^* parameter at each sampling point.

The multi-potential TI runs were analyzed according to Ankeny et al. (1991) to estimate the soil hydraulic conductivity at pressure heads of -10 (K_{10}), -30 (K_{30}), -60 (K_{60}) and -120 mm (K_{120}).

The BEST-steady algorithm was also applied to estimate K_s for the one-potential experiments carried out with both the TI and the MDI.

Eq.(15) by Bagarello et al. (2004) was used to determine K_s for the SFH infiltration runs, by assuming an α^* parameter of 4 m^{-1} (Elrick and Reynolds, 1992).

Finally, eq.(10) by Nimmo et al. (2009) was used to estimate K_s for each applied water volume during the BB experiment, assuming $\lambda_c = 1/\alpha^* = 0.25$ m. The last two determinations of K_s were averaged to obtain an estimate of K_s at a given sampling point.

Testing BEST against independent soil data

The hydraulic properties predicted with BEST were compared with independent measurements of water retention, saturated soil hydraulic conductivity, K_s, and unsaturated soil hydraulic conductivity, K. The water retention data were obtained by standard laboratory techniques (Dane and Hopmans, 2002). The K_s and K data were collected in the field by the PI and the TI (multi-potential experiment), respectively, considering that these techniques have become in the last 25 years near-standard approaches for field measurement of soil hydraulic conductivity (Angulo-Jaramillo et al., 2000; Bagarello et al., 2000; Reynolds et al., 2000; Verbist et al., 2013).

For each established pressure head in the laboratory, a mean value of θ was calculated using the valid laboratory data to obtain a single experimental water retention curve for the sampled site, and the vG model with the Burdine condition and $\theta_r = 0$ was fitted to the mean (θ, h) data pairs. The fitting was performed by minimizing the sum of the squared residuals between the model and the data.

Taking into account that the fitted saturated soil water content, θ_s, was appreciably lower than the porosity, ϕ, determined from the bulk density measurements (fitted $\theta_s = 0.3996$ m^3m^{-3}, i.e. 76% of ϕ), the three BEST algorithms, i.e. BEST-slope, BEST-intercept and BEST-steady, were applied with both $\theta_s = \phi$ (BSL-ϕ, BIN-ϕ, and BST-ϕ, respectively) and θ_s equal to the fitted value (BSL-fit, BIN-fit, and BST-fit, respectively). The hydraulic parameters estimated with BEST were used to calculate θ at the experimentally imposed pressure heads for each sampling point and a mean value of θ was obtained for each h value by averaging the valid results with BEST. The θ values predicted with BEST were then compared with the measured θ values by linear regression analysis techniques.

The K_s values obtained with BEST were compared with the K_s data collected by the PI with the TPD approach since these calculations do not need any subjective estimation of soil parameters, that could affect the comparison between datasets. At first, the normality of the distribution of both the untransformed and the ln-transformed K_s data was tested by the Lilliefors (1967) test. Then, a two-tailed t test was applied to compare the K_s data obtained with the PI and the BEST procedure. This comparison was made for each applied BEST algorithm.

Another test of the K_s data obtained with BEST was carried out by establishing a comparison with the unsaturated soil hydraulic conductivity, K, measured with the TI. According to Bagarello et al. (2014a), this comparison can allow to discriminate between

possible ($K_s > K$ at the highest pressure head, equal to -10 mm in this investigation) and physically impossible ($K_s < K_{10}$) situations. Also for the TI measurements, the normality of the distribution of both the untransformed and the ln-transformed K values was preliminarily tested.

Finally, for each established pressure head in the field by the TI, a mean value of K was calculated by using the individual K values obtained at each sampling point with this device to obtain a single experimental hydraulic conductivity function for the sampled site. The hydraulic parameters estimated with the six BEST algorithms were used to calculate K at the experimentally imposed pressure heads for each sampling point and a mean value of K was obtained for each h value by averaging the valid results with BEST. The K values predicted by BEST were then compared with the K values obtained with the TI.

Comparing methods to determine saturated soil hydraulic conductivity

A comparison among the K_s values obtained with different infiltrometer techniques was carried out. In particular, six independent sets of K_s data were obtained with the following techniques and procedures: 1) PI with the TPD approach (PI dataset); 2) BST-ϕ algorithm (BEST); 3) one-potential TI experiment, i.e. $h = 0$, steady algorithm, $\theta_s = \phi$ (TI); 4) MDI experiment, $h = 0$, steady algorithm, $\theta_s = \phi$ (MDI); 5) simplified falling head technique (SFH); and 6) bottomless bucket method (BB). The normality of the distribution of both the untransformed and the ln-transformed K_s data was tested. Then, the Tukey Honestly Significant Difference test was applied to compare the six datasets.

The choices to assume $\theta_s = \phi$ to analyze the BEST, SFH, TI and MDI data and to apply the steady algorithm for the analysis of the BEST, TI and MDI infiltration runs were made for the following reasons: i) assuming $\theta_s = \phi$ allowed to include the SFH experiment in the comparison. With θ_s set at the fitted value by the vG model, the hypothesis of 1D flow could be violated and the wetting front could be expected to go beyond the bottom of the cylinder as infiltration proceeded; ii) with $\theta_s = \phi$, the steady algorithm yielded K_s data for seven TI runs and for all MDI and BEST runs (sample sizes, $N_s = 20$ for the MDI and 10 for BEST), but lower success rates were obtained with both the slope ($N_s = 7$ for the TI, 20 for the MDI and 9 for BEST) and the intercept ($N_s = 3$, 18 and 10, respectively) algorithms. Therefore, the steady algorithm allowed to establish the K_s comparison by considering the highest possible number of runs; iii) from a practical point of view, simple approaches are obviously desirable. The steady algorithm is simpler to apply than the slope and intercept

algorithms, and porosity determination is simpler than the determination of the soil water content at exactly the end of the infiltration run; iv) in any case, there was no certainty that the θ_s value obtained by fitting the vG model to the laboratory water retention data was really representative of the volumetric soil water content at the end of the infiltration runs because of the possible disturbance of soil structure during soil core collection; and v) the sensitivity of the K_s values obtained with BEST and different estimates of θ_s ($\theta_s = \phi$ or fitted θ_s value) was small according to the existing criteria of evaluation (Elrick and Reynolds, 1992), with differences between means, not exceeding a factor of 1.6, that were particularly small for the intercept and steady algorithms (factor of difference $\leq$ 1.35).

The two K_s comparisons between BEST and the PI carried out in this investigation differed from a methodological point of view (comparison between two independent datasets; multiple comparison among six independent datasets) since they had different objectives and particularly i) testing the BEST performances against the most established and accepted infiltration technique for measuring K_s, and ii) assessing the relative performances of six infiltration techniques varying from a near-standard technique (PI) to an almost never tested technique (BB method).

A.2.3. Results and discussion

Texture and soil characteristics during the sampling period

The soil was loam at eight sampling points and clay-loam at other two locations (Table 1). The dry bulk density ranged from 1.21 to 1.36 Mg m^{-3} during the sampling period, and it varied over an appreciably smaller range (1.21-1.26 Mg m^{-3}) for all but one sampling dates, suggesting that changes in ρ_b were generally small. All field runs were carried out at an antecedent soil water content of $\leq$ 0.19 m^3m^{-3}.

Testing BEST against independent soil data

Due to a malfunctioning of the laboratory equipment, seven experimentally determined water retention curves were usable. Depending on the pressure head, the coefficient of variation, *CV*, of θ varied from 2.7 to 7.5%. These values were small and consistent with those reported in the literature (e.g., Shouse et al., 1995; Hillel, 1998), supporting the choice to test the BEST procedure against the laboratory measured water retention data.

Table 1 Sample size, N_s, minimum, *Min*, maximum, *Max*, mean and coefficient of variation, *CV*, of the clay, *cl*, silt, *si*, and sand, *sa*, percentages, gravimetric soil water content, *w*, and dry soil bulk density, ρ_b, sampled at the field site.

Variable	Sampling date	N_s	Min	Max	Mean	CV (%)
cl (%)	15/04/2013	10	21.6	31.3	24.9	12.7
si (%)		10	29.4	42.2	37.4	10.5
sa (%)		10	35.6	40.7	37.7	5.1
w (g g^{-1})	15/04/2013	20	0.11	0.27	0.15	24.1
	29/04/2013	3	0.18	0.19	0.18	1.9
	18/05/2013	3	0.10	0.13	0.11	13.8
	27/05/2013	3	0.10	0.13	0.12	16.2
	08/07/2013	20	0.03	0.08	0.05	23.9
	24/09/2013	2	0.12	0.14	0.13	14.8
	3/10/2013	5	0.07	0.09	0.08	12.1
ρ_b (Mg m^{-3})	15/04/2013	20	1.11	1.57	1.25	10.0
	29/04/2013	3	1.13	1.29	1.21	6.7
	18/05/2013	3	1.17	1.32	1.26	6.1
	27/05/2013	3	1.21	1.53	1.36	12.1
	24/09/2013	2	1.16	1.34	1.25	9.8
	3/10/2013	5	1.15	1.50	1.26	11.2

The vG model fitted well to the data since the coefficient of determination, R^2, was equal to 0.973 and the relative error, *Er*, expressing the quality of the fit (Lassabatère et al., 2006), was of 4.2% (Figure 1). The fitted saturated soil water content, θ_s, equal to 0.3996 m^3m^{-3}, was lower than the calculated porosity, ϕ, equal to 0.5280 m^3m^{-3}. Different investigations have suggested that θ_s should be approximately 85-95% of ϕ (Somaratne and Smettem, 1993; Dane and Hopmans, 2002; Mubarak et al., 2009b; Verbist et al., 2013) but this indication has not a general validity since, for example, Gonzalez-Sosa et al. (2010) determined a mean θ_s/ϕ ratio of 0.7 using θ_s values measured in the field. Therefore, $\theta_s/\phi = 0.76$ was plausible.

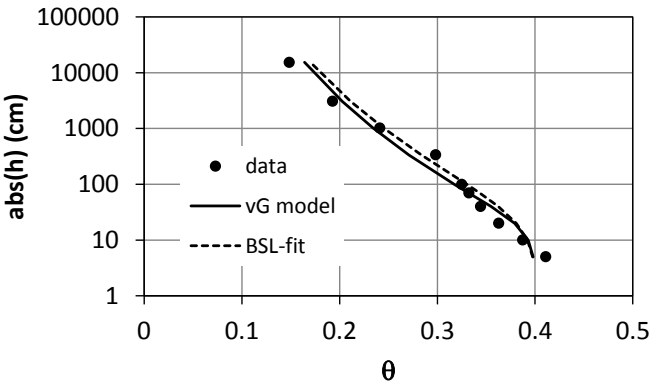

Fig. 1 Measured water retention values, fitted van Genuchten's (1980) model to the data and predicted soil water retention curve with the BSL-fit algorithm.

Regardless of the estimate of θ_s (ϕ, fitted value), the BIN and BST algorithms were successful at each sampling point (N_s = 10). The BSL algorithm yielded unacceptable results in a few cases, impeding soil hydraulic characterization at one (with BSL-ϕ) or three (BSL-fit) locations.

In the comparison between the predicted and the measured water retention values, the three BEST algorithms (BSL, BIN and BST) applied with the same θ_s value (ϕ or the fitted value) showed similar performances and, in particular, the BIN and BST algorithms yielded identical results since the estimates of θ did not vary between these two algorithms (Table 2). This last result was due to the dependence of the h_g scale parameter of the water retention curve on the S^2/K_s ratio, S being the soil sorptivity, that is expected to be the same for both the BIN and BST algorithms (Lassabatère et al., 2006; Bagarello et al., 2014c). All regressions were statistically significant (P = 0.05). With $\theta_s = \phi$, the linear regression line between the predicted and the experimental values was different from the identity line according to the calculated 95% confidence intervals for the intercept and the slope, and high E_r values (18.2-27.6%) were obtained. With θ_s set at the fitted value, all algorithms yielded a linear regression line between the predicted θ values and the data that did not differ from the identity line, and the relative errors were much smaller (Er = 4.5-8.4%).

Table 2 Results of the linear regression analysis between the volumetric soil water content predicted by different BEST approaches for 10 pressure head values, h ($-153 \leq h \leq -0.05$ m), and the laboratory measured volumetric soil water content.

Predictive approach	Regression coefficients			95% confidence intervals		Relative error (%)
	Intercept	Slope	R^2	Intercept	Slope	
BSL-ϕ	0.0029	1.2619	0.9752	-0.05 – 0.05	1.10 – 1.43	27.6
BIN-ϕ and BST-ϕ	-0.0276	1.2522	0.9588	-0.09 – 0.04	1.04 – 1.46	18.2
BSL-fit	0.0278	0.9325	0.9791	-0.01 – 0.06	0.82 – 1.04	4.5
BIN-fit and BST-fit	-0.0127	0.9701	0.9660	-0.06 – 0.03	0.82 – 1.12	8.4

R^2 = coefficient of determination. All R values were > 0 according to a one-tailed t test (P = 0.05).

Therefore, it was possible to detect a satisfactory correspondence of the predicted soil water retention values with the experimental data, and the choice of θ_s was more important than the applied algorithm to reproduce the laboratory measured θ values since signs of a good predictive ability of BEST were only detected when θ_s was set at the indirectly determined experimental value. This last result might represent another support to the robustness of the BEST procedure because a ponding infiltration process, such as the one established with the Beerkan experiment, implies that some air can be entrapped in the sampled soil volume (Reynolds, 1993), physically determining $\theta_s < \phi$. With θ_s = fitted value, the three BEST algorithms showed similar, and consistently acceptable, predictive performances since all algorithms yielded regression lines statistically coinciding with the identity line. However, the BSL algorithm performed slightly better than the other two

algorithms since a higher R^2 value and a lower *Er* value were obtained in the former case. In addition, the water retention curve predicted with BSL was very similar to that obtained by fitting the vG model to the data (Figure 1).

The statistical frequency distribution of the K_s data was assumed to be ln-normal, since the normality hypothesis was not rejected for all tested datasets only with reference to the ln-transformed K_s data (Table 3). Therefore, geometric means and associated coefficients of variations, *CV*s, were calculated to summarize the data using the appropriate ln-normal equations (Lee et al., 1985).

Table 3 Results of the normality test and geometric mean and associated coefficient of variation of the saturated soil hydraulic conductivity values, K_s, obtained with the Pressure infiltrometer with the TPD approach (PI) and with different applicative scenarios of the BEST procedure of soil hydraulic characterization.

Method	Sample size	Normality test		Mean	Coefficient of variation (%)
		N	LN		
PI	10	yes	yes	97.6 a,b,c,d,e,f	113.4
BSL-ϕ	9	no	yes	56.2 a	185.9
BIN-ϕ	10	no	yes	133.8 b	113.0
BST-ϕ	10	no	yes	111.5 c	114.3
BSL-fit	7	yes	yes	35.1 d	235.5
BIN-fit	10	no	yes	99.5 e	111.8
BST-fit	10	no	yes	82.5 f	113.9

N = normality of the untransformed K_s data; LN normality of the ln-transformed K_s data; yes = the normality hypothesis was not rejected at $P = 0.05$; no = the normality hypothesis was rejected.
Mean values followed by the same letter were compared and the differences were not significant according to a two-tailed t test ($P = 0.05$).

From a statistical point of view, the K_s values obtained with BEST and the PI were similar regardless of the applied algorithm (Table 3). However, the highest, and almost perfect, similarity between the PI and BEST estimates of K_s was detected with the BIN-fit algorithm, since the means and the associated *CV*s of K_s differed by 1.9% and 1.6 percentage units, respectively. The largest differences were detected with the BSL-fit algorithm, with means and *CV*s of K_s differing by 64.0% and 122.1 percentage units, respectively. Therefore, even the K_s comparison allowed to find a good correspondence between the BEST predictions and independent data obtained with a near-standard measurement technique. The appropriateness of using $\theta_s < \phi$ was confirmed but the BEST algorithm allowing a good reproduction of the PI data was not the one best predicting the laboratory measured water retention values. In particular, the algorithm performing best in terms of water retention predictions performed worst with reference to K_s.

The BST-ϕ algorithm yielded practically equivalent K_s values to the BIN-fit algorithm since the means and the *CV*s differed by a negligible 12% and 2.5 percentage units, respectively. This last result reinforced the choice to apply the simplest approach for the K_s comparison among different infiltrometer techniques.

The estimates of a mean K_s obtained with the three BEST algorithms differed at the most by a factor of 2.4-2.8, depending on the assumed θ_s value (Table 3), and they decreased with the passage from the BIN algorithm to the BSL one, confirming previous findings (Bagarello et al., 2014c). These levels of difference could be negligible for some practical purposes taking into account that K_s is expected to vary by several orders of magnitude in the field (Elrick and Reynolds, 1992). However the three algorithms also differed in terms of relative variability of the predicted K_s values (*CV*s differing by 1.6-2.1 times, depending on θ_s) and BSL showed a tendency to yield particularly high *CV* values. Therefore, the choice of the BEST algorithm should be expected to have an appreciable impact on the predicted variability of K_s. On the basis of the established comparison with the PI data, the BIN and BST algorithms appear to yield more reliable variability predictions than BSL.

The statistical frequency distribution of the K_{10}, K_{30}, K_{60} and K_{120} data was assumed to be ln-normal, since the normality hypothesis was never rejected for all tested datasets with reference to both the untransformed and the ln-transformed data. This choice allowed to establish a comparison between the geometric mean values of the measured saturated and unsaturated hydraulic conductivities. On the basis of this comparison, a physically impossible K_s value was only detected with reference to the BSL-fit algorithm since K_s = 35.1 mm h^{-1} and K_{10} = 42.5 mm h^{-1} was obtained (Figure 2). Therefore, the suspect that the BSL-fit algorithm yielded unreliable K_s values was reinforced by this independent test. The K_s values obtained with both the other BEST procedures and the PI were considered more plausible than those obtained with the BSL-fit algorithm since they were all greater than K_{10}. However, some question about the information contained in the K_s data was legitimate

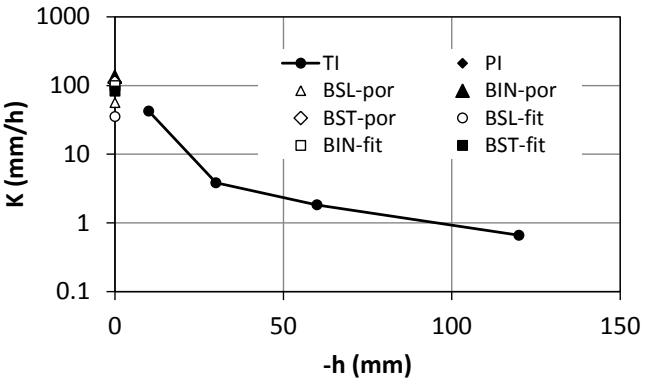

Fig. 2 Soil hydraulic conductivity, *K*, vs. pressure head, *h*, relationship obtained with the Tension Infiltrometer (TI) and comparison with the saturated soil hydraulic conductivity (*h* = 0) obtained with the Pressure Infiltrometer (PI) and different applicative scenarios of the BEST procedure of soil hydraulic characterization.

because the $K(h)$ relationship in the pressure head range from 0 to -10 mm appeared to be flatter than expected on the basis of its detected slope in the -10 to -30 mm range.

The geometric means of K at a given pressure head from -10 to -120 mm were always higher with BEST than the TI, regardless of the applied BEST algorithm and the considered pressure head (Figure 3). Differences between the two experimental methods were particularly noticeable for $h \leq$ -30 mm, since BEST yielded K values higher by a factor of 9 to 35 than the TI, depending on both the algorithm and h. The differences were considerably smaller (i.e., by a factor of 1.2-3.0, depending on the algorithm), and maybe negligible in practice, for the highest pressure head (h = -10 mm). Moreover, these differences were slightly smaller with the algorithms using the fitted θ_s (1.2-2.3) than those setting θ_s at ϕ (1.3-3.0). Therefore, this check confirmed the recent finding by Bagarello et al. (2014a) that the BEST- and the TI-predicted unsaturated soil hydraulic conductivities can be expected to be relatively similar only very close to saturation, probably because the assumed hydraulic conductivity function in BEST does not reproduce satisfactorily the changes in the pore system of a real soil for $h <$ -10 mm. In any case, even this test confirmed that setting θ_s at the fitted value was more appropriate than assuming $\theta_s = \phi$.

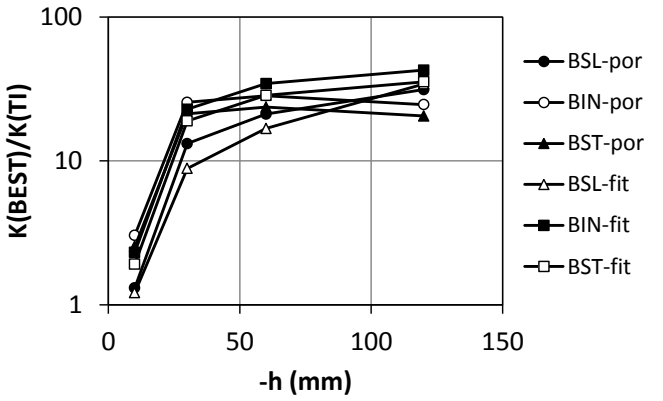

Fig. 3 Ratio between the unsaturated soil hydraulic conductivity predicted with different applicative scenarios of the BEST procedure of soil hydraulic characterization, K(BEST), and the measured conductivity with the Tension Infiltrometer, K(TI), for different pressure head, h, values.

In summary, the BIN-fit algorithm performed best among the tested ones for the following reasons: i) relatively good prediction of laboratory measured water retention values; ii) almost perfect correspondence with saturated soil hydraulic conductivity measured with the PI; iii) plausible K_s values, although slightly lower than those expected on the basis of the TI experiment; and iv) ability to reproduce the TI-measured unsaturated soil hydraulic conductivity, but only close to saturation. The BSL-fit algorithm allowed to improve water retention prediction but it was not a good choice for soil hydraulic conductivity prediction.

This investigation was in line with the conclusion by Aiello et al. (2014) that the applicative methodology of the BEST procedure has to be adapted to the particular situation under consideration. Additional developments can be thought, including the choice of the

constants of the infiltration model, since Nasta et al. (2012) suggested that a proper choice of these constants should be expected to improve the soil hydraulic parameters estimated with BEST. However, estimation procedures of the constants as a function of soil type have still to be developed. Another point deserving consideration is the representation of the soil as a single-permeability system in the current BEST procedure. This representation could be responsible of the poor matching between predicted and measured unsaturated soil hydraulic conductivity. An extension of the infiltration model used in BEST (Haverkamp et al., 1994) for cumulative infiltration into dual-permeability soils has recently been developed (Lassabatère et al., 2014). Further work should be carried out to derive an adapted BEST method for dual-permeability soils. Then, it should be established if this adaption improves prediction of soil hydraulic conductivity.

Comparing methods to determine saturated soil hydraulic conductivity

Geometric means and associated *CV*s were calculated to summarize the K_s data obtained with the six infiltration techniques since the normality hypothesis was not rejected for all tested datasets only with reference to the ln-transformed K_s data (Table 4). The means of K_s varied within a relatively narrow range (98 to 284 mm h^{-1}, i.e by a factor of not more than 2.9) and the relative variability of the K_s data was similar for all tested methods but the MDI one (*CV* = 36% for the MDI and 95-122% for the other methods). Differences between methods were not statistically significant at $P = 0.05$ according to the THSD test. This last result, and the suggestion by Elrick and Reynolds (1992) that a difference in K_s by a factor of two or three can be considered negligible for different practical purposes, indicated that the tested methods yielded a similar information on the mean K_s for the sampled area. This was an encouraging result from a practical point of view since it suggested that one of the factors that are known to influence the experimental determination of K_s, i.e. the applied measurement technique, had no more than a reduced impact on K_s determination.

However, an effect of the applied measurement method on the estimated values of K_s was also sensed. The reason was that K_s was highest for the TI and the MDI methods, intermediate for the SFH technique and lowest for the BB, BEST and PI methods, and a difference between these three groups of methods was thought to be possible considering the probability to alter the infiltration surface during the run. In particular, the TI and the MDI were the less perturbing methods since water was applied with a reasonably negligible kinetic energy. With the SFH technique, free water was applied on the soil surface only once. Water was repeatedly applied within the ring with the BB and BEST methods, and a constant head

of water was maintained for the PI method with a device making use of the Mariotte bottle principle to supply repeatedly water to the infiltration surface. Therefore, the data suggested that the non-significant decrease of K_s from 284 to 98 mm h^{-1} was due, at least in part, to soil changes during the run. A partial support to this suggestion was given by Bagarello et al. (2012, 2013b), who concluded that a more noticeable disturbance of the infiltration surface should be expected with the PI device than with the SFH technique. Another support was found in an investigation by Assouline and Mualem (2002), which suggested that the distribution of steady-state infiltration rates can be expected to be normal in an unsealed, i.e. undisturbed, soil and log-normal in a sealed, i.e. more or less disturbed, soil. In this investigation, the normal distribution hypothesis of the untransformed K_s data was only rejected with reference to the BB and BEST datasets (Table 4), both obtained by a repeated application of a given water volume. In other terms, also the normality test was more or less in line with the suggested interpretation. A practical implication of this investigation is that the tested techniques can be used indifferently to obtain at least an estimate of the order of magnitude of K_s for the sampled soil, but also that using different techniques may allow an improved interpretation and/or simulation of hydrological processes such as rainfall partition into infiltration and rainfall excess (Bagarello et al., 2012, 2013b). The soil initial condition, i.e. before occurrence of rainfall, can be described with the TI, the MDI and maybe the SFH technique because the infiltration run is expected to alter only minimally the infiltration surface. A long and intense rainfall event can disturb appreciably the soil surface and this circumstance can be taken into account in terms of measured K_s, at least approximately, by carrying out a run with a PI device similar to the one used in this investigation or also with the BEST and BB techniques.

Table 4 Results of the normality test and geometric mean and associated coefficient of variation of the saturated soil hydraulic conductivity values, K_s (mm h^{-1}), obtained with the Tension Infiltrometer (TI), the Mini Disk tension Infiltrometer (MDI), the Simplified Falling Head technique (SFH), the Bottomless Bucket method (BB), the BEST procedure of soil hydraulic characterization (BEST) and the Pressure infiltrometer (PI).

Method	Sample size	Normality test		Mean	Coefficient of variation (%)
		N	LN		
TI	7	yes	yes	284.3	95.3
MDI	20	yes	yes	236.9	36.1
SFH	10	yes	yes	170.9	122.1
BB	10	no	yes	131.6	98.7
BEST	10	no	yes	111.5	114.3
PI	10	yes	yes	97.6	113.4

All differences between two mean values were not statistically significant according to the Tukey Honestly Significant Difference test (P = 0.05).

Another factor potentially affecting the detected differences between the applied methods to determine K_s was thought to be an incorrect choice of the α^* and λ_c parameters for the calculation of K_s with the SFH technique and the BB method, respectively. However, the choice of $\alpha^* = 4$ m^{-1} ($\lambda_c = 0.25$ m) was found to be appropriate for the sampled field soil since the two-level PI experiment yielded a geometric mean value of α^* equal to 5 m^{-1}, very close to the assumed value for this parameter.

The duration of the infiltration run was another possible factor affecting the observed differences because a longer run can determine more appreciable swelling phenomena, resulting in a decrease of K_s (Bagarello et al., 2012, 2013b). The mean duration of the TI, MDI and SFH test ranged from 4 to 25 min whereas it was of 25 to 112 min for the BB, BEST and PI runs, with the longest runs performed with this last technique. However, the duration was similar (25 min) for the TI and BEST runs. Therefore, lower K_s values were generally obtained with longer runs, although with some exception, suggesting that the run duration was a contributing factor to the observed differences.

Another point to be considered is the appreciably lower variability of the K_s data obtained with the MDI as compared with the other methods. An effect of soil disturbance due to the run cannot be suggested in this case because an appreciably higher *CV* was detected with the TI, similar to the MDI in terms of water application procedure at the infiltration surface. Some soil heterogeneity, such as macropores, likely occurred at the sampled site since even the lowest mean of K_s (98 mm h^{-1}) was approximately an order of magnitude higher than the expected K_s for a soil with a similar loam texture (10.4 mm h^{-1}, Carsel and Parrish, 1988). Therefore, a smaller soil volume was found to be more homogeneous than a larger volume probably because, as suggested by Lai and Ren (2007), the probability to sample only a part of the range of K_s values increases with a smaller source. As a matter of fact, a relatively few runs with the TI yielded K_s values ranging from 57 to 636 mm h^{-1} whereas an appreciably larger number of runs with the MDI yielded a smaller range of K_s values, varying from 127 to 405 mm h^{-1}. An implication of this interpretation is that a larger ring or disc was more appropriate to represent field soil heterogeneity (Bagarello et al., 2013a; Youngs, 1987). Moreover, a source having a diameter of 0.15-0.24 m was enough to give a representation of this variability because all randomly conducted experiments with sources of this size yielded similar *CV* values.

The measured conductivity with both the TI and the MDI was considered to be the field-saturated soil hydraulic conductivity or very close to K_s for the following reasons: i) a

null pressure head was established on the porous plate of the two devices; ii) the contact material layer was thin (i.e, 2-3 mm) for the MDI or the pressure head offset between the membrane of the TI and the soil was explicitly accounted for in setting the pressure head at the soil surface; iii) the data analysis procedure was sound from a theoretical point of view since it was based on a three-dimensional infiltration model (Haverkamp et al., 1994) that is valid for the case of a null pressure head on the infiltration surface; and iv) the "ex-post" check of the data supported the validity of the experimental and theoretical assumptions and procedures because, with the TI, $K_s = 6.7 \times K_{10}$ was obtained on average. Therefore, a very small increase of h (from -10 mm to zero or nearly zero) determined much larger conductivities, which is a plausible result in terms of macropore effects on flow transport processes under near-saturated conditions. Moreover, the TI and MDI techniques yielded the highest K_s values among the tested infiltrometer techniques, suggesting that macropores were not excluded from the flow process established with these two devices.

The fact that the same order of magnitude of K_s was obtained with the six tested approaches can be viewed as a sign of robustness of the infiltrometer methods for determining this hydrodynamic parameter. This investigation also confirmed that the intended use of the data has to be taken into account in the choice of the most appropriate measurement method (Verbist et al., 2013; Bagarello et al., 2014b). This topic should further be developed also because some investigations questioned the usability of the infiltrometer data, at least in some circumstances (van de Giesen et al., 2000). Probably, more comparisons should be carried out between experimentally measured hydrological processes (e.g., surface runoff at the base of a plot) and the corresponding processes simulated with mechanistic models and the measured soil hydraulic properties (Aiello et al., 2014; Vandervaere et al., 1998). Another implication of the approximate similarity of the K_s results is that simple methods can be viewed as a good substitute of more demanding methods. This is a promising result since the importance of intensively sampling the soil to obtain a reliable characterization of the porous medium is known (Gómez et al., 2005; Verbist et al., 2010; Bagarello et al., 2010; 2013c) and simple approaches, requiring practically sustainable efforts, appear usable at this aim.

A.2.4. Conclusions

Comparing different techniques to estimate soil hydraulic properties is frequent in the scientific literature and uncertainties in the data interpretation are more or less unavoidable since reference values of these properties cannot generally be established. However, these

comparisons help to understand the information contained in a particular measurement. What we are measuring with a particular method and a specific procedure remains a point to be further developed to improve interpretation and/or simulation of hydrological processes on the basis of the measured soil hydraulic properties.

In this investigation, carried out on a loam soil, the BEST-intercept algorithm with a saturated soil water content, θ_s, appreciably lower than the soil porosity was found to be the best choice, among the tested alternatives, to obtain a reasonably good prediction of laboratory measured water retention values, an almost perfect correspondence with the saturated soil hydraulic conductivity measured with the pressure infiltrometer (PI), plausible K_s values, although slightly lower than those expected on the basis of a multi-potential tension infiltrometer (TI) experiment, and a relatively good reproduction of the unsaturated soil hydraulic conductivity measured with the TI, but only very close to saturation. The θ_s value used for the BEST calculations was obtained in the laboratory and there was no proof that it did coincide with the saturated soil water content at the end of the field infiltration run. Notwithstanding this, sampling the soil confined by the ring at the end of this run to obtain an experimental value of θ_s appears a step of the application procedure of the BEST experiment that could yield a more reliable estimation of soil hydraulic properties in comparison with that obtained with the assumption of coincidence between θ_s and the soil porosity.

BEST, the PI, one-potential experiments with both the TI and the mini disk infiltrometer (MDI), the simplified falling head (SFH) technique and the bottomless bucket (BB) method yielded statistically similar estimates of K_s for the sampled area. However, the methods were not perfectly equivalent probably because they differed by the run duration and determined different levels of soil disturbance at the infiltration surface during the run. The conclusion was that any of the tested technique appears usable to obtain the order of magnitude of K_s at the field site. However, the TI, MDI and SFH data should be considered more appropriate to characterize the soil before wetting by a rainfall event. The BEST, BB and PI data seem more appropriate to characterize a soil at some later stage during a rainfall event.

In conclusion, BEST is promising to simply characterize a soil but additional investigations should be carried out in other soils texturally similar to the sampled soil to understand if the methodology performing reasonably well in this investigation can be suggested for a general use in loam soils. Another point deserving consideration is an improved representation of the unsaturated soil hydraulic conductivity function in the BEST

procedure. This investigation suggested that, in general, soil stability upon wetting influences the relative performances of the considered infiltrometer methods to determine K_s. This suggestion could be tested by replicating the experiment in a more stable (or unstable) soil than the loam soil of this investigation. A practical support to the choice of the most appropriate measurement method could also be given by functional evaluation, that involves comparing an experimentally measured hydrological process (i.e., surface runoff at the base of a plot) with the corresponding process simulated with mechanistic models and the measured soil hydraulic properties.

References

Aiello R, Bagarello V, Barbagallo S, Consoli S, Di Prima S, Giordano G, Iovino M. 2014. An assessment of the Beerkan method for determining the hydraulic properties of a sandy loam soil. *Geoderma* 235–236:300–307.

Angulo-Jaramillo R, Vandervaere JP, Roulier S, Thony JL, Gaudet JP, Vauclin M. 2000. Invited Review – Field measurement of soil surface hydraulic properties by disc and ring infiltrometers. A review and recent developments. *Soil & Tillage Research* 55: 1-29.

Ankeny M.D, Ahmed M, Kaspar TC, Horton R. 1991. Simple field method for determining unsaturated hydraulic conductivity. *Soil Science Society of America Journal* 55: 467-470.

Assouline S, Mualem Y. 2002. Infiltration during soil sealing: The effect of areal heterogeneity of soil hydraulic properties. *Water Resources Research* 38(12): 22-1–22-9.

Bagarello V, Iovino M. 2012. Testing the BEST procedure to estimate the soil water retention curve. *Geoderma* 187-188: 67-76.

Bagarello V, Iovino M, Tusa G. 2000. Factors affecting measurement of the near sat-urated soil hydraulic conductivity. *Soil Science Society of America Journal*, 64: 1203-1210.

Bagarello V, Iovino M, Tusa G. 2001. Effect of contact material on tension infiltrometer measurements. *Transactions of the ASAE* 44(4): 911-916.

Bagarello V, Iovino M, Elrick D. 2004. A simplified falling head technique for rapid determination of field-saturated hydraulic conductivity. *Soil Science Society of America Journal* 68: 66-73.

Bagarello V, Castellini M, Iovino M. 2005. Influence of the pressure head sequence on the soil hydraulic conductivity determined with tension infiltrometer. *Applied Engineering in Agriculture* 21(3): 383-391.

Bagarello V, Castellini M, Iovino M. 2007. Comparison of unconfined and confined unsaturated hydraulic conductivity. *Geoderma* 137: 394-400.

Bagarello V, Provenzano G, Sgroi A. 2009. Fitting particle size distribution models to data from Burundian soils for the BEST procedure and other purposes. *Biosystems Engineering* 104: 435-441, doi:10.1016/j.biosystemseng.2009.07.008.

Bagarello V, Di Stefano C, Ferro V, Iovino M, Sgroi A. 2010. Physical and hydraulic characterization of a clay soil at the plot scale. *Journal of Hydrology* 387: 54-64, doi:10.1016/j.hydrol.1010.03.029.

Bagarello V, Di Prima S, Iovino M, Provenzano G, Sgroi A. 2011. Testing different approaches to characterize Burundian soils by the BEST procedure. *Geoderma* 162: 141-150, doi: 10.1016/j.geoderma.2011.01.014.

Bagarello V, D'Asaro F, Iovino M. 2012. A field assessment of the Simplified Falling Head technique to measure the saturated soil hydraulic conductivity. *Geoderma* 187-188: 49-58, doi: 10.1016/j.geoderma.2012.04.008.

Bagarello V, Iovino M, Lai J. 2013a. Field and numerical tests of the two-ponding depth procedure for analysis of single-ring pressure infiltrometer data. *Pedosphere* 23(6): 779-789.

Bagarello V, Baiamonte G, Castellini M, Di Prima S, Iovino M. 2013b. A comparison between the single ring pressure infiltrometer and simplified falling head techniques. In press on *Hydrological Processes* doi: 10.1002/hyp.9980.

Bagarello V, Di Stefano C, Iovino M, Sgroi A. 2013c Using a transient infiltrometric technique for intensively sampling field-saturated hydraulic conductivity of a clay soil in two runoff plots. *Hydrological Processes* 27: 3415-3423, doi: 10.1002/hyp.9448.

Bagarello V, Di Prima S, Giordano G, Iovino M. 2014a. A test of the Beerkan Estimation of Soil Transfer parameters (BEST) procedure. *Geoderma* 221-222: 20-27, doi: 10.1016/j.geoderma.2014.01.017.

Bagarello V, Castellini M, Di Prima S, Iovino M. 2014b. Soil hydraulic properties determined by infiltration experiments and different heights of water pouring. *Geoderma* 213: 492-501, doi: 10.1016/j.geoderma.2013.08.032.

Bagarello V, Di Prima S, Iovino M. 2014c. Comparing alternative algorithms to analyze the beerkan infiltration experiment. In press on *Soil Science Society of America Journal* doi:10.2136/sssaj2013.06.0231.

Bouma J. 1982. Measuring the hydraulic conductivity of soil horizons with continuous macropores. *Soil Science Society of America Journal* 46: 438-441.

Brooks RH, Corey CT. 1964. Hydraulic properties of porous media. *Hydrol*. Paper 3, Colorado State University, Fort Collins.

Burdine NT. 1953. Relative permeability calculation from pore size distribution data. *Petr. Trans. Am. Inst. Min. Metall. Eng*. 198: 71-77.

Carsel RF, Parrish RS. 1988. Developing joint probability distributions of soil water retention characteristics. *Water Resources Research* 24: 755-769.

Ciollaro G, Lamaddalena N. 1998. Effect of tillage on the hydraulic properties of a vertic soil. *Journal of Agricultural Engineering Research* 71: 147-155.

Dane JH, Hopmans JW. 2002. *Water retention and storage: laboratory*. p. 688–692. In: J.H. Dane and G.C. Topp (Eds.). Methods of Soil Analysis, Physical Methods, Part 4, 3rd edition. Soil Sci. Soc. Am, Madison, WI.

Dohnal M, Dusek J, Vogel T. 2010. Improving hydraulic conductivity estimates from minidisk infiltrometer measurements for soils with wide pore-size distributions. *Soil Science Society of America Journal* 74(3): 804-811.

Elrick DE, Reynolds WD. 1992. Methods for analyzing constant-head well permeameter data. *Soil Science Society of America Journal* 56: 320-323.

Gee GW, Bauder JW. 1986. *Particle-size analysis.* p. 383-411. In: A. Klute (ed.). Methods of Soil Analysis, Part 1: Physical and Mineralogical Methods, 2nd ed. Agron. Monogr. 9. ASA and SSSA, Madison, WI.

Gómez JA, Vanderlinden K, Nearing MA. 2005. Spatial variability of surface roughness and hydraulic conductivity after disk tillage: implications for runoff variability. *Journal of Hydrology* 311: 143-156.

Gonzalez-Sosa E, Braud I, Dehotin J, Lassabatère L, Angulo-Jaramillo R, Lagouy M, Branger F, Jacqueminet C, Kermadi S, Michel M. 2010. Impact of land use on the hydraulic properties of the topsoil in a small French catchment. *Hydrological Processes* 24: 2382-2399.

Haverkamp R, Ross PJ, Smettem KRJ, Parlange JY. 1994. Three-dimensional analysis of infiltration from the disc infiltrometer: 2. Physically based infiltration equation. *Water Resources Research* 30(11): 2931-2935.

Hillel D. 1998. *Environmental soil physics*. Academic Press, San Diego, 771 pp.

Jarvis N, Koestel J, Messing I, Moeys J, Lindahl A. 2013. Influence of soil, land use and climatic factors on the hydraulic conductivity of soil. *Hydrology and Earth System Sciences* 17: 5185-5195.

Lai J, Ren L. 2007. Assessing the size dependency of measured hydraulic conductivity using double-ring infiltrometers and numerical simulation. *Soil Science Society of America Journal* 71: 1667-1675.

Lassabatère L, Angulo-Jaramillo R, Soria Ugalde JM, Cuenca R, Braud I, Haverkamp R. 2006. Beerkan estimation of soil transfer parameters through infiltration experiments – BEST. *Soil Science Society of America Journal* 70: 521-532.

Lassabatère L, Angulo-Jaramillo R, Goutaland D, Letellier L, Gaudet JP, Winiarski T, Delolme C. 2010. Effect of settlement of sediments on water infiltration in two urban infiltration basins. *Geoderma* 156: 316-325.

Lassabatère L, Yilmaz D, Peyrard X, Peyneau PE, Lenoir T, Šimůnek J, Angulo-Jaramillo R. 2014. New analytical model for cumulative infiltration into dual-permeability soils. *Vadose Zone Journal* 13(12), 15 pp.

Lauren JG, Wagenet RJ, Bouma J, Wosten JHM. 1988. Variability of saturated hydraulic conductivity in a glossaquic hapludalf with macropores. *Soil Science* 145(1): 20-28.

Lee DM, Reynolds WD, Elrick DE, Clothier BE. 1985. A comparison of three field methods for measuring saturated hydraulic conductivity. *Canadian Journal of Soil Science* 65: 563-573.

Lilliefors HW. 1967. On the Kolmogorov-Smirnov test for normality with mean and variance unknown. *Journal of the American Statistical Association* 62(318): 399-402.

Logsdon SD, Jaynes DB. 1996. Spatial variability of hydraulic conductivity in a cultivated field at different times. *Soil Science Society of America Journal* 60: 703-709.

Madsen MD, Chandler DG. 2007. Automation and use of mini disk infiltrometers. *Soil Science Society of America Journal* 71(5):1469-1472.

Mertens J, Jacques D, Vanderborght J, Feyen J. 2002. Characterisation of the field-saturated hydraulic conductivity on a hillslope: in situ single ring pressure infiltrometer measurements. *Journal of Hydrology* 263: 217-229.

Minasny B, McBratney AB. 2007. Estimating the water retention shape parameter from sand and clay content. *Soil Science Society of America Journal* 71: 1105-1110.

Mubarak I, Mailhol JC, Angulo-Jaramillo R, Ruelle P, Boivin P, Khaledian M. 2009a. Temporal variability in soil hydraulic properties under drip irrigation. *Geoderma* 150: 158-165.

Mubarak I, Mailhol JC, Angulo-Jaramillo R, Bouarfa S, Ruelle P. 2009b. Effect of temporal variability in soil hydraulic properties on simulated water transfer under high-frequency drip irrigation. *Agricultural Water Management* 96: 1547-1559.

Mubarak I, Angulo-Jaramillo R, Mailhol JC, Ruelle P, Khaledian M, Vauclin M. 2010. Spatial analysis of soil surface hydraulic properties: Is infiltration method dependent? *Agricultural Water Management* 97: 1517-1526.

Nasta P, Lassabatere L, Kandelous MM, Šimůnek J, Angulo-Jaramillo R. 2012. Analysis of the role of tortuosity and infiltration constants in the Beerkan method. *Soil Science Society of America Journal* doi: 10.2136/sssaj/2012.0117n.

Nimmo JR, Schmidt KM, Perkins KS, Stock JD. 2009. Rapid measurement of field-saturated hydraulic conductivity for areal characterization. *Vadose Zone Journal* 8: 142-149.

Perroux KM, White I. 1988. Designs for disc permeameters. *Soil Science Society of America Journal* 52: 1205-1215.

Prieksat MA, Kaspar TC, Ankeny MD. 1994. Positional and temporal changes in ponded infiltration in corn field. *Soil Science Society of America Journal* 58: 181-184.

Reynolds WD. 1993. *Saturated hydraulic conductivity: field measurement*. In: M.R.Carter (ed.). Soil Sampling and Methods of Analysis, Canadian Society of Soil Science, Lewis Publishers, Boca Raton, FL, USA. Chapter 56, p., 599-613.

Reynolds WD. 2006. Tension infiltrometer measurements: implications of pressure head offset due to contact sand. *Vadose Zone Journal* 5: 1287-1292.

Reynolds WD, Elrick DE. 1990. Ponded infiltration from a single ring: I. Analysis of steady flow. *Soil Science Society of America Journal* 54: 1233-1241.

Reynolds WD, Elrick DE. 1991. Determination of hydraulic conductivity using a tension infiltrometer. *Soil Science Society of America Journal* 55: 633-639.

Reynolds WD, Zebchuk WD. 1996. Use of contact material in tension infiltrometer measurements. *Soil Technology* 9: 141-159.

Reynolds WD, Elrick DE. 2002. *3.4.3.2.b Pressure infiltrometer*. p. 826–836. In: J.H. Dane and G.C. Topp (Eds.). Methods of Soil Analysis, Physical Methods, Part 4, 3rd edition. Soil Sci. Soc. Am, Madison, WI.

Reynolds WD, Elrick DE. 2005. *Chapter 6 Measurement and characterization of soil hydraulic properties*. p.197-252. In J.Álvarez-Benedí and R.Muñoz-Carpena (co-eds.), Soil-Water-Solute Process Characterization – An Integrated Approach, CRC Press, Boca Raton, Florida, USA.

Reynolds WD, Bowman BT, Brunke RR, Drury CF, Tan CS. 2000. Comparison of tension infiltrometer, pressure infiltrometer, and soil core estimates of saturated hydraulic conductivity. *Soil Science Society of America Journal* 64: 478–484.

Shouse PJ, Russell WB, Burden DS, Selim HM, Sisson JB, van Genuchten MTh. 1995. Spatial variability of soil water retention functions in a silt loam soil. *Soil Science* 159(1): 1-12.

Somaratne NM, Smettem KRJ. 1993. Effect of cultivation and raindrop impact on the surface hydraulic-properties of an Alfisol under wheat. *Soil & Tillage Research* 26: 115-125.

van de Giesen NC, Stomph TJ, de Ridder N. 2000. Scale effects of Hortonian overland flow and rainfall–runoff dynamics in a West African catena landscape. *Hydrological Processes* 14: 165-175.

van Genuchten MTh. 1980. A closed form equation for predicting the hydraulic conductivity of unsaturated soils. *Soil Science Society of America Journal* 44: 892-898.

Vandervaere JP, Vauclin M, Haverkamp R, Peugeot C, Thony JL, Gilfedder M. 1998. Prediction of crust-induced surface runoff with disc infiltrometer data. *Soil Science* 163: 9-21.

Vauclin M, Elrick DE, Thony JL, Vachaud G, Revol Ph, Ruelle P. 1994. Hydraulic conductivity measurements of the spatial variability of a loamy soil. *Soil Technology* 7: 181-195.

Vepraskas MJ, Williams JP. 1995. Hydraulic conductivity of saprolite as a function of sample dimensions and measurement technique. *Soil Science Society of America Journal* 59: 975-981.

Verbist KMJ, Baetens J, Cornelis WM, Gabriels D, Torres C, Soto G. 2009. Hydraulic conductivity as influenced by stoniness in degrade drylands of Chile. *Soil Science Society of America Journal* 73(2): 471-484.

Verbist KMJ, Torfs S, Cornelis WM, Oyarzún R, Soto G, Gabriels D. 2010. Comparison of single- and double-ring infiltrometer methods on stony soils. *Vadose Zone Journal* 9: 462-475.

Verbist KMJ, Cornelis WM, Torfs S, Gabriels D. 2013. Comparing methods to determine hydraulic conductivities on stony soils. *Soil Science Society of America Journal* 77(1): 25-42, doi:10.2136/sssaj2012.0025.

Wainwright J, Parsons AJ. 2002. The effect of temporal variations in rainfall on scale dependency in runoff coefficients. *Water Resources Research*, 38(12): 1271, doi:10.1029/2000WR000188, 7-1 – 7-10.

Xu X, Lewis C, Liu W, Albertson JD, Kiely G. 2012. Analysis of single-ring infiltrometer data for soil hydraulic properties estimation: comparison of BEST and Wu methods. *Agricultural Water Management* 107: 34-41.

Yilmaz D, Lassabatère L, Angulo-Jaramillo R, Deneele D, Legret M. 2010. Hydrodynamic characterization of basic oxygen furnace slag through an adapted BEST method. *Vadose Zone Journal* 9:1-10.

Youngs EG. 1987. Estimating hydraulic conductivity values from ring infiltrometer measurements. *Journal of Soil Science* 38: 623-632.

Part B: Effect of sealing process and surface crust on water infiltration

B.1 Background

Sealing formation and surface crust are widespread phenomena in many soils, especially in arid and semi-arid regions characterized by high intensity rainfall and unstable soil structure.

In literature there is not a clearly distinction between sealing and crust. According to Remly and Bradford (1989) sealing is the initial or wet phase of crust formation whereas crusting is the consequence of the subsequent drying process. Sealing manifests during rainfall events and it is a complex process which depends on many factors, including rainfall intensity and energy, soil surface slope, aggregate stability, soil texture, land cover and anthropogenic factors like mechanical treatment (soil tillage). Sealing includes physical actions such as compaction of soil surface due to the impact of raindrops, clogging of pores and deposition of clay particles on the soil surface. Crust is the result of sealing process which results in a thin layer with greater bulk density, higher shear strength and lower hydraulic conductivity than the underlying soil.

Hydraulic characteristics of crust have an important role in rainfall partition between infiltration and runoff, even if the crust is only a few millimeters thick (Assouline and Mualem, 2002, 2006; Šimůnek et al., 1998; Vandervaere et al., 1997, 1998). Seals and crusts are unfavorable for several reasons, i.e. they hamper seeds germination, reduce root aeration, water availability trough reduced infiltration and retention capacity, require more energy for soil tillage (Bresson et al., 2006; Goldshleger et al., 2004; Ben-Dor et al., 2003, 2004; Cerdan et al., 2001; Stolte et al., 1997; De Jong, 1992). Surface crusts form rapidly when soil is wetted, even if farmers frequently remove them by harrowing or plowing (e.g., Ben-Dor et al., 2003). The negative impact of sealing and crust on soil erosion, flooding and agricultural productivity have long been recognized (Bressoon et al., 2006; McIntyre, 1958). Crust classification is mainly based on the formation mechanisms. Even if crust classification may vary in literature, there is an agreement on two major types: structural and depositional crust (Chen et al., 1980). Structural crusts do not involve any external imported materials in the formation processes. Depositional crusts form when external soil particles, transported in suspension by surface flow, are deposited on the soil surface as water infiltrates or evaporates.

In the formation of surface crusts and seals a key role is played by aggregate stability, intensity of rainfall and its kinetic energy and raindrops size. The aggregates stability is the

ability of aggregates to withstand disaggregation when subjected to internal or external stresses. Le Bissonnais (1996) identified four mechanisms of aggregate breakdown: (1) slaking by the compression of entrapped air during wetting, (2) differential swelling of clay, (3) raindrop impact and (4) physico-chemical dispersion due to osmotic stress that reduces the attractive forces between colloidal particles during wetting. Aggregate stability is influenced by a wide range of factors like texture, organic matter content, mineralogy, calcium and iron content, sodium content and moisture (Goldshleger et al., 2004; Roth and Eggert, 1994; Shainberg et al., 1992; Le Bissionais, 1990; Farres, 1978, 1985). Organic matter acts as a binding agent both between primary particles and aggregates themselves. Furthermore, organic matter is a water-absorbing agent that reduces clay wettability and, consequently, aggregates breakdown.

Rainfall or irrigation water may destroy soil aggregates by two processes: i) slaking, that is the breakdown of aggregates into small individual particles when immersed in water; and ii) mechanical destruction of aggregates operated by direct impact of water drops. According to Le Bissonais (1990), two different situations can occur during rainfall: i) if aggregates are saturated before rainfall, breakdown is caused by contact between water and aggregates, and the involved processes are slaking and micro-cracking, ii) when aggregates are dry before rainfall, breakdown is due to kinetic energy of raindrop and the most important process is mechanical breakdown or splash erosion. The kinetic energy of raindrops depends on the falling velocity (Le Bissonnais, 1996; Geeves, 1997). Agassi et al., (1985) and Geeves (1997) investigated the threshold kinetic energy that causes aggregates breakdown. According to these authors, sealing occurred when raindrops have a kinetic energy greater than 23 J mm^{-1} m^{-2}. Particularly on bare soils, the aggregates are simultaneously subject to the direct impact of raindrops and wetting, so, the loose particles fill and clog the voids between other aggregates by a “washing in” process described by McIntyre (1958).

According to Assouline (2011), the thickness of structural crusts formed under high kinetic energy rainfall can vary by more than two orders of magnitude, i.e. from 0.1 mm to 20 mm. Geeves (1997) used two kinetic energy levels (0.3 and 27.3 J mm^{-1} m^{-2}) showing higher run-off and lower infiltrations rates with the higher kinetic energy compared to the lower one. McIntyre (1958) concluded that a crust only 0.1 mm thick may reduce the infiltration rate by more than a factor of ten. However, the infiltration rate in crusted soils depends also on several factors such as rainfall intensity, wetting rate and antecedent soil moisture content.

The saturated hydraulic conductivity of the crust is related to the conditions and to the factors that prevail during the crust or seal formation processes. Wetting and drying cycles

influences the crust forming process and consequently its hydraulic properties. In fact, depending on the processes involved on soil sealing or crusting, several types of crusts may arise whose characteristics can be classified as summarized in Table 1 (Valentin and Bresson, 1992; Bresson et al., 2006).

Table 1 Crust types, crust formation processes and specific features of crust according to Valentin and Bresson (1992) and Bresson et al., (2006) (adapted from De Jong et al., 2011)

Crust type	Thickness (mm)	Total porosity	Other features	Infiltration (mm/h)	Formation process
Structural crusts					
Slaking	1-3	Moderate	Thin, dense layer, with sharp lower boundary	5-20	Aggregate breakdown
Infilling	2-5	Low	Thin, dense layer, with textural separation and rather sharp lower boundary. Porosity partly filled with bare silts	5-8	Filling of pores/cracks
Coalescing	3->15	Moderate	Thick, continuos layer, with convexo-concave voids and progressive lower boundary	3-9	Compaction
Sieving crust	1-3	Low	Loose sand grains upper layer overlying a thin plasmic layer	0-15	Downward movement, sieving
Depositional crusts					
Runoff	2->50	Low	Sorted micro-bedding	1-5	Sedimentation
Still water	2->50	Very low	Higly sorted micro-bedding	0-2	Sedimentation
Erosion crusts	<1	Very low	Thin plasmic layer at the surface	0-2	Removal of top layer

Due to its importance on hydrological processes, investigation on the effects of surface crusting on infiltration rates has been the subject of several studies from the middle of the 20th century. In this time frame, several approaches were suggested to model water infiltration on sealed and crusted soils. A simple approach to model a crust-soil system consists of considering the crust as a well-established layer with constant values of thickness and saturated hydraulic conductivity. This approach assesses the crust effect through the hydraulic resistance, R_c (T), which is the ratio between the crust thickness, L_c (L), and the corresponding conductivity, K_c (L T^{-1}), (Hillel and Gardner, 1969). The method is based on an infiltration test in which water is supplied at the upper surface of the soil crust under zero ponded conditions in order to measure the steady state water flux across the crust. Moreover, the knowledge of the unsaturated hydraulic conductivity function of the subsoil, K_{hs} (L T^{-1}), is required that can be measured after the removal of the crust. The approach proposed by Hillel

and Gardner (1969) allows the determination of hydraulic resistance of the crust and the quantification of its effects on infiltration process directly in the field. Others approaches consider the system formed by two individual layers with the upper one having uniform properties (Chu, 1985; Romkens et al., 1990; Ahuja and Swartzendruber, 1992; Philip, 1998; Simunek et al., 1998; Smith et al., 1999; Corradini et al., 2000) or non-uniform properties with bulk density that is maximum at the soil surface and then decrease with depth to a minimum corresponding to that of underlying soil (Mualem and Assouline, 1989). The two-layer models, either uniform or not, are more realistic, but their practical implementation and parameterization can be problematic for the large number of input parameters required (Rawls et al., 1990; Nearing et al., 1996). Moreover, these models require calibration with laboratory-simulated rainfall experiments and others data like pressure head measurements (Diekkruger and Bork, 1994) or bulk density (Augeard et al., 2007), that are difficult to collect in the field. For these reasons, simpler approaches as like the one proposed by Hillel and Gardner (1969), which do not required calibration, are preferred.

B.1.1. Field techniques for hydraulic characterization of soil crust

During the last decades several field approaches have been suggested to determine the hydraulic properties of crusted soils. Vandervaere et al. (1997) proposed a direct method to determine hydrodynamic properties of soil crust which uses tension disk infiltration data at several water supply potentials together with information collect by a minitensiometer installed below the soil crust. The minitensiometer, having a cup 20-mm-long and 2.2-mm-diam, is placed horizontally at the crust-subsoil interface with the aim of predicting the arrival of the wetting front beneath the crust. The method applies the infiltration model proposed by Haverkamp et al. (1994) to estimate the sorptivity of the crust, S_c (L $T^{-0.5}$), at different pressure heads, h_0 (L), imposed on the soil surface, using cumulative infiltration data collected until the wetting front reaches the crust-subsoil interface which is identified by a rise in tensiometer readings. The matric flux potential, ϕ_c (L^2T^{-1}), is computed from the corresponding sorptivity value using each value of pressure heads, h_0, applied during the infiltration test. Finally, the hydraulic conductivity of the soil crust is obtained by differentiating the matric flux potential with respect to the pressure heads.

Due to the fragility of the crust, insertion of the porous cup below the crust without altering the soil may be difficult particularly in dry conditions. To avoid soil disturbance,

Vandervaere et al. (1997) inserted the minitensiometer into a hole made 24 hours before and moistened with a 1 cm^3 of water.

The approach proposed by Šimůnek et al. (1998) allows a complete hydraulic characterization of the two layered crust-subsoil system. This alternative approach involves the use of the inverse method and two transient infiltration experiments conducted with disk infiltrometer in the same site. After the first infiltration experiment the crust is removed and the second infiltration experiment is carried out in the underlying soil. The second experiment allows a complete hydraulic characterization of the lower layer by application of inverse method to the solution of the axisymmetric flow out of a disk infiltrometer in a unsaturated porous media (Šimůnek and van Genuchten, 1996, 1997). Then, application of the inverse method to the infiltration data collected during the first experiment conducted on the two-layered system, with known hydraulic properties of the subsoil, allows to estimate the hydraulic properties of the surface crust. Unfortunately, also this method has drawbacks related to the fact that inverse modeling experiences non-uniqueness problems (Šimůnek et al., 1998; Hopmans and Šimůnek, 1999) and lack of convergence in solutions (Wildenschild and Jensen, 1999).

Touma et al. (2011), on the basis of early work by Hillel and Gardner (1969), proposed a method to estimate the hydraulic characteristics of the surface crust that combines a rain simulation experiment and a single-ring infiltration test applied on the same soil after the removal of the crust. Rainfall simulation yields steady-state infiltration rate through the crust surface which is computed as the difference between the runoff rate and the applied rainfall intensity. A single-ring infiltration test based on BEST (Beerkan Estimation of Soil Transfer parameters) procedure is conducted after removing of the crust to estimate the hydraulic properties of the subsoil. Once the hydraulic properties of the subsoil, i.e. the water retention curve and the hydraulic conductivity function, are determined, the crust hydraulic resistance is computed as the ratio between the crust thickness and the corresponding hydraulic conductivity assumed equal to the steady-state infiltration rate measured in the crust-subsoil system. It should be emphasized that the use of rainfall simulator in the field may be complex, in addition, the two experiments do not sample the same area (1 m^2, or more, for the simulated rainfall against <0.02 m^2 for ring test).

Instead in a recent investigation, Souza et al. (2014) detected the effect of soil surface crusting on the mechanical and hydrodynamic properties of a cropped soil, under field and natural rainfall conditions, by a single-ring infiltration experiment with BEST algorithm and shear strength measures.

An alternative to the use of rainfall simulator and a simplification of the method is proposed in chapter B.2. In particular, a minidisk infiltrometer (MDI, Decagon Devices Inc., Pullman, WA) is used in place of the rainfall simulator for measuring the steady-state infiltration rates through the soil-crust system. The BEST procedure (Lassabatère et al., 2006) is applied to estimate the hydraulic properties of underlying soil after removal the sealed layer. The theory on which the method is based and the practical application of the procedure to two crusted soils are outlined in chapter B.2.

The MDI requires a small amount of water, it is of practical use in the field and minimizes disturbance of the sampled soil. Furthermore, the MDI samples a small area (i.e., approximately 16 cm^2) and potentially allows assessment of small-scale spatial variability of hydraulic properties of the soil crust. Despite the small size of the sampled area Alagna et al. (2016a) have proved that the device is a practical alternative to the classical tension infiltrometer to estimate hydrodynamic properties of a loam soil (chapter A.2).

In bare soil of Mediterranean areas the development of sealing processes are very common phenomena due to intense rainfall events associated to the lack of the advantageous protective effects of vegetation cover. In chapter B.3, the ability of the BEST method to detect the effect of sealing induced by natural rainfall is showed. Pairwise infiltration tests were conducted along and between the vineyard rows to compare the soil hydraulic conductivity before and after an intense rainfall event. The bare soil between the rows developed a weak but clearly detectable surface seal that was not observed along the rows probably due to the protective effects of plant cover. It was concluded that extemporaneous measurements conducted by a simple infiltrometer under ponded condition were able to evaluate the influence of surface sealing. In fact, due to the presence of surface sealing that developed between the sampling campaigns, the values of hydraulic conductivity between the rows decreased by a factor of 1.5 whereas it remained along the row. Given the extremely dynamic nature of the processes involved in crust formation measurement and prediction of infiltration in crusted soils can be difficult. Therefore, efforts should be made to identify procedures for investigating the development of surface sealing as a consequence of a given perturbative event. This assessment is also relevant to establish to what extent the common ponded infiltrometer measurements could perturbate the soil surface thus yielding unreliable predictions of the soil hydraulic characteristics. In chapter B.4, an indirect method to characterize the development of the soil surface sealing is proposed by comparing the results of infiltrometric experiments that apply water with different energy levels at the soil surface. The water application procedure can have a substantial effect on the estimates of soil water

transmission properties. The disturbance induced by the height of water pouring mimics breakdown of aggregates caused by rainfall. Therefore, water application determines the possibility of particle detachment and clogging of the largest pores resulting in the development of a surface sealing layer. The investigation was conducted on a sandy-loam soil with the BEST procedure. Two heights of water pouring were used low (0.03 m) and high (1.5 m) under three different initial soil water content, θ_i (cm^{-3} cm^{-3}), conditions. Depending on θ_i, the results showed a decrease in hydraulic conductivity from 13 to 27 times when water was poured by high height. It was concluded that runs carried out with a high height of pouring of water appear more appropriate to obtain data usable to explain surface runoff generation phenomena during intense rainfall events which can develop sealing layers, especially when the soil is relatively dry at the time of sampling.

References

Agassi, M., Morin, J., Shainberg, I. 1985. Effect of raindrop impact energy and water salinity on infiltration rates of sodic soils. Soil Sci Soc Am J., 49, 186–190.

Alagna, V., Bagarello, V., Di Prima, S., Iovino, M. 2016. Determining hydraulic properties of a loam soil by alternative infiltrometer techniques. Hydrol. Processes, 30(2), 263–275.

Ahuja, L.R., Swartzendruber, D. 1992. Flow through crusted soils: analytical and numerical approaches. In: Sumner, M.E., Stewart, B.A. (Eds.), Soil Crusting: Chemical and Physical Processes. Advances in Soil Science. Lewis Publishers, USA, pp. 93–122.

Assouline, S. 2011. Soil surface sealing and crusting. In J. Glinski, J. Horabik, J. Lipiec (eds.). Encyclopedia of Agrophysics. Encyclopedia of Earth Sciences Series. 1st Edition, XLVI, 1028 p. Springer.

Assouline, S., Mualem, Y. 2002. Infiltration during soil sealing: The effect of areal heterogeneity of soil hydraulic properties. Water Resources Research, 38(12), 1286, doi:10.1029/2001WR001168.

Assouline, S., Mualem, Y. 2006. Runoff from heterogeneous small bare catchments during soil surface sealing. Water Resources Research, 42:W12405, doi:10.1029/2005WR004592.

Augeard, B., Assouline, S., Fonty, A., Kao, C., Vauclin, M. 2007. Estimating hydraulic properties of rainfall-induced soil surface seals from infiltration experiments and X-ray bulk density measurements. Journal of Hydrology, 341, 12–26.

Ben-Dor, E., Goldshleger, N., Benyamini, Y., Agassi, M., Blumberg, D.G. 2003. The spectral reflectance properties of soil structural crusts in the 1.2- to 1.25- μm spectral region. Soil Science Society of America Journal, 67, 289–299.

Ben-Dor, E., Goldshleger, N., Braun, O., Gindel, B., Goetz, A.F.H., Bonfil, D., Margalit, N., Binayminy, Y., Karnieli, A., Agassi, M. 2004. Monitoring of the infiltration rate in semi-arid soils using airborne hyperspectral technology. International Journal of Remote Sensing, 25, 2607–2624.

Bresson, L.M., Le Bissonnais, Y., Andrieux, P. 2006. Soil surface crusting and structure slumping in Europe. In: Boardman, J., Poesen, J. (Eds.), Soil Erosion in Europe. Wiley & Sons Ltd, West Sussex, pp. 489–500.

Cerdan, O., Souchére, V., Lecomte, V., Couturier, V., Le Bissonais, Y. 2001. Incorporating soil surface crusting processes in an expert-based runoff model: sealing and transfer by runoff and erosion related to agricultural management. Catena, 46, 189–205.

Chen, Y., Tarchitzky, J., Brouwer, J., Morin, J., Banin, A. 1980. Scanning electron microscope observations on soil crusts and their formation. Soil Science, 130(1), 49-55.

Chu, S., 1985. Modelling infiltration into tilled soil during non-uniform rainfall. Transactions American Society of Agricultural Engineers, 28 (4), 1226–1232.

Corradini, C., Melone, F., Smith, R.E. 2000. Modeling local infiltration for a two-layered soil under complex rainfall patterns. Journal of Hydrology, 237, 58– 73.

De Jong, S.M. 1992. The analysis of spectroscopical data to map soil types and soil crusts of Mediterranean eroded soils. Soil Technology, 5, 199– 211.

De Jong, S. M., Addink, E. A., Van Beek, L. P. H., Duijsings, D. 2011. Physical characterization, spectral response and remotely sensed mapping of Mediterranean soil surface crusts. Catena, 86(1), 24-35.

Diekkruger, B., Bork, H.R. 1994. Temporal variability of soil surface crust conductivity. Soil Technology, 7, 1–18.

Farres, P.J. 1978. The role of time and aggregate size in the crusting process. Earth Surface Processes and Landforms, 3, 243– 254.

Farres, P.J. 1985. Feedback relationships between aggregate stability, rainsplash erosion and soil crusting , Assessment of soil surface sealing and crusting. Proceedings of the Symposium Held in Ghent, Belgium, pp. 82– 90 (ISBN: 90-9001289-3).

Geeves, D.W. 1997. Aggregate breakdown and soil surface sealing under rainfall [PhD thesis]. Canberra: Australian National University.

Goldshleger, N., Ben-Dor, E., Benyamini, Y., Agassi, M. 2004. Soil reflectance as a tool for assessing physical crust arrangement of four typical soil in Israel. Soil Science, 169, 677–687.

Haverkamp, R., Ross, P.J., Smettem, K.R.J., Parlange, J.Y. 1994. Threedimensional analysis of infiltration from the disc infiltrometer. 2. Physically based infiltration equation. Water Resources Research, 30, 2931-2935.

Hillel, D., Gardner, W.R. 1969. Steady infiltration into crust-topped profiles. Soil Science, 108, 137–142.

Hopmans, J., Simunek, J. 1999. Review of inverse estimation of soil hydraulic properties. In: Van Genuchten, M., Leij., F., Wu, L. (Eds.), International Workshop on Characterization and Measurement of the Hydraulic Properties of Unsaturated Porous Media. University of California, Riverside, California, pp. 643–659.

Lassabatère, L., Angulo-Jaramillo, R., Soria Ugalde, J.M., Cuenca, R., Braud, I., Haverkamp, R. 2006. Beerkan estimation of soil transfer parameters through infiltration experiments – BEST. Soil Science Society of America Journal, 70, 521-532.

Le Bissionais, Y. 1990. Experimental study and modelling of soil surface crusting processes. Catena, 16, 13–28.

Le Bissonnais, Y. 1996. Aggregate stability and assessment of soil crustability and erodibility: I. Theory and methodology. Eur J Soil Sci., 47, 425–437.

McIntyre, D.S. 1958. Permeability measurements of soil crusts formed by raindrop impact. Soil Science, 85, 185–189.

Mualem, Y., Assouline, S. 1989. Modeling soil seal as a nonuniform layer. Water Resources Research, 25, 2101–2108.

Nearing, M., Liu, B., Risse, L., Zhang, X. 1996. Curve numbers and Green and Ampt effective hydraulic conductivities. Water Resources Bulletin, 32, 125–136.

Philip, J.R. 1998. Infiltration into crusted soils. Water Resources Research, 34, 1919–1927

Rawls, W., Brakensiek, D., Simanton, J., Kohl, K. 1990. Development of a crust factor for the Green and Ampt model. Transactions American Society of Agricultural Engineers, 33, 1224–122

Remley, P.A., Bradford, J.M. 1989. Relationship of soil crust morphology to inter-rill erosion parameters. Soil Sci. Soc. Am. J., 53, 1215-1221.

Romkens, M.J.M., Prasad, S.N., Whisler, F.D. 1990. Surface sealing and infiltration. In: Anderson, M.G., Burt, T.P. (Eds.), Process Studies in Hillslope Hydrology. John Wiley and Sons Ltd., New York, pp. 127–172.

Roth, C.H., Eggert, T. 1994. Mechanisms of aggregate breakdown involved in surface sealing, runoff generation and sediment concentration on Loess soils. Soil and Tillage Research, 32, 253–268.

Shainberg, I., Levy, G.J., Rengasamy, P., Frenkel, H. 1992. Aggregate stability and seal formation as affected by drop impact energy and soil amendments. Soil Sciences, 154, 113–119.

Šimůnek, J., van Genuchten, M.T. 1996. Estimating unsaturated soil hydraulic properties from tension disc infiltrometer data by numerical inversion. Water Resources Research, 32, 2683–2696.

Šimůnek, J., van Genuchten, M.T. 1997. Estimating unsaturated soil hydraulic properties from multiple tension disc infiltrometer data. Soil Science, 162, 383–398.

Šimůnek, J., Angulo-Jaramillo, R., Schaap, M.G., Vandervaere, J.P., van Genuchten, M.T. 1998. Using an inverse method to estimate the hydraulic properties of crusted soils from tension disc infiltrometer data. Geoderma, 86, 61-81.

Smith, R.E., Corradini, C., Melone, F. 1999. A conceptual model for infiltration and redistribution in crusted soils. Water Resources Research, 35, 1385–1393.

Souza, E.S., Antonino, A.C.D., Heck, R.J., Montenegro, S.M.G.L., Lima, J.R.S., Sampaio, E.V.S.B., Angulo-Jaramillo, R., Vauclin, M. 2014. Effect of crusting on the physical and hydraulic properties of a soil cropped with Castor beans (Ricinus communis L.) in the northeastern region of Brazil. Soil and Tillage Research, 141, 55–61. doi:10.1016/j.still.2014.04.004

Stolte, J., Ritsema, C.J., De Roo, A.P.J. 1997. Effects of crust and cracks on simulated catchment discharge and soil loss. Journal of Hydrology, 195, 279–290.

Touma, J., Raclot, D., Al-Ali, Y., Zante, P., Hamrouni, H., Dridi, B. 2011. In situ determination of the soil surface crust resistance. Journal of Hydrology, 403, 253-260.

Vandervaere, J.P., Peugeot, C., Vauclin, M., Angulo-Jaramillo, R., Lebel, T. 1997. Estimating hy-draulic conductivity of crusted soils using disc infiltrometers and minitensiometers. Journal of Hydrology, 188(189), 209-223.

Vandervaere, J.P., Vauclin, M., Haverkamp, R., Peugeot, C., Thony, J.L., Gilfedder, M. 1998. Pre-diction of crust-induced surface runoff with disc infiltrometer data. Soil Science, 163, 9-21.

Valentin, C., Bresson, L.M. 1992. Morphology, genesis and classification of surface crusts in loamy sand and sandy soils. Geoderma, 55, 225–245.

Wildenschild, D., Jensen, K. 1999. Numerical modeling of observed effective flow behavior in unsaturated heterogeneous sands. Water Resources Research, 35, 29–42.

B.2. A simple field method to measure the hydrodynamic properties of soil surface crust*

V. Alagna, V. Bagarello, S. Di Prima, G. Giordano, M. Iovino*

Dipartimento di Scienze Agrarie e Forestali, Università degli Studi di Palermo, Italy
*Corresponding author E-mail: massimo.iovino@unipa.it; Tel. +39 091 23897070, Fax +39 091 484035.

Abstract

The hydraulic resistance of the surface crust was determined by a combination of two infiltrometric techniques: first, a surface measurement of steady-state infiltration rate is conducted by a mini-disk tension infiltrometer (MDI); then, the surface crust is removed, its thickness is measured, and a ponded infiltration test is performed at the same site. The Beerkan Estimation of Soil Transfer parameters (BEST) method is applied to estimate the hydraulic properties of the underlying soil provided the particle-size distribution and the bulk density are known. Under the assumption of a unit gradient of hydraulic head below the soil crust, the pressure head at the interface crust-soil is derived. Finally, the hydraulic conductivity of the crust is calculated from the steady-state water flow measured by the MDI and the Darcy law.

The method was tested in a sandy loam and a clay soil. In the sandy loam soil, a 2-3 mm thick slaking crust was visually observed, but no increased surface hydraulic resistance was detected in 10 out of 11 cases. In the clay soil, a 5-7 mm thick crust was formed by gradual coalescence of the plastic, wet aggregates by rainfall compaction. In 10 out of 15 tests, the steady-state infiltration rate with the crust was lower than the underlying soil saturated hydraulic conductivity, denoting an increased hydraulic resistance of the surface crust. For the clay soil, the mean value of the hydraulic resistance was practically independent of the crust thickness and varied between 78 and 81 min.

Key words: Soil Surface Crust, Mini Disk Tension Infiltrometer, BEST procedure.

*This is a post-refereeing final draft. When citing, please refer to the published version: Alagna, V., Bagarello, V., Di Prima, S., Giordano, G., Iovino, M. (2013). A simple field method to measure the hydrodynamic properties of soil surface crust. Journal of Agricultural Engineering 2013; XLIV(s2):e14. doi:10.4081/jae.2013.(s1):e14

B.2.1. Introduction

In many arid and semi-arid regions, the combination of high intensity rainfall and unstable soil aggregation frequently leads to the development of a surface crust characterized by higher bulk density and lower porosity than the underlying soil. It acts as a barrier to water infiltration, hampers germination of seeds and reduces root aeration and water availability. Preventing these problems requires an understanding and prediction of how soil degradation develops in the field (Bresson and Boiffin, 1990). In the formation of surface crusts, aggregate stability plays a key role. Rainfall or irrigation water may destroy soil aggregates by two processes. First, breakdown of aggregates as consequence of slaking when immersed in water. Second, mechanical destruction of aggregates as consequence of water drop impacts (De Jong et al., 2011). In both cases, the loose particles are partially moved by splash erosion and carried into the soil mass by the infiltrating water where they fill the voids between the aggregates. Valentin and Bresson (1992) referred to this as *structural crust*. Fine particles, resulting from aggregates breakdown, can be translocated to a certain distance from their original location. After the rainstorm, a *depositional crust* of variable thickness can be deposited on the soil surface, mainly consisting of clay that was in suspension during rainstorms. A detailed classification of structural and depositional crusts was proposed by Valentin and Bresson (1992).

Investigations on the effects of surface crusting on infiltration rate were conducted since the middle of the 20th century. A review of laboratory and field studies aimed at investigating the factors involved in rainfall-induced seal formation and improving the knowledge about soil crusting effects can be found in Assouline (2004). A simple approach to model the effect of surface sealing on infiltration consists of considering a well established saturated crust with constant thickness and saturated conductivity. Hillel and Gardner (1969) accounted for the crust effect through the hydraulic resistance which is the ratio between the crust thickness and the corresponding conductivity. Under ponded condition, if the crust is less pervious than the lower layer, a negative pressure head can develop in the subsoil (Hillel and Gardner, 1969). A measurement of the pressure head at the crust-soil interface can be obtained by minitensiomenter horizontally inserted beneath the soil crust.

Vandervaere et al. (1997) proposed a method which uses tension disk infiltration data at several water supply potential, together with information from pre-installed minitensiometer below the soil crust to estimate hydraulic conductivity, matric flux potential and sorptivity. An alternative approach involves the use of the inverse solution and two transient infiltration experiments conducted in the same site by a disk infiltrometer before and

after the removal of the soil crust (Šimůnek et al, 1998). However, tensiometers insertion may be problematic in situ whereas the inverse modeling raises problems of non-uniqueness of the solution (Šimůnek and van Genuchten, 1997). Touma et al. (2011) proposed a method to determine the surface crust resistance that combines two types of in situ experiments: i) a rain simulation experiment, and ii) a single ring infiltration test on the same soil after removal of the crust. Steady state infiltration rate through the crust is calculated as the difference between the runoff rate and the applied rainfall intensity. The subsoil hydraulic properties are determined by the combination of pedotransfer functions and a transient model for 3D infiltration in a homogeneous, uniformly unsaturated soil. The method appeared reliable even if it was applied to only one soil type and texture. However, the field use of the rainfall simulator is complicated and the spatial support for the proposed method is questionable. In fact, the two experiments do not sample the same area (1 m^2, or more, for the simulated rainfall against <0.02 m^2 for ring test).

An alternative to the rainfall simulator for measuring the steady state infiltration rate through the soil crust could be the use of the minidisk tension infiltrometer (MDI) that requires a small amount of water and it is easily transportable in the field (Lichner et al., 2007; Madsen and Chandler, 2007; Dohnal et al., 2010). A laboratory application of the MDI to measure the infiltration rates of badlands crust was conducted by Li et al. (2005). The MDI samples a limited area (approximately 15 cm^2) with a very limited disturbance of soil surface. This small sampled area implies that local crust characteristics, including thickness, can be precisely determined. The minimization of disturbance is a great advantage for the characterization of the soil surface crust in the field given the nature of the thin sealing layer, that can easily be disrupted under minimal mechanical action.

The purpose of this investigation was to develop and test a simplified method to determine the hydrodinamic properties of the surface crust. Following the approach by Touma et al. (2011), the hydraulic resistance of the crust is determined by a combination of two infiltrometric techniques: first, a surface measurement of steady-state infiltration rate is conducted by a MDI; then, the surface crust is removed, its thickness is measured, and a ponded infiltration test is performed at the same site. The Beerkan Estimation of Soil Transfer parameters (BEST) procedure (Lassabatère et al., 2006) is applied to estimate the hydraulic properties of the underlying soil provided the particle-size distribution and the bulk density are known. The method was tested in a sandy loam and a clay soil exhibiting a structural crust that developed due to the autumn-winter rainstorms typically occurring under Mediterranean climate.

Theory

The method is based on the earlier work by Hillel and Gardner (1969). The flux across a surface crust of thickness L_c (L) is given by:

$$q_c = -K_c \frac{h_s - L_c - h_0}{L_c} \tag{1}$$

in which h_0 (L) is the water pressure head at the crust surface, h_s (L) is the pressure head at the soil-crust interface and K_c (L T^{-1}) is the hydraulic conductivity of the soil crust. For zero ponded conditions, h_0 becomes zero; furthermore, the thickness of the crust (of the order of a few mm) can be neglected in the numerator of eq. (1) which becomes:

$$q_c = -K_c \frac{h_s}{L_c} = -\frac{h_s}{R_c} \tag{2}$$

where R_c (T) is the crust resistance. For a transient infiltration process, h_s increases with time up to a constant value when steady state condition is reached. Then, the water flux entering the subsoil, q_s (L T^{-1}), can be calculated by the Darcy law:

$$q_s = -K(h_s)\left(\frac{dh}{dz} - 1\right) \tag{3}$$

Where $K(h_s)$ is the unsaturated hydraulic conductivity of the subsoil corresponding to a pressure head h_s and ($dh/dz - 1$) is the hydraulic gradient at soil-crust interface. Due to the continuity of the flux at the soil-crust interface, $q_c = q_s$. Furthermore, when steady state is reached, dh/dz tends to become a negligible quantity and eq. (3) reduces to:

$$q_s = K(h_s) \tag{4}$$

Combining eqs. (2) and (4), the following equation for the crust hydraulic resistance is obtained:

$$R_c = -\frac{h_s}{K(h_s)} \tag{5}$$

When the crust thickness cannot be neglected in the numerator of eq. (1), the crust resistance will be given by:

$$R_c = -\frac{h_s - L_c}{K(h_s)} \tag{6}$$

Therefore, determination of the soil crust resistance needs the knowledge of the soil hydraulic properties of the subsoil, $\theta(h)$ e $K(h)$, and execution of an infiltration test in which water is supplied at the upper surface of the soil crust under zero ponded conditions. Under steady state conditions, the unsaturated hydraulic conductivity of the subsoil $K(h_s)$ is

determined by eq. (4) and, then, the pressure head at the crust-subsoil interface is derived by inverting the $K(h)$ relationship. Crust hydraulic resistance is finally obtained by eqs. (5) or (6).

The hydraulic properties of the subsoil can be determined by the BEST method (Lassabatère et al., 2006) that focuses specifically on the van Genuchten (1980) relationship for the water retention curve with the Burdine (1953) condition and the Brooks and Corey (1964) relationship for hydraulic conductivity:

$$\frac{\theta-\theta_r}{\theta_{fs}-\theta_r}=\left[1+\left(\frac{h}{h_g}\right)^n\right]^{-m} \tag{7a}$$

$$m=1-\frac{2}{n} \tag{7b}$$

$$\frac{K(\theta)}{K_{fs}}=\left(\frac{\theta-\theta_r}{\theta_{fs}-\theta_r}\right)^{\eta} \tag{8a}$$

$$\eta=\frac{2}{m\times n}+3 \tag{8b}$$

where θ (L^3L^{-3}) is the volumetric soil water content, h (L) is the soil water pressure head, K ($L\ T^{-1}$) is the soil hydraulic conductivity, n, m and η are shape parameters, and h_g (L), θ_{fs} (L^3L^{-3}, field saturated soil water content), θ_r (L^3L^{-3}, residual soil water content) and K_{fs} ($L\ T^{-1}$, field saturated soil hydraulic conductivity) are scale parameters. In the BEST procedure, θ_r is assumed to be zero.

Estimation of the shape parameters is based on the soil particle size distribution (PSD), whereas the scale parameter are estimated by means of an inverse analysis of infiltration data. Cumulative infiltration data, I (L), are fitted to the analytical formulation derived by Haverkamp et al. (1994) for a transient zero ponded infiltration from a circular surface:

$$I(t)=S\sqrt{t}+\left(A\,S^2+B\,K_{fs}\right)t \tag{9}$$

where t (T) is the time, S ($L\ T^{-1/2}$) is soil sorptivity, and A (L^{-1}) and B are constants that depend on the shape parameter η, the scale parameter θ_{fs}, the ring radius, r (L), and the initial water content, θ_0 (L^3L^{-3}). The initial and field saturated water contents are measured at the beginning and the end of the infiltration experiment, respectively. BEST first estimates sorptivity by eq.(9) with K_{fs} replaced by its sorptivity function and the experimental steady state infiltration rate, i_s ($L\ T^{-1}$):

$$K_{fs}=i_s-A\,S^2 \tag{10}$$

Once sorptivity is estimated, K_{fs} is driven through eq.(10), assuming that steady state has been reached. As eq.(9) is valid only at transient state, the considered duration of the experiment has to be lower than a maximum time, t_{max} (T):

$$t_{max} = \frac{1}{4(1-B)^2}\left(\frac{S}{K_{fs}}\right)^2 \tag{11}$$

The pressure head scale parameter, h_g, is finally estimated by the following relationship (Lassabatere et al., 2010):

$$h_g = -\frac{S^2}{c_p K_{fs}\left(\theta_{fs}-\theta_0\right)\left[1-\left(\frac{\theta_0}{\theta_{fs}}\right)^{\eta}\right]} \tag{12}$$

in which c_p is a texture parameter that can be derived from the shape parameters (m, n and η).

B.2.2. Materials and methods

Validation of the proposed method was performed in two differently textured soils. The first experimental site (Site 1) is located near the Agricultural Faculty of the University of Palermo (UTM: 355500E, 4218950N) in a citrus orchard having a canopy that covers almost completely the soil surface. The soil had received no tillage in the last three years and, in late autumn when the experiments were conducted, uncontrolled weeds covered diffusely but not uniformly the soil surface. According to the USDA classification, the soil is sandy loam with percentages of clay, *cl* = 15.6% silt, *si* = 27.4% and sand, *sa* = 50.7%. Hydraulic resistance of the surface crust was measured at 11 randomly selected points in which a surface crust was visually observed. Site 2 is located in a vineyard near Marsala, western Sicily (UTM: 286250E, 4187250N). The soil is classified as clay (*cl* = 54.3%, *si* = 29.2%, *sa* = 16.5%). In late spring, after the winter rainfalls, 15 measurement points were randomly selected approximately in the middle of the crop rows (spaced 2.50 m) where soil was not covered by vegetation.

Measurement of the hydraulic resistance of the crust involved a two step experiment (Figure 1). First, the MDI was applied on the surface of the crust to measure the steady state infiltration rate, q_c. The original MDI device (Decagon Devices, Inc., Pullman, WA) with a disk diameter of 3.2 cm was used. The pressure head at the soil surface can be regulated from -0.5 to -7 cm by a suction control tube at the top of the infiltrometer. A very thin layer of contact material (Spheriglass no.2227, Potter Industries, LaPraire, Canada) was spread on the

surface crust to level small irregularities and assure a good hydraulic contact between the porous disk and the soil. Then the MDI was accurately placed on the surface to avoid any disturbance of the crust and the air tube open to start infiltration. The instrument was assured to a rod to keep it in vertical position and to avoid loss of contact with the crust surface during infiltration (Figure 1). The imposed pressure head at the base of the device was not set to zero, as established by theory, but a small suction (approximately 5 mm) was applied to consider the thickness of the contact material layer and also to avoid lateral leakage when water is applied onto an unconfined surface at zero (or positive) pressure head. According to Reynolds (2006), the imposed pressure head on the soil surface is higher than the one established at the base of the device by a quantity depending on the thickness of the contact material (i.e., established h_0 value > –5 mm). In addition, considering the low porosity of the sealed surface soil, the use of a slightly negative pressure head at the soil surface should not influence the measurement of the hydraulic resistance of the crust. Visual readings of the water level in the MDI supply tube were taken at 30 s interval until the complete empting of the reservoir that occurred in approximately 8 min in the sandy loam soil and 15 min in the clay soil. Apparent steady-state infiltration rate was deduced from the slope of the linear portion of the cumulative infiltration vs. time plot.

Fig. 1 Experimental procedure for determining the hydraulic resistance of the surface soil crust: a) surface crust; b) MDI experiment; c) crust removal; d) ring infiltration test.

Three days after the MDI measurement, the surface crust was accurately removed and its thickness measured by a gauge. The average of 5-6 measurements was assumed as thickness of the crust at a given measurement point. A ring with an inner diameter of 80 mm was inserted into the subsoil to a depth of about 10 mm to avoid lateral loss of the ponded water. A known volume of water (50 mL) was poured in the cylinder at the start of the measurement and the elapsed time during the infiltration was measured. When the amount of water had completely infiltrated, an identical amount of water was poured into the cylinder, and the time needed for the water to infiltrate was logged. The procedure was repeated until the difference in infiltration time between three consecutive trials became negligible, signaling a practically steady-state infiltration. To avoid disturbance of the soil surface, the water energy was dissipated against a shield placed 10-20 mm above the soil surface (Figure 1). The number of collected (t, I) data points varied with the run between 10 and 16.

Before conducting the experiment, a disturbed soil sample was collected to estimate the initial gravimetric water content and to determine the PSD, using conventional methods following H_2O_2 pretreatment to eliminate organic matter and clay deflocculation using sodium hexametaphosphate and mechanical agitation (Gee and Bauder, 1986). When the last volume of water had infiltrated, a small sample was collected within the ring to determined the field saturated gravimetric water content. Both initial and field saturated gravimetric water content values were converted into volumetric ones, i.e. θ_0 and θ_{fs}, by the dry soil bulk density, ρ_b (Mg m^{-3}), measured on an undisturbed soil core (0.05 m in height by 0.05 m in diameter) collected in the subsoil in close vicinity of the infiltrometer ring.

B.2.3. Results and discussion

In site 1, the steady state infiltration rate, q_c, through the surface crust ranged from a minimum value of 390 to a maximum value of 755 mm h^{-1} with a mean value of 561 mm h^{-1} (Table 1) In site 2, q_c ranged from 117 to 200 mm h^{-1} (average 147 mm h^{-1}). As expected, a lower q_c values were observed in the clay soil where the relatively weaker structure of the soil aggregates lead to the formation of a more compact surface crust (Figure 1). The coefficient of variation of q_c in the two soils were similar, even if the hydrodinamic characteristics of the surface crust could be considered more homogeneous in the clay soil (CV = 23%) than in the sandy loam soil (CV = 19%) at the time of field tests.

The hydraulic properties, i.e. the water retention curve and the hydraulic conductivity function, of the soil underneath the crust showed similarities between the two soils. The relationships $\theta(h)$ were more variable with the considered run in the sandy loam soil than in

the clay soil. The opposite result was found for the hydraulic conductivity functions (Figure 2). The shape parameters (*n*, *m* and η), that basically depend on the PSD, were characterized by small coefficients of variation (CV < 2.5%) for both soils. For the sandy loam soil, the average values of *n*, *m* and η (*N* = 11), were 2.15, 0.07 and 16.0. For the clay soils (*N* = 15), *n* = 2.07, *m* = 0.03 and η = 31.4. These results did not coincide with the mean values listed by Minasny and McBratney (2007) for the USDA textural categories, which is obvious given the differences in terms of both origin and sample size of the datasets. However, the shape parameters of this investigation were relatively close to the ones reported by the cited Authors and also in line with the circumstance that a lower *n* and a higher η value should be expected for a clay soil than a sandy loam soil.

Table 1 Statistics of the hydraulic parameters of the van Genuchten-Broooks and Corey model (*n*, *m*, η, θ_{fs}, h_g and K_{fs}) for the subsoil and steady state infiltration rate through the surface crust (q_c).

	n	*m*	η	θ_{fs} (m^3m^{-3})	h_g (mm)	K_{fs} (mm h^{-1})	q_c (mm h^{-1})
site 1 sandy loam N = 11							
min	2.149	0.069	15.6	0.576	-180	193	390
max	2.159	0.074	16.4	0.649	-26	623	755
mean	2.154	0.071	16.0	0.615	-87	346	561
CV (%)	0.2	2.5	2.2	5.0	61.0	43.5	23.2
site 2 clay N = 15							
min	2.067	0.032	30.5	0.514	-886	14	117
max	2.073	0.035	33.0	0.622	-51	1777	200
mean	2.070	0.034	31.4	0.557	-241	731	147
CV (%)	0.1	2.4	2.3	5.8	118.0	86.6	18.7

The mean values of θ_{fs} were 0.62 cm^3cm^{-3} (CV = 5.0%) in site 1 and 0.56 cm^3cm^{-3} (CV = 5.8%) in site 2. Actually, estimations of total porosity conducted from independently measured soil bulk densities by assuming a particle density of 2.65 kg m^{-3}, yielded similar results, i.e. a mean value of 0.59 cm^3cm^{-3} for the sandy loam of site 1 and 0.55 cm^3cm^{-3} for the clay soil (site 2). The pressure head scale parameter, h_g, and the field saturated hydraulic conductivity, K_{fs}, that mainly depend on the infiltration experiments, were characterized by a greater variability. The mean values of the two scale parameters were h_g = –87 mm (CV = 61%) and K_{fs} = 346 mm h^{-1} (CV = 44%) for site 1, and h_g = –241 mm (CV = 118%) and K_{fs} = 731 mm h^{-1} (CV = 87%) for site 2. The estimated values of h_g are in agreement with the texture of the two soils given that a higher absolute value of the pressure scale parameter is

expected in fine soils exhibiting a smaller modal pore size (Haverkamp et al., 2006). A higher mean K_{fs} value in the clay soil probably occurred because soils rich in clay often show macropores, microcraks and other structural discontinuities that help water transmission (Bagarello et al., 2010). In this case, the variability of the measured K_{fs} also increases depending on whether the macropores are sampled or not (Bagarello et al, 2012). In fact, the K_{fs} values measured by the BEST procedure in the clay soil extended over two orders of magnitude from a minimum of 14 mm h^{-1} to a maximum of 1777 mm h^{-1} whereas in the sandy loam soil the field saturated hydraulic conductivity values differed, at the most, by a factor of 3.2.

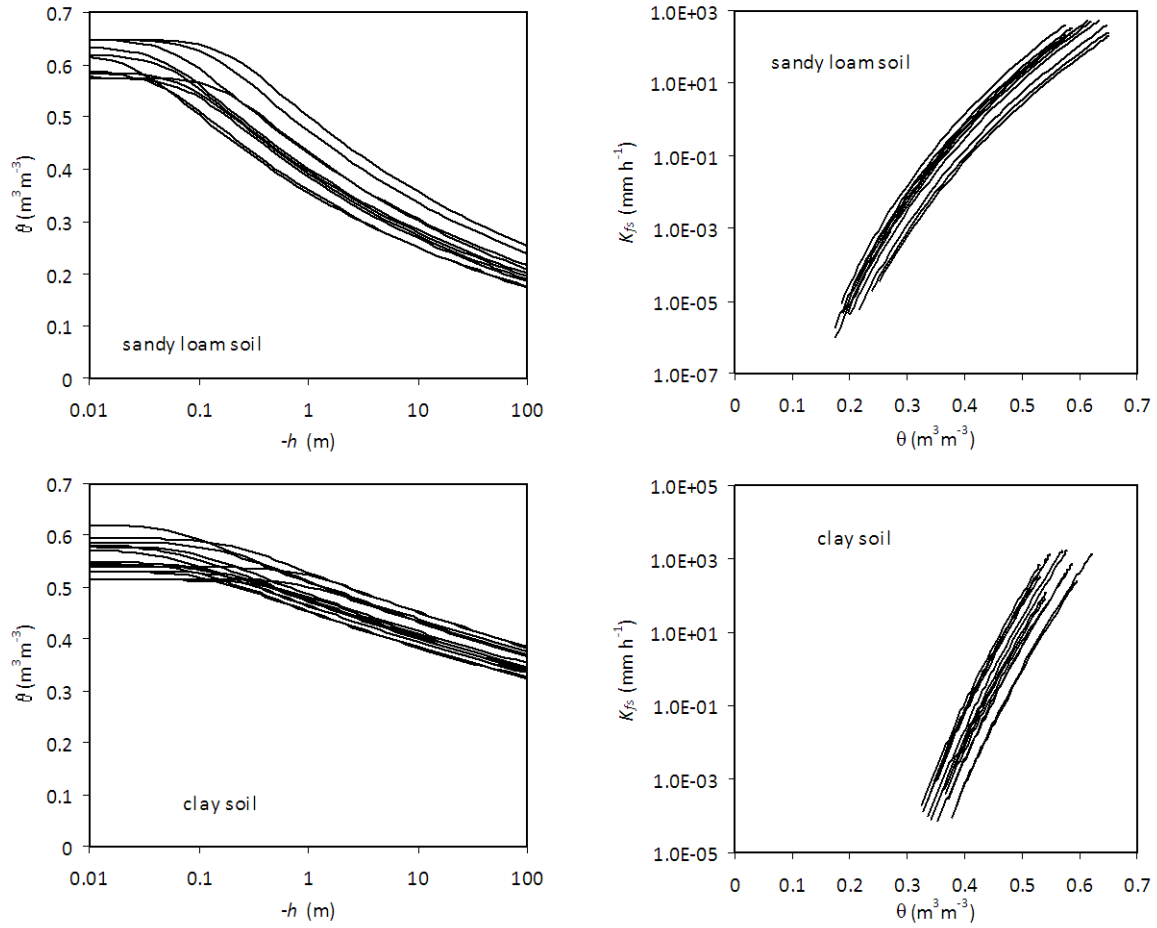

Fig. 2 Water retention curves and hydraulic conductivity functions for the subsoil of site 1 (a and b) and site 2 (c and d).

In site 1, the ratio of the steady state flow rate though the crust to the field saturated hydarulic conductivity of the subsoil, q_c/K_{fs}, was greater than one in 10 out of 11 experiments (mean value, q_c/K_{fs} = 1.56) and also for the only experiment in which $q_c < K_{fs}$, the ratio q_c/K_{fs} was very close to one (q_c/K_{fs} = 0.93). It was concluded that the visually observed surface crust was not hydraulically effective in reducing infiltration in this soil. Surface soil crust in

the sandy loam site was thinner (L_c = 2-3 mm) and less developed than in the clay soil. As can be seen in figure 3, it includes many sand particles that avoided excessive compaction of the surface layer. According to Valentin and Bresson (1992), in cultivated soils of loamy type slaking crusts develop as a result of aggregate breakdown probably induced by entrapped air compression when the soil is dry before rainfall. Such crusts are thin (1-3 mm), rather porous with a no clear textural separation between coarse and fine particles and the infiltration rate is relatively high (De Jong et al., 2011). Another factor that lead to the formation of a slaking crust in the sandy loam soil of site 1, could be the protective effect of the tree canopy that prevented the soil surface from the direct impact of the drops. Therefore, the main mechanism for disaggregation was the wetting of the dry aggregate rather than the kinetic energy of the rainfall.

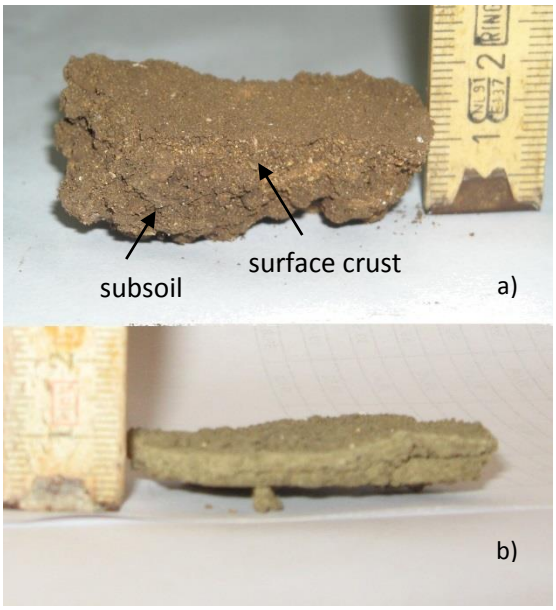

Fig. 3 Slaking structural crust on the sandy loam soil of site 1 (a) and coalescing crust on the clay soil of site 2 (b).

In the clay soil, the condition $q_c/K_{fs} < 1$ was observed in 10 experiments out of 15 experiments denoting an increased hydraulic resistance of the surface crust. With the exclusion of one experiment that yielded a value of q_c/K_{fs} = 9.1, mainly as a consequence of an extremely low value on the subsoil field saturated hydraulic conductivity (K_{fs} = 14 mm h^{-1}), the q_c/K_{fs} values ranged from 0.09 to 1.59 with a mean value of 0.49 (CV = 108%). Therefore, the formation of a surface crust acted as a barrier to water infiltration in the clay soil. The crust in clay soil was thicker (L_c = 5-7 mm) and probably more compact than in the sandy loam soil (Figure 3). Physical characterization of the soil crust should be carried out in additional testing of the proposed field method. However, visual inspection of the removed crust showed a distinct structural separation between the compacted surface layer and underlying undisturbed subsoil that, according to Valentin and Bresson (1992), typical occurs in the coalescing crust. Such crusts results mainly from gradual compaction due to aggregate coalescence by deformation under plastic conditions. This crusting process is observed in wet soils under heavy rainfall intensity.

For the experiments in which $q_c/K_{fs} < 1$ (N = 10), the pressure head at the soil-crust interface, h_s, varied between –263 and –77 mm with a mean value of –180 mm (CV = 35.5%) (Table 2). Considering that water is supplied at the surface of the crust with a pressure head

close to zero ($h_0 \approx -5$ mm) this result shows what marked reduction of the water pressure head occurs in the first mm of the profile due to the hydraulic resistance of the crust. If the thickness of the crust is neglected, the hydraulic resistance calculated from eq. (5) ranged from 0.39 to 2.24 h with a mean value of 1.31 h (78 min). The corresponding mean value of the hydraulic conductivity of the crust was 5.8 mm h^{-1}. Considering the thickness of the crust (eq. 6) the mean value of the crust hydraulic resistance was 1.35 h (81 min), with a mean value of the hydraulic conductivity of 5.5 mm h^{-1}. Therefore, calculation of the hydraulic parameters of the crust were not appreciably affected by L_c. A practical implication of this result is that measuring the crust thickness is not strictly necessary to calculate its conductivity and hydraulic resistance.

B.2.4. Conclusions

Soil surface crusting may severely affect agricultural soils as it significantly reduces infiltration, hampers germination of seeds and reduces root aeration and water availability. Knowledge of the hydrodinamic properties of the surface soil crust is important to predict and mitigate its negative effects. A simplified method to determine the hydraulic resistance of the surface crust is presented that is based on the approach by Hillel and Gardner (1969). It requires the knowledge of the steady state infiltration rate in the crusted soil and the hydraulic properties of the soil underlying the crust and combines two in situ infiltrometric experiments. A mini-disk tension infiltrometer is first conducted at the soil surface to measure the steady-state infiltration rate. Then, the surface crust is removed, its thickness is measured, and a ponded infiltration test is performed at the same site to determine the hydraulic properties of the underlying soil by the Beerkan Estimation of Soil Transfer parameters (BEST) procedure.

The method was tested in a sandy loam and a clay soil after a prolonged rainfall period that allowed the formation a surface crust. In the sandy loam soil, a 2-3 mm thick slaking crust was visually observed, but ratio of the steady state flow rate to the field saturated hydarulic conductivity of the subsoil, q_c/K_{fs}, was greater than one in 10 out of 11 experiments thus detecting no increase of the surface hydraulic resistance. In the clay soil, a 5-7 mm thick crust was formed that was attributed to gradual coalescence of the plastic, wet aggregates by rainfall compaction. In this soil, the condition $q_c/K_{fs} < 1$ was observed in 10 out of 15 experiments denoting an increased hydraulic resistance of the surface crust. The hydraulic resistance was not appreciably affected by the crust thickness. The mean value of the crust hydraulic resistance was 1.31-1.35 h (78-81 min), with a mean value of the hydraulic

conductivity of 5.5-5.8 mm h^{-1}. The developed method is particularly simple and appears to be suitable to discriminate between different levels of the hydraulic resistance of the surface crust. However, further investigations involving different soil and crust types is necessary in order to confirm its reliability.

Acknowledgements: the Authors would like to thank Giuseppe Nicolosi for his help in the experimental work.

Contributions: theory was developed by V. Bagarello and M. Iovino. All authors analyzed the data and contributed to write the manuscript.

Funding: the study was supported by grants of the Sicilian Region (Progetto Tristezza).

References

Assouline S. 2004. Rainfall-induced soil surface sealing: a critical review of observations, conceptual models, and solutions. Vadose Zone Journal, 3:570-591.

Bagarello V., Di Stefano C., Ferro V., Iovino M., Sgroi A., 2010. Physical and hydraulic characterization of a clay soil at the plot scale. Journal of Hydrology, 387: 54-64.

Bagarello V, D'Asaro F, Iovino M. 2012. A field assessment of the Simplified Falling Head technique to measure the saturated soil hydraulic conductivity. Geoderma 187-188: 49-58.

Bresson L.-M., Boiffin J. 1990. Morphological characterization of soil crust development stages on an experimental field. Geoderma, 47:301-325.

Brooks R.H., Corey C.T. 1964. Hydraulic properties of porous media. Hydrol. Paper 3, Colorado State University, Fort Collins.

Burdine N.T. 1953. Relative permeability calculation from pore size distribution data. Petr. Trans. Am. Inst. Min. Metall. Eng., 198:71-77.

De Jong S.M., Addink E.A., van Beek L.P.H., Duijsings D. 2011. Physical characterization, spectral rensponse and remotely sensed mapping of Mediterranean soil surface crusts. Catena, 86:24-35.

Dohnal, M., Dusek, J., Vogel, T., 2010. Improving hydraulic conductivity estimates from minidisk infiltrometer measurements for soils with wide pore-size distributions. Soil Sci. Soc. Am. J. 74(3), 804-811.

Gee G.W., Bauder J.W. 1986. Particle-size analysis. In Methods of soil analysis. Part 1, Klute A (ed), 2nd ed, ASA and SSSA, Madison, WI, USA, 383-411.

Haverkamp R., Debionne S., Vialet P., Angulo-Jaramillo R., de Condappa D. 2006. Soil properties and moisture movement in the unsaturated zone. In J.W. Delleur (ed.), The handbook of groundwater engineering, CRC, Boca Raton, FL.

Haverkamp R. Ross P.J., Smettem K.R.J., Parlange J.Y. 1994. Three-dimensional analysis of infiltration from the disc infiltrometer. 2. Physically based infiltration equation. Water Resources Research, 30:2931-2935.

Hillel D., Gardner W.R. 1969. Steady infiltration into crust-topped profiles. Soil Science, 180(2):137-142.

Lassabatère L., Angulo-Jaramillo R., Goutaland D., Letellier L., Gaudet J.P., Winiarski T., Delolme C. 2010.. Effect of settlement of sediments on water infiltration in two urban infiltration basins. Geoderma, 156:316-325.

Lassabatère, L., Angulo-Jaramillo, R., Soria Ugalde, J.M., Cuenca, R., Braud, I., Haverkamp, R., 2006. Beerkan estimation of soil transfer parameters through infiltration experiments – BEST. Soil Science Society of America Journal 70, 521-532.

Li X.-Y., González A., Solé-Benet A. 2005. Laboratory methods for the estimation of infiltration rate of soil crusts in the Tabernas Desert badlands. Catena, 60:255-266.

Lichner L., Hallett P.D., Feeney D.S., Ďugová O. Šír M., Tesař M. 1997. Field measurement of soil water repellency and its impact on water flow under different vegetation. Biologia, 62(5):537-541.

Madsen M.D., Chandler D.G. 2007. Automation and use of Mini Disk Infiltrometer. Soil Science Society of America Journal, 71:1469-1472.

Minasny B., McBratney A.B. 2007. Estimating the water retention shape parameter from sand and clay content. Soil Science Society of America Journal, 71:1105-1110.

Reynolds W.D. 2006: Tension infiltrometer measurements: implication of pressure head offset due to contact sand. Vadose Zone Journal, 5:1287-1292.

Šimůnek J., Angulo-Jaramillo R., Schaap M.G., Vandervaere J.P., van Genuchten M.T. 1998. Using an inverse method to estimate the hydraulic properties of crusted soils from tension disc infiltrometer data. Geoderma, 86:61-81.

Šimůnek J., van Genuchten M.Th. 1997. Estimating unsaturated soil hydraulic proper-ties from multiple tension disc infiltrometer data. Soil Science, 162(6):383-398.

Touma J., Raclot D., Al-Ali Y., Zante P., Hamrouni H., Dridi B. 2011. In situ determination of the soil surface crust resistance. Journal of Hydrology, 403:253-260.

Valentin C., Bresson L.-M. 1992. Morphology, genesis and classification of surface crusts in loamy and sandy soils. Geoderma, 55:225-245.

van Genuchten M.Th. 1980. A closed form equation for predicting the hydraulic conductivity of unsaturated soils. Soil Science Society of America Journal, 44:892-898.

Vandervaere J.P., Peugeot C., Vauclin M., Angulo-Jaramillo R., Lebel T. 1997. Estimating hydraulic conductivity of crusted soils using disc infiltrometers and minitensiometers. Journal of Hydrology, 188-189:209-223.

B.3. Estimating hydraulic conductivity of a sealed loamy soil from beerkan experiments in a Mediterranean vineyard*

V. Alagna[1], V. Bagarello[1], A. Cerdà[2,3], S. Di Prima[4]*, F. Guaitoli[5], M. Iovino[1], S. Keesstra[3]

[1] Department of Agricultural and Forest Sciences, University of Palermo, Viale delle Scienze, 90128 Palermo, Italy

[2] Department of Geography, University of Valencia, Blasco Ibáñez, 28, 46010 València, Spain

[3] Soil Physics and Land Management Group, Wageningen University, Droevendaalsesteeg 4, 6708PB Wageningen, The Netherlands.

[4] Agricultural Department, University of Sassari, Viale Italia, 39, 07100 Sassari, Italy

[5] Assessorato regionale dell'Agricoltura, dello Sviluppo Rurale e della Pesca Mediterranea, UO S5.05, Viale Regione Siciliana 2771, 90145 Palermo Italy

* Corresponding Author. E-mail: sdiprima@uniss.it

Abstract

In bare soils of semi-arid areas, surface sealing is a rather common phenomenon due to the beating action of rainfall. Water infiltration measurements under ponding conditions constitute a common way for an approximate characterization of sealed soils. In this study, the impact of sealing on soil hydraulic conductivity was checked in a Mediterranean vineyard (western Sicily, Italy) under conventional tillage. The BEST (Beerkan Estimation of Soil Transfer parameters) algorithm was applied to the infiltration data to obtain the hydraulic conductivity of sealed and unsealed soils. Soil hydraulic conductivity was found to vary during the year and also spatially (i.e., rows vs. inter-rows) due to sealing, tillage and vegetation cover. A 55 mm rainfall depth determined a decrease of the saturated soil hydraulic conductivity, K_s, by a factor close to two in the inter-row areas, due to the formation of a sealed layer at the surface. The same rainfall was practically ineffective in the row areas (i.e., K_s varied by only 1.1 times) since the vegetation cover intercepted raindrops which prevented surface soil. Thus, the comparison between the K_s values obtained along the rows and in the inter-rows was found to yield a valuable information on the effect of sealing with reference to a particular sampling date. Finally, the ability of the beerkan infiltration test to detect the effect of the seal on flow and BEST estimates of the soil hydraulic parameters was demonstrated.

Keywords: Hydraulic conductivity, Water infiltration measurements, Sealing, Vineyard

* This is a pre-refereeing draft submitted to Soil in 2016.

B.3.1. Introduction

Collision of raindrops on a bare soil surface can result in physical and chemical changes of the exposed soils. The mechanical alteration of the upper soil aggregates, expressed in terms of compaction, splash, and particle detachment, contribute to form a surface crust (Assouline, 2004). This type of crust, named structural, differs from the depositional crust (West *et al.*, 1992), which is formed by deposition of detached, fine particles carried out in suspension by runoff (Fox and Le Bissonnais, 1998). The hydraulic properties of the crusts vary significantly (Fox *et al.*, 1998a, 1998b). Different physical rainfall properties may be related with structural crust development, such as intensity (Morin and Benyamini, 1977; Baumhardt *et al.*, 1990; Freebairn *et al.*, 1991), kinetic energy (Eigel and Moore, 1983; Mohammed and Kohl, 1987) and momentum (Rose, 1960; Brodie and Rosewell, 2007). The initial or wetting phase in crust formation is defined as surface sealing (Römkens, 1979). During the drying cycle, this layer consolidates and may differ from the wetting phase in its mechanical and hydraulic properties (Mualem *et al.*, 1990). This drying phase is kwon as crusting (Römkens, 1979).

The hydrodynamic properties of such a layered system (seal layer, underlying soil), may deeply affect the partition between infiltration and runoff at the soil surface, especially in arid and semi-arid areas where crusting is a rather common phenomenon (Angulo-Jaramillo *et al.*, 2016). Water infiltration measurements constitute a common way for an indirect characterization of sealed/crusted soils (Bedaiwy, 2008; Alagna *et al.*, 2013). The Beerkan Estimation of Soil Transfer (BEST) parameters procedure by Lassabatere et al. (2006) is very attractive for practical use since it allows an estimation of both the soil water retention and the hydraulic conductivity functions. The BEST method considers certain analytical formulae for the hydraulic characteristic curves and estimates their shape parameters, which are texture dependent, from particle-size analysis by physical-empirical pedotransfer functions. Structure dependent scale parameters are estimated by a beerkan experiment (Haverkamp *et al.*, 1996), i.e. a three-dimensional (3D) field infiltration experiment at ideally zero pressure head. BEST substantially facilitates the hydraulic characterization of unsaturated soils, and it is gaining popularity in soil science (Gonzalez-Sosa *et al.*, 2010; Mubarak *et al.*, 2010; Bagarello *et al.*, 2014b; Di Prima, 2015; Castellini *et al.*, 2016; Di Prima *et al.*, 2016b). Alternative data analysis (Yilmaz *et al.*, 2010; Bagarello *et al.*, 2014c) and field (Bagarello *et al.*, 2014a; Alagna *et al.*, 2016; Di Prima *et al.*, 2016a) procedures based on BEST method were developed. The ability of the BEST method to distinguish between crusted and non-crusted soils was demonstrated by Souza *et al*. (2014). Moreover, Di Prima et al. (2016a) successfully

applied a beerkan derived procedure to explain surface runoff and sealing generation phenomena occurring during intense rainfall events. These authors concluded that if any seal forms at the surface, beerkan infiltration test should detect its impact on flow and BEST estimates should essentially be expressive of the hydraulic properties of the surface layer. In fact, the BEST method is dedicated to non-layered soils that should also be uniform and with a uniform soil water content at the beginning of the infiltration run (Lassabatere *et al.*, 2006, 2009) and contain no macropore network (Lassabatere *et al.*, 2014). However, completely homogeneous soils probably do not exist in natural environments (Reynolds and Elrick, 2002). Therefore, the hydraulic conductivity obtained by an infiltrometer method, such as BEST, should probably be considered as an equivalent conductivity, i.e. the conductivity of a rigid, homogeneous and isotropic porous medium characterized by infiltration rates that are those actually measured on the real soil (Bagarello *et al.*, 2010). For the case of stratified media, the layer with the lowest hydraulic conductivity may control flow and consequently cumulative infiltration at the surface (Alagna *et al.*, 2013). Therefore, water infiltration data can be regarded as more representative of the hydraulic behavior of the less permeable layer, and BEST parameters can be assigned to the less permeable layer. Such approach was proposed by Lassabatere *et al*. (2010) for a stratified medium with a low permeability sedimentary layer at the surface, by Yilmaz et al. (2010, 2013), for the characterization of crusted reactive materials, and, recently, by Coutinho *et al.* (2016) for a permeable pavement for stormwater management in an urban area.

The main objective of the paper was to carry out a hydraulic characterization of a loamy soil in a vineyard under conventional tillage located at Marsala (western Sicily, Italy). In particular, the specific objectives were to: i) check the ability of the BEST method to yield estimates of soil saturated hydraulic conductivity on sealed and non-sealed soils; and ii) establish changes on soil hydraulic conductivity due to soil sealing.

B.3.2. Material and methods

Study site

The experimental site is located close to Marsala (western Sicily, Italy), in the homeland of Sicilian viticulture, at the coordinates 37°48'5.10" N and 12°30'44.79" E. Elevation is 111 m a.s.l. and soil surface is flat. The soil is a typic Rhodoxeralf with a depth of 1 m and a small amount of gravel. According to USDA classification, the soil texture, determined on two replicated soil samples, is loam (Table 1). A weather station is located 5 km away from the

sampling site, at the coordinates 37°79'35.64"N and 12°56'81.59"E. It is positioned at the same elevation of the sampling site and it is part of a network of stations managed by Servizio Informativo Agrometeorologico Siciliano –SIAS.

Table 1 Clay (%), silt (%) and sand (%) content (USDA classification system), soil textural classification, dry soil bulk density, ρ_b (g cm^{-3}), and saturated soil water content, θ_s (cm^3cm^{-3}), of the sampled vineyard soil. Coefficient of variation (%) in brackets.

Variable	Site characteristic
clay	19.7
silt	49.6
sand	30.7
Textural classification	loam
ρ_b	1.128 (5.1)
θ_s	0.575 (3.8)

At the sampling site, the common soil management for the vineyards of Marsala was applied during the two years of sampling (2015 and 2016) (Figure 1). The soil is shallow-harrowed to a depth of 0.10-0.15 m in October, after the first autumn rainfalls. Faba bean (*Vicia faba* L. var. *minor*) is sown in November between the rows. In March, the legume biomass is cut and immediately incorporated into the soil with a rotary tiller to a depth of 0.20 m. Finally, a new rotary tillage is performed in May and, only for the second year, it was also performed in June. This soil management practice is applied between the rows. Along the rows, a mechanical topper is used at each soil tillage date to a depth of 0.10 m.

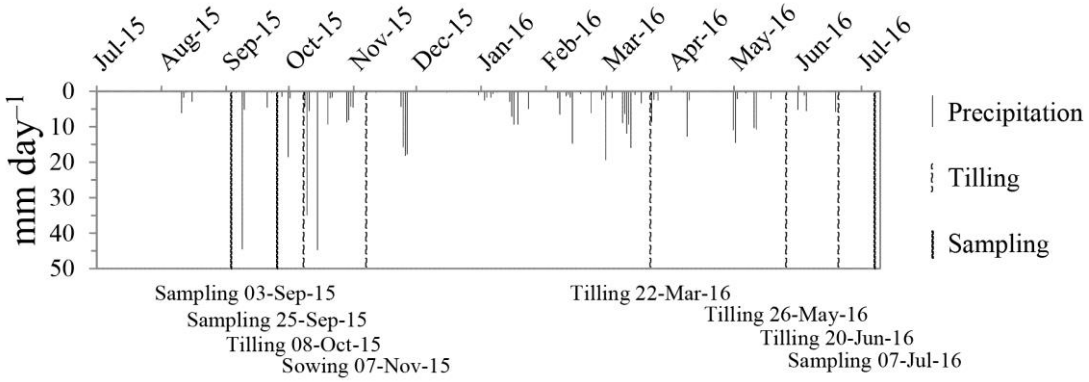

Fig. 1 Precipitation and soil management program during the study period. The sapling dates are reported.

Soil sampling

An area of approximately 150 m^2 was sampled on three different sampling campaigns covering two growing seasons. The first two campaigns were carried out at the beginning and the end of September 2015, respectively, and the third campaign was performed at the beginning of July 2016. Between the first two sampling campaigns, soil was not tilled and a total rainfall of 55 mm occurred (Figure 1), which is approximately 10% of the average annual precipitation for the area. In particular, a 29-mm event occurred during the morning of

9 September, with a maximum recorded intensity of 25 mm h^{-1}. During the same day, total precipitation was of 44.6 mm. This rainfall led to the development of a weak but clearly detectable surface seal (Figure 2). This phenomenon was only observed between the rows and not along the rows, probably due to the protective effects of plant cover. The second sampling was performed one week after the last rainfall. Finally, a third sampling campaign was carried out during the following dry season in order to sample the soil after the ordinary tillage practices and with moisture conditions comparable to the first sampling date.

On each sampling date, a total of 10 undisturbed soil cores (5 cm in height by 5 cm in diameter) were collected at the soil surface close to the points where the infiltration tests were performed, 5 along the rows and 5 between the rows. These cores were used to determine the dry soil bulk density, ρ_b (g cm^{-3}), and the soil water content at the time of the experiment, θ_i (cm^3 cm^{-3}). The soil porosity was calculated from the ρ_b data, assuming a soil particle density of 2.65 g cm^{-3}. A disturbed soil sample (0–10-cm depth), collected both along and between the rows, was used to determine the particle size distribution (PSD), using conventional methods (Gee and Bauder, 1986). Fine size fractions were determined by the hydrometer method, whereas the coarse fractions were obtained by mechanical dry sieving. The clay, silt and sand percentages were determined from the measured PSD according to the USDA standards.

Fig. 2 Surface seal layer developed after the intense storms fallen in September 2015.

Beerkan experiments

For each sampling date, an area of approximately 100 m^2 was chosen and 14 beerkan infiltration runs (Lassabatere *et al.*, 2006) were carried out using a 15 cm inner-diameter ring. Seven runs were carried out along the rows and seven on the bare inter-rows area (Figure 3). The steel ring was positioned between two vine stocks along the row and in the same orthogonal direction between the rows. The ring was inserted to a depth of about 0.01 m into the soil surface to avoid lateral loss of the ponded water. On sealed soil, to avoid crack and soil disturbance during the ring insertion, the soil outside the hedge of the ring was moistened with 5 cm^3 of water by means of a syringe before insertion. After ten minutes the ring was

carefully inserted applying a slight pressure and rotation. These expedients ensured a reasonable accuracy in site preparation and they were essential to prevent the crust surface perturbation.

According to the guidelines by Lassabatère et al. (2006), for each run a known volume of water (150 mL) was poured in the cylinder at the start of the experiment and the elapsed time during its infiltration was measured. When the amount of water had completely infiltrated, another identical volume of water was poured on the confined infiltration surface and the time needed for the complete infiltration was logged. The procedure was repeated 15 times for each run by applying water at a small distance (3 cm of height) from the infiltration surface. As is commonly suggested in practical application of a ponding infiltration method, the energy of the water due to the application was dissipated on the fingers of a hand in order to minimize soil disturbance (Reynolds, 2008).

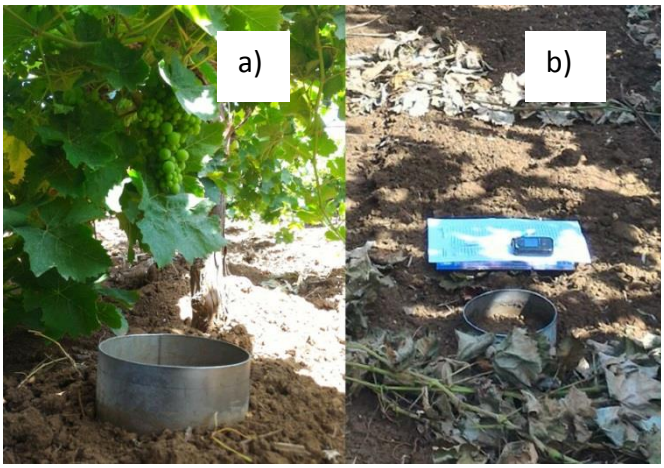

Fig. 3 Beerkan infiltration runs carried out (a) along the rows and (b) on the bare inter-rows area.

Di Prima *et al.* (2016b) showed that all BEST derived methods, i.e. BEST-slope, BEST-intercept and BEST-steady, led to similar results in most cases. However, BEST-slope appeared to yield more accurate estimates, especially of the saturated soil hydraulic conductivity, K_s (mm h^{-1}), but it was affected by a failure rate higher than others algorithms (Bagarello *et al.*, 2014c). In this study, such a problem did not occur and, therefore, the BEST-slope algorithm (Lassabatere *et al.*, 2006) was considered to estimate the whole set of parameters of the hydraulic conductivity function. BEST focuses specifically on the Brook and Corey (1964) relationship:

$$\frac{K(\theta)}{K_s} = \left(\frac{\theta - \theta_r}{\theta_s - \theta_r} \right)^{\eta} \quad (1)$$

where K (L T^{-1}) is the soil hydraulic conductivity, θ (L^3L^{-3}) is the volumetric soil water content, θ_r (L^3L^{-3}) is the residual volumetric soil water content, θ_s (L^3L^{-3}) is the saturated volumetric soil water content, and η is a shape parameter linked to the soil textural properties. In BEST, η is estimated from the analysis of the PSD with the pedotransfer function included in the procedure, whereas θ_s, θ_r and K_s are scale parameters. BEST considers θ_r to be zero,

and θ_s was assumed to coincide with soil porosity in this investigation, as suggested by many authors (Xu *et al.*, 2009; Mubarak *et al.*, 2010; Bagarello *et al.*, 2011; Di Prima, 2015; Di Prima *et al.*, 2016a). In particular, Di Prima *et al.* (2016a) demonstrated that the assumed coincidence between saturated soil water content and porosity did not practically affect the K_s estimation.

BEST-slope estimates sorptivity, S (mm $h^{-0.5}$), by fitting the experimental cumulative infiltration data on the explicit transient two-term equation by Haverkamp *et al.* (1994):

$$I(t) = S\sqrt{t} + \left[A(1-B)S^2 + B\, i_s\right] t \quad (2)$$

where I (mm) is 3D cumulative infiltration and t (h) is the time. Then, K_s (mm h^{-1})is estimated as a function of S as follow:

$$K_s = i_s - AS^2 \quad (3)$$

where i_s (mm h^{-1}) is the experimental steady-state infiltration rate, which is estimated by linear regression analysis of the last data points describing steady-state conditions on the I vs. t plot and corresponds to the slope of the regression line. The constants A (mm^{-1}) and B can be defined for the specific case of a Brooks and Corey relation (Eq. 1) and taking into account initial soil water content, θ_i (L^3L^{-3}), as (Haverkamp *et al.*, 1994):

$$A = \frac{\gamma}{r(\theta_s - \theta_i)} \quad (4a)$$

$$B = \frac{2-\beta}{3}\left[1 - \left(\frac{\theta_i}{\theta_s}\right)^{\eta}\right] + \left(\frac{\theta_i}{\theta_s}\right)^{\eta} \quad (4b)$$

where γ (parameter for geometrical correction of the infiltration front shape) and β are coefficients that are commonly set at 0.75 and 0.6 for $\theta_i < 0.25\ \theta_s$, and r (mm) is the radius of the source.

Data analysis

Data sets were summarized by calculating the mean, M, and the associated coefficient of variation, CV. In particular, *cl*, *si*, *sa*, ρ_b, θ_s values were considered site specific and therefore they were determined only in duplicate (*cl*, *si*, *sa*, N = 2), or considering their low variability (ρ_b, θ_s), the arithmetic mean and the associated CV were calculated (Table 1). Temporal variability of θ_i was determined on the basis of ten replicate samples on each sampling date (Table 2). The K_s data were assumed to be log-normally distributed since the statistical distribution of these data is generally log-normal (Lee *et al.*, 1985; Warrick, 1998). The geometric mean and the associated CV were therefore calculated to summarize K_s values

using the appropriate ‘‘log-normal equations” (Lee *et al.*, 1985). Statistical comparison between two sets of data was conducted using two-tailed t-tests, whereas the Tukey Honestly Significant Difference test was applied to compare three sets of data. The ln-transformed K_s data were used in the statistical comparison. A probability level, P = 0.05, was used for all statistical analyses.

Table 2 Sample size (N), minimum (Min), maximum (Max), mean, and coefficient of variation (CV, in %) of the soil water content at the time of sampling, θ_i (cm^3cm^{-3}), values for different sampling dates.

Statistic	Sept 3, 2015	Sept 25, 2015	Jul 7, 2016
N	10	10	10
Min	0.051	0.093	0.047
Max	0.073	0.133	0.087
Mean	0.064 A	0.114 B	0.067 A
CV	12.0	10.9	18.1

The values in a row followed by the same upper case letter were not significantly different according to the Tukey Honestly Significant Difference test (P = 0.05).

B.3.3. Results and discussion

All the 42 infiltrations runs were analyzable with the BEST-slope algorithm, yielding positive K_S values. In addition, the fitting of the infiltration model to the transient phase of the infiltration run always yielded relative errors lower than 5.5% (Lassabatere *et al.*, 2006), denoting an acceptable error for transient cumulative infiltration (Figure 4).

For the first and the third campaign, the beerkan runs carried out between the rows yielded comparable and statistically similar (Table 3) K_s values (Figure 5). In both cases, the average K_s values were approximately 20 times higher than the expected saturated conductivity on the basis of the soil textural characteristics alone (e.g., K_s = 10.4 mm h^{-1} for a loam soil according to Carsel and Parrish, 1988). This circumstance suggested that soil macroporosity generated by soil tillage in the ploughed horizon likely influenced measurement of K_s (Josa *et al.*, 2010; Alagna *et al.*, 2016; Di Prima *et al.*, 2016a). In these conditions, the soil structure is expected to be particularly fragile, especially with reference to macroporosity, and hence unstable (Jarvis *et al.*, 2008), which implies that

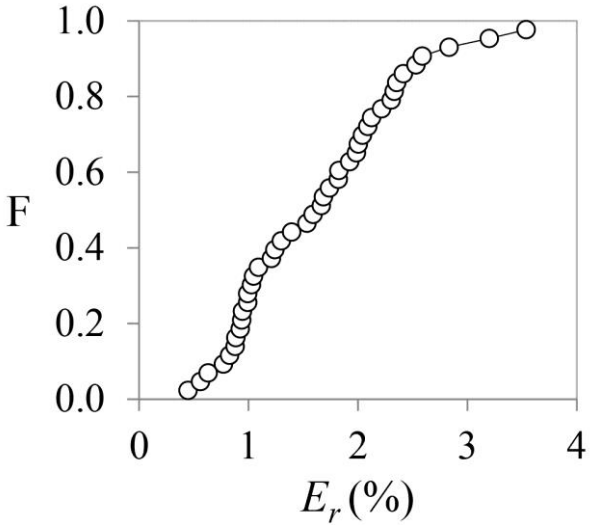

Fig. 4 Cumulative frequency distribution of the relative errors, E_r (%), of the fitting of the infiltration model to the transient phase of the infiltration runs.

clogging of the largest pores at the soil surface, as a consequence of the aggregates breakdown occurring during a rainstorm, can easily mitigate tillage effects on soil hydraulic properties (Ciollaro and Lamaddalena, 1998). The presence of the seal layer during the second field campaign clearly affected water infiltration between the rows. In particular, the presence of this layer implied that K_s was 1.5-1.8 times lower than that measured in the absence of the sealed layer (Figure 5). Sealing at the soil surface determined an increased hydraulic resistance to water penetration into soil (Alagna *et al.*, 2013) since differences between the K_s datasets (second against first and third sampling campaigns) were statistically significant. Sealing also resulted in a decrease of the minimum K_s measurable values, while the maximum values remained unchanged (Table 3). The tillage practices carried out in the spring 2016 removed any existing soil crust and thereby increased soil infiltration properties (Figure 5) (Zhai *et al.*, 1990; Xu and Mermoud, 2001; Ndiaye *et al.*, 2005; Chahinian *et al.*, 2006; Strudley *et al.*, 2008; Pare *et al.*, 2011), suggesting a cycling occurrence of crusting phenomena within the year.

Table 3 Sample size (N), minimum(Min), maximum(Max),mean, and coefficient of variation (CV, in %) of the saturated soil hydraulic conductivity, K_s (mm h^{-1}), values obtained from BEST experiments carried out along and within the rows on different sampling dates.

Variable	Rows/Inter-rows	Statistic	Sept 3, 2015	Sept 25, 2015	Jul 7, 2016
K_s	Rows	N	7	7	7
		Min	188.1	159.1	158.4
		Max	289.1	369.1	234.2
		Mean	223.6 a A	212.4 a A	199.2 a A
		CV	15.4	27.6	14.1
	Inter-rows	N	7	7	7
		Min	193.0	97.0	160.6
		Max	261.8	251.3	272.3
		Mean	229.5 a A	129.3 b B	192.5 a A
		CV	10.3	31.7	20.2

The values in a column followed by a different lower case letter were significantly different according to a two tailed t test (P = 0.05). The values in a row followed by the same upper case letter were not significantly different according to the Tukey Honestly Significant Difference test (P = 0.05). The values followed by a different upper case letter were significantly different.

Many studies in the literature have reported similar temporal dynamics within the year, even in vineyards. In fact, infiltration experiments constitute an indirect measurement closely associated with sealing or crusting (Römkens *et al.*, 1990), and the saturated hydraulic conductivity may vary considerably within the year if these phenomena occur. In particular, rainfall and wetting–drying cycles favor soil reconsolidation and soil-surface sealing or

crusting, whereas tillage removes existing layering (Pare *et al.*, 2011). For instance, Biddoccu *et al.* (2017) studied temporal variability of soil hydraulic properties in a vineyard on a silt loam soil. These authors reported hydraulic conductivity values measured during the summer four times lower than those measured during the wet season, due to the presence of a structural crust resulting from rainfall events following the late spring tillage. Bradford *et al.* (1987) reported for 20 soils (varying in texture from sand to clay) a reduction in infiltration rate after a 60 min of simulated rainfall (intensity of 63 mm h^{-1}), due to the effect of surface sealing on infiltration. Bagarello *et al*. (2014a), Alagna *et al*. (2016) and Di Prima *et al*. (2016a) applied on five soils having different texture a beerkan derived procedure to explain surface runoff and disturbance phenomena at the soil surface occurring during intense rainfall events. These authors reported saturated hydraulic conductivity values of the disturbed soil from nine to 33 times lower than the undisturbed soils. In particular, Di Prima *et al.* (2016a) applied this methodology in a vineyard with a sandy-loam texture. These authors compared this simple methodology with rainfall simulation experiments establishing a physical link between the two methodologies through the kinetic energy of the rainfall and the gravitational potential energy of the water used for the beerkan runs. They also indirectly demonstrated the occurrence of a certain degree of compaction and mechanical breakdown using a mini disk infiltrometer (Decagon, 2014). With this device, they reported a reduction of the unsaturated hydraulic conductivity by 2.3 times, due to the seal formation. In another investigation carried out in Brazil with the BEST procedure, non-crusted soils were three times more conductive then the crusted soil (Souza *et al.*, 2014).

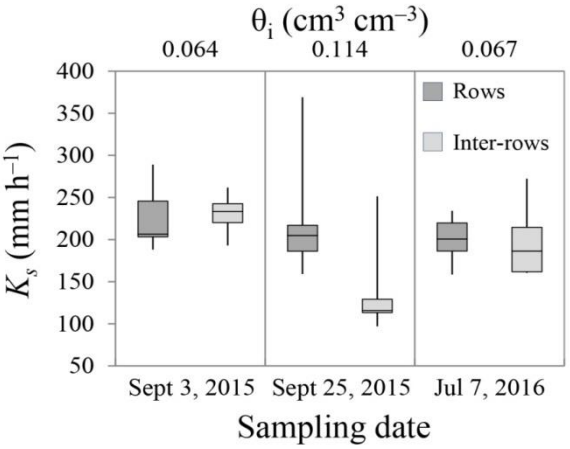

Fig. 5 Box plots of the saturated soil hydraulic conductivity, K_s (mm h^{-1}), values obtained from BEST experiments carried out along and between the rows on different sampling dates and for different initial soil water content, θ_i (cm^3cm^{-3}), values. On the box plots, boundaries indicates median, 25th and 75th quantiles, the top and bottom whiskers indicate the minimum and maximum values.

The results reported in this investigation suggested that our hypothesis about the ability of the beerkan infiltration test to detect the effect of the seal on flow and soil hydraulic characteristics estimated by BEST was reasonable. Indeed, the hydrodynamic properties of both the seal and the underlying soil play a key role during a rainstorm affecting the partition between infiltration and runoff (Vandervaere *et al.*, 1997; Assouline and Mualem, 2002, 2006). Hence, a transient method, as the beerkan one, appears appropriate to characterize

sealed soils. Recently, Di Prima et al. (2016b) showed that BEST-slope is less sensitive to the attainment of steady-state and allows to obtain accurate estimates of saturated soil hydraulic conductivity with less water and hence shorter experimental times than the other two BEST algorithms. For these reasons, BEST-slope appears suitable, among the alternative algorithms, to characterize a seal layer.

During the second field campaign, the seal layer only affected water infiltration between the rows (Table 3), suggesting that the protective role of vegetation along the rows was effective. The cover intercepted raindrop energy preventing surface sealing (Dunne *et al.*, 1991). The protective role along the vine-rows is well known, while in vine inter-rows the mulching practice is commonly applied to protect soil from raindrop impact (Celette *et al.*, 2008; Prosdocimi *et al.*, 2016). For the second campaign, the mean K_s value obtained between the rows was 1.6 times lower than the one obtained along the rows (Figure 5). In particular, this latter value, equal to 212.4 mm h^{-1}, did not significantly differ from those of the first and third sampling dates (Table 3). On the other hand, during these campaigns, beerkan runs carried out along and between the rows also yielded similar K_s values, due to the absence of a seal between the rows. This experimental information suggested that the sealing occurrence, the adopted soil management and the cover influenced both the temporal and the spatial variation of the soil hydrological characteristics at the field-scale.

The saturated conductivity of the seal layers can be two orders of magnitude or more lower than the conductivity of the underlying undisturbed soil (Torri *et al.*, 1999; Assouline and Mualem, 2002). In this investigation, 55 mm of rainfall determined development of a seal layer but not a substantial reduction of K_s. The applied methodology in this investigation seems suitable to explore in the future the functional dynamic of the seal layer under natural rainfall conditions. A perplexity on the possibility to collect reliable data on sealed soils by a ponding infiltration experiment is related to the need to insert the ring into the soil. The doubt is that ring insertion could determine fractures in the sealed layer and this fractures could directly connect the ponded depth of water during the run with the underlying, non-sealed, soil layer (Vandervaere *et al.*, 1997). In other terms, ring insertion could impede, in practice, measurement of fluxes though the sealed layer. In this investigation, fracture were not visually detected at the soil surface, perhaps because the soil was not very dry where the experiment on the sealed layer was performed (Table 2), the ring insertion depth was small (0.01 m), and insertion was carried out a few minutes after wetting the insertion circumference. Other ponding infiltration techniques, such as the single-ring pressure infiltrometer (Reynolds and Elrick, 1990) and, particularly, the simplified falling head technique (Bagarello *et al.*, 2004),

presuppose appreciably deeper insertions of the ring and, consequently, more risk to disrupt or alter the fragile seal layer at the soil surface during ring insertion. Therefore, the beerkan run seems a more appropriate ponding infiltration run to prevent, or minimize, substantial alteration of the surface to be sampled. Obviously, this conclusion needs additional testing but the premises are encouraging, also considering that beerkan runs were successfully conducted in other sealed soils (Souza *et al.*, 2014).

B.3.4. Conclusions

A loam soil was sampled in a Mediterranean vineyard located at Marsala (western Sicily, Italy), with beerkan infiltration experiments carried out along the rows direction and in the inter-rows within two consecutive growing seasons. Beerkan tests along with BEST-slope algorithm led to accurate estimates in both sealed and un-sealed conditions, allowing to assess the effect of the cycling occurrence of sealing due to rainfalls and wetting–drying cycles on the vineyard inter-rows.

A sampling strategy implying beerkan tests carried out along and between the vine-rows was successfully applied. This strategy allowed to assess the reduction in hydraulic conductivity with extemporaneous measurements alone. Its main advantage is that it allows a rapid assessment of sealing severity affecting water infiltration. At the sampled site, the impact of sealing on saturated soil hydraulic conductivity was moderate.

In conclusion, the hypothesis that the beerkan runs are suitable enough to detect the effect of the seal on flow and BEST estimates appeared reasonable. In the future, testing the proposed procedure in conjunction with others field methodologies for soil hydraulic characterization implying alteration at the soil surface, such as rainfall simulation experiments or the beerkan derived procedure discussed above, should contribute to a better understanding of sealing severity affecting water infiltration on bare soils.

Acknowledgements

This study was supported by grants from the Research Project CISV under grant n° 2014COMM-0363 CUP 872114000570002. A.V. carried out the experimental work. S.D.P. analyzed the results. All authors contributed to write the paper. S.D.P. also thanks I.A., E.B. and R.D.O.

References

Alagna V, Bagarello V, Di Prima S, Giordano G, Iovino M. 2013. A simple field method to measure the hydrodynamic properties of soil surface crust. *Journal of Agricultural Engineering* 44 (25): 74–79 DOI: 10.4081/jae.2013.(s1):e14

Alagna V, Bagarello V, Di Prima S, Giordano G, Iovino M. 2016. Testing infiltration run effects on the estimated water transmission properties of a sandy-loam soil. *Geoderma* 267: 24–33 DOI: 10.1016/j.geoderma.2015.12.029

Angulo-Jaramillo R, Bagarello V, Iovino M, Lassabatere L. 2016. Soils with Specific Features. In *Infiltration Measurements for Soil Hydraulic Characterization* Springer International Publishing; 289–354. Available at: http://link.springer.com/chapter/10.1007/978-3-319-31788-5_4

Assouline S. 2004. Rainfall-Induced Soil Surface Sealing. *Vadose Zone Journal* 3 (2): 570–591

Assouline S, Mualem Y. 2002. Infiltration during soil sealing: The effect of areal heterogeneity of soil hydraulic properties. *Water Resources Research* 38 (12): 1286 DOI: 10.1029/2001WR001168

Assouline S, Mualem Y. 2006. Runoff from heterogeneous small bare catchments during soil surface sealing: runoff from heterogeneous catchments. *Water Resources Research* 42 (12): n/a-n/a DOI: 10.1029/2005WR004592

Bagarello V, Castellini M, Di Prima S, Iovino M. 2014a. Soil hydraulic properties determined by infiltration experiments and different heights of water pouring. *Geoderma* 213: 492–501 DOI: 10.1016/j.geoderma.2013.08.032

Bagarello V, Di Prima S, Giordano G, Iovino M. 2014b. A test of the Beerkan Estimation of Soil Transfer parameters (BEST) procedure. *Geoderma* 221–222: 20–27 DOI: 10.1016/j.geoderma.2014.01.017

Bagarello V, Di Prima S, Iovino M. 2014c. Comparing Alternative Algorithms to Analyze the Beerkan Infiltration Experiment. *Soil Science Society of America Journal* 78 (3): 724 DOI: 10.2136/sssaj2013.06.0231

Bagarello V, Di Prima S, Iovino M, Provenzano G, Sgroi A. 2011. Testing different approaches to characterize Burundian soils by the BEST procedure. *Geoderma* 162 (1–2): 141–150 DOI: 10.1016/j.geoderma.2011.01.014

Bagarello V, Iovino M, Elrick D. 2004. A Simplified Falling-Head Technique for Rapid Determination of Field-Saturated Hydraulic Conductivity. *Soil Science Society of America Journal* 68 (1): 66 DOI: 10.2136/sssaj2004.6600

Bagarello V, Stefano CD, Ferro V, Iovino M, Sgroi A. 2010. Physical and hydraulic characterization of a clay soil at the plot scale. *Journal of Hydrology* 387 (1–2): 54–64 DOI: 10.1016/j.jhydrol.2010.03.029

Baumhardt RL, Römkens MJM, Whisler FD, Parlange J-Y. 1990. Modeling infiltration into a sealing soil. *Water Resources Research* 26 (10): 2497–2505 DOI: 10.1029/WR026i010p02497

Bedaiwy MNA. 2008. Mechanical and hydraulic resistance relations in crust-topped soils. *CATENA* 72 (2): 270–281 DOI: 10.1016/j.catena.2007.05.012

Biddoccu M, Ferraris S, Pitacco A, Cavallo E. 2017. Temporal variability of soil management effects on soil hydrological properties, runoff and erosion at the field scale in a hillslope vineyard, North-West Italy. *Soil and Tillage Research* 165: 46–58 DOI: 10.1016/j.still.2016.07.017

Bradford JM, Ferris JE, Remley PA. 1987. Interrill soil erosion processes: I. Effect of surface sealing on infiltration, runoff, and soil splash detachment. *Soil Science Society of America Journal* 51 (6): 1566–1571 Available at: https://dl.sciencesocieties.org/publications/sssaj/abstracts/51/6/SS0510061566 [Accessed 4 November 2015]

Brodie I, Rosewell C. 2007. Theoretical relationships between rainfall intensity and kinetic energy variants associated with stormwater particle washoff. *Journal of Hydrology* 340 (1–2): 40–47 DOI: 10.1016/j.jhydrol.2007.03.019

Brooks RH, Corey T. 1964. hydraulic properties of porous media. *Hydrol. Paper 3., Colorado State University, Fort Collins.*

Carsel RF, Parrish RS. 1988. Developing joint probability distributions of soil water retention characteristics. *Water Resources Research* 24 (5): 755–769 DOI: 10.1029/WR024i005p00755

Castellini M, Iovino M, Pirastru M, Niedda M, Bagarello V. 2016. Use of BEST Procedure to Assess Soil Physical Quality in the Baratz Lake Catchment (Sardinia, Italy). *Soil Science Society of America Journal* 0 (0): 0 DOI: 10.2136/sssaj2015.11.0389

Celette F, Gaudin R, Gary C. 2008. Spatial and temporal changes to the water regime of a Mediterranean vineyard due to the adoption of cover cropping. *European Journal of Agronomy* 29 (4): 153–162 DOI: 10.1016/j.eja.2008.04.007

Chahinian N, Moussa R, Andrieux P, Voltz M. 2006. Accounting for temporal variation in soil hydrological properties when simulating surface runoff on tilled plots. *Journal of Hydrology* 326 (1–4): 135–152 DOI: 10.1016/j.jhydrol.2005.10.038

Ciollaro G, Lamaddalena N. 1998. Effect of Tillage on the Hydraulic Properties of a Vertic Soil. *Journal of Agricultural Engineering Research* 71 (2): 147–155 DOI: 10.1006/jaer.1998.0312

Coutinho AP, Lassabatere L, Montenegro S, Antonino ACD, Angulo-Jaramillo R, Cabral JJSP. 2016. Hydraulic characterization and hydrological behavior of a pilot permeable pavement in an urban center, Brazil. *Hydrological Processes*: n/a-n/a DOI: 10.1002/hyp.10985

Decagon. 2014. Minidisk Infiltrometer User's Manual. *Decagon Devices, Inc., Pullman, USA*: 24

Di Prima S. 2015. Automated single ring infiltrometer with a low-cost microcontroller circuit. *Computers and Electronics in Agriculture* 118: 390–395 DOI: 10.1016/j.compag.2015.09.022

Di Prima S, Bagarello V, Angulo-Jaramillo R, Bautista I, Burguet M, Cerdà A, Iovino M, Lassabatère L, Prosdocimi M. 2016a. Comparing Beerkan infiltration tests with rainfall simulation experiments for hydraulic characterization of a sandy-loam soil. *Submitted to Hydrological Processes*

Di Prima S, Lassabatere L, Bagarello V, Iovino M, Angulo-Jaramillo R. 2016b. Testing a new automated single ring infiltrometer for Beerkan infiltration experiments. *Geoderma* 262: 20–34 DOI: 10.1016/j.geoderma.2015.08.006

Dunne T, Zhang W, Aubry BF. 1991. Effects of Rainfall, Vegetation, and Microtopography on Infiltration and Runoff. *Water Resources Research* 27 (9): 2271–2285 DOI: 10.1029/91WR01585

Eigel JD, Moore I. 1983. Effect of rainfall energy on infiltration into a bare soil

Fox DM, Le Bissonnais Y. 1998. Process-based analysis of aggregate stability effects on sealing, infiltration, and interrill erosion. *Soil Science Society of America Journal* 62 (3): 717–724 Available at: https://dl.sciencesocieties.org/publications/sssaj/abstracts/62/3/SS0620030717 [Accessed 9 November 2015]

Fox DM, Le Bissonnais Y, Bruand A. 1998a. The effect of ponding depth on infiltration in a crusted surface depression. *CATENA* 32 (2): 87–100 DOI: 10.1016/S0341-8162(98)00042-3

Fox DM, Le Bissonnais Y, Quétin P. 1998b. The implications of spatial variability in surface seal hydraulic resistance for infiltration in a mound and depression microtopography. *CATENA* 32 (2): 101–114 DOI: 10.1016/S0341-8162(98)00043-5

Freebairn DM, Gupta SC, Rawls WJ. 1991. Influence of Aggregate Size and Microrelief on Development of Surface Soil Crusts. *Soil Science Society of America Journal* 55 (1): 188 DOI: 10.2136/sssaj1991.03615995005500010033x

Gee GW, Bauder JW. 1986. Particle-size Analysis. In *SSSA Book Series*Soil Science Society of America, American Society of Agronomy; 383–411.

Gonzalez-Sosa E, Braud I, Dehotin J, Lassabatère L, Angulo-Jaramillo R, Lagouy M, Branger F, Jacqueminet C, Kermadi S, Michel K. 2010. Impact of land use on the hydraulic properties of the topsoil in a small French catchment. *Hydrological Processes* 24 (17): 2382–2399 DOI: 10.1002/hyp.7640

Haverkamp R, Arrúe J, Vandervaere J, Braud I, Boulet G, Laurent J, Taha A, Ross P, Angulo-Jaramillo R. 1996. Hydrological and thermal behaviour of the vadose zone in the area of Barrax and Tomelloso (Spain): Experimental study, analysis and modeling. *Project UE n. EV5C-CT* 92: 00–90

Haverkamp R, Ross PJ, Smettem KRJ, Parlange JY. 1994. Three-dimensional analysis of infiltration from the disc infiltrometer: 2. Physically based infiltration equation. *Water Resources Research* 30 (11): 2931–2935 DOI: 10.1029/94WR01788

Jarvis N, Etana A, Stagnitti F. 2008. Water repellency, near-saturated infiltration and preferential solute transport in a macroporous clay soil. *Geoderma* 143 (3–4): 223–230 DOI: 10.1016/j.geoderma.2007.11.015

Josa R, Ginovart M, Solé A, others. 2010. Effects of two tillage techniques on soil macroporosity in sub-humid environment. *Int. Agrophys* 24: 139–147

Lassabatere L, Angulo-Jaramillo R, Goutaland D, Letellier L, Gaudet JP, Winiarski T, Delolme C. 2010. Effect of the settlement of sediments on water infiltration in two urban infiltration basins. *Geoderma* 156 (3–4): 316–325 DOI: 10.1016/j.geoderma.2010.02.031

Lassabatere L, Angulo-Jaramillo R, Soria Ugalde JM, Cuenca R, Braud I, Haverkamp R. 2006. Beerkan Estimation of Soil Transfer Parameters through Infiltration Experiments—BEST. *Soil Science Society of America Journal* 70 (2): 521 DOI: 10.2136/sssaj2005.0026

Lassabatere L, Angulo-Jaramillo R, Soria-Ugalde JM, Šimůnek J, Haverkamp R. 2009. Numerical evaluation of a set of analytical infiltration equations: EVALUATION INFILTRATION. *Water Resources Research* 45 (12): n/a-n/a DOI: 10.1029/2009WR007941

Lassabatere L, Yilmaz D, Peyrard X, Peyneau PE, Lenoir T, Šimůnek J, Angulo-Jaramillo R. 2014. New Analytical Model for Cumulative Infiltration into Dual-Permeability Soils. *Vadose Zone Journal* 0 (0): 0 DOI: 10.2136/vzj2013.10.0181

Lee DM, ELRICK D, REYNOLDS W, Clothier BE. 1985. A comparison of three field methods for measuring saturated hydraulic conductivity. *Canadian journal of soil science* 65 (3): 563–573 Available at: http://pubs.aic.ca/doi/abs/10.4141/cjss85-060 [Accessed 27 January 2015]

Mohammed D, Kohl R. 1987. Infiltration response to kinetic energy. *Transactions of the ASAE-American Society of Agricultural Engineers (USA)*

Morin J, Benyamini Y. 1977. Rainfall infiltration into bare soils. *Water Resources Research* 13 (5): 813–817 DOI: 10.1029/WR013i005p00813

Mualem Y, Assouline S, Rohdenburg H. 1990. Rainfall induced soil seal (A) A critical review of observations and models. *Catena* 17 (2): 185–203

Mubarak I, Angulo-Jaramillo R, Mailhol JC, Ruelle P, Khaledian M, Vauclin M. 2010. Spatial analysis of soil surface hydraulic properties: Is infiltration method dependent? *Agricultural Water Management* 97 (10): 1517–1526 DOI: 10.1016/j.agwat.2010.05.005

Ndiaye B, Esteves M, Vandervaere J-P, Lapetite J-M, Vauclin M. 2005. Effect of rainfall and tillage direction on the evolution of surface crusts, soil hydraulic properties and runoff

generation for a sandy loam soil. *Journal of Hydrology* 307 (1–4): 294–311 DOI: 10.1016/j.jhydrol.2004.10.016

Pare N, Andrieux P, Louchart X, Biarnes A, Voltz M. 2011. Predicting the spatio-temporal dynamic of soil surface characteristics after tillage. *Soil and Tillage Research* 114 (2): 135–145 DOI: 10.1016/j.still.2011.04.003

Prosdocimi M, Tarolli P, Cerdà A. 2016. Mulching practices for reducing soil water erosion: A review. *Earth-Science Reviews* Available at: http://www.sciencedirect.com/science/article/pii/S0012825216302264 [Accessed 2 September 2016]

Reynolds W, Elrick D. 2002. Pressure infiltrometer. *DANE, JH E TOPP, G.C. Methods of Soil Analysis, Part* 4: 826–836

Reynolds WD, Elrick DE. 1990. Ponded Infiltration From a Single Ring: I. Analysis of Steady Flow. *Soil Science Society of America Journal* 54 (5): 1233 DOI: 10.2136/sssaj1990.03615995005400050006x

Römkens M. 1979. Soil crusting: when crusts form and quantifying their effects [Soil hydraulic properties]. *Agricultural Reviews and Manuals ARM NC*

Römkens M, Prasad S, Parlange J, others. 1990. Surface seal development in relation to rainstorm intensity. *Catena, Supplement* (17): 1–11

Rose C. 1960. Soil detachment caused by rainfall. *Soil Science* 89 (1): 28–35

Souza ES, Antonino ACD, Heck RJ, Montenegro SMGL, Lima JRS, Sampaio EVSB, Angulo-Jaramillo R, Vauclin M. 2014. Effect of crusting on the physical and hydraulic properties of a soil cropped with Castor beans (Ricinus communis L.) in the northeastern region of Brazil. *Soil and Tillage Research* 141: 55–61 DOI: 10.1016/j.still.2014.04.004

Strudley MW, Green TR, Ascough II JC. 2008. Tillage effects on soil hydraulic properties in space and time: State of the science. *Soil and Tillage Research* 99 (1): 4–48 DOI: 10.1016/j.still.2008.01.007

Torri D, Regüés D, Pellegrini S, Bazzoffi P. 1999. Within-storm soil surface dynamics and erosive effects of rainstorms. *CATENA* 38 (2): 131–150 DOI: 10.1016/S0341-8162(99)00059-4

Vandervaere J-P, Peugeot C, Vauclin M, Angulo Jaramillo R, Lebel T. 1997. Estimating hydraulic conductivity of crusted soils using disc infiltrometers and minitensiometers. *Journal of Hydrology* 188–189: 203–223 DOI: 10.1016/S0022-1694(96)03160-5

Warrick AW. 1998. Spatial variability. In: Hillel, D. (Ed.), Environmental Soil Physics. Academic Press, San Diego, CA, pp. 655–675.

West L, Chiang S, Norton L. 1992. The morphology of surface crusts. *Soil Crusting: Chemical and Physical Processes*: 301–308

Xu D, Mermoud A. 2001. Topsoil properties as affected by tillage practices in North China. *Soil and Tillage Research* 60 (1–2): 11–19 DOI: 10.1016/S0167-1987(01)00167-2

Xu X, Kiely G, Lewis C. 2009. Estimation and analysis of soil hydraulic properties through infiltration experiments: comparison of BEST and DL fitting methods. *Soil Use and Management* 25 (4): 354–361 DOI: 10.1111/j.1475-2743.2009.00218.x

Yilmaz D, Lassabatere L, Angulo-Jaramillo R, Deneele D, Legret M. 2010. Hydrodynamic Characterization of Basic Oxygen Furnace Slag through an Adapted BEST Method. *Vadose Zone Journal* 9 (1): 107 DOI: 10.2136/vzj2009.0039

Yilmaz D, Lassabatere L, Deneele D, Angulo-Jaramillo R, Legret M. 2013. Influence of Carbonation on the Microstructure and Hydraulic Properties of a Basic Oxygen Furnace Slag. *Vadose Zone Journal* 12 (2): 0 DOI: 10.2136/vzj2012.0121

Zhai R, Kachanoski RG, Voroney RP. 1990. Tillage Effects on the Spatial and Temporal Variations of Soil Water. *Soil Science Society of America Journal* 54 (1): 186 DOI: 10.2136/sssaj1990.03615995005400010029x

B.4. Testing infiltration run effects on the estimated water transmission properties of a sandy-loam soil*

V. Alagna, V. Bagarello*, S. Di Prima, G. Giordano, M. Iovino

Dipartimento di Scienze Agrarie e Forestali, Università degli Studi di Palermo, Viale delle Scienze, 90128, Palermo, Italy.
*Corresponding author: E-mail vincenzo.bagarello@unipa.it., Tel.: +39 091 23897053

Abstract

Testing factors influencing determination of soil water transmission properties by an infiltrometer method helps to better interpret the collected data and allows to develop appropriate sampling strategies for the intended use of the data. These factors include the soil water content at the start of the experiment, the height from which water is poured onto the soil surface, and the duration of the infiltration run. A sandy-loam soil was sampled with the BEST (Beerkan Estimation of Soil Transfer parameters) procedure of soil hydraulic characterization and two heights of pouring of water (0.03 and 1.5 m) under three different initial soil water content, θ_i ($0.12 \leq \theta_i \leq 0.20$ m^3m^{-3}), conditions. According to the BEST guidelines, relatively short infiltration runs (average run duration $\leq$ 1.5 hours, depending on both the date and the height from which water was poured) were carried out. However, three long infiltration runs (10 hours) were also carried out when θ_i was of 0.075 m^3m^{-3}. The saturated soil hydraulic conductivity, K_s, and the soil water sorptivity, S, were estimated for each infiltration run with the BEST-steady algorithm. The mean values of K_s varied with the height of pouring of water and θ_i from 13 to 496 mm h^{-1}, and a low height from which water was poured yielded 13 to 27 times higher K_s means than a high height, depending on θ_i. An inverse relationship between K_s and θ_i was clearer with the low height of pouring of water than the high one. The mean saturated hydraulic conductivity obtained with the long runs (15 mm h^{-1}) was close to the means of K_s obtained with the high and shorter runs (13-19 mm h^{-1}, depending on θ_i). The means of S varied from 35 to 126 mm $h^{-0.5}$, with the low runs yielding 2.3 to 2.8 times higher means than the high runs. The high sorptivity obtained with the long runs (160 mm $h^{-0.5}$) was in line with the low initial soil water content. In conclusion, the water application procedure and the duration of the infiltration run can have a noticeable effect on the estimated soil water transmission properties. Long duration runs or runs carried out with a high height of pouring of water appear more appropriate than short duration runs with a low

height of pouring of water to obtain data usable to explain surface runoff generation phenomena during intense rainfall events, especially when the soil is relatively dry at the time of sampling. In the future, the effects of both the height from which water is poured and the run duration on the water transmission properties measured with BEST should be tested for different initial soil water conditions in other soils. The usability of the height from which water is poured onto the soil surface as a parameter to mimic high intensity rain should also be investigated specifically.

Keywords: Soil hydraulic properties; beerkan infiltration run; BEST procedure; height of pouring of water; run duration

* This is the peer reviewed version of the article and it may be used for non-commercial purposes in accordance with Wiley Terms and Conditions for Self-Archiving. When citing, please refer to: Alagna, V., Bagarello, V., Di Prima, S., Giordano, G., Iovino, M. (2016). Testing infiltration run effects on the estimated water transmission properties of a sandy-loam soil. Geoderma, 267, 24-33.

B.4.1. Introduction

Measuring soil hydraulic properties is necessary for interpreting and simulating many hydrological processes having environmental and economic importance, such as rainfall partition into infiltration and runoff. Especially for the soil water transmission properties, that depend strongly on soil structure, field measurement techniques should be used to minimize disturbance of the sampled soil volume and to maintain its functional connection with the surrounding soil (Bouma, 1982). Many replicated measurements of these properties have to be carried out to characterize an area of interest since they are known to vary widely both in space and time (e.g., Prieksat et al., 1994; Logsdon and Jaynes, 1996). Therefore, the technique to be applied at the near point scale should be simple and rapid.

Reasons for using ponding infiltrometer techniques to determine soil water transmission properties in the field include robust theory, simple devices, relatively small volumes of water, generally rapid experiment, extensive testing, and possibility to determine different water transmission properties, such as saturated soil hydraulic conductivity, K_s, and sorptivity, S (Reynolds, 2008a,b). Infiltrometer runs can also be used to obtain a complete soil hydraulic characterization, i.e. not limited to soil water transmission parameters. In particular, in the BEST (Beerkan Estimation of Soil Transfer parameters) procedure of soil hydraulic characterization (Lassabatère et al., 2006; Yilmaz et al., 2010; Bagarello et al., 2014a), the shape parameters of certain analytic formulae for the hydraulic characteristic curves are

estimated from particle-size analysis whereas the structure dependent scale parameters are obtained by a three-dimensional field infiltration experiment at theoretically zero pressure head, using the infiltration model by Haverkamp et al. (1994).

Generally, the analysis of the infiltration data is based on an idealized representation of the sampled soil that is assumed to be rigid, homogeneous, isotropic and uniformly unsaturated before the run (e.g., Reynolds and Elrick, 1990; Lassabatère et al., 2006). However, structure dependent soil properties have a dynamic nature and they can vary appreciably upon wetting due to different phenomena, such as aggregate breakdown promoted by raindrop impact or weakening of interparticle bonds (Collis-George and Laryea, 1971; Assouline and Mualem, 2002, 2006; Chen et al., 2013). Therefore, there is the need to explore the link between hydraulic characterization of initially unsaturated real soils and experimentally controllable factors of the infiltration run. This is still an open issue although some investigations developing this topic can be found in the literature. For example, K_s under rainfall conditions appears to be better represented by the tension infiltrometer than ponded head infiltrometers in stony soils (Verbist et al., 2013) but the opposite was suggested for other soils (Alagna et al., 2015; Bagarello et al., 2012, 2014b).

Although BEST appears attractive for a simple, rapid and complete soil hydraulic characterization, little is known about the dependence of the calculated soil water transmission properties on the applied experimental procedure in the field. Bagarello et al. (2014c) suggested that the K_s values determined by applying water at a relatively large distance from the soil surface could be more appropriate than those obtained with a low height of pouring of water to explain surface runoff generation phenomena during intense rainfall events. However, it should be established, for a given soil, to what extent the height from which water is poured influences the calculated soil water transmission properties under different initial soil water conditions since changes in soil structure due to wetting depend on the antecedent wetness conditions (e.g., Le Bissonnais, 1996; Cerdà, 1998). Another factor needing consideration is the duration of the infiltration run, that is often chosen quite subjectively. BEST calculations need measurement of steady-state infiltration rate but relatively short runs are generally carried out in the field. Although the measured infiltration rates generally suggest rapid attainment of quasi steady-state conditions (Reynolds et al., 2000; Lassabatère et al., 2006), a long run could be expected to yield more robust estimates of steady-state infiltration rates than a short run (e.g. Elrick et al., 1990). However, a long run may also imply more time and opportunities for altering the sampled soil volume due, for example, to swelling and weakening of particle bonds (Hillel and Mottes, 1966; Talsma and

Lelij, 1976). Therefore, long runs may not be a valid alternative to short runs in any case. Even in this case, it is necessary to establish what happens in the field with runs of different duration to make an appropriate use of the calculated soil parameters. In addition, repeatedly pouring water on the surface of an initially dry soil, according to the BEST original procedure, implies a possible effect of deterioration of the exposed soil surface and air entrapment in the sampled soil volume on the measured infiltration rates. These factors have to be considered because alteration of soil surface during the run and even small changes in the entrapped air content may have a noticeable effect on the experimentally determined K_s values (Arya et al., 1998; Faybishenko, 1995; Reynolds, 2008a,b; Sakaguchi et al., 2005).

The relationship between the applied experimental approach and the measured parameter is not totally clear for sandy-loam soils. For example, similar estimates of K_s were obtained with two infiltrometer techniques differing by several factors, including flow field (one- or three-dimensional), stage of the infiltration process used for K_s calculation (transient, steady-state), and expected soil disturbance effects during the run (more noticeable with the steady-state technique than the transient one; Bagarello and Sgroi, 2007), but this similarity was only partially confirmed in a subsequent investigation (Bagarello et al., 2014b). Moreover, a noticeable dependence of K_s on the height from which water was poured was detected for BEST but not for the Simplified Falling Head technique (Bagarello et al., 2004, 2014c). The high percentage of coarse particles in these soils could suggest a certain rigidity of the porous medium, and hence a reduced sensitivity to disturbance due to wetting. However, the limited content in clay particles could also imply weak soil aggregation and hence the possibility that water application determines particle detachment and clogging of the largest pores. Moreover, soil swelling during the infiltration run cannot be completely excluded due to the clay that is present in the soil. The importance to establish factors specifically influencing measurement of K_s of sandy-loam soils was also acknowledged by other Authors (Somaratne and Smettem, 1993; Lado et al., 2004).

The investigation reported in this manuscript was carried out on a sandy-loam soil to test how the height from which water was poured for the BEST infiltration experiment affected estimation of saturated soil hydraulic conductivity and sorptivity for different initial soil water contents. The dependence of the K_s and S estimates on the duration of the infiltration run was also tested.

B.4.2. Materials and methos

The study was performed at the Department of Agriculture and Forestry Sciences of the Palermo's (Italy) University, in a citrus orchard with trees spaced 4 m × 4 m apart. The soil (Typic Rhodoxeralf), having a relatively high gravel content and an organic matter content in the 0-0.1 depth range of 3.9% (Bagarello et al., 2014c), was classified as sandy-loam (Table 1). The soil surface was gently levelled and smoothed before sampling. The superficial herbaceous vegetation was cut with a knife while the roots remained in situ.

Table 1 Coordinates, land use, management practices, clay (%), silt (%) and sand (%) content (USDA classification system) in the 0–0.1 m depth range and soil textural classification. Standard deviations are indicated in parentheses.

Variable	Site characteristic
Coordinates	33S 355511E - 4218990N
Land use	Citrus orchard
Management practices	Conventional tillage
clay	17.6 (1.9)
silt	29.8 (2.8)
sand	52.6 (4.7)
Textural classification	Sandy-loam

Height of pouring of water

An area of approximately 150 m^2, already used for an earlier investigation (Bagarello et al., 2014c), was sampled on May 2014 and January 2015.

On a sampling date, a total of 20 undisturbed soil cores (0.05 m in height by 0.05 m in diameter) were collected at the 0 to 0.05 m and 0.05 to 0.10 m depths in randomly chosen sampling points. These cores were used to determine the dry soil bulk density, ρ_b, and the soil water content at the time of the experiment, θ_i. The soil porosity, f, was calculated from the ρ_b data, assuming a soil particle density of 2.65 Mg m^{-3}. According to other investigations, the field saturated soil water content, θ_s, was assumed to coincide with f (Mubarak et al., 2009; Bagarello et al., 2011, 2014c).

Small diameter (i.e., 0.08 m) rings inserted to a depth of 0.01 m were used for the beerkan infiltration runs (Lassabatère et al., 2006). Ring insertion was conducted by gently using a rubber hammer and ensuring that the upper rim of the ring remained horizontal during insertion. The rings were particularly small to more clearly detect possible effects of soil disturbance due to water application. A total of 20 runs were carried out at randomly selected locations on a sampling date. Following the existing guidelines (Lassabatère et al., 2006), for each run 15 water volumes, each of 57 mL, were successively poured in 3-5 s on the confined infiltration surface. Ten runs were carried out by applying water at a small distance from the infiltration surface, i.e. approximately at a height, h_w, of 0.03 m, and dissipating its energy on the fingers of the hand, in an attempt to minimize soil disturbance due to water application

(low, L, runs), as is commonly suggested in practical application of a ponding infiltration method (Reynolds, 2008a). Water was applied from h_w = 1.5 m at the other 10 sampling points (high, H, runs). The soil surface was not shielded in this case to maximize possible damaging effects of water impact. To ensure flow verticality and prevent wind effects, the device developed by Bagarello et al. (2014c) was used. The mean infiltration time of each applied water volume was calculated for both the low, Δt_L (T), and the high, Δt_H (T), runs. For a given water volume (first, second, …, fifteenth), the infiltration time was measured from water application to disappearance of all water, and the mean infiltration time was calculated by averaging the individual infiltration times. These calculations were made since, for a given amount of applied water, run duration is inversely related to infiltration rate.

The BEST procedure (Lassabatère et al., 2006) was applied to estimate the whole set of parameters for the water retention (van Genuchten, 1980; Burdine, 1953) and hydraulic conductivity (Brooks and Corey, 1964) curves. According to this procedure, residual water content is supposed to be zero and shape parameters of these curves are estimated from particle size distribution and porosity, using specific pedo-transfer functions. With the BEST-steady algorithm (Bagarello et al., 2014a), calculation of soil sorptivity, S (L $T^{-0.5}$), and saturated soil hydraulic conductivity, K_s (L T^{-1}), makes use of the intercept, b_s^{exp} (L), and the slope, i_s^{exp} (L T^{-1}), of the straight line fitted to the data describing steady-state conditions on the cumulative infiltration, I (L), vs. time, t (T), plot. The following relationships are used to calculate S and K_s:

$$S = \sqrt{\frac{i_s^{exp}}{A + \frac{C}{b_s^{exp}}}} \tag{1}$$

$$K_S = \frac{C\, i_s^{exp}}{A\, b_s^{exp} + C} \tag{2}$$

where A (L^{-1}) and C are constants in the steady-state expansion of the infiltration model by Haverkamp et al. (1994). The scale parameter for water pressure head, that is related to the air-entry pressure head, is finally estimated from S and K_s. For each infiltration run, a linear regression line was therefore fitted to the last data points, describing the near steady-state conditions, in order to estimate b_s^{exp} and i_s^{exp} on the I vs. t plot. Eqs.(1) and (2) were then applied to estimate S and K_s, respectively. For these calculations, the site was considered homogeneous in terms of particle-size distribution (PSD) and ρ_b, f, θ_i and θ_s values. The mean PSD determined by Bagarello et al. (2014c) was also used in this investigation. The

representative ρ_b, f, θ_i and θ_s values were obtained by averaging the individual determinations of each variable obtained from the undisturbed soil cores on a given sampling date.

The BEST-steady algorithm was considered in this investigation because it allows a simple calculation of S and K_s. Another reason was that a higher success percentage of the infiltration runs, implying more experimental information, was expected with BEST-steady than with other possible algorithms. In particular, Di Prima et al. (2015) showed that the BEST-slope (Lassabatère et al., 2006) and BEST-intercept (Yilmaz et al., 2010) algorithms can fail when the transient phase of the infiltration process is too short or it is described by a too small number of data points. Failure of these two algorithms was considered possible because a rapid attainment of near steady flow conditions was expected for this relatively coarse textured soil.

The hypothesis of normality was checked by the Lillefors (1967) test for both the untransformed and the ln-transformed S and K_s data. Then, for a given height of pouring of water, the data were summarized by calculating the mean, M, and the associated coefficient of variation, CV.

Two different sampling campaigns were carried out in this investigation but a third dataset was developed by re-analyzing with the BEST-steady algorithm the data collected on June 2012 at the same field site (Bagarello et al., 2014c). In 2012, a different number of cores were collected to determine θ_i and ρ_b (10 instead of 20), the ring was slightly larger (inner diameter = 0.085 m instead of 0.08 m), and more water was applied with each pouring (64 mL instead of 57 mL). However, the experimental differences between the earlier (2012) and later (2014, 2015) sampling campaigns were considered to be practically negligible and inconsequential, and this circumstance made it possible to consider three different sampling dates for testing effects of the height from which water was poured.

Attempting to check soundness of the estimated sorptivities, it was considered that, according to Reynolds and Elrick (2002), S can be approximated by:

$$S = \left[\gamma_w(\theta_s - \theta_i)\,\phi_m\right]^{1/2} \tag{3}$$

where γ_w is a dimensionless constant (White and Sully, 1987) related to the shape of the wetting (or drainage) front and ϕ_m (L^2T^{-1}) is the matric flux potential, defined by (Gardner, 1958):

$$\phi_m = \int_{h_i}^{0} K(h)\,dh = \frac{K_s - K_i}{\alpha} \qquad h_i \le h \le 0 \tag{4}$$

where h (L) is the soil water pressure head, h_i (L) is the initial value of h, K (L T^{-1}) is the soil hydraulic conductivity ($K_i = K(h_i)$), and α (L^{-1}) is the slope of ln K versus h. Substituting eq.(4) into eq.(3) and assuming $K_i = 0$ yields:

$$S = \left[\gamma_w (\theta_s - \theta_i) \frac{K_s}{\alpha} \right]^{1/2} \quad (5)$$

Duration of the infiltration run

On July 2014, three long duration (10 hours) infiltration runs were carried out at randomly chosen points of the selected field site by using rings with an inner diameter of 0.15 m inserted to a depth of 0.01 m into the soil. From seven to 10 water volumes of 150 mL, depending on the run, were poured in succession on the confined infiltration surface to monitor the initial, transient stage of the process with the common procedure for a beerkan experiment (Lassabatère et al., 2006). Then, to continue the run for a long period of time, a large Mariotte bottle was connected to the ring by a pipe immediately after infiltration of the last applied volume of water, and a small constant head (i.e., ~ 5 mm) was established until the end of the run. The bottle consisted of a graduated, transparent cylinder with an inner diameter of 0.144 m and a height of 1.9 m (figure 1). The large capacity (~ 30 L) of this reservoir avoided the need of frequent refilling. The time interval between visual readings at the reservoir was of 1 to 15 min. A total of six undisturbed soil cores were also collected to determine θ_i and ρ_b at the 0-0.05 m and 0.05-0.10 m sampling depths.

Fig. 1 Mariotte bottle used for the long duration infiltration runs

Each run was repeatedly analysed to detect possible changes in the calculated S and K_s values with the duration of the run. In particular, for a given number of collected (I, t) data, the last five points were assumed to represent the steady-state phase of the process and S and K_s were calculated with BEST-steady. Calculations were repeated by assuming a variable number of collected data points, ranging from a minimum of eight (Lassabatère et al., 2006) to a maximum of 78-93, depending on the run, corresponding to an infiltration process of 10 hours. In particular, an estimate of S and K_s was obtained by considering the first eight (I, t) data points that were collected (shortest run duration, = t_8). Then, the subsequent (I, t) data pair was included in the

data set to be analysed and a new estimate of S and K_s was obtained (run duration = t_9, $t_9 > t_8$). This procedure was repeated until all collected data pairs were included in the analysed data set (longest run duration).

To check if the assumption of near steady-state conditions was plausible for each assumed run duration, the gravity time, t_{grav} (T), was calculated (Philip, 1969):

$$t_{grav} = \left(\frac{S}{K_s} \right)^2 \tag{6}$$

The fractional influence of gravity on cumulative three-dimensional infiltration, ε, was also determined as a function of time by the following relationship (Smettem et al., 1995):

$$I(1-\varepsilon) = St^{1/2} + \frac{\gamma S^2}{r(\theta_s - \theta_i)} t \tag{7}$$

Therefore, in this investigation a high (or H) run denoted an infiltration run carried out by establishing a large (1.5 m) vertical distance between the confined infiltration surface and the water pouring point, i.e. the point from which water was made free to reach the soil. This vertical distance was small (0.03 m) for the low (or L) runs. The terms high (H) and low (L) runs were already used by Bagarello et al. (2014) to denote the same kind of infiltration runs and they were maintained here for terminological consistency with the previous investigation. Long runs had a fixed duration of 10 hours. Runs carried out by applying a sequence of 15 water volumes, each of 57-64 mL depending on the sampling date, were denoted as short.

B.4.3. Results and discussion

B.4.3.1. Height of pouring of water

Initial conditions

The antecedent soil water content differed appreciably among the three sampling dates ($0.118 \leq \theta_i \leq 0.202$ m^3m^{-3}, Table 2) but the dry soil bulk density ($1.126 < \rho_b < 1.144$ Mg m^{-3}) and, hence, the estimated saturated soil water content ($0.568 \leq \theta_s \leq 0.575$ m^3m^{-3}) remained practically constant (i.e., differences by not more than 1.6%). Consequently, the ratio between θ_i and θ_s varied from 0.20 to 0.35.

Duration of the infiltration process

The initial check of the field data suggested that the height from which water was poured influenced the infiltration process on all sampling dates since the mean duration of the H runs, varying with the date from 3500 s to 5400 s, was 4.0 to 5.4 times longer than the mean

duration varying with the date from 3500 s to 5400 s, was 4.0 to 5.4 times longer than the mean duration of the L runs (640 - 1020 s).

Table 2 Sample size (*N*), minimum (*Min*), maximum (*Max*), mean, and coefficient of variation (*CV*, in %) of the soil water content at the time of sampling, θ_i (m^3m^{-3}), dry soil bulk density, ρ_b (Mg m^{-3}), and saturated soil hydraulic conductivity, K_s (mm h^{-1}), and sorptivity, *S* (mm $h^{-0.5}$), values obtained on different years with the BEST experiment by pouring water into the cylinder from two different heights

Variable	Height of water pouring (m)	Statistic	June 2012	May 2014	January 2015
θ_i		N	10	20	20
		Min	0.103	0.094	0.155
		Max	0.132	0.201	0.239
		Mean	0.118	0.158	0.202
		CV	9.1	17.4	10
ρ_b		N	10	20	20
		Min	1.054	1.039	1.002
		Max	1.194	1.302	1.249
		Mean	1.127	1.144	1.126
		CV	4.2	6.3	4.4
K_s	0.03	N	10	9	10
		Min	169.2	97.7	36.6
		Max	854.7	958.1	457.6
		Mean	496.4 a A	299.2 a AB	168.8 a B
		CV	43.5	95.2	74.3
	1.5	N	10	10	9
		Min	13.1	3.2	5.4
		Max	23.8	45.0	22.0
		Mean	18.1 b A	18.9 b A	12.8 b A
		CV	22.8	77.5	44.1
S	0.03	N	10	9	10
		Min	54.7	63.3	48.6
		Max	181.8	117.6	116.1
		Mean	126.3 a A	84.8 a B	83.1 a B
		CV	31.8	23.7	28.3
	1.5	N	10	10	9
		Min	39.5	24.0	24.6
		Max	52.3	54.9	49.3
		Mean	45.7 b A	37.3 b AB	34.8 b B
		CV	9.3	30.4	23.0

For a given variable, the values in a column followed by a different lower case letter were significantly different according to a two tailed t test (P = 0.05). The values in a row followed by the same upper case letter were not significantly different according to the Tukey Honestly Significant Difference test (P = 0.05). The values followed by a different upper case letter were significantly different

In all cases, $\Delta t_H/\Delta t_L$ ($1.2 \leq \Delta t_H/\Delta t_L \leq 9.5$) increased with the number of the applied volumes of water, N_v (figure 2), indicating that Δt_H increased more than Δt_L during the run. Differences between the three $\Delta t_H/\Delta t_L$ vs. N_v relationships started to become clear after infiltration of six

volumes of water, and relatively dry initial soil conditions ($\theta_i \leq 0.16$ m^3m^{-3}) yielded similar $\Delta t_H/\Delta t_L$ ratios, higher than those detected for the wetter soil.

The H and L runs differed only by the height from which water was poured since averaging 10 runs for a given height should be appropriate to obtain representative values for the field site (Reynolds et al., 2002; Verbist et al., 2010). Therefore, the differences between Δt_H and Δt_L were expressive of a progressive deterioration of the infiltration surface with the repeated application of a given amount of water from a great height. Disturbance occurred soon, since $\Delta t_H/\Delta t_L$ was systematically greater than one even in the early stages of the infiltration run, and it increased with a prolonged exposure of the soil surface to water. For a small number of applied water volumes, $\Delta t_H/\Delta t_L$ was independent of the soil water content at the time of the experiment. However, an initially wet soil condition reduced the effect of the height from which water was poured for relatively large infiltrated water volumes.

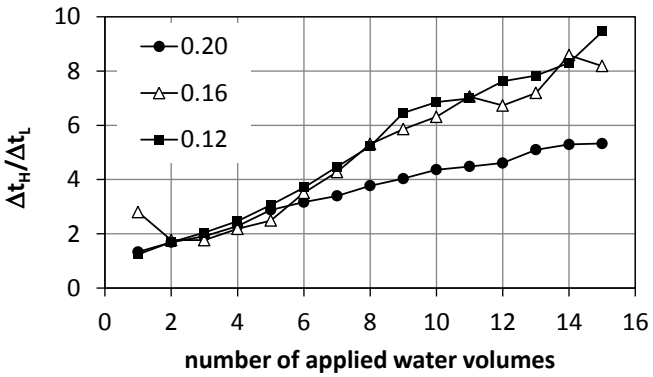

Fig. 2 Ratio between the mean infiltration time for a water application height of 1.5 (Δt_H) and 0.03 (Δt_L) m during the BEST runs plotted against the number of the applied volumes of water for different values of the initial soil water content, θ_i, ranging from 0.12 to 0.20 m^3m^{-3}

Statistical distribution of the data

According to the Lilliefors (1967) test, the hypothesis of a normal distribution for both the untransformed and the ln-transformed K_s and S data was never rejected ($P = 0.05$) for the 12 tested datasets, developed by considering a given initial soil water content and a height of pouring of water. However, the largest difference between the empirical cumulative distribution function and the corresponding theoretical function was generally smaller with reference to the untransformed data (Table 3). Therefore, K_s and S were assumed to be normally distributed, and the data were summarized by calculating the arithmetic mean and the associated coefficient of variation.

Saturated soil hydraulic conductivity

The mean values of K_s varied from 13 to 496 mm h^{-1} (difference by a factor of approximately 39) and the associated *CV*s ranged from 23% to 95% (Table 2). Soil macroporosity likely influenced the results of the L runs since a mean $K_s \geq 169$ mm h^{-1} was obtained and this value was higher than the expected saturated conductivity on the basis of the soil textural

characteristics alone (e.g., K_s = 44.2 mm h^{-1} for a sandy-loam soil according to Carsel and Parrish, 1988). The effect of the height from which water was poured on K_s was statistically significant, and also noticeable, on all sampling dates because $M(K_{sL})$ (mean of K_s obtained with a low run) was 13 to 27 times higher than $M(K_{sH})$ (K_s for a high run), depending on the sampling date. The ratio between the two means decreased from the driest to the wettest soil conditions. Relative variability of K_s was larger with the low runs than the high ones. The $M(K_{sL})$ values differed at the most by a factor of three. Some differences were statistically significant according to the Tukey Honestly Significant Difference test (P = 0.05) and the mean values clearly decreased with an increase in the initial soil water content (figure 3). The $M(K_{sH})$ values differed by not more than a factor of 1.5, the differences were not statistically significant and the inverse relationship between K_s and θ_i was less clear (figure 3).

Table 3 Results of the Lillefors (1967) test for each developed dataset

Variable	Sampling date	Type of run	Sample size	D_{max}		D_{crit}
				N	LN	
K_s	June 2012	L	10	0.1209	<u>0.1159</u>	0.258
		H	10	<u>0.1458</u>	0.1464	0.258
	May 2014	L	9	0.2326	<u>0.1553</u>	0.271
		H	10	<u>0.1582</u>	0.1822	0.258
	January 2015	L	10	<u>0.1055</u>	0.1601	0.258
		H	9	<u>0.1299</u>	0.1478	0.271
S	June 2012	L	10	<u>0.0999</u>	0.1637	0.258
		H	10	<u>0.1132</u>	0.1228	0.258
	May 2014	L	9	<u>0.1358</u>	0.1485	0.271
		H	10	<u>0.1262</u>	0.1299	0.258
	January 2015	L	10	<u>0.1381</u>	0.1858	0.258
		H	9	0.1173	<u>0.1145</u>	0.271

K_s = saturated soil hydraulic conductivity; S = soil sorptivity; L = low (height of water application = 0.03 m); H = high (height of water application = 1.50 m); D_{max} = largest difference between the empirical cumulative distribution function and the corresponding theoretical function (smaller values are underlined); D_{crit} = critical value of D_{max}; N = normal; LN = log-normal.

An inverse relationship between K_s and θ_i was expected for the sampled sandy-loam soil due to moderate swelling phenomena and weakening of the interparticle bonds reducing macropore volume in wet soil (Bagarello and Sgroi, 2007). Air entrapment did not explain this relationship since an initially higher soil water content should imply less opportunities for air entrapment during the infiltration run and hence higher K_s results (Reynolds, 2008a,b).

The more soil perturbing experiment (H infiltration runs) reduced the dependence of K_s on θ_i and a drier soil condition determined larger differences between K_{sL} and K_{sH}.

Therefore, the applied experimental methodology had a noticeable effect on the measured conductivity under all antecedent conditions, but a dry soil was more sensitive to the height from which water was poured than a wet soil. Likely, a larger height from which water was poured implied more energy applied to the soil surface and therefore more opportunities for aggregate breakdown, compaction of the exposed soil surface and macropore obstruction, particularly in more macroporous conditions (lower θ_i, higher K_s).

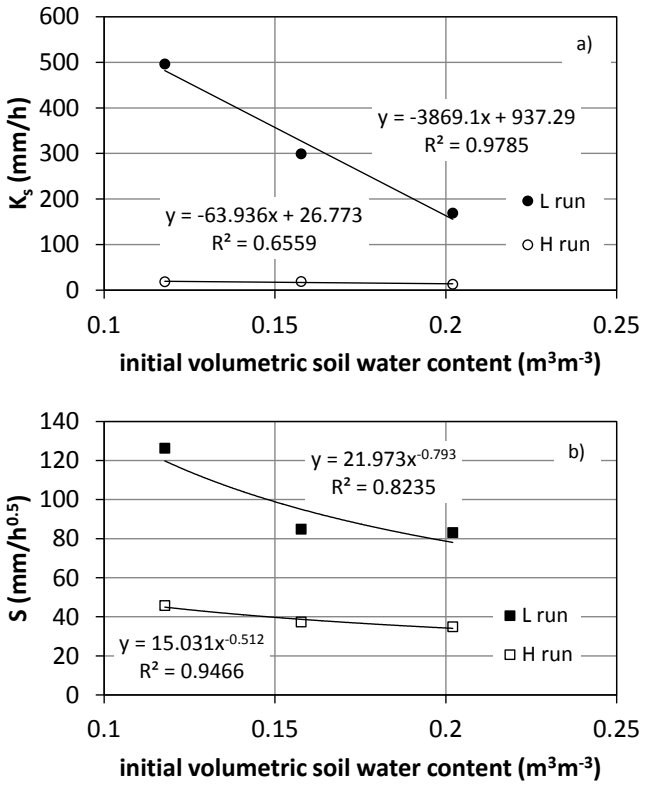

Fig. 3 Effect of the initial volumetric soil water content on the mean values of a) the saturated soil hydraulic conductivity, K_s, and b) the soil sorptivity, S, for both the low (L) and high (H) infiltration runs

The mean K_s values obtained with the BEST runs and a low height of pouring of water were in line with the saturated conductivity previously measured at the same field site with the SFH and PI techniques (figure 4) (Bagarello and Sgroi, 2007; Bagarello et al., 2014c). The information collected by a BEST run with high pouring height on a relatively dry soil was closer to that collected by less perturbative approaches (SFH, PI techniques) in relatively wet soil conditions.

Soil sorptivity

The means of S varied from 35 to 126 mm $h^{-0.5}$ (difference by a factor of 3.6) and the associated *CV*s ranged from 9% to 32% (Table 2). In all cases (initial soil water content, height from which water was poured), relative variability was smaller for S than for K_s. The effect of the height from which water was poured on S was statistically significant on all sampling dates and it varied only slightly for the three sampling campaigns because $M(S_L)$ (the mean of S obtained with a low run) was 2.3 to 2.8 times higher than $M(S_H)$ (S for a high run), depending on the period. The three $M(S_L)$ values differed at the most by a factor of 1.5 whereas $M(S_H)$ changed by not more than 1.3 times and some differences were statistically significant in both cases. This result and the plot of S against θ_i (figure 3) suggested a tendency of S to decrease with an increase of θ_i. The S data collected in this investigation

were consistent with the expected effect of both θ_i and K_s on this soil property according to eq.(5). For a given θ_i (i.e., for a given sampling date), S decreased with a decrease in K_s and, for a given type of run (L or H), S showed a tendency to decrease as θ_i increased and K_s decreased.

Soil disturbance determined a reduced ability of the porous medium to adsorb water due to capillarity and, in the range of the tested θ_i values, this effect was more noticeable than that produced by an increase of θ_i. Even the fact that $CV(S) < CV(K_s)$ was always obtained was considered physically plausible. The reason was that K_s strongly depends on the highly variable soil structure, particularly influencing the largest pores and their hydraulic continuity (e.g., Somaratne and Smettem, 1993; Jarvis et al., 2013), whereas S is more expressive of the capillary forces exerted by the soil matrix, which is known not to vary much in space. Therefore, the estimates of S appeared plausible on the basis of the physical meaning of this variable. This result was not expected a priori because data were collected by a ponding infiltration experiment which is not the best choice to detect capillarity effects on the established flow process (Reynolds and Elrick, 1990). Perhaps, the fact that the ponding depth was small (i.e., close to zero) was an appropriate choice to obtain plausible S data.

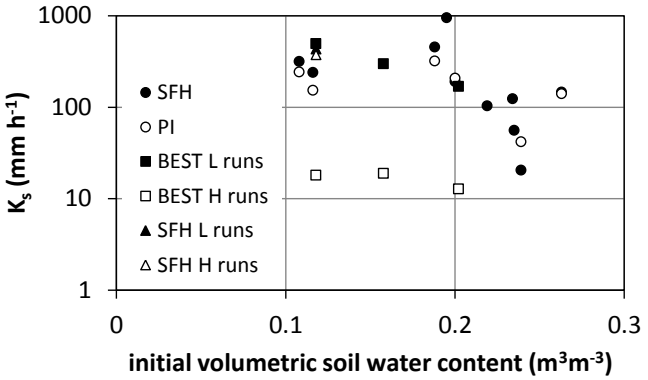

Fig. 4 Effect of the initial volumetric soil water content on the mean saturated soil hydraulic conductivity obtained at the field site in this and other investigations (Bagarello and Sgroi, 2007; Bagarello et al., 2014c) with different experimental methodologies.

Link between field soil data and hydrological processes

Establishing a conceptual link between the applied experimental methodology for characterizing the soil and the interpretable hydrological processes is important to understand the practical usefulness of a particular measurement. For example, Amezketa et al. (1996) and Le Bissonnais (1996) suggested that testing aggregate stability under fast wetting is appropriate to assess effects of heavy rain storms occurring in summer on the soil. Slow wetting experiments corresponds to a field condition of wetting under gentle rain. Liu et al. (2011) suggested that double ring infiltrometer experiments are useful to mimic effects of fast wetting of initially dry soil under high rainfall intensities. According to other investigations, however, K_s data collected by infiltrometer methods could be expected to be unusable for interpreting field hydrological processes, and particularly infiltration, for different reasons.

For example, the high K_s values obtained by van de Giesen et al. (2000) with ring infiltrometers were not considered to be the actual values during rainstorms because they would have precluded occurrence of the measured runoff. To explain this inconsistency, van de Giesen et al. (2000) suggested that massive air inclusion in the soil and crust formation and associated particle sorting phenomena, decreasing overall permeability during the rainstorm, influenced runoff production. These phenomena did not occur or were less noticeable when K_s was measured with the infiltrometer. Flow at saturation is dominated by structural macropores, that are known to be fragile (Jarvis et al., 2013). Moreover, runoff generation often presupposes development of a surface seal layer (Assouline and Mualem, 2006; Chen et al., 2013) but it can also happen that rainfall does not induce significant changes in K_s (Schiettecatte et al., 2005). A significant decrease of K_s can occur after an intense rainfall but not as a consequence of a light rain (Liu and Chen, 2015).

The methodology applied in this investigation, combining low and high infiltration runs, seems appropriate to test the effect of intense and prolonged rainfall events on the hydraulic characteristics of the surface soil layer, and it is also simpler than an approach involving soil characterization both before and after natural or simulated rainfall since it needs less equipment and field work.

Other investigations appear to give some indirect support to the suggested method. For example, the fact that the height from which water was poured had a more noticeable effect on K_s than S was consistent with the results obtained by Somaratne and Smettem (1993) in another sandy-loam soil, since simulating intense rainfall in initially dry soil conditions triggered a decrease of the average hydraulic conductivity whereas sorptivity remained unaffected. The homogenizing effect of the runs with a high height for water pouring on K_s was in line with the conclusion by Assouline and Mualem (2006) that the formation of soil surface seal apparently reduces the effect of the field areal variability on the steady infiltration rate.

An intense and prolonged rainfall event has a soil surface perturbing effect that, reasonably, was better represented by the runs with a high height for water pouring than those with a low height. Therefore, K_s can be expected to be high and highly variable, depending on the soil water content, before occurrence of high energy rainfall events. Rainfall determines a decrease of K_s in the upper soil layer, that assumes a value that does not depend strongly on the antecedent soil water content. The manner in which water is applied has an appreciable effect on both S and K_s, particularly in initially dry soil conditions. A noticeable soil

disturbance during wetting reduces in general infiltration and it also reduces the effect of θ_i on this hydrological process.

B.4.3.2. Duration of the infiltration run

Field data and saturated soil hydraulic conductivity and soil sorptivity calculations

The experimentally measured cumulative infiltration curves appeared consistent with the theoretically expected curve **(**figure 5). The small concavity was plausible since the soil had a relatively coarse texture (Lassabatère et al., 2009). For long runs 1 and 2, the infiltration rate, i_r, was initially high (figure 6) but it soon decreased and approached a near steady value (i.e., approximately after less than 200 s). This near steady condition persisted for a relatively long period and it was more noisy in its early stages than at later times. At a later stage of the infiltration process (i.e., after more or less 8000 s), i_r started to decrease again until the end of the run. Long run 3 evolved as the other two runs but, in addition, i_r increased abruptly and permanently at the beginning of the near steady condition. For run durations of less than approximately 8000-10000 s, depending on the run, K_s was nearly independent of t but it showed appreciable oscillations, at least for two runs (figure 7a). Then, K_s decreased progressively with t. Sorptivity did not vary systematically with t for both relatively short and long durations of the run but a long run yielded consistently higher S values than a short run (figure 7b). Moreover, clear oscillations of S were only detected for relatively short durations of the run. The calculated final values of K_s and S were relatively similar for the three runs ($10.2 \leq K_s \leq 19.4$ mm h^{-1}, mean = 14.7 mm h^{-1}; $134.8 \leq S \leq 186.2$ mm $h^{-0.5}$, mean = 159.9 mm $h^{-0.5}$).

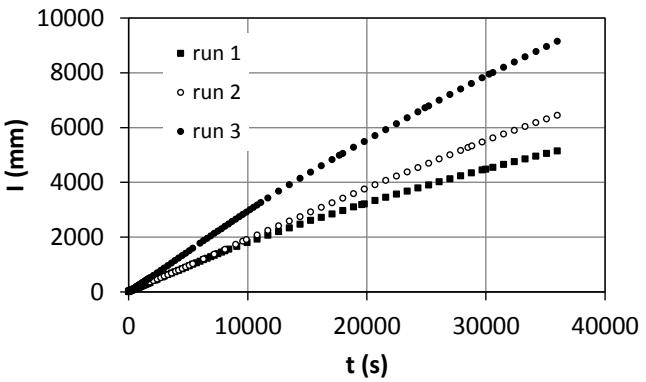

Fig. 5 Cumulative infiltration, *I*, against time, *t*, for the long duration infiltration runs.

Early stage of the infiltration run

Initially, K_s and S were relatively high and low, respectively, suggesting a significant role of macropores and other large voids on water transport processes in the soil. As a matter of fact,

the lowest K_s value during this phase was 230 mm h^{-1} (figure 7) that is appreciably higher than the expected saturated conductivity for a sandy-loam soil (Carsel and Parrish, 1988).

The oscillations of S and K_s were associated with oscillations in infiltration rates that can occur under air confining conditions (Jarrett and Fritton, 1978; Wang et al., 1998). According to Wang et al. (1998), in particular, when the air pressure ahead of the wetting front reaches an air-breaking value, soil air escapes from the surface, leading to an immediate decrease in the air pressure and an increase in the infiltration rate. When the air pressure falls below a certain air-closing value, air escape stops, the infiltration rate decreases again and the air pressure increases. In this investigation, air confining conditions could be considered unlikely or even impossible due to the absence of physical obstacles to air escape. However, air entrapment is common in three-dimensional ponding infiltration experiments (Reynolds, 2008a,b), notwithstanding that water flow is free to diverge below the ring insertion depth, and the experimental conditions likely favored entrapment of air in the sampled soil volume. Indeed, ponding conditions were established on the surface of an initially very dry soil (θ_i = 0.075 m^3m^{-3}) and, in the early stages of the run, a new volume of water was applied after complete infiltration of the previously poured volume. Therefore, a cyclic infiltration process maybe occurred because much air was present in the soil at the beginning of the run and the experimental approach favored air entrapment during wetting. The attenuation of the phenomenon at later stages of the run probably occurred because a small positive head was steadily established on the soil surface at a certain moment and the opportunities for air entrapment decreased. In other words, steadily establishing ponding conditions avoided exposure of soil surface to air which instead occurred, although for no more than a few seconds, when a new water volume was poured after complete infiltration of the previous amount of water. Moreover, the i_r vs. t plot suggested a very rapid attainment of

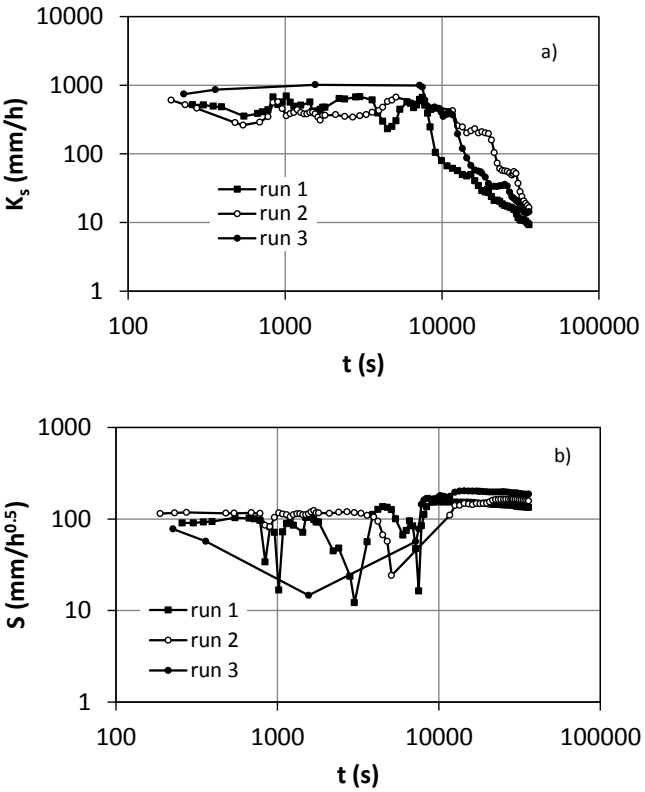

Fig. 7 Estimated values of a) the saturated soil hydraulic conductivity, K_s, and b) the soil sorptivity for different assumed durations, t, of the three long duration infiltration runs.

near steady conditions and, in these conditions, the field-saturated zone under the infiltration surface should remain essentially constant in size and shape (Elrick and Reynolds, 1992). Therefore, as the run proceeded, there were more and more opportunities for a permanent removal of the entrapped air from the field-saturated bulb.

Probably, an effect of the entrapped air was not detected with the shorter L and H runs for the following reasons: i) limited number of water volumes used for the run and hence insufficient experimental information to detect a clear oscillating pattern in the measured infiltration rates, and ii) higher initial water content of the sampled soil as compared with the long duration infiltration runs, implying less opportunities for air entrapment during the run.

Late stage of the infiltration run

To explain the effect of time on K_s and S during the late phase of the infiltration process, the hypothesis that the infiltration process did not reach the necessary steady conditions required by BEST-steady was initially excluded. As a matter of fact, the decreasing stage in the i_r vs. t plot followed a long phase suggesting practically constant i_r values (figure 6). Moreover, the comparison between the considered run duration for the calculation of S and K_s and the corresponding gravity time, t_{grav} (T) (figure 8), suggested that the choice to analyze the infiltration process by BEST-steady (i.e., assuming that a near steady-state condition was reached) was appropriate even for relatively short duration runs. At later times, $t < t_{grav}$ was detected and a change from $t > t_{grav}$ to $t < t_{grav}$ with longer infiltration times suggested that the sampled soil was not

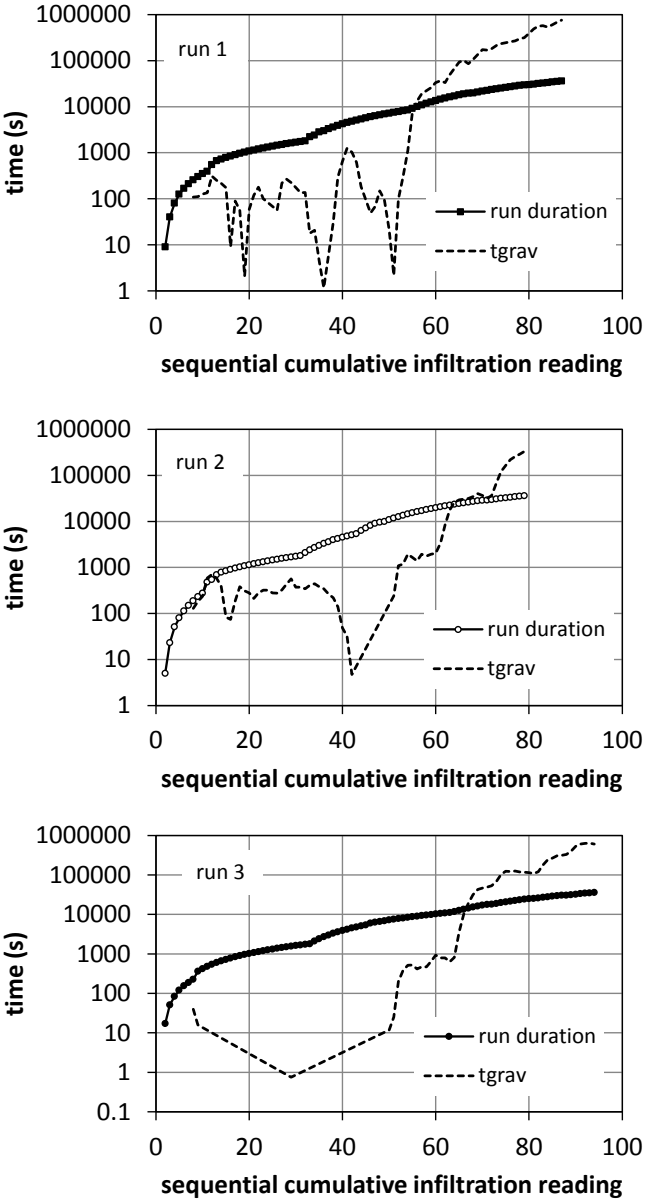

Fig. 8 Comparison between the run duration and the gravity time, t_{grav}, for the three long duration infiltration runs.m^3m^{-3}

ideal as required by theory (Haverkamp et al., 1994). Moreover, the sampled soil was presumably thick since a large amount of water infiltrated the soil before i_r started to decrease permanently (figures 5 and 6). Therefore, an effect of non-homogeneous subsurface soil characteristics (wetter conditions, less permeable layer) on the measured infiltration rates cannot be excluded.

Alteration phenomena occurring at or close to the soil surface were considered to be at least a concomitant cause of the late time decreasing infiltration rates since the soil remained saturated for several hours before the infiltration rates started to decrease. There was time for some macropore narrowing promoted by swelling, that maybe was moderate due to the relatively low clay content of the soil, but it certainly occurred since the surface swelled upward, almost blocking the outlet tube. Consequently, the water outlet tip of the device needed to be raised by a few mm during the run not to obstruct water discharge from the reservoir. Moreover, due to the long wetting period, weakening of the particle bonds likely occurred. Water was applied by a Mariotte bottle as subsequent impulses and, after each impulse, a few soil particles were noted to float in the established water ponding layer until they were deposited on the soil surface, possibly clogging exposed pores. The long duration of this phase of the infiltration process (decreasing i_r vs. t relationship) implied a long available time for the occurrence of these phenomena and revealed that they were continuous until the end of the run. A test of this last interpretation was made in the laboratory on an undisturbed soil core (diameter = 8 cm, height = 5 cm) that was saturated from the bottom to reproduce more or less the soil condition at the beginning of the late time i_r vs. t relationship for the field experiment (wetted soil). Then, flux densities were measured under a constant head of 1 cm for several hours. Flux densities decreased with time (figure 9), supporting the suggestion that physical soil deterioration phenomena occurring at or close to the soil surface were a possibility not to be excluded. In the field, soil alteration determined a progressive decrease of K_s but it left S practically unchanged, which is reasonable taking into account that sorptivity is more expressive of capillary effects, that mainly depend on soil matrix properties.

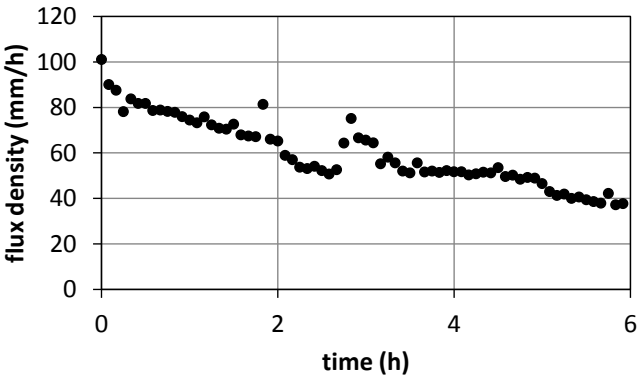

Fig. 9 Flux density against time for a constant head laboratory experiment.

For the three long runs, gravity contributed appreciably to the infiltration process in the early stages of the run (figure 10), which was in line with other findings on field soils (Smettem et al., 1998). Late time decrease of infiltration rates (figure 6) had the effect to substantially decrease this contribution.

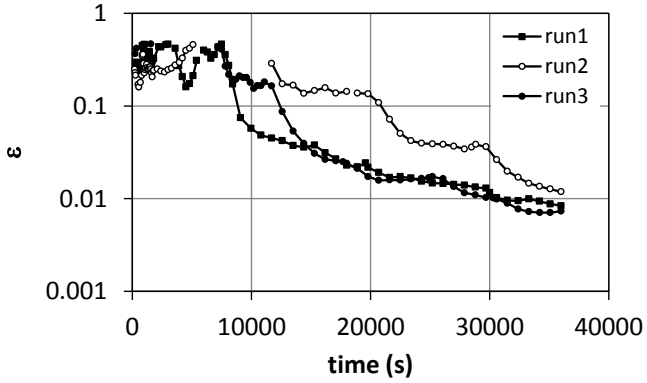

Fig. 10 Fractional influence of gravity on cumulative 3D infiltration, ε, as a function of time for the three long duration infiltration runs

Comparison between long and high runs

The results of the long duration runs and those obtained by shorter runs and a high pouring height were compared taking into account that both experiments determined some kind of soil alteration. This comparison suggested that the two perturbation factors (height from which water was poured and duration of the run) had a similar impact on the measured parameters. In particular, the mean value of K_s obtained with the long runs was within the range, not particularly wide (maximum/minimum = 1.5), of the mean K_s values obtained with the H runs. The sorptivity calculated with the long runs was appreciably higher (i.e., by a factor of 3.5) than the highest S value obtained with the H runs. Even this result was considered to be plausible since the long runs were carried out in an initially drier soil than the H runs.

B.4.3.3. Possible experimental improvements in future research

This investigation improved our knowledge of the factors affecting measurement of water transmission properties by an infiltrometer method and also allowed us to recognize what experimental improvements could be advisable to give independent support to suggested interpretations of the field data. In particular, X-ray tomography could be used to experimentally assess the reasons for the dependence of the K_s measurements on θ_i and height from which water is applied (Luo et al., 2008; Peth et al., 2010). A direct measurement of θ_s at the end of the infiltration run should also be made to check the impact of the assumed coincidence between saturated soil water content and porosity on the S and K_s calculations (Luo et al., 2008; Koestel and Larsbo, 2014; Snehota et al., 2015; Alagna et al., 2015). The problem is that measuring θ immediately after the run is difficult because of the very wet condition of the sample. Probably, the best way to make this measurement is to use the gravimetric method because indirect methods are not accurate enough. However, doing it

gravimetrically has the problem of the sample falling apart and water flowing out before one gets the sample collected. Finally, water temperature should be measured during the long infiltration runs taking into account that production of air bubbles and changes in water viscosity are expected consequences of water temperature changes (Clancy and Alba, 2011).

B.4.4. Conclusions

The height from which water was poured onto the infiltration surface influenced significantly measurement of saturated soil hydraulic conductivity, K_s, and soil sorptivity, S, with the low runs yielding higher mean values than the high runs. The effects of the height from which water was poured were particularly noticeable for K_s probably because this property depends strongly on soil structure that is susceptible to alteration due to water application. Sorptivity was less affected by the height of pouring of water since this property depends more than K_s on soil matrix, which does not change with the water application procedure. The height from which water was poured had more appreciable effects on K_s in the initially drier soil conditions, and a more soil perturbing experiment (high infiltration runs) reduced the dependence of K_s on θ_i detected with the low and less perturbing runs. High runs also had a homogenizing effect on the measured conductivity. With the long duration runs, the estimated mean conductivity was close to the means of K_s obtained with the high, but shorter, runs.

In conclusion, the application procedure of a given experimental method has to be considered a source of variability of the measured soil properties.

The results of this investigation may allow to better explain the infiltration process at the field site and also provide suggestions on how to sample the soil depending on the intended use of the data. If water application does not perturb appreciably the exposed soil surface, initially wetter soil conditions lead to less infiltration due to the reduced ability of the soil to adsorb water but also because K_s decreases as the initial soil water content increases. Disturbing the soil surface by water pouring reduces in general infiltration and it also attenuates the effect of θ_i on this process. If the objective of the field campaign is to obtain data usable to explain surface runoff generation phenomena during intense rainfall events, the most appropriate choice should be a high run, to mimic relatively prolonged rainfall effects on the soil surface. A low run is more appropriate to determine the saturated conductivity of a soil that is not directly impacted by rainfall, due for example to the presence of a mulching on the soil surface. In any case, the height from which water is poured has a reduced impact on the measured soil properties in relatively wet soil conditions. Moreover, a high and relatively

short run seems usable to test what happens, in terms of estimated saturated conductivity, when a ponding water condition is maintained on the soil surface for a long time.

In the future, the effects of the height of pouring of water and the run duration on the measured water transmission properties should be tested for different initial soil water conditions in other soils in an attempt to improve our ability to use measured soil properties for both interpreting and simulating hydrological processes, including runoff generation phenomena.

The hypothesis that the height from which water is poured onto the soil surface is a parameter useful in infiltration experiments to mimic the effect of high intensity rain on the soil hydraulic properties needs specific experimental testing. At this aim, infiltration rates should also be measured during natural or simulated rainstorms.

Acknowledgements

This study was supported by grants of the Università degli Studi di Palermo (Dottorato di Ricerca in Sistemi Agro-Ambientali, indirizzo Idronomia Ambientale; Dottorato di Ricerca in Scienze Agrarie, Forestali e Ambientali) and the Sicilian Region (Progetto CISV). All authors contributed to outline the investigation, analyze and discuss the results, and write the manuscript. Vincenzo Alagna and Simone Di Prima carried out the experimental work. The Authors wish to acknowledge the constructive review made by two anonymous Reviewers, helping us to improve the manuscript.

References

Alagna V., Bagarello V., Di Prima S., Iovino M. 2015. Determining hydraulic properties of a loam soil by alternative infiltrometer techniques. Hydrological Processes, published online, doi: 10.1002/hyp.10607

Amezketa E., Singer M.J., Le Bissonnais Y. 1996. Testing a new procedure for measuring water-stable aggregation. Soil Science Society of America Journal, 60: 888-894.

Arya L.M., Dierolf T.S., Sofyan A., Widjaja-Adhi I.P.G., van Genuchten M. 1998. Field measurement of the saturated hydraulic conductivity of a macroporous soil with unstable subsoil structure. Soil Science, 163(11): 841-852.

Assouline S., Mualem Y. 2002. Infiltration during soil sealing: The effect of areal heterogeneity of soil hydraulic properties. Water Resources Research, 38(12), 1286: 22-1 – 22-9, W12405, 11 pages.

Assouline S., Mualem Y. 2006. Runoff from heterogeneous small bare catchments during soil surface sealing. Water Resources Research, 42, W12405, 11 pages.

Bagarello V., Sgroi A. 2007. Using the simplified falling head technique to detect temporal changes in field-saturated hydraulic conductivity at the surface of a sandy loam soil. Soil & Tillage Research, 94: 283-294.

Bagarello V., Iovino M., Elrick D. 2004. A simplified falling head technique for rapid determination of field-saturated hydraulic conductivity. Soil Science Society of America Journal, 68: 66-73.

Bagarello V., Di Prima S., Iovino M., Provenzano G., Sgroi A. 2011. Testing different approaches to characterize Burundian soils by the BEST procedure. Geoderma, 162: 141-150, doi: 10.1016/j.geoderma.2011.01.014.

Bagarello V., D'Asaro F., Iovino M. 2012. A field assessment of the Simplified Falling Head technique to measure the saturated soil hydraulic conductivity. Geoderma, 187-188: 49-58, doi: 10.1016/j.geoderma.2012.04.008.

Bagarello V., Di Prima S., Iovino M. 2014a. Comparing alternative algorithms to analyze the beerkan infiltration experiment. Soil Science Society of America Journal, 78: 724-736, doi:10.2136/sssaj2013.06.0231.

Bagarello V., Baiamonte G., Castellini M., Di Prima S., Iovino M. 2014b. A comparison between the single ring pressure infiltrometer and simplified falling head techniques. Hydrological Processes, 28: 4843-4853, doi: 10.1002/hyp.9980.

Bagarello V., Castellini M., Di Prima S., Iovino M. 2014c. Soil hydraulic properties determined by infiltration experiments and different heights of water pouring. Geoderma, 213: 492-501, doi: 10.1016/j.geoderma.2013.08.032.

Bouma J. 1982. Measuring the hydraulic conductivity of soil horizons with continuous macropores. Soil Science Society of America Journal, 46: 438-441.

Brooks R.H., Corey C.T. 1964. Hydraulic properties of porous media. Hydrol. Paper 3, Colorado State University, Fort Collins.

Burdine N.T. 1953. Relative permeability calculation from pore size distribution data. Petr. Trans. Am. Inst. Min. Metall. Eng., 198: 71-77.

Carsel R.F., Parrish R.S. 1988. Developing joint probability distributions of soil water retention characteristics. Water Resources Research, 24: 755-769.

Cerdà A. 1998. Soil aggregate stability under different Mediterranean vegetation types. Catena, 32: 73-86.

Chen, L., Sela, S., Svoray, T., Assouline, S. 2013. The role of soil surface sealing, microtopography and vegetation patches in rainfall-runoff processes in semiarid areas. Water Resources Research, 49(9): 5585-5599.

Clancy K., Alba V.M. 2011. Temperature and time of day influence on double-ring infiltrometer steady-state infiltration rates. Soil Science Society of America Journal, 75(1): 241-245.

Collis-George N., Laryea K.B. 1971. Infiltration behaviour of structurally unstable soils under ponded and non-ponded conditions. Australian Journal of Soil Research, 9: 7-20.

Di Prima S., Lassabatere L., Angulo-Jaramillo R. Bagarello V., Iovino M. 2015. Testing a new automated single ring infiltrometer for Beerkan infiltration experiments. Geoderma, 262: 20–34, doi: 10.1016/j.geoderma.2015.08.006.

Elrick D.E., Reynolds W.D. 1992. Infiltration from constant-head well permeameters and infiltrometers. p.1-24. In G.C. Topp, W.D. Reynolds and R.E. Green (eds.), Advances in Measurement of Soil Physical Properties: Bringing Theory into Practice, SSSA Special Publication no.30, Madison, WI, USA.

Elrick D.E., Reynolds W.D., Geering H.R., Tan K.A. 1990. Estimating steady infiltration rate times for infiltrometers and permeameters. Water Resources Research, 26(4): 759-769.

Faybishenko B.A. 1995. Hydraulic behavior of quasi-saturated soils in the presence of entrapped air. Water Resources Research, 31: 2421-2435.

Gardner W.R. 1958. Some steady-state solutions of the unsaturated moisture flow equation with application to evaporation from a water table. Soil Science, 85(4): 228-232.

Haverkamp R., Ross P.J., Smettem K.R.J., Parlange J.Y. 1994. Three-dimensional analysis of infiltration from the disc infiltrometer: 2. Physically based infiltration equation. Water Resources Research, 30(11): 2931-2935.

Hillel D., Mottes J. 1966. Effect of plate impedance, wetting method and aging on soil moisture retention. Soil Science, 102: 135-140.

Jarrett A.R., Fritton D.D. 1978. Effect of entrapped soil air on infiltration. Transactions of the ASAE, 21(5): 901-906.

Jarvis N., Koestel J., Messing I., Moeys J., Lindahl A. 2013. Influence of soil, land use and climatic factors on the hydraulic conductivity of soil. Hydrology and Earth System Sciences, 17: 5185-5195.

Koestel J., Larsbo M. 2014. Imaging and quantification of preferential solute transport in soil macropores. Water Resources Research, 50: 4357-4378.

Lado M., Paz A., Ben-Hur M. 2004. Organic matter and aggregate size interactions in infiltration, seal formation, and soil loss. Soil Science Society of America Journal, 68: 935-942.

Lassabatère L., Angulo-Jaramillo R., Soria Ugalde J.M., Cuenca R., Braud I., Haverkamp R. 2006. Beerkan estimation of soil transfer parameters through infiltration experiments – BEST. Soil Science Society of America Journal, 70: 521-532.

Lassabatere L., Angulo-Jaramillo R., Soria-Ugalde J.M., Šimůnek J. Haverkamp R. 2009. Numerical evaluation of a set of analytical infiltration equations. Water Resources Research, 45, W12415, 20 pages.

Le Bissonnais Y. 1996. Aggregate stability and assessment of soil crustability and erodibility: I. Theory and methodology. European Journal of Soil Science, 47(4): 425-437.

Lilliefors H.W. 1967. On the Kolmogorov-Smirnov test for normality with mean and variance unknown. Journal of the American Statistical Association, 62(318): 399-402.

Liu L., Chen J. 2015. The effect of conservation practices in sloped croplands on soil hydraulic properties and root-zone moisture dynamics. Hydrological Processes, 29: 2079-2088, doi: 10.1002/hyp.10348.

Liu H., Lei T.W., Zhao J., Yuan C.P., Fan Y.T., Qu L.Q. 2011. Effects of rainfall intensity and antecedent soil water content on soil infiltrability under ranfall conditions using the run off-on-out method. Journal of Hydrology, 396: 24-32.

Logsdon S.D., Jaynes D.B. 1996. Spatial variability of hydraulic conductivity in a cultivated field at different times. Soil Science Society of America Journal, 60: 703-709.

Luo L., Lin H., Halleck P. 2008. Quantifying soil structure and preferential flow in intact soil using X-ray computed tomography. Soil Science Society of America Journal, 72: 1058-1069.

Mubarak I., Mailhol J.C., Angulo-Jaramillo R., Ruelle P., Boivin P., Khaledian M. 2009. Temporal variability in soil hydraulic properties under drip irrigation. Geoderma, 150: 158-165.

Peth S., Nellesen J., Fischer G., Horn R. 2010. Non-invasive 3D analysis of local soil deformation under mechanical and hydraulic stresses by mu CT and digital image correlation. Soil & Tillage Research, 111: 3-18.

Philip J.R. 1969. Theory of infiltration. Advances in Hydroscience, 5: 215-296.

Prieksat, M.A., Kaspar, T.C., Ankeny, M.D. 1994. Positional and temporal changes in ponded infiltration in corn field. Soil Science Society of America Journal, 58: 181-184.

Reynolds W.D. 2008a. Chapter 76. Saturated hydraulic properties: well permeameter. p.1025-1042 in Carter M.R. and Gregorich E.G. (eds.), Soil Sampling and Methods of Analysis, 2nd edition. Canadian Society of Soil Science, Boca Raton, FL, USA.

Reynolds W.D. 2008b. Chapter 77. Saturated hydraulic properties: ring infiltrometer. p.1043-1056 in Carter M.R. and Gregorich E.G. (eds.), Soil Sampling and Methods of Analysis, 2nd edition. Canadian Society of Soil Science, Boca Raton, FL, USA.

Reynolds W.D., Elrick D.E. 1990. Ponded infiltration from a single ring: I. Analysis of steady flow. Soil Science Society of America Journal, 54: 1233-1241.

Reynolds W.D., Elrick D.E. 2002. 3.4.3.2.b Pressure infiltrometer. p.826-836. In J.H. Dane and G.C. Topp (co-eds.), Methods of Soil Analysis, Part 4, Physical Methods, Number 5 in the Soil Science Society of America Book Series, Soil Science Society of America, Inc., Madison, WI, USA.

Reynolds W.D., Bowman B.T., Brunke R.R., Drury C.F., Tan C.S. 2000. Comparison of tension infiltrometer, pressure infiltrometer, and soil core estimates of saturated hydraulic conductivity. Soil Science Society of America Journal, 64: 478–484.

Reynolds W.D., Elrick D.E., Youngs E.G. 2002. 3.4.3.2.a Single-ring and double- or concentric-ring infiltrometers. p.821-826. In J.H. Dane and G.C. Topp (co-eds.), Methods of Soil Analysis, Part 4, Physical Methods, Number 5 in the Soil Science Society of America Book Series, Soil Science Society of America, Inc., Madison, WI, USA.

Sakaguchi A., Nishimura T., Kato M. 2005. The effect of entrapped air on the quasi-saturated soil hydraulic conductivity and comparison with the unsaturated hydraulic conductivity. Vadose Zone Journal, 4: 139-144.

Schiettecatte W., Jin K., Yao Y., Cornelis W.M., Lu J., Wu H., Verbist K., Cai D., Gabriels D., Hartmann R. 2005. Influence of simulated rainfall on physical properties of a conventionally tilled loess soil. Catena, 64: 209-221.

Smettem K.R.J., Ross P.J., Haverkamp R., Parlange J.Y. 1995. Three-dimensional analysis of infiltration from the disk infiltrometer. 3. Parameter estimation using a double-disk tension infiltrometer. Water Resources Research, 31(10): 2491-2495.

Smettem K.R.J., Ross P.J., Haverkamp R., Parlange J.Y.,Gregory P.J. 1998. Laboratory and field application of a twin disc infiltrometer for measurement of soil hydraulic properties. p.41-51. In P. Dillon and I. Simmer (eds.), Shallow Groundwater Systems, IAH International Contribution to Hydrogeology 18. Taylor & Francis, London, UK.

Snehota M., Jelinkova V., Sobotkova M., Sacha J., Vontobel P., Hovind J. 2015. Water and entrapped air redistribution in heterogeneous sand sample: Quantitative neutron imaging of the process. Water Resources Research, 51: 1359-1371.

Somaratne N.M., Smettem K.R.J. 1993. Effect of cultivation and raindrop impact on the surface properties of an Alfisol under wheat. Soil & Tillage Research, 26: 115-125.

Talsma T., Lelij A.V.D. 1976. Infiltration and water movement in an in situ swelling soil during prolonged ponding. Australian Journal of Soil Research, 14(3): 337-349.

van de Giesen N.C., Stomph T.J., de Ridder N. 2000. Scale effects of Hortonian overland flow and rainfall–runoff dynamics in a West African catena landscape. Hydrological Processes, 14: 165-175.

van Genuchten M.Th. 1980. A closed form equation for predicting the hydraulic conductivity of unsaturated soils. Soil Science Society of America Journal, 44: 892-898.

Verbist K., Torfs S., Cornelis W.M., Oyarzún R., Soto G., Gabriels D. 2010. Comparison of single- and double-ring infiltrometer methods on stony soils. Vadose Zone Journal, 9: 462-475.

Verbist K.M.J., Cornelis W.M., Torfs S., Gabriels D. 2013. Comparing methods to determine hydraulic conductivities on stony soils. Soil Science Society of America Journal, 77: 25-42.

Wang Z., Feyen J., van Genuchten M.Th., Nielsen D. 1998. Air entrapment effects on infiltration rate and flow instability. Water Resources Research, 34(2): 213-222.

White I., Sully M.J. 1987. Macroscopic and microscopic capillary length and time scales from field infiltration. Water Resources Research, 23(8): 1514-1522.

Yilmaz D., Lassabatère L., Angulo-Jaramillo R., Deneele D., Legret M. 2010. Hydrodynamic characterization of basic oxygen furnace slag through an adapted BEST method. Vadose Zone Journal, 9: 1-10.

Part C: Effect of water repellency on infiltration processes

C.1 Background

Soil water repellency (SWR) or hydrophobicity is a surface property of soil particles (Doerr and Ritsema, 2005) and it is due to coating of mineral particles with organic compounds which reduces soil wettability. Water repellency is a worldwide phenomenon so that it seems not to be geographically or climatically dependent (Angulo-Jaramillo et al., 2016). Moreover, soil water repellency has been reported in different soil types from sand dune to forest soils, burned areal, under several vegetation covers and land uses (e.g. Ritsema, 2001; Buczko et al., 2005; Robichaud 2010; Chrenková et al., 2014). This soil property, which may vary from few to 50 cm deep (Dekker and Ritsema 1994), has a high impact on soil hydrological processes and hydraulic properties (Doerr et al., 2000). Indeed, it can reduce water infiltration capacity with a consequent increased surface runoff and soil erosion, especially in hilly areas. It reduces hysteresis of the water retention characteristic (Ritsema et al., 1998; Bauters et al., 2000) and the hydraulic conductivity function (Nieber et al., 2000). In repellent soils the filtering function can be reduced with development of preferential flow paths, commonly named fingers (Ritsema and Dekker, 1994). Therefore, the vertical water flow is concentrated on a small section resulting in increased risk of groundwater contamination by leaching of soluble nutrients or pollutants. Soil water repellency has repercussions on microbial activity and agricultural production because the reduced availability of water in the root zone causes reduction of seed emergence and plant growth (Blackwell, 2000). However, when slight, this phenomenon can have positive effects on aggregates stability (Piccolo and Mbagwu, 1999; Mataix-Solera and Doerr, 2004; Goebel et al., 2005) and, moreover, it may reduce the soil water evaporation (Imeson et al., 1992; Yang et al., 1996). Hydrophobicity is not a irreversible soil property but is known to follow short-term or seasonal variations. Its reversible nature seems mainly associated with fluctuations in soil moisture, but knowledge of the processes involved in the changes of status from hydrophobic to hydrophilic and vice versa is still incomplete (Doerr et al., 2000).

The study of soil water repellency is challenging due to the combined influence of several factors. However, organic matter is the main and most documented contributor of soil water repellency. Organic matter content decreases along soil profile and, therefore, water repellency can be reduced with soil depth (Doerr et al., 2000; Vogelmann et al., 2010) but leaching of hydrophobic compounds can increase hydrophobicity of lower soil layers (Vogelmann et al., 2013a). Although organic matter is the main cause of hydrophobicity, it

was argued in some studies that soil organic matter (SOM) and SWR may have both a negative correlation (Teramura, 1980) or no relationship (DeBano, 1992; Wallis et al., 1993). This leads to the conclusion that the degree of SWR depends on the quality rather than the quantity of soil organic matter (Wallis and Horne, 1992).

The hydrophobic compounds contained in soil organic matter depend on types of decomposed plant material (McGhie and Posner, 1987; Mataix-Solera and Doerr, 2004; Ellies et al., 2005), exudates produced by roots fungi or by microbial activity (Bond and Harris, 1964; Savage et al., 1969; Dekker and Ritsema, 1996; Schaumann et al., 2007; Fisher et al., 2010), trees resins, waxes or aromatic oils (Doerr et al., 2000; Ferreira et al., 2000). The humic substances contained in SOM have a high molecular weight, long-chains of carbon and different structural formula. They can be divided in: (i) fulvic acids which are soluble in water under all pH conditions, (ii) humic acids which are not soluble in water under acidic conditions (pH < 2) but are soluble at higher pH values and (iii) humins which are not soluble in water (Stevenson, 1994). Different compounds are suspected to be the cause of soil water repellency that can be divided into two groups. The first group is represented by the aliphatic hydrocarbons, which are elongated chain containing hydrogen and carbon atoms. These molecules are non-polar, therefore they do not have positive or negative charges at either end of the chain thus resulting almost insoluble in water. The second consist of amphiphilic compounds formed by hydrocarbon chain. These substances are soluble given they have a functional group with a positive or negative charge in one end. This end of the chain is hydrophilic, whereas the other is hydrophobic (Fig. 1(I)). Generally, the amphiphilic molecules are water soluble, but when their polar ends are bonded to a surface, they produce a hydrophobic coating as illustrated in Fig. 1 (IIa). It was stated by McIntosh and Horne (1994) that both groups cause water repellency, but others authors have claimed that the polar molecules like fatty acids or waxes are mainly responsible of the hydrophobic coating on soil particles (Ma'shum et al., 1988; Hudson et al., 1994; Franco et al,. 2000).

The organic coating of mineral soil particles with a continuous film containing hydrophobic compounds increases the contact angle at the liquid-solid interface, ω, to values greater than 90°. In these circumstances water does not wet the soil spontaneously (Letey et al., 2000).

Soil water repellency is a function of soil surface chemistry (Roy and McGill, 2002), in particularly it is a function of the surface tension (also called surface free energy) of the solid-vapor interface, γ^{sv}, in soil. For understand this concept and consequently the water entry in a repellent soil, let us consider a system consisting of three adjacent phases: soil (s),

liquid (l), and vapor (v) that are meeting at a common interline TPL (three phase line) (Sheludko, 1966; de Gennes, 1985), as depicted in figure 2. Water repellent soils have a lower surface tension at soil vapor interface, γ^{sv}, than the wettable soils. Measuring the surface tension at soil-vapor interface is difficult, but it can be evaluated using related parameters. A useful indicator of the free energy of the solid-vapor interface in soils is represented by the contact angle, ω. The contact angle is related to the free energies of the three interfaces meeting at the solid-liquid-vapor contact line by Young equation (1855):

$$\cos\omega = \frac{\gamma^{sv} - \gamma^{sl}}{\gamma^{lv}} \qquad (1)$$

where γ^{sv}, γ^{sl}, and γ^{lv} are the free energies (J m^{-2}) at solid-vapor, solid-liquid and liquid-vapor interfaces, respectively.

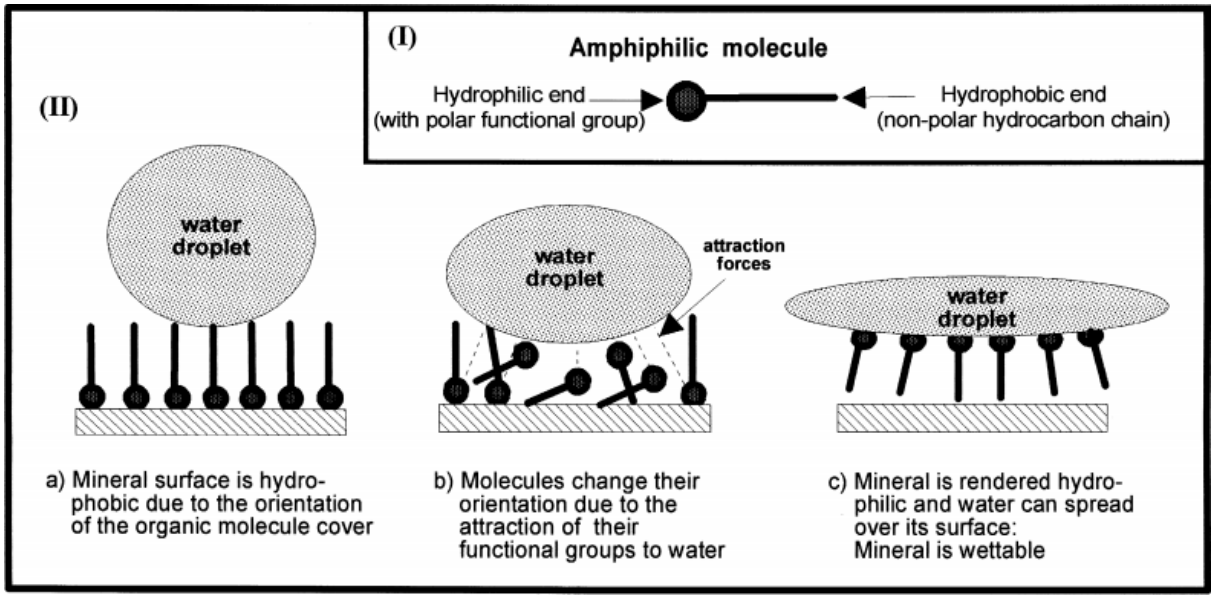

Fig. 1. Schematic representation of (I) an amphiphilic molecule and (II/a–c) changes in orientation of such molecules on a mineral surface while in contact with water (based on Tschapek, 1984; Ma'shum and Farmer, 1985; Velmulapalli, 1993) (adapted from Doerr et al., 2000).

The surface free energy of water, γ^{lv}, is equal to 72.75 x 10^{-3} J m^{-2} at 21 °C (Adamson and Petry, 1997), and for a complete wetting condition, the soils must have a surface free energy γ^{sv} significantly higher than surface tension of water. When water comes in contact with soil surface two cases may occur:

a) for $\gamma^{sv} \geq \gamma^{sl} + \gamma^{lv}$, no mechanical equilibrium is possible between the three phases and the contact angle is zero because three phase line does not exists. Water spreads spontaneously in a continuous film on soil surface (Figure 2 A).

b) for $\gamma^{sv} < \gamma^{sl} + \gamma^{lv}$ water forms a droplet on the smooth surface soil in mechanical equilibrium and the contact angle ω is defined by the Young equation (eq. 1). In this case, the following possibilities may arise:

   i. if $\gamma^{sv} > \gamma^{sl}$ then cos ω > 0, since ω < 90° water is on a hydrophilic soil (Figure 2 B),

   ii. if $\gamma^{sv} = \gamma^{sl}$ then cos ω = 0, then ω = 90° that is the limit case between complete wetting and partial wetting of soil (Figure 2 C),

   iii. if $\gamma^{sv} < \gamma^{sl}$ then cos ω < 0, therefore ω > 90° water is on a hydrophobic soil (Figure 2 D).

Summing up, if ω is greater than 90° water will not spontaneously penetrate into the soil, and therefore an external force is required to move the air and wet the soil. This conditions is referred to as "extreme water repellency. In contrast, subcritical repellency conditions can occur when the water-solid contact angle is less than 90° but not zero (Tillman et al., 1989). In this case the water infiltration is not prevented entirely but it is delayed by the time required to displace air.

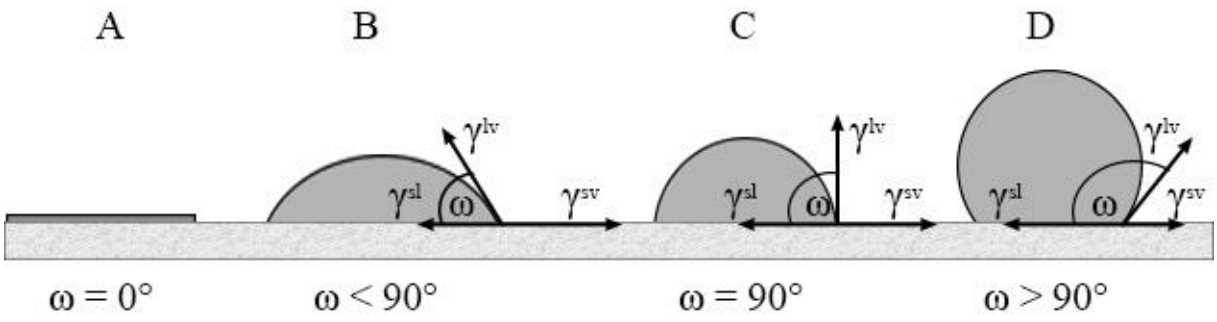

Fig. 2. Interfacial tensions at the three phase line (TPL) of the adjacent liquid (l), solid (s) and vapour (v) phase for various contact angles ω (readapted from Diehl, D. 2009)

Additional factors involved in SWR are pH, soil texture, temperature and water content. Acid soils seem to be more prone to develop SWR than alkaline soils (Dekker and Jungerius, 1990; Cerdà and Doerr, 2007; Mataix-Solera et al., 2007). However, Mataix-Solera and Doerr (2004) found manifestation of the phenomenon in calcareous soils of Spain. Soils with coarser particles are more susceptible to develop water repellency due to their smaller surface area (De Bano, 1981), but also soils with large amount of clay were found to exhibit extreme water repellency (Crockford et al., 1991). Temperature play an important role in SWR because water surface tension and viscosity change. High temperature reached during wildfire determines the volatilization of hydrophobic organic substances which condense in

cooler soil regions thus causing an increase of SWR (Savage, 1974). Several authors have investigated the effects of temperature on oven-dried soils and they found higher SWR levels than those measured on air-dried or field-moist samples (e.g. Dekker et al., 2001; de Jonge et al., 1999; Buczko et al., 2002-2005). They referred to "potential water repellency" if SWR was determined on oven-dried samples, whereas "actual water repellency" if SWR was determined on air-dried or field-moist samples.

The interaction between amphiphilic organic molecules and soil particles is largely governed by water content (Doerr et al., 2000; Ellies et al., 2005). As soil dries, organic particles bind to soil particles. When soil is being wetted, these particles are liberated into solution. Drying may intensify soil water repellency as larger hydrophobic portions of organic matter remain exposed, while wetting can mitigate soil water repellency by exposing hydrophilic portions (Doerr, 1998; Lichner et al., 2013a). Therefore, severe water repellency is expected following prolonged dry, warm summers with a transition from water repellent (hydrophobic) to wettable (hydrophilic) conditions during the autumn/winter months (Buczko et al., 2005; Lichner et al., 2013a; Rodríguez-Alleres et al., 2007). Dry soil becomes wettable above a threshold water content. Likewise moist, wettable soil may become water repellent when dried. This threshold is called the critical water content (CWC). However, rather than a single soil moisture value, it is most commonly reported as a range or a transition zone defined by two water contents (de Jonge et al., 1999; Dekker and Ritsema, 1994; Dekker et al., 2001). The lower one defines the water content below which the soil is water repellent, whereas the higher one represents the water content above which the soil is wettable. Despite the soil moisture vs. water repellency relationship has been the subject of several studies (e.g. Doerr et al., 2000; Dekker et al., 2001; Vogelmann et al., 2013b) little is known about the mechanisms involved in the breakdown and re-establishment of water repellency that follow under prolonged wet conditions and during extended dry periods and on the effects of soil moisture on hydrophobicity.

C.1.1. Assessment of soil water repellency

Soil water repellency can be measured either in the field or in the laboratory, however, not all the existing techniques may be used in both circumstances. Several techniques were proposed to measure the contact angle between water and soil surface, but direct measurement of ω is difficult and inconsistent (Letey et al., 2000). Some of these methods, like the capillary rise method (Emerson and Bond, 1963), the Wilhelmy plate (Bachmann et al., 2003) and the

sessile drop (Bachmann et al., 2000) require expensive equipments and are time-consuming and therefore were not largely applied.

Water repellent soils can be characterized quantitatively, both in situ and in laboratory, by the Water Drop Penetration Time (WDPT) test (Van't Woudt, 1959) and the Molarity of an Ethanol Droplet (MED) test that is also known as the Ethanol Percentage, EP, test or the Critical Surface Tension, CST, test (Letey, 1969). The two tests convey two different information of the same phenomenon which has a dynamic nature.

The WDPT indicates the dynamics of the contact angle in water-soil interface, namely the time required for ω to change from its original value (> 90°) to a value approaching 90° that allows drop infiltration. Therefore, it is not necessarily an index of the water repellency but more precisely an index of the persistence of water repellency (Cerdà and Doerr, 2007; Letey et al., 2000). The test involves applying a drop of distilled water onto the smoothed soil surface and recording the time required for its complete penetration. Initially, the water drop applied on soil surface does not penetrate indicating that ω is greater than 90°. As time of soil exposure to water increases, the characteristics of soil surface change so that the contact angle decreases from more than 90° to less than 90° and the drop eventually penetrates. To distinguish between wettable and repellent soils, an arbitrary time threshold of 5 s was taken into account for the complete drop infiltration without a specific physical meaning (Richardson, 1984) . Therefore, if the WDPT exceeds 5 s the soil is considered water repellent (ω >90°) vice versa hydrophilic (ω <90°). However, over the years, several authors proposed WDPT classifications with different categories (Table 1). However, the time limit of 5 s was generally adopted to identify wettable conditions.

The time required for the complete penetration of the drop can vary from a few seconds to hours. Therefore, drop can be subject to evaporation phenomena that influence the results especially in very hydrophobic soils. To avoid this inconvenient, the drops should be covered by a transparent capsule.

There is not a standard protocol regarding the number of drops to be used as well the volume of each drop. On repacked samples prepared with sieved soil from three to five drops can be enough to obtain representative data due to the smoothed surface and low variability of soil properties (e.g. Dekker and Ritsema, 1994; Doerr et al., 2006; Wallach and Graber, 2007). Hallin et al. (2013) proposed a standard protocol that allows to estimate the mean WDPT value with an error of ±10% at 95% confidence using 30 drops of 80 to 200 μL size.

Table 1 Classes of water repellency persistence based on WDPT (s) values according to various authors

Notation	Classes	Adams et al. (1969)	Roberts and Carbon (1971)	Dekker and Jungerius (1990)	Bisdom et al. (1993)
Wettable	0	< 10	< 1	< 5	< 5
Slightly repellent	1	10 – 60	1 – 10	5 – 60	5 – 60
Strongly repellent	2	–	10 – 60	60 – 600	60 – 600
Severely repellent	3	> 60	> 60	600 – 3600	600 – 3600
	4	–	–	3600 – 10800	> 3600
Extremely repellent	5	–	–	10800 – 21600	–
	6	–	–	> 21600	–

The WDPT test, especially in conditions of high hydrophobicity, may yield uncertain results due to the complicated identification of the time when infiltration of water drop applied into the soil is complete. Despite these drawbacks, the WDPT test, for its simplicity, and the low cost of equipment required is the most commonly adopted method by the scientific community to assess SWR.

The MED (or EP) test is a rapid method to assess soil water repellency. It represents an indirect measurement of the soil surface tension. As mentioned in the previous paragraph, the liquid-solid angle ω is related to the surface tension of the liquid applied. Therefore, reducing the surface tension of the liquid (γ^{lv}) increases the wettability of a repellent soil because the contact angle between the two media decreases. The surface tension can be lowered through the use of a non-polar solvent such as ethanol. As matter of fact, the ethanol has an effective zero contact angle (Tillman et al., 1989). Therefore, preparing different mixtures with increasing ethanol to water concentration decreases the surface tension of water so that the mixture can infiltrate spontaneously within a specified time. The surface tension of such mixtures depends in a nonlinear way from the volumetric ethanol content (Butler and Wightman, 1932; Vazquez et al., 1995). According to Roy and McGill (2002) the surface tension of water–ethanol mixtures γ^{lv} can be calculated as follow:

$$\gamma^{lv} = 0.06105 - 0.01475 \times \ln\left(\frac{EP}{5.8} + 0.5\right) \quad (2)$$

where EP is the volumetric ethanol content (%).

The test involves the application of drops of mixtures, with known concentration of ethanol, which must infiltrates within a predetermined time (generally 5 s). Therefore, the test consists in finding the surface tension of the mixture which is able to wet a soil with contact angle of 90°. If the surface tension of the drop mixture applied into the soil is lower than that

corresponding to 90°, it will penetrate rapidly. Vice versa the infiltration of the applied liquid mixture will be slightly retarded thus indicating a higher surface tension than the 90° soil surface tension. In other words, if a droplet of mixture with high ethanol concentration, i.e. lower liquid surface tension (γ^{lv}), is absorbed within the time threshold chosen it denotes high degree of soil hydrophobicity. Obviously the smaller is the ethanol increment used, the more accurate is the determination of the surface tension. For instance, Buczko et al. (2002) used ethanol concentrations of 0, 1, 2, 3, 4, 5, 6, 8, 10, 15, 20, 30 and 40% by volume.

The threshold time within which the droplet should infiltrate varies with the author from 3 to 10 s (King, 1981; Crockford et al., 1991; Harper and Gilkes, 1994; Doerr, 1998; Buczko et al., 2002). However, Doerr (1998) suggested short penetration time to avoid the possible decay of hydrophobicity and the fast evaporation of ethanol which has a lower evaporation temperature of water. The drop volume seems to have no effects on the ω that depends only on the ethanol concentration and temperature.

King (1981) and Doerr (1998) on basis of their investigations carried out on soils from Portugal and Australia, respectively, have proposed the classifications listed on table 2 to assess the degree of water repellency.

Table 2 Classes of degree of water repellency proposed by King (1981) and Doerr (1998)

King (1981)			Doerr (1998)		
Notation	Classes	MED	Notation	Classes	EP %
Not significant	1	-	Very hydrophilic	1	0
Very low	2	-	Hydrophilic	2	3
Low	3, 4, 5	0 - 1	Slightly hydrophobic	3	5
Moderate	6, 7, 8	1.2 - 2.2	Moderately hydrophobic	4	8.5
Severe	9, 10	2.4 - 3	Strongly hydrophobic	5	13
Very severe	11, 12	> 3.2	Very strongly hydrophobic	6	24
-	-	-	Extremely hydrophobic	7	36

The degree of water repellency can be expressed either as surface tension, molarity or ethanol percentage of the solution that infiltrates the soil in less than the chosen penetration time.

Satisfactory correlations between WDPT and MED were obtained for instance by Crockford et al. (1991) or Harper and Gilkes (1994) but not in the investigation carried out by Dekker and Ritsema (1994). According to Doerr (1998) for high level of hydrophobicity a good correlation should be expected which can worsen for low water repellency conditions. According to Buczko et al. (2002) reasons for scattering in correlation are the i) different physical meaning of the two tests since the WDPT gives information about the persistence

whereas the MED test about the degree of SWR, and ii) the applied measurement process and support volumes, because the WDPT test is related to the infiltration of a single water droplet while the MED test gathers information by several drops that inevitably must be applied in different points on the soil. Thus, despite synthesized in a single value, the MED or EP test is to a greater extent affected by intrinsic small-scale heterogeneity.

The MED test is advantageous because it is faster than the WDPT test but the second has a more direct hydrological relevance (Doerr, 1998).

However, both tests do not seem to be suitable to evaluate conditions of subcritical water repellency since the drops of applied liquid rapidly infiltrate. To overcome this problem Tillman et al. (1989) developed a more sensitive and physically meaningful index of water repellency based on measurement of soil sorptivity. This index, called water repellency index (*RI*), is based on soil infiltration measured with water and ethanol. As for the MED test, it is used to describe the degree of soil water repellency. In particular, RI is the adjusted ratio between soil sorptivity values measured ethanol and water. The first presents lower contact angle with the hydrophobic surface, so it is not influenced by repellency and provides a measurement of transport of liquid in soil.

Tension infiltrometers were usually used to determine the sorpitivities of both infiltrating liquids. A small negative pressure head is applied so that the flow is driven by capillarity rather than gravity and the macropore influence is reduced or negligible. A miniaturized laboratory infiltrometer (Leeds-Harrison et al. 1994) was used by Hallett et al. (2001) and Vogelmann et al. (2013a) to determine soil water repellency at the aggregate scale. The minidisk infiltrometer (MDI, Decagon Device Inc., 1998) and standard infiltrometers (Perroux and White, 1988) were used in situ by Jarvis et al. (2008), Lewis et al. (2006), Robichaud et al. (2008) and Hunter et al. (2011). The impact of disc size on measurements of soil water repellency index (RI) was studied by Hunter et al. (2011) who suggested that the MDI is appropriate for field assessment of SWR. According to these authors the MDI has to be preferred to the standard tension infiltrometer because it is more compact, less expensive, easily portable and requires less liquid and sampling time.

The sorptivities, S (L $T^{-1/2}$), of both liquid is determined by the following equation:

$$S = \sqrt{\frac{Qf}{4br}} \tag{3}$$

where: Q (L^3T^{-1}) corresponds at the steady rate of flow during early-time infiltration (Hallett et al., 2001), f is the total porosity, b is a parameter taken as 0.55 (White and Sully, 1987) and r (L) is the radius of the infiltrometer.

The repellency index, RI, as suggested by Tillman et al. (1989) relates the sorptivity of pure water, S_w, and ethanol, S_e, in the following relationship:

$$S_w = \left[\frac{(\mu_e / \gamma_e)^{1/2}}{(\mu_w / \gamma_w)^{1/2}} \right] S_e \quad (4)$$

where: μ_e is the viscosity of ethanol (95%) at 20 °C (0.0012 N s m^{-2}), γ_e is the surface tension of ethanol (0.023 N m^{-1} at 20 °C), μ_w is the viscosity of water (0.0010 N s m^{-2} at 20 °C) and γ_w is the surface tension of water (0.073 N m^{-1} at 20 °C). Using these values the eq. (4) is simplified into:

$$S_w = 1.95 \cdot S_e \quad (5)$$

Consequently, the Tillman et al. (1989) RI index becomes:

$$RI = 1.95 \frac{S_e}{S_w} \quad (6)$$

The constant 1.95 takes into account the differences of surface tension and viscosity between ethanol and water. Consequently, in a non-repellent soil the ethanol sorptivity can never be greater than the sorptivity of water. Therefore, RI cannot be greater than 1.95 (Wallis et al., 1991).

Gryze et al. (2006) used the RI value obtained with eq. (6) to estimate the soil-water contact angle, ω, as:

$$\omega = \arccos\left(\frac{1}{RI} \right) \quad (7)$$

The RI index, given its robustness and being a hydrologically-based index, is becoming commonly used in field investigation on soil water repellency. Also the use of MDI to determine the sorptivities of both infiltrating liquids is equally popular (e.g. Lewis et al., 2006; Robichaud et al., 2008). In contrast to the droplet scale methods, the use of this device allows to evaluate the effect of water repellency on infiltration process. Moreover, the

sampled area by the MDI is 100 times greater than that sampled with a droplet test (0.14 cm^2) thus allowing to take into account the small-spatial variability of SWR.

In chapter C.2, the minidisk infiltrometer was used with the aim to investigate the effects of vegetation and soil water content on SWR in the upper soil layers of a Mediterranean managed pine woodland. The SWR was detected by the common WDPT test and the RI index in two sampling dates and at two sampling depths along the soil profile. In particular, the thatch formed by decomposed vegetal material and the underlying mineral soil were sampled. Investigation highlights a inner drawback of the RI index in that the two experiments cannot be conducted at exactly the same site due to the influence of the antecedent soil water content on both ethanol and water sorptivities. To overcome spatial variability problems related to double infiltration experiment, in the investigation the possibility to use repellency indices obtained by a single infiltration experiment like the index proposed by Lichner et al. (2013b) is tested. This index, called water repellency cessation time, *WRCT*, is defined as the time corresponding to the intersection of the two straight lines representing the cumulative infiltration vs. square root of time relationship for hydrophobic and near wettable conditions. All the water repellency indices used in the investigation unanimously detected a severe hydrophobicity of the *Pinus pinaster* thatch but also a severe occurrence of SWR in the underlying mineral soil. In a glade area, within the forested site, the WRCT was able to detect sub-critical water repellency conditions that were not identified by the classical WDPT test.

In chapter C.3, the results obtained from the previous investigation were compared with those collected in another pine forest located in Eastern Spain. The two Mediterranean forests are planted with different tree species of pine family (*Pinus pinaster* in Italy and *Pinus halepensis* in Spain) but undergo similar climatic, pedological and management conditions. A specific objective of the investigation is focused on the individuation of indices derived from a single MDI experiments carried out only with water. Given that the possibility to derive a repellency index from a unique water infiltration experiment conducted by the MDI at a single site has been recognized as extremely advantageous also considering the potential simplicity of the technique a modified repellency index, RI_m, is proposed and developed in the chapter. The proposed repellency index RI_m follows the same approach of WRCT index but, unlike this, is based on a measurements of an intrinsic soil property. In fact, it is defined as the ratio of the sorptivities estimated at the late (wettable) and early (repellent) stages of the water cumulative infiltration data. Both the WRCT and RI_m indices were found

to be correlated with the traditional WDPT test and more common and cumbersome RI test, therefore can be proposed as alternative procedures for SWR assessment. The MDI-based indices were more able to signal sub-critical SWR than the traditional WDPT tests. Finally, it was found that the vertical distribution of hydrophobic compounds was led by the hydraulic conductivity of the overlying thatch given that the mineral soil of Spanish site did not showed water repellency conditions compared to the same Italian soil layer.

The chapter C.4 deals with a another different issue linked to the use of MDI infiltrometer. The datasets considered is that of chapter C.3 incremented with data collected in a fire-affected forest located in Spain in which different post-fire management strategies were implemented. The main focus was on the use of different methods of sorptivity estimation to assess the best calculation procedure of the water repellency index from water/ethanol sorptivity measurements conducted by the MDI. Based on current knowledge, most authors (e.g. Lewis et al., 2006; Robichaud et al., 2008; Hunter et al., 2011) estimate the sorptivity, S_0 ($L\ T^{-0.5}$) to be included in Eq. (6), as the infiltration rate out of a MDI during a fixed time interval, generally 1-5 min according the Philip's (1957) equation for horizontal infiltration

$$S = \frac{I}{\sqrt{t}} \tag{8}$$

where I (L) is cumulative infiltration and t (T) is time. However, investigation showed that the early-time linear regression of the I vs. √t data neglects the effects of gravity and lateral capillary flux at the source thus resulting in S_0 overestimations especially for the ethanol infiltration test in which the liquid flow is very fast and the steady-state flow was generally reached in less than 1 min. For the water infiltration experiments, flow out of the MDI did not start during the first 1 min of the run thus making it impossible to estimate S_0 according the criteria based on the use of Eq. (8). To overcome this drawbacks, it is proposed to fit the infiltration data collected from early to intermediate times with the two-term cumulative infiltration equation proposed by Haverkamp et al. (1994). Unbiased estimation of soil sorptivity were obtained applying the two linearization techniques known as Cumulative Linearization, CL, method and Differentiated Linearization, DL, method (see chapter A.1). Finally, using the total cumulative water infiltration data linearized in the form of both CL or DL methods it was possible to obtain the new repellency index RI_s defined as the ratio between the slopes of the linearized data in the wettable and repellent stages of the infiltration process. For the experimental conditions considered, the mean values of the new repellency index RI_s were once again significantly correlated with the RI and WDPT indices thus

showing the potential reliability of soil hydrophobicity assessment by this new index. Compared to the two other indices derived from a single experiment with water (WRCT and RI_m), the new index RI_s includes information on both sorptivity and conductivity measured in the wettable and repellent stages of the infiltration process, and can be therefore considered more directly linked to the hydrological processes affected by SWR.

Finally, chapter C.5 investigated the effects of soil water contents on SWR with the specific aim to detect the existence of a critical water contents functioning as a soil moisture threshold between hydrophobic and hydrophilic conditions. The investigation was conducted on forest floor of the main exotic (*Pinus pinaster* and *Eucaliptus camaldulensis*) and native (*Quercus ilex* and *Quercus pubescens*) species used in Sicilian reforestations. The study was carried out on sieved soil samples moistened at different water contents under standard laboratory conditions to avoid environmental disturbances (e.g. temperature or humidity changes) which may distort the measurements. The SWR was detected by the common droplet tests WDPT and EP. In addition, the samples were leached by fixed water volume to investigate the extent of hydrophobic compounds transmission between the upper and lower layers of the soil profile as a consequence of prolonged rainfall events.

Both the WDPT and EP tests showed that the *Quercus pubescens* was the tree species that originated less repellency in the forest floor whereas the *Eucaliptus camaldulensis* was the species that conferred higher degree of water repellency to the forest floor. Leaching of hydrophobic molecules contained in the forest floor determined a reduction of hydrophobicity because removes the more hydrophobic organic compounds and consequently the liquid-soil contact angle is reduced to values less 90° causing lower WDPT and EP values.

References

Adams, S., Strain, B.R., Adams, M.S. 1969. 'Water-repellent soils and annual plant cover in a desert scrub community of southeastern California', Proc. Symp. Water-repellent Soils, Uniu. Galf., 289-295.

Adamson, A.W., Petry, A.1997. Physical chemistry of surfaces. John Wiley and Sons, New York.

Angulo-Jaramillo, R., Bagarello, V., Iovino, M., Lassabatere. 2016. Infiltration Measurements for Soil Hydraulic Characterization. Springer International Publishing. pp 289. DOI: 10.1007/978-3-319-31788-5.

Bachmann, J., Ellies, A., Hartage, K.H. 2000. Development and application of a new sessile drop contact angle method to assess soil water repellency. J. Hydrol., 231(232), 66-75.

Bachmann, J., Woche, S.K., Goebel, M.-O. 2003. Extended methodology for determining wetting properties of porous media. Water Resour. Res., 39, 1353-1366.

Bauters, T.W.J., Steenhuis, T.S., DiCarlo, D.A., Nieber, J.L., Dekker, L.W., Ritsema, C.J., Parlange, J.-Y., Haverkamp, R. 2000. Physics of water repellent soils. J. Hydrol., 231(232), 233– 243.

Bisdom, E.B.A., Dekker, L.W., Schoute, J.F.T. 1993. Water repellency of sieve fractions from sandy soils and relationships with organic material and soil structure. Geoderma, 56, 105–118.

Blackwell, P.S. 2000. Management of water repellency in Australia, and risks associated with preferential flow, pesticide concentration and leaching. Journal of Hydrology, 231(232), 384-395.

Bond, R.D., Harris, J.R. 1964. The influence of the microflora on physical properties of soils: I. Effects associated with filamentous algae and fungi. Aust. J. Soil Res., 2, 111-122.

Buczko, U., Bens, O., Hüttl, R.F. 2005. Variability of soil water repellency in sandy forest soils with different stand structure under Scots pine (Pinus sylvestris) and beech (Fagus sylvatica). Geoderma 126(3–4), 317–336.

Buczko U., Bens O., Fischer H., Hüttl R.F. 2002. Water repellency in sandy luvisol under different forest transformation stages in northeast Germany. Geoderma, 109, 1-18.

Butler, J.A.V., Wightman, A. 1932. Adsorption at the surface of solutions: Part I. The surface composition of water–alcohol solutions. J. Chem. Soc. Part II, 2089– 2097.

Cerdà, A., Doerr, S.H. 2007. Soil wettability, runoff and erodibility of major dryMediterranean land use types on calcareous soils. Hydrological Processes, 21, 2325-2336.

Chrenková, K., Mataix-Solera, J., Dlapa, P., Arcenegui, V. 2014. Long-term changes in soil aggregation comparing forest and agricultural land use in different Mediterranean soil types. Geoderma, 235, 290-299.

Crockford, S., Topalidis, S., Richardson, D.P. 1991. Water repellency in a dry sclerophyll forest — measurements and processes. Hydrological Processes, 5, 405–420.

Debano, L.F. 1992. The effect of fire to soil properties. pp. 151-156. USDA Forest Service General Technical Report, Portland.

DeBano L.F. 1981. Water repellent soils: a state-of-the-art. USDA Forest Service General Technical Report PSW-46, 21 pp.

de Jonge, L.W., Jacobsen, O.H., Moldrup, P. 1999. Soil Water Repellency: Effects of Water Content, Temperature, and Particle Size. Soil Science Society of America Journal, 63, 437-442.

Dekker, L.W., Doerr, S.H., Oostindie, K., Ziogas, A.K., Ritsema, C.J. 2001. Water repellency and critical soil water content in a dune sand. Soil Science Society of America Journal, 65, 1667-1674.

Dekker, L.W., Jungerius, P.D. 1990. Water repellency in the dunes with special reference to the Netherlands. In: Dunes of the European coasts (ed. Bakker, T.W.), pp. 173-183. Catena-Verlag, Cremlingen-Destedt.

Dekker, L.W., Ritsema, C.J. 1994. How water moves in a water repellent sandy soil. 1. Potential and actual water repellency. Water Resour. Res., 30, 2507-25 17.

Dekker, L.W., Ritsema, C.J. 1996. Variation in water content and wetting patterns in Dutch water repellent peaty clay and clayey peat soils. Catena, 28, 89-105

de Gennes, P. G. 1985. Wetting: statics and dynamics. Rev. Mod. Phys. 57:827–863.

Diehl, D. 2009. The role of organic matter for hydrophobicity in urban soils. PhD Thesis, University Koblenz-Landau, Landau.

Doerr S.H. 1998. On standardizing the 'Water Drop penetration Time' and the 'Molarity of an Ethanol Droplet' techniques to classify soil hydrophobicity: a case study using medium textured soils. Earth Surface Processes and Landforms, 23, 663-668.

Doerr, S.H., Ritsema, C.J. 2005. Water movement in hydrophobic soils. In: *Encyclopedia of Hydrological Sciences* (eds. Anderson, M.G. & McDonnell, J.). John Wiley & Sons.

Doerr, S.H., Shakesby, S.H., Walsh, R.P.D. 2000. Soil water repellency: its causes, characteristics and hydro-geomorphological significance. Earth-Science Reviews, 51, 33-65

Doerr, S.H., Shakesby, R.A., Dekker, L.W., Ritsema, C.J. 2006. Occurrence, predictionband hydrological effects of water repellency amongst major soil and land-use types in a humid temperate climate. European Journal of Soil Science, 57, 741- 754.

Ellies, A., Ramírez, C., Mac Donald, R. 2005. Organic matter and wetting capacity distribution in aggregates of Chilean soils. Catena, 59, 69-78

Emerson, W.W., Bond, R.D. 1963. The rate of water entry into dry sand and calculation of the advancing contact angle. Aust. J. Soil Res., 1, 9-16.

Ferreira, A.J.D., Coelho, C.O.A., Walsh, R.P.D., Shakesby, R.A., Ceballos, A., Doerr, S.H. 2000. Hydrological implications of soil water-repellency in Eucalyptus globulus forests, north-central Portugal. Journal of Hydrology, 231(232), 165-177.

Fisher, T., Veste, M., Wiche, W., Lange, P. 2010. Water repellency and pore clogging at early succession stages of microbiotic crusts on inland dunes, Brandenburg, NE Germany. Catena, 80, 47-52.

Franco, C.M.M., Clarke, P.J., Tate, M.E., Oades, J.M. 2000. Studies on non-wetting sands: II. Hydrophobic properties and chemical characterisation of natural water-repellent materials. Journal of Hydrology, 231, 47-58.

Goebel, M.-O., Bachmann, J., Woche, S.K., Fischer, W.R. 2005. Soil wettability, aggregate stability, and the decomposition of soil organic matter. Geoderma, 128, 80-93.

Gryze, S., Jassogne, L., Bossuyt, H., Six, J., Merckx, R. 2006. Water repellence and soil aggregate dynamics in a loamy grassland soil as affected by texture. European Journal of Soil Science, 57, 235-246.

Hallett, P.D., Baumgartl, T., Young, I.M. 2001. Subcritical water repellency of aggregates from a range of soil management practices. Soil Science Society of America Journal, 65, 184-190.

Hallin, I., Douglas, P., Doerr, S.H., Bryant, R. 2013. The role of drop volume and number on soil water repellency determination. Soil Science Society of America Journal, 77(5), 1732-1743.

Harper, R.J., Gilkes, R.J. 1994. Soil attributes related to water-repellency and the utility of soil survey for predicting its occurrence. Australian Journal of Soil Research, 32, 1109-1124.

Haverkamp, R., Ross, P.J., Smettem, K.R.J., Parlange, J.Y. 1994. Three-dimensional analysis of infiltration from the disc infiltrometer. 2. Physically based infiltration equation. Water Re-sources Research, 30, 2931-2935

Hudson, R.A., Traina, S.J., Shane, W.W., 1994. Organic matter comparison of wettable and non-wettable soils from bentgrass sand greens. Journal of the Soil Science Society of America, 58, 361–367.

Hunter, A.E., Chau, H.W., Si, B.C. 2011. Impact of tension infiltrometer disc size on measured soil water repellency index. Can. J. Soil Sci., 91(1) 77–81.

King, P.M. 1981. Comparison of methods for measuring severity of water repellence of sandy soils and assessment of some factors that affect its measurement. Australian Journal of Soil Research, 19, 275-285.

Imeson, A.C., Verstraten, J.M., Van Mullingen, E.J., Sevink, J. 1992. The effects of fire and water repellency on infiltration and runoff under Mediterranean type forest. Catena, 19, 345-361.

Jarvis, N., Etana, A., Stagnitti, F. 2008. Water repellency, near-saturated infiltration and preferential solute transport in a macroporous clay soil. Geoderma, 143, 223-230.

Leeds-Harrison, P.B., Youngs, E.G., Uddin, B. 1994. A device for determining the sorptivity of soil aggregates. Eur. J. Soil Sci., 45, 269212.

Letey, J., 1969. Measurement of contact angle, water drop penetration time, and critical surface tension. Proceedings of the Symposium on Water-Repellent Soils, University of California, May 1968, pp. 43–47

Letey, J., Carrillo, M.L.K., Pang, X.P. 2000. Approaches to characterize the degree of water repellency. Journal of Hydrology, 231(232),61-65.

Lewis, S.A., Wu, J.Q., Robichaud, P.R. 2006. Assessing burn severity and comparing soil water repellency, Hayman Fire, Colorado. Hydrological Processes, 20, 1-16.

Lichner, L., Capuliak, J., Zhukova, N., Holko, L., Czachor, H., Kollar, J. 2013a. Pines influence hydrophysical parameters and water flow in a sandy soil. Biologia, 68(6), 1104–1108.

Lichner, L., Hallett, P.D., Drongová, Z., Czachor, H., Kovacik, L., Mataix-Solera, J., Homolák, M. 2013b. Algae influence the hydrophysical parameters of a sandy soil. Catena, 108, 58–68.

Ma'shum, M., Farmer, V.C. 1985. Origin and assessment of water repellency of a sandy South Australian Soil. Australian Journal of Soil Research, 23, 623-626.

Ma'shum, M., Tate, M.E., Jones, G.P., Oades, J.M. 1988. Extraction and characterisation of water-repellent material from Australian soils. Soil Science, 39, 99–110.

Mataix-Solera, J., Arcenegui, V., Guerrero, C., Mayoral, A.M., Morales, J., González, J., García-Orenes, F., Gómez, I. 2007. Water repellency under different plant species in a calcareous forest soil in a semiarid Mediterranean environment. Hydrological Processes, 21, 2300-2309.

Mataix-Solera, J., Doerr, S.H. 2004. Hydrophobicity and aggregate stability in calcareous topsoils from fire-affected pine forests in south-eastern Spain. Geoderma, 118, 77-88.

McGhie, D.A., Posner, A.M. 1987. The effect of plant top material on the water repellency of fired sands and water repellent soils. Aust. J. Agr. Res., 32, 609-620

McIntosh, J.C., Horne, D.J. 1994. Causes of repellency: I. The nature of the hydrophobic compounds found in a New Zealand development sequence of yellow–brown sands. Proceedings of the 2nd National Water Repellency Workshop, 1–5 August, Perth, Western Australia. pp. 8–12.

Nieber, J.L., Bauters, T.W.J., Steenhuis, T.S., Parlange, J.-Y. 2000. Numerical simulation of experimental gravity-driven unstable flow in water repellent sand. J. Hydrol., 231(232), 295–307.

Perroux, K.M., White, I. 1988. Designs for disc permeameters. Soil Sci. Soc. Am. J., 52, 1205-1215.

Philip, J.R. 1957. The theory of infiltration: 4. Sorptivity and algebraic infiltration equations. Soil Sci., 84, 257–264.

Piccolo, A., Mbagwu, J.S.C. 1999. Role of Hydrophobic Components of Soil Organic Matter in Soil Aggregate Stability. Soil Science Society of America Journal, 63, 1801-1810.

Richardson, J.L. 1984. Field observation and measurement of water repellency for soil surveyors, Soil Surv. Horiz., 25, 32-36.

Ritsema, C.J. 2001. Water repellency and critical soil water content in a dune sand. Soil Sci. Soc. Am. J., 65, 1667–1674.

Ritsema, C.J., Dekker, L.W. 1994. Soil moisture and dry bulk density patterns in bare dune sands. Journal of Hydrology, 154, 107-131.

Ritsema, C.J., Dekker, L.W., Nieber, J.L., Steenhuis, T.S. 1998. Modeling and field evidence of finger formation and finger recurrence in a water repellent sandy soil. Water Resour. Res., 34, 555–567.

Roberts, F.J., Carbon, B.A. 1971. Water repellence in sandy soils of south-western Australia: 1. Some studies related to field occurrence. Division of Plant Industry CSIRO (Australia). Field Station Record, 10, 13–20

Robichaud, P.R. 2010. Post-fire treatment effectiveness for hillslope stabilization. DIANE Publishing.

Robichaud, P.R., Lewis, S.A., Ashmun, L.E. 2008. New procedure for sampling infiltration to assess post-fire soil water repellency. USDA Forest Service Research Note RMRS-RN-33, 14 pp.

Rodríguez-Alleres, M., Benito, E., de Blas, E. 2007. Extent and persistence of water repellency in north-western Spanish soils. Hydrological Processes 21(17), 2291-2299.

Roy, J.L., McGill, W.B. 2002. Assessing soil water repellency using the molarity of ethanol droplet (MED) test. Soil Sci., 167, 83–97.

Savage, S.M. 1974. Mechanism of fire-induced water repellency in soil. Soil Science Society of America Proceedings, 38, 652-657

Savage, S.M., Martin, J.P., Letey, J. 1969. Contribution of some soil fungi to natural and heat-induced water repellency in sand. Soil Sci. Soc. Am. J., 33, 405-409

Schaumann, G.E., Braun, B., Kirchner, D., Rotard, W., Szewzyk, U., Grohmann, E. 2007. Influence of biofilms on the water repellency of urban soil samples. Hydrol. Process., 21, 2276-2284.

Sheludko, A.(ed.). 1966. Physical chemistry of surfaces. In Colloid Chemistry, 3rd Ed. Elsevier, Amsterdam, pp. 90–92

Stevenson, F.J. 1994. Humus Chemistry: Genesis, Composition, Reactions. Wiley, New York.

Teramura, A.H. 1980. Relationships between Stand Age and Water Repellency of Chaparral Soils. Bulletin of the Torrey Botanical Club, 107, 42-46.

Tillman, R.W., Scotter, D.R., Wallis, M.G., Clothier, B.E. 1989. Water-repellency and its measurement by using intrinsic sorptivity. Australian Journal of Soil Research, 27, 637-644.

Tschapek, M. 1984. Criteria for determining the hydrophilicity - hydrophobicity of soils. Zeitschrift für Pflanzenernährung und Bodenkunde, 147, 137-149.

Van't Woudt, B.D. 1959. Particle coatings affecting the wettability of soils. Journal of Geophysical Research 64, 263–267.

Vazquez, G., Alvarez, E., Navaza, J.M. 1995. Surface tension of alcohol + water from 20 to 50 jC. J. Chem. Eng. Data, 40, 611– 614.

Velmulapalli, G.K. 1993. Physical Chemistry. Prentice-Hall, London, 991 pp.

Vogelmann, E.S., Reichert, J.M., Prevedello, J., Awe, G.O., Mataix-Solera, J. 2013a. Can occurrence of soil hydrophobicity promote the increase of aggregates stability? Catena, 110, 24-31.

Vogelmann, E. S., Reichert, J. M., Prevedello, J., Consensa, C. O. B., Oliveira, A. É., Awe, G. O., Mataix-Solera, J. 2013b. Threshold water content beyond which hydrophobic soils become hydrophilic: The role of soil texture and organic matter content. Geoderma, 209, 177-187.

Vogelmann, E.S., Reichert, J.M., Reinert, D.J., Mentges, M.I., Vieira, D.A., de Barros, C.A.P., Fasinmirin, J.T. 2010. Water repellency in soils of humid subtropical climate of Rio Grande do Sul, Brazil. Soil and Tillage Research, 110, 126-133.

Wallach, R., Graber, E.R. 2007. Infiltration into effluent irrigation-induced repellent soils and the dependence of repellency on ambient relative humidity. Hydrological Processes, 21, 2346-2355.

Wallis, M.G., Horne, D.J. 1992. Soil water repellency. Advances in Soil Science, 20, 91-146.

Wallis, M.G., Scotter, D.R., Horne, D.J. 1991. An evaluation of the intrinsic sorptivity water repellency index on a range of New Zealand soils. Aust. J. Soil Res., 29, 353-362.

Wallis, M.G., Horne, D.J., Palmer, A.S. 1993. Water-repellency in a New Zealand development sequence of yellow-brown sands. Australian Journal of Soil Research, 31, 641-654.

White ,I., Sully, M.J. 1987. Macroscopic and microscopic capillary length and time scales from field infiltration. Water Resources Research, 23(8), 1514-1522.

Yang, B., Blackwell, P.S., Nicholson, D.F. 1996. A numerical model of heat and water movement in furrow-sown water repellent sandy soils. Water Resources Research, 32, 3051-3061.

Young, T. 1855. Miscellaneous Works of the Late Thomas Young. Murray, London.

C.2. Indagine sull'idrorepellenza del suolo di una pineta artificiale mediterranea*

Investigation on soil water repellency in a Mediterranean managed pine woodland

V. Alagna*, V. Bagarello, G. Giordano, M. Iovino

Dipartimento di Scienze Agrarie e Forestali, Università degli Studi di Palermo, Viale delle Scienze, 90128, Palermo, Italy.
*Corresponding Author: Vincenzo Alagna, tel.: 09123897065; fax: 091484035; e-mail: vincenzo.alagna01@unipa.it.

Sommario

Nell'indagine è stata caratterizzata l'idrorepellenza del suolo di una pineta artificiale Mediterranea utilizzando sia il tradizionale Water Drop Penetration Time (*WDPT*) test che due indici desunti da esperimenti di infiltrazione condotti con il MiniDisk Infiltrometer (MDI). In particolare, il Repellency Index (*RI*) è stato calcolato come rapporto tra i valori di sorptività misurati con etanolo e acqua, mentre il Water Repellency Cessation Time (*WRCT*) è stato ricavato utilizzando l'informazione acquisita nella fase idrofobica e in quella idrofila del processo di infiltrazione con acqua. Tutti gli indici hanno inequivocabilmente indicato che la lettiera di *Pinus pinaster* è altamente idrofobica come conseguenza dell'elevato contenuto di sostanza organica. Tuttavia, il suolo minerale della pineta ha presentato livelli di idrorepellenza significativamente maggiori di quelli di un suolo non-boscato avente un contenuto di sostanza organica confrontabile, portando a concludere che la bagnabilità del suolo è influenzata dalla composizione piuttosto che dalla disponibilità complessiva della sostanza organica. Gli indici *RI* e *WRCT* hanno fornito risultati confrontabili con l'indice *WDPT*, consentendo però di segnalare condizioni di idrorepellenza sub-critica non rilevate con il tradizionale test *WDPT*. Essendo ricavati da un esperimento infiltrometrico, gli indici *RI* e *WRCT* sono stati ritenuti particolarmente adatti a caratterizzare l'idrorepellenza in termini di effetti sui processi idrologici del suolo.

Abstract

The soil water repellency of a Mediterranean managed pine woodland was investigated by the Water Drop Penetration Time (*WDPT*) test and two indices derived from infiltration experiments carried out by the MiniDisk Infiltrometer (MDI). Specifically, the Repellency Index (*RI*) was calculated as the adjusted ratio between ethanol and water soil sorptivities

whereas the Water Repellency Cessation Time (*WRCT*) was obtained from the hydrophobic and wettable stages of a water infiltration test. All the water repellency indices unanimously detected a severe hydrophobicity of the *Pinus pinaster* thatch as a consequence of its high organic matter content. High hydrophobicity was also observed in the underlying mineral soil but not in the soil of a glade area, close to the forest site, that was characterized by similar organic matter contents. It was concluded that soil wetting properties are more influenced by composition rather than overall quantity of organic matter. The *WRCT* and *RI* indices yielded water repellency estimations comparable to those obtained by *WDPT*, even if they allowed detection of sub-critical water repellency conditions that were not observed by the *WDPT* test. Both *RI* and *WRCT* rely on infiltration data collected by a much larger spatial support than *WDPT* test. Therefore, they were considered specifically focused to assess the effects of water repellency on the hydrologic processes.

*This is a post-refereeing final draft. When citing, please refer to the published version: Alagna, V., Bagarello, V., Giordano, G., Iovino, M. (2016). Investigation on soil water repellency in a Mediterranean managed pine woodland. Quaderni di idronomia Montana, EdiBios, 34, 379-391

C.2.1. Introduzione

Ampie aree marginali della Sicilia sono state impiantate con specie protettive sempreverdi a rapida crescita, tra cui conifere e eucalipti, per contrastare la degradazione del suolo e mitigare il rischio idrogeologico. Tuttavia, le resine, le cere e gli altri composti organici contenuti nei tessuti di queste specie si depositano sulla superficie delle particelle di suolo e possono dare origine a fenomeni di idrorepellenza che rallentano i processi di infiltrazione provocando un aumento del deflusso e dell'erosione idrica superficiale (Cerdà e Doerr, 2007; DeBano, 2000; Doerr et al., 2000). Seguendo le variazioni stagionali di umidità del suolo, l'idrorepellenza è massima in occasione delle prolungate siccità estive che caratterizzano il clima Mediterraneo e diminuisce durante i mesi invernali come conseguenza degli apporti meteorici (Buczko et al., 2005; Lichner et al., 2013a; Rodríguez-Alleres et al., 2007). La distribuzione verticale dell'idrorepellenza è influenzata dall'interazione vegetazione-suolo e, nel caso delle pinete, ci si attende che sia limitata allo spessore della lettiera formata da aghi parzialmente decomposti (Buczko et al., 2002). Tuttavia, l'influenza dei composti idrofobici sul suolo minerale sottostante risulta in gran parte sconosciuta.

L'idrorepellenza del suolo è comunemente valutata con il test Water Drop Penetration Time (*WDPT*) che consiste nel posizionare una goccia di acqua sul suolo e misurare il tempo

necessario affinché penetri completamente (Watson e Letey, 1970). Un suolo è considerato idrorepellente quando *WDPT* > 5 s (Doerr, 1998). Tuttavia, essendo una misura del tempo necessario affinché l'angolo di contatto acqua-suolo passi da valori maggiori di 90° (condizione di idrorepellenza) a valori inferiori a 90° (condizione di bagnamento), si ritiene che il test sia una misura della stabilità della repellenza e non necessariamente un indice della sua intensità (Letey et al., 2000). Gli approcci più diffusi per misurare il grado di idrorepellenza si basano sull'uso di liquidi non-polari, come l'etanolo, che bagnano la superficie delle particelle. Con il Repellency Index, *RI*, la misura dell'intensità dell'idrorepellenza è data dal rapporto tra le sorptività del suolo misurate con etanolo e acqua, corretto per tener conto della diversa viscosità e tensione superficiale dei due liquidi utilizzati (Tillmann et al., 1989). Sulla base di test di infiltrazione effettuati in laboratorio con un infiltrometro miniaturizzato, Lichner et al. (2013b) hanno proposto l'indice Water Repellency Cessation Time (*WRCT*) che misura il tempo necessario per passare dalla condizione di suolo idrorepellente a quella di suolo bagnabile.

Rispetto agli esperimenti *droplet,* condotti a scala della singola goccia, il MiniDisk Infiltrometer (MDI) consente stime della sorptività del suolo maggiormente rappresentative dei processi idrologici interessati dal fenomeno dell'idrorepellenza (Hunter et al., 2011) e, in forza della maggiore semplicità di impiego, costituisce una valida alternativa al classico infiltrometro a depressione (Alagna et al., 2016).

La presente indagine è stata condotta con l'obiettivo di valutare l'effetto della copertura vegetale sull'idrorepellenza degli strati più superficiali del suolo di una pineta in ambiente mediterraneo. A tal fine, le stime dedotte con gli usuali indicatori di idrorepellenza (*WDPT* e *RI*) sono state confrontate con quelle dedotte dall'indice *WRCT* che si basa su un unico esperimento infiltrometrico eseguito con il MDI.

C.2.2. Materiali e metodi

L'area sperimentale è ubicata all'interno della pineta artificiale di Ciavolo a Marsala (37°45'40.6" N, 12°34'09.0" E) che può essere considerata rappresentativa degli interventi di forestazione diffusamente effettuati nel passato in Sicilia (figura 1).

Il suolo è un *Typic Rhodoxeralf*, poco profondo (0.40-0.60 m), che sovrasta una formazione calcarenitica di base. Secondo la classificazione USDA, la tessitura è franco-argillosa (argilla = 31.1%; limo = 44.3%; sabbia = 24.6%).

All'interno dell'area sono stati scelti due siti di campionamento (approssimativamente di 25 m^2 ciascuno), il primo comprendente piante di *Pinus pinaster* di 30 anni di età che

ricoprono completamente il suolo (sito P) e il secondo ubicato in una adiacente radura (bare land, B) su cui cresce vegetazione erbacea spontanea costituita prevalentemente da *Avena fatua* L., *Galactites elegans* (All.) Soldano, *Hypochaeris achyrophorus* L., *Oxalis pes-caprae* L. e *Vulpia ciliata* Dumort,. La distanza fra i due siti, circa 50 m, è stata ritenuta sufficiente ad escludere ogni influenza dei composti organici prodotti dalla specie forestale sulle caratteristiche di idrofobicità del suolo del sito B.

Fig. 1 *Vista dell'area sperimentale di Ciavolo: (a) pineta; (b) radura*

Nel sito P è stata campionata sia la lettiera (Thatch, T), costituita da residui vegetali parzialmente decomposti per uno spessore di circa 5 cm, che il suolo minerale sottostante (Subsoil, S). Al fine di esplorare differenti contenuti idrici del suolo, sono state eseguite due campagne di misura: a settembre 2014, dopo un prolungato periodo siccitoso (I epoca), e a novembre dello stesso anno, dopo le piogge autunnali (II epoca). Tra la prima e la seconda campagna di misura, si sono registrati 108 mm di pioggia pari a circa il 20% della precipitazione media annua dell'area. Nel sito B è stata effettuata una sola campagna di misura nel novembre 2014. In tal caso, il campionamento si è limitato allo strato superficiale di suolo minerale dal momento che non è presente lettiera organica.

Per ciascuna epoca e profondità di campionamento, il protocollo sperimentale ha previsto: il prelievo di 10 campioni (5 x 5 cm) di suolo indisturbato per la determinazione della densità apparente, ρ_b (Mg m^{-3}), e del contenuto idrico iniziale, θ_0 (m^3m^{-3}); il prelievo di campioni di suolo rimaneggiato per la determinazione del contenuto in sostanza organica con il metodo Walkley-Black (Nelson e Sommers, 1982); l'esecuzione dei test *WDPT* e degli esperimenti infiltrometrici secondo le modalità precisate in seguito. Per ciascuna epoca, il protocollo sperimentale è stato completato in 10 giorni durante i quali non si sono verificate precipitazioni.

Il test *WDPT* è stato effettuato posizionando sulla superficie del suolo, precedentemente livellata, 30 gocce di acqua distillata di circa 70 µL ciascuna mediante un contagocce medicale e misurando il tempo necessario alla loro completa penetrazione. Secondo Hallin et al. (2013), l'utilizzo di 30 gocce consente di stimare il valore medio di *WDPT* con un errore del ±10% al livello di confidenza del 95%.

Gli esperimenti infiltrometrici sono stati effettuati utilizzando il MDI prodotto dalla Decagon Devices avente diametro del disco poroso di 4.5 cm. Per ciascuna epoca e profondità di campionamento, in punti scelti in maniera casuale all'interno dell'area sperimentale, sono stati effettuati 10 esperimenti con acqua e 10 con una soluzione di etanolo al 95% v/v. Il potenziale imposto sulla superficie di infiltrazione è stato di -2 cm e il disco dello strumento è stato posizionato direttamente sulla superficie del suolo precedentemente livellata con l'apporto di modeste quantità di terreno setacciato sul luogo. I volumi cumulati di infiltrazione sono stati misurati visivamente a intervalli di tempo, Δt, ravvicinati per le prove condotte con etanolo (Δt = 10-60 s) e più prolungati per quelle con acqua (Δt = 1-30 min). In ogni caso, le prove sono state protratte fino allo svuotamento del serbatoio dello strumento (volume, V = 80 cm^3). La sorptività del suolo è stata stimata dalla pendenza del tratto iniziale della curva di infiltrazione cumulata, I (L), in funzione della radice quadrata del tempo, t (T) (Philip, 1957). Dalla medesima rappresentazione, estesa all'intera durata della prova effettuata con acqua, è stato calcolato l'indice *WRCT* come istante di tempo corrispondente al punto di intersezione delle due rette interpolanti la parte iniziale e finale dei punti sperimentali I vs. $t^{0.5}$ (Lichner et al, 2013b). Per il calcolo del Repellency Index è stata utilizzata la seguente relazione (Tillman et al., 1989):

$$RI = 1.95 \frac{S_e}{S_w} \qquad (1)$$

in cui S_e (L T$^{-0.5}$) è il valore della sorptività del suolo misurata con etanolo e S_w (L T$^{-0.5}$) è la sorptività misurata con acqua. A causa dell'influenza del contenuto idrico iniziale sulla stima di S, le prove per la determinazione di *RI* non possono essere effettuate in sequenza nello stesso punto. Per tener conto dell'incertezza nella stima di *RI* legata alla variabilità spaziale delle proprietà idrauliche del suolo, Pekarova et al. (2015) hanno considerato l'intero set di valori di *RI* ottenuti combinando gli m valori di S_e con n valori di S_w effettuati all'interno di una data area sperimentale. Con questo approccio è pertanto possibile ottenere una caratterizzazione dell'indice *RI* in termini di valore centrale e dispersione della distribuzione di frequenza empirica.

L'individuazione della legge di probabilità teorica che meglio descrive le distribuzioni delle variabili *WDPT*, *WRCT* e *RI* è stata eseguita con il test di Lilliefors (1967) (P = 0.05) e gli statistici calcolati secondo le corrispondenti relazioni (Lee et al., 1985). I confronti tra medie sono stati eseguiti con il t-test (P = 0.05).

C.2.3. Risultati e Discussione

Al termine della stagione estiva, il contenuto idrico, θ_0, della lettiera di pino, T, è risultato significativamente più basso e più variabile di quello del suolo minerale sottostante, S (tabella 1). A seguito delle precipitazioni autunnali intercorse fra le due date di campionamento, si è osservato un aumento significativo dell'umidità nella lettiera ma non nel suolo minerale della pineta. Ciò ha determinato una ridistribuzione del contenuto idrico che, infatti, nella seconda epoca di campionamento è risultato maggiormente uniforme sia in direzione orizzontale (CV = 5.80-8.01%) che verticale, come segnalato dai valori medi di θ_0 non significativamente differenti per le due profondità (T-II e S-II). A causa della ridotta traspirazione e intercettazione, il valore medio di θ_0 nella radura (sito B) è risultato 1.7 volte maggiore di quello dell'area boscata (tabella 1).

Tabella 1 Statistici del contenuto idrico iniziale del suolo, θ_0, della densità apparente, ρ_b, e del contenuto di sostanza organica, OM, per differenti profondità e epoche di campionamento (T = lettiera pineta, S = suolo pineta; B = suolo radura; I = prima epoca di campionamento; II = seconda epoca di campionamento; valori medi seguiti dalla stessa lettera racchiusa tra parentesi indicano differenze statisticamente significative, P = 0.05).

	T-I	T-II	S-I	S-II	B-II
			Contenuto idrico iniziale, θ_0 ($cm^3\ cm^{-3}$)		
min	0.104	0.149	0.149	0.155	0.245
max	0.16	0.199	0.18	0.182	0.312
mean	0.128 (a),(c)	0.175 (a),d	0.166 b,(c)	0.169 b,d,(e)	0.281 (e)
CV (%)	16.89	8.01	6.33	5.80	7.51
			Densità apparente, ρ_b ($g\ cm^{-3}$)		
min	0.45	0.641	1.108	1.011	1.12
max	1.077	0.891	1.242	1.219	1.291
mean	0.725 a,(c)	0.749 a,(d)	1.172 (b),(c)	1.089 (b),(d),(e)	1.192 (e)
CV (%)	32.42	9.5	4.14	5.70	4.73
			Sostanza organica, OM (%)		
min	19.10	21.31	4.60	3.80	4.43
max	21.66	21.74	4.80	4.04	5.00
mean	20.03 a,(c)	21.48 a,(d)	4.66 (b),(c)	3.93 (b),(d),(e)	4.71 (e)
CV (%)	7.04	1.07	2.41	3.11	6.02

Come atteso, nella lettiera T i valori di densità apparente, ρ_b, sono risultati significativamente più bassi e quelli di sostanza organica, OM, significativamente più alti rispetto al suolo sottostante S (tabella 1). In particolare, il rapporto tra i valori medi di ρ_b della lettiera T e del suolo S è risultato pari a 0.62 per la prima epoca di campionamento e 0.69 per la seconda, mentre per OM tale rapporto è stato rispettivamente di 4.3 e 5.5. La lettiera T non ha evidenziato una significativa variabilità temporale di ρ_b e OM (tabella 1) mentre nel suolo S entrambe le grandezza si sono ridotte nell'intervallo fra i due campionamenti di un fattore 0.93 e 0.84, rispettivamente. Il suolo della radura (B) ha evidenziato valori di ρ_b e OM più alti di quelli del suolo della pineta (S) anche se l'intervallo di variabilità complessivo dei valori puntuali delle due grandezze (ρ_b = 1.01-1.29; OM = 3.8-5.0) è nel complesso abbastanza contenuto.

Per il suolo B, il test *WDPT* non ha evidenziato fenomeni di idrorepellenza dal momento che le gocce di acqua si sono sempre infiltrate entro il tempo limite di 5 s. Al contrario, sia la lettiera T che il suolo S del sito forestato hanno evidenziato chiari fenomeni di idrorepellenza con valori del *WDPT* compresi tra 100 e 6890 s (tabella 2). Con riferimento a questi ultimi siti, l'ipotesi di distribuzione log-normale dei valori di *WDPT* non è stata mai rigettata mentre quella normale è stata rigettata in un caso su quattro (S-I). Inoltre, il test statistico di Lilliefors (1967) ha restituito valori assoluti della massima differenza tra la distribuzione empirica e quella teorica sempre più bassi per i dati log-trasformati. Pertanto, la distribuzione log-normale è stata ritenuta più adatta a descrivere le misure di *WDPT*.

Indipendentemente dall'epoca di campionamento, la lettiera T è risultata più idrorepellente del suolo S sottostante con un rapporto fra i valori medi di *WDPT* (media geometrica, GM) compreso tra 2.0 e 5.3. Secondo la classificazione proposta da Dekker e Ritsema (1994), la lettiera di pino può essere considerata severamente idrorepellente. Come conseguenza dell'aumento del contenuto idrico verificatosi tra le due date di campionamento, il *WDPT* della lettiera T è diminuito di un non significativo 14%. Viceversa, nel suolo S sottostante, l'idrofobicità è aumentata nello stesso intervallo di tempo passando da fortemente idrorepellente (GM = 317 s) a severamente idrorepellente (GM = 745 s). Tale incremento si è verificato nonostante il contenuto idrico del suolo sia rimasto invariato e il quantitativo di sostanza organica sia diminuito (tabella 1) suggerendo, pertanto, che parte dei composti anfifilici responsabili della idrofobicità del suolo si siano ridistribuiti dalla lettiera verso il suolo minerale sottostante veicolati delle piogge autunnali. Considerato che nel suolo S si è registrato un valore di *WDPT* non inferiore a 100 s, si può concludere che la presenza della

lettiera di aghi di pino induce un aumento della persistenza dell'idrorepellenza di almeno 20 volte rispetto al suolo della radura B (*WDPT* < 5 s).

Tabella 2 Statistici degli indici Water Drop Penetration Time, WDPT, Water Repellency Cessation Time, WRCT, e Repellency Index, RI, per differenti profondità e epoche di campionamento (T = lettiera pineta, S = suolo pineta; B = suolo radura; I = prima epoca di campionamento; II = seconda epoca di campionamento; valori medi seguiti dalla stessa lettera racchiusa tra parentesi indicano differenze statisticamente significative, P = 0.05).

	T-I	T-II	S-I	S-II	B-II
			Water Drop Penetration Time, *WDPT* (s)		
min	868	150	113	100	
max	3534	6890	1660	4425	
GM	1689 a,(c)	1454 a,(d)	317 (b),(c)	745 (b),(d)	<5
CV (%)	48.41	182.00	63.78	136.67	
			Water Repellency Cessation Time, *WRCT* (s)		
min	9736	3067	2446	1701	479
max	20204	13678	8502	8772	861
GM	13933 (a),(c)	8007 (a),(d)	4344 b,(c)	3534 b,(d),(e)	631 (e)
CV (%)	25.4	49.3	45.0	56.4	21.5
			Repellency Index, *RI*		
min	11.9	10.3	1.9	3.3	1.4
max	224.0	129.6	27.7	31.2	4.7
GM	55.1 (a),(c)	32.5 (a),(d)	6.1 (b),(c)	9.7 (b),(d),(e)	2.7 (e)
CV (%)	68.8	70.5	69.7	54.6	26.1

I test di infiltrazione eseguiti con l'etanolo sono risultati in linea con la teoria che prescrive una più o meno prolungata fase transitoria, nella quale la velocità di infiltrazione diminuisce, seguita da una fase stazionaria in cui la velocità di infiltrazione è praticamente costante (figura 2). Invece, le prove effettuate con acqua hanno incontrovertibilmente evidenziato fenomeni di idrorepellenza nel sito forestato come segnalato dai grafici delle altezze cumulate di infiltrazione, *I*, in funzione del tempo, *t*, che mostrano una curvatura rivolta verso l'alto caratteristica di un comportamento idrofobico (figura 2). Infatti, dopo una fase iniziale in cui l'infiltrazione è ostacolata, la rimozione dello strato di composti anfifilici che rivestono le particelle solide determina il bagnamento delle superfici e, quindi, un repentino aumento della velocità di infiltrazione (Doerr et al., 2000). Tale andamento della curva di infiltrazione cumulata è stato osservato, sebbene in misura notevolmente ridotta, anche nel suolo della radura (B) evidenziando che l'idrorepellenza ha interessato anche questo sito (figura 2).

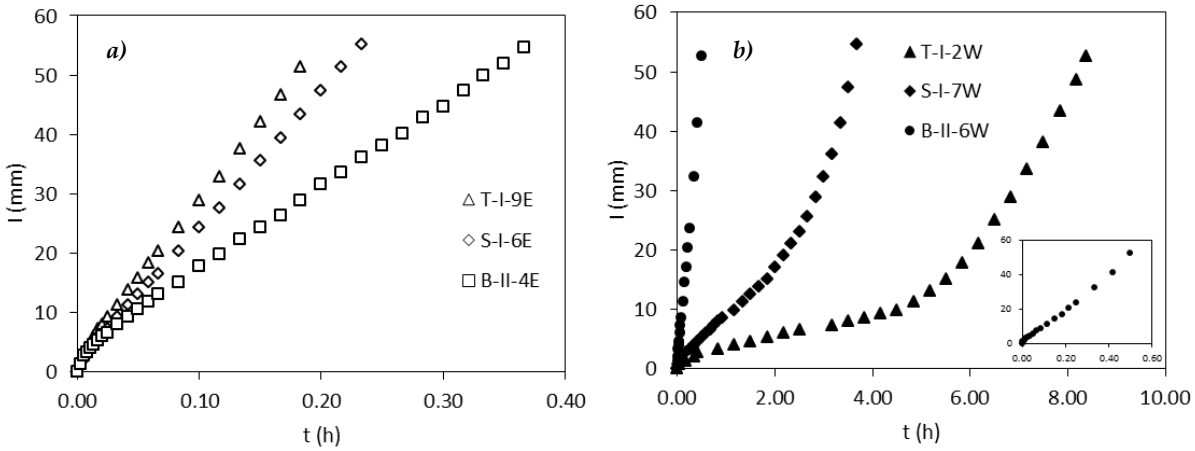

Fig. 2 Esempi di curve di infiltrazione cumulata, I, in funzione del tempo, t, misurate con il MDI utilizzando (a) etanolo, (b) acqua

L'effetto dell'idrorepellenza sul processo di infiltrazione è risultato anche più evidente quando i dati di infiltrazione sono stati rappresentati nella forma I vs. $t^{0.5}$ (figura 3). In questo caso, tutte le prove eseguite con acqua nel sito forestato, ma anche nella radura, hanno evidenziato una più o meno accentuata forma a mazza da "hockey" indicativa secondo Lichner et al. (2013) del passaggio dalla condizione di suolo idrorepellente a quella di suolo bagnabile.

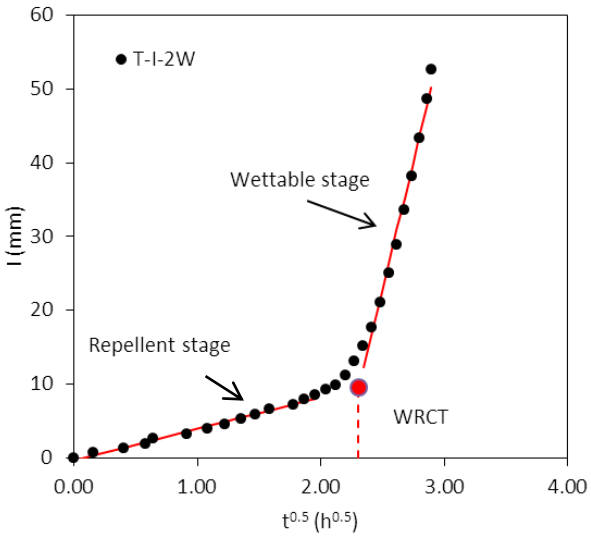

Fig. 3 Esempio di stima del Water Repellency Cessation Time, WRCT, dal diagramma dell'infiltrazione cumulata, I, in funzione della radice quadrata del tempo, t.

Anche per l'indice *WRCT*, la legge log-normale è sempre risultata più adatta della legge normale a descrivere la distribuzione di frequenza empirica dei dati sperimentali. La lettiera T ha evidenziato valori medi di *WRCT* (media geometrica, GM) 2.3-3.2 volte maggiori del suolo S sottostante (tabella 2) e differenze anche maggiori sono state riscontrate tra i due suoli minerali della pineta (S) e della radura (B) (rapporti fra GM pari a 5.4-6.7). Nelle condizioni sperimentali considerate, diverse per vegetazione, tipo di suolo e contenuto idrico, gli indici *WRCT* e *WDPT* sono risultati significativamente correlati (R^2 = 0.8449) anche se i valori medi dei due indici hanno evidenziato differenze di più di un ordine di grandezza (tabella 2). In particolare, *WRCT* è risultato sempre maggiore di *WDPT* con discrepanze che si riducevano all'aumentare dell'idrorepellenza. Condizioni di idrorepellenza

deboli, come quelle che caratterizzano la radura, sono state evidenziate da *WRCT* ma non con il tradizionale test *WDPT*. Si è pertanto dedotto che l'indice *WRCT*, ottenuto da un singolo esperimento MDI effettuato con acqua, è potenzialmente più indicato a segnalare condizioni di cosiddetta idrorepellenza sub-critica. Questa circostanza si verifica quando l'angolo di contatto tra l'acqua e il suolo è minore di 90° ma non pari a zero (bagnabilità totale) per cui la velocità di infiltrazione dell'acqua è ridotta ma non del tutto impedita come nel caso di condizioni di idrofobicità severe (Tillman et al., 1989).

Per l'indice *RI*, l'ipotesi di distribuzione log-normale è stata rigettata in un caso su cinque a differenza di quella normale che è stata sempre rigettata. Per il calcolo degli statistici di tale indice si è pertanto assunta una distribuzione log-normale (tabella 2). Il sito P si è confermato più idrorepellente del sito B con valori medi di *RI* nella lettiera T compresi fra 33 e 55, a seconda dell'epoca di campionamento, e pari a 9.0 e 3.4 volte quelli del suolo S sottostante. Tuttavia, anche nel suolo S l'influenza dei composti idrofobi prodotti dagli alberi di pino è risultata significativa, dato che i valori medi di *RI* sono stati mediamente 2.4-3.7 volte maggiori di quelli del suolo della radura (B). Inoltre, la variabilità spaziale di *RI* per la pineta, indipendentemente dall'epoca (I o II) e dalla profondità di campionamento (T o S) è risultata doppia rispetto a quella della radura (tabella 2). In accordo con quanto evidenziato per il *WDPT*, nell'intervallo di tempo trascorso tra i due campionamenti anche l'indice *RI* è diminuito di un fattore due nella lettiera T ed aumentato di un fattore 1.5 nel suolo S confermando che il processo di lisciviazione dei composti idrofobi dalla lettiera e l'accumulo negli strati immediatamente inferiori gioca un ruolo importante sulla dinamica spazio-temporale del fenomeno.

Gli indici considerati hanno fornito stime congruenti delle variabilità del fenomeno dell'idrorepellenza del suolo alla scala parcellare. Infatti, il coefficiente di variazione, CV, è risultato generalmente minore nella lettiera T rispetto al suolo S sottostante e nella radura B rispetto al sito boscato (tabella 2). Tuttavia, rispetto al range di valori di CV generalmente osservati (CV = 20-70%), la variabilità di *WDPT* è risultata in alcuni casi notevolmente maggiore. La superficie di suolo campionata con il *droplet* test è dell'ordine di 0.14 cm^2 mentre quella campionata con il MDI risulta almeno 100 volte più grande (A = 15.90 cm^2). Pertanto, la differente informazione sulla variabilità dell'idrorepellenza è da attribuire alle diverse dimensioni delle superfici campionate in campo (Moody e Schlossberg, 2010).

Correlazioni statisticamente significative sono state osservate fra l'indice *RI* e gli indici *WDPT* e *WRCT* (N = 5). Tuttavia, per l'indice *WRCT*, il coefficiente di determinazione è risultato più alto (R^2 = 0.954) rispetto all'indice *WDPT* (R^2 = 0.880)

confermando che i test infiltrometrici (*RI* e *WRCT*) forniscono stime dell'idrorepellenza maggiormente confrontabili e, probabilmente, più rispondenti alle implicazioni idrologiche del fenomeno.

C.2.4. Conclusioni

I diversi indici di idrorepellenza considerati (*WDPT*, *WRCT* e *RI*) unanimemente concordano nel segnalare elevati livelli di idrorepellenza nella lettiera del *Pinus pinaster* che presenta livelli di sostanza organica del 20%. Tuttavia, anche il suolo minerale sottostante la lettiera ha evidenziato livelli di idrorepellenza maggiori di quelli del suolo di un'adiacente radura avente contenuti di sostanza organica confrontabili e dell'ordine del 4%. Inoltre, l'idrorepellenza del suolo boscato è aumentata dopo le piogge autunnali come conseguenza del dilavamento dei composti idrofobici (resine e cere) dalle superfici degli aghi in decomposizione. Tale incremento, che corrisponde ad una diminuzione del contenuto di sostanza organica, induce a ritenere che la bagnabilità del suolo è prevalentemente influenzata dalla composizione piuttosto che dalla disponibilità complessiva della sostanza organica.

Gli indici *RI* e *WRCT* hanno evidenziato condizioni di idrorepellenza sub-critica per il suolo della radura che non sono state rilevate con il tradizionale test *WDPT* secondo il quale tale suolo è classificabile come non idrorepellente (*WDPT* < 5 s). Tale condizione, che si verifica quando l'angolo di contatto acqua-suolo è inferiore a 90°, può influenzare negativamente il comportamento idrologico del suolo perché riduce la velocità di infiltrazione rispetto alle condizioni di completa bagnabilità. I due indici *RI* e *WRCT*, ricavati attraverso gli esperimenti infiltrometrici, sono risultati correlati fra loro e con l'indice *WDPT*. Inoltre, essendo rappresentativi di un processo di infiltrazione condotto ad una scala spaziale almeno 100 volte maggiore dell'esperimento *WDPT*, sono stati ritenuti maggiormente appropriati a caratterizzare l'idrorepellenza in termini di effetti sui processi idrologici del suolo. In particolare, l'indice *WRCT*, che richiede l'esecuzione di un unico esperimento infiltrometrico con acqua, può essere considerato un indice alternativo in grado di superare gli inconvenienti sperimentali legati alle stime di idrorepellenza effettuate utilizzando etanolo e acqua.

Bibliografia

Alagna V., Bagarello V., Di Prima S., Iovino M., Determining hydraulic properties of a loam soil by alternative infiltrometer techniques. Hydrological Processes, 30, 263-275, (2016) DOI: 10.1002/hyp.10607.

Buczko U., Bens O., Fischer H., Hüttl R.F., Water repellency in sandy luvisols under different forest transformation stages in Northeast-Germany. Geoderma, 109, 1–18, (2002).

Buczko U., Bens O., Hüttl R.F., Variability of soil water repellency in sandy forest soils with different stand structure under Scots pine (Pinus sylvestris) and beech (Fagus sylvatica). Geoderma, 126(3–4), 317–336, (2005).

Cerdà A., Doerr S.H., Soil wettability, runoff and erodibility of major dry-Mediterranean land use type on calcareous soil. Hydrological Processes, 21, 2325-2336, (2007).

DeBano L.F., The role of fire and soil heating on water repellency in wild-land environments: A review. Journal of Hydrology, 231-232, 195-206, (2000).

Dekker L.W., Ritsema C.J., How water moves in a water-repellent sandy soil: 1. Potential and actual water-repellency. Water Resources Research, 30, 2507–2517, (1994).

Doerr S.H., On standardising the "Water Drop Penetration Time" and the "Molarity of an Ethanol Droplet" techniques to classify soil water repellency: a case study using medium textured soils. Earth Surface Processes and Landforms 23, 663–668, (1998).

Doerr S.H., Shakesby R.A., Walsh R.P.D., Soil water repellency: its causes, characteristics and hydro-geomorphological significance. Earth-Science Reviews 51(1–4), 33–65, (2000).

Hallin I., Douglas P., Doerr S. H., Bryant R., The role of drop volume and number on soil water repellency determination. Soil Science Society of America Journal, 77(5), 1732-1743, (2013).

Hunter A.E., Chau H.W., Si B.C., Impact of tension infiltrometer disc size on measured soil water repellency index. Canadian Journal of Soil Science, 91, 77-81, (2011).

Letey J., Carrillo M.L.K., Pang X.P., Approaches to characterize the degree of water repellency. Journal of Hydrology, 231–232, 61–65, (2000).

Lichner L., Capuliak J., Zhukova N., Holko L., Czachor H., Kollar J., Pines influence hydrophysical parameters and water flow in a sandy soil. Biologia, 68(6), 1104–1108, (2013a).

Lichner L., Hallett P.D., Drongová Z., Czachor H., Kovacik L., Mataix-Solera J., Homolák M., Algae influence hydrophysical parameters of a sandy soil. Catena, 108, 58–68, (2013b).

Lee D.M., Reynolds W.D., Elrick D.E., Clothier B.E., A comparison of three field methods for measuring saturated hydraulic conductivity. Canadian Journal of Soil Science, 65, 563–573, (1985).

Lilliefors H.W., On the Kolmogorov–Smirnov test for normality with mean and variance unknown. Journal of the American Statistical Association, 62(318): 399–402, (1967).

Moody D.R., Schlossberg M.J., Soil water repellency index prediction using the molarity of ethanol droplet test. Vadose Zone Journal, 9(4), 1046–1051, (2010).

Nelson D.V., Sommers L.E., Total carbon, organic carbon, and organic matter. In: Page, A.L. (Ed.), Methods of soil analysis, Part 2. Chemical and biological meth-ods, (1982).

Pekarova P., Pekar J., Lichner L., A new method for estimating soil water repellency index. Biologia, 70, 1450-1455 (2015).

Philips J.R., The Theory of infiltration: the infiltration equation and its solution. Soil Science, 83, 345- 357, (1957).

Rodríguez-Alleres M., Benito E., de Blas E., Extent and persistence of water repellency in north-western Spanish soils. Hydrological Processes, 21(17), 2291-2299, (2007).

Tillman R.W., Scotter D.R., Wallis M.G., Clothier B.E., Water-repellency and its measurement by using intrinsic sorptivity. Australian Journal of Soil Research, 27(4), 637–644, (1989).

Watson C.L., Letey J., Indices for characterizing soil-water repellency based upon contact angle-surface tension relationships. Soil Science Society of America Proceedings, 34(6), 841–844, (1970).

C.3. Application of minidisk infiltrometer to estimate water repellency in Mediterranean pine forest soils*

V.Alagna[1], M. Iovino[1]*, V. Bagarello[1], J. Mataix-Solera[2], Ľ Lichner[3]

[1] Dipartimento di Scienze Agrarie e Forestali, Università degli Studi di Palermo, Viale delle Scienze, Ed. 4 Ingr. E, 90128 Palermo, Italy

[2] Departamento de Agroquímica y Medio Ambiente, Universidad Miguel Hernández, Edificio Alcudia, Avda de la Universidad, 03202 Elche Alicante, Spain

[3] Institute of Hydrology, Slovak Academy of Sciences, Dúbravská cesta 9, 841 04 Bratislava, Slovak Republic

[*] Corresponding author. E-mail: massimo.iovino@unipa.it, tel +39 091 23897070, fax +39 091 484035

Abstract

Assessment of soil water repellency (SWR) was conducted in the decomposed organic floor layer (duff) and in the mineral soil layer of two Mediterranean pine forests, one in Italy and the other in Spain, by the widely-used water drop penetration time (WDPT) test and alternative indices derived from infiltration experiments carried out by the minidisk infiltrometer (MDI). In particular, the repellency index (RI) was calculated as the adjusted ratio between ethanol and water soil sorptivities whereas the water repellency cessation time (WRCT) and the specifically proposed modified repellency index (RI_m) were derived from the hydrophobic and wettable stages of a single water infiltration experiment. Time evolution of SWR and vegetation cover influence was also investigated at the Italian site. All indices unanimously detected severe SWR conditions in the duff of the pine forests. The mineral subsoils in the two forests showed different wettability and the clay-loam subsoil at Ciavolo forest was hydrophobic even if characterized by organic matter (OM) content similar to the wettable soil of an adjacent glade. It was therefore assumed that the composition rather than the total amount of OM influenced SWR. The hydraulic conductivity of the duff differed by a factor of 3.8-5.8 between the two forested sites thus influencing the vertical extent of SWR. Indeed, the mineral subsoil of Javea showed wettable or weak hydrophobic conditions probably because leaching of hydrophobic compounds was slowed or prevented at all. Estimations of SWR according to the different indices were in general agreement even if some discrepancies were observed. In particular, at low hydrophobicity levels the SWR indices gathered from the MDI tests were able to signal sub-critical SWR conditions that were not detected by the traditional WDPT index. The WRCT and modified repellency index RI_m yielded SWR estimates in reasonable agreement with those obtained with the more cumbersome RI test and, therefore, can be proposed as alternative procedures for SWR

assessment.

Keywords: Pine forest, Soil water repellency, Minidisk infiltrometer, Modified repellency index

*This is a post-refereeing final draft. When citing, please refer to the published version: Alagna, V., Iovino, M., Bagarello, Mataix-Solera, J., Lichner, Ľ. (2016). Application of minidisk infiltrometer to estimate water repellency in Mediterranean pine forest soils. Accepted by Journal of Hydrology and Hydromechanics, published online, DOI: 10.1515/johh-2017-0009

C.3.1. Introduction

Fast-growing protective woodlands, mostly of evergreen trees including pine and eucalyptus, have been planted in large marginal areas in the Mediterranean region to tackle land degradation and control water runoff, soil erosion and compaction, landslides, and organic matter decline (Iovino et al., 2016). Resins, waxes, aromatic oils and other organic substances in the tissues of these trees can cause organic coating on soil particles which is responsible of soil water repellency (SWR) or hydrophobicity (Doerr et al., 2000). Hydrological processes can be affected by SWR through reduced matrix infiltration, development of fingered flow, irregular wetting fronts, and overall increased runoff generation and soil erosion (Cerdà and Doerr, 2007; DeBano, 2000; Doerr et al., 2000).

Hydrophobicity is not a static soil property but is known to follow short-term or seasonal variations. It is generally found to be most extreme when soils are dry, declining and eventually disappearing as soils become wet (e.g., de Jonge et al., 1999; Dekker and Ritsema, 1994; Fer et al., 2016; Lichner et al., 2013a; Vogelmann et al., 2013) although the soil moisture water repellency relationship is nevertheless complex (Doerr et al., 2000). When wet, amphiphilic compounds produced by plants are hydrophilic, but below a critical moisture threshold, their hydrophilic ends are bond strongly with one another and the soil particles, while hydrophobic ends are oriented towards the free space inducing water repellency (Ma'shum and Farmer, 1985; Tschapek, 1984). Severe water repellency is therefore expected following prolonged dry, warm summers that are typical of Mediterranean region with a transition from water repellent (hydrophobic) to wettable (hydrophilic) conditions during the autumn/winter months (Buczko et al., 2005; Lichner et al., 2013a; Rodríguez-Alleres et al., 2007).

The vertical extent of hydrophobicity within soil profiles was reported to vary from only a few centimeters (Buczko et al., 2002; Jungerius and Dejong, 1989) to over 50 cm depth (Dekker and Ritsema, 1994). In young pine forest, it is expected that SWR is limited to the

decomposed organic floor layer (duff) including large amount of partially decomposed vegetal material (Doerr et al., 1996). However, the extent and the conditions under which hydrophobic compounds influence SWR of underlying mineral soils remain unclear (Buczko et al., 2002). The persistence of soil water repellency can be quantitatively characterized either in the field or in the laboratory by the water drop penetration time (WDPT) test that consists of placing a drop of water on the soil surface and measuring the time for it to penetrate (Van't Woudt, 1959; Watson and Letey, 1970). WDPT value determines how long water repellency persists in the contact area between a water droplet and the soil surface. A soil is considered to be water repellent if the WDPT exceeds 5 s (Doerr, 1998).

The adjusted ratio between the soil-ethanol and soil-water sorptivities was proposed as a measure of the degree of hydrophobicity (Tillman et al., 1989). At the aim of estimating soil sorptivity, tension infiltration experiments are preferred to ponded ones to exclude the contribution of macropores that may overwhelm soil hydrophobicity (Cerdà, 1996; Ebel et al., 2012; Nyman et al., 2010). Miniaturized tension infiltrometers were proposed to determine SWR (Hallett et al., 2001; Vogelmann et al., 2013), but their use is confined to the aggregate scale and, for field use, standard infiltrometers are more suited. Hunter et al. (2011) assessed the influence of disk size suggesting that the minidisk infiltrometer (MDI), having a 45 mm diameter disk, is appropriate for field assessment of SWR. In a recent investigation, the MDI proved to be a practical alternative to the classical tension infiltrometer to estimate hydrodynamic properties of a loam soil (Alagna et al., 2016). Furthermore, repellency assessment based on MDI tests appears inherently scaled to account for soil physical properties other than hydrophobicity (e.g., the volume, connectivity and the geometry of pores) that directly influence the hydrological processes.

Lichner et al. (2013b) assessed hydrophobicity of biological soil crusts by the water repellency cessation time (WRCT), estimated from the intersection of the two straight lines representing the cumulative infiltration vs. square root of time relationship for hydrophobic and near wettable conditions. For their miniaturized tension infiltration experiments, the WRCT increased with an increase in WDPT despite coefficients of determination were hardly significant (Lichner et al., 2013b). Use of WRCT to assess SWR from field experiments conducted by the MDI are still lacking in literature and there is the need to test the reliability of this index also considering the potential advantages that stem from its simplicity (small volumes of water, only one test site).

The objective of this research was to test alternative indices for assessing SWR from infiltration experiments conducted with the MDI in two Mediterranean pine woodlands. In

particular, the investigation was focused on the capability of MDI experiments carried out with either ethanol and water or water alone to assess SWR and to better understand the vertical evolution of SWR into the upper part of a forest soil profile.

C.3.2. Materials and methods

The investigation was conducted in two managed pine woodlands of the coastal Mediterranean region that can be considered representative of the reforestations widely applied in the past decades to tackle land degradation (Figure 1). The first site is located in the artificial woodland of Ciavolo close to Marsala, Italy (37°45'40.6" N, 12°34'09.0" E). Elevation is 105 m a.s.l. and surface slope is low (4.4%). The soil is a *Typic Rhodoxeralf* (Soil Survey Staff, 2014) with a depth of 0.40–0.60 m and the parent material is calcareous sandstone. According to USDA classification, the soil texture is clay loam (Table 1).

Two sampling sites (approximately 5 x 5 m^2 each) were arranged in an area including 30 years old *Pinus pinaster* trees. The first sampling site was located under the tree canopy fully covering the soil surface (site CF), the second sampling site was located in a glade vegetated with spontaneous annual grasses (*Avena fatua* L., *Galactites elegans* (All.) Soldano, *Hypochaeris achyrophorus* L., *Oxalis pes-caprae* L. and *Vulpia ciliata* Dumort) (site CG).

Fig. 1 Location of experimental sites.

Table 1 Physical and chemical properties of soils from the Mediterranean pine woodland sites at Ciavolo (Italy) and Javea (Spain).

Site	Depth (cm)	Soil texture	Sand (%)	Silt (%)	Clay (%)	$CaCO_3$ (%)	pH (H_2O)	pH ($CaCl_2$)
Ciavolo (forest)	5 - 10	clay-loam	23.6	43.0	33.4	2.05	7.39	6.76
Ciavolo (glade)	0 - 10	clay-loam	36.9	34.5	28.5	3.80	7.77	6.97
Javea	5 - 10	silty-clay	15.7	43.3	40.8	4.11	7.55	6.78

The second site was selected for comparative purposes given that any effect of pine stands on SWR can be excluded in this case due to the distance (approximately 50 m) between the two sites. In site CF, both the 5-cm thick surface duff formed by decomposed vegetal material (CFO) and the underlying 5-cm thick mineral soil layer (CFM) were sampled two times in 2014, at exactly the same location, to explore different initial soil moisture conditions. The first sampling was conducted in late summer (from 11th to 22th September) after a long dry period. Cumulative precipitation in the three months prior to sampling was 4.8 mm, whereas mean daily air temperature was 24.6 °C. The second sampling was conducted from 24th November to 3rd December after 108 mm rainfalls had occurred that is approximately 20% of the average annual precipitation for the location. Average air temperature on the two sampling dates were 24.7 °C and 18.2 °C, respectively. Only the 5-cm thick surface layer of mineral soil was sampled in the glade at the second date (CGM) given that a well-developed organic layer was not detectable in this case.

The second experimental site is located at Javea close to Alicante, Spain (38°48'15.0"N 0°09'18.8"E, elevation 213 m a.s.l.), in a 40-years old afforested plantation of *Pinus halepensis* (site JF). In the past, the site was cultivated as shown by the presence of abandoned agricultural terraces. The soil is *Lithic Rhodoxeralf* (Soil Survey Staff, 2014) developed over a karstified limestone with variable depth, generally lower than 0.5 m. According to USDA classification, the soil is silty clay (Table 1). On 8th and 16th July 2015, the surface duff (JFO) and the underlying mineral soil layer (JFM) were sampled at a selected flat area (approximately 5 x 5 m^2) located under the tree canopy. The mean daily air temperature at the two sampling dates were, respectively, 27.1 °C and 26.0 °C. No rainfall occurred in between the two dates and in the three months prior to sampling. In the same period (April to June) the mean daily air temperature was 21.1 °C. Only dry soil moisture condition was sampled at Javea site given the main focus of the study was on the SWR distribution in the upper soil profile of the two Mediterranean pine forests. Hereinafter, information from the seven sets of data, resulting from different sites, vegetation habitats, sampling depths and initial soil water contents, is abbreviated as follows: C: Ciavolo, J: Javea,

F: pine forest, G: glade with spontaneous grass vegetation, O: decomposed organic floor layer (duff), M: mineral soil, 1: first sampling date, 2: second sampling date.

For each sampling condition (i.e., for each soil layer and time of sampling), 10 undisturbed soil cores (0.05 m in height by 0.05 m in diameter) were randomly collected to determine soil bulk density, ρ_b (Mg m^{-3}), and volumetric water content at the time of sampling, θ_0 (m^3m^{-3}). Scrubbed soil samples were also collected to determine organic matter (OM) content by the Walkley-Black method (Nelson and Sommers, 1982). The water drop penetration time (WDPT) test was carried out by placing 30 drops of deionized water in different smoothed locations within the sampling area from a standard height of 10 mm and recording the time for their complete penetration, A medical dropper was used that yielded drops of uniform volume (70 ± 5 μL). Despite there is not a standard protocol for WDPT measurement, this drop size was close to the minimum volume recommended by Hallin et al. (2013) to accurately account for soil microtopographical variability. According to these authors, the applied protocol allows estimating the mean WDPT value with an error of ±10% at 95% confidence. For long infiltration time (WDPT > 600 s) the drop was protected from direct sun and covered by a plastic can to limit evaporation. Five classes of repellency were considered according to Dekker and Ritsema (1994): wettable (WDPT <5 s); slightly water repellent (WDPT = 5-60 s); strongly water repellent (WDPT = 60-600 s); severe water repellent (WDPT = 600-3600 s) and extremely water repellent (WDPT > 3600 s).

Twenty tension infiltration tests were conducted by a standard MDI (Decagon Devices, Inc., Pullman, WA). Both 95% ethanol and deionized water were used, setting the applied pressure head at –2 cm to reduce macropore flow (Beatty and Smith, 2013; Hallet et al., 2001; Lichner et al., 2013b) and placing the disk of the MDI directly on the soil surface previously levelled using a small amount of 2-mm sieved soil collected near the infiltration point. Cumulative infiltration of ethanol was visually recorded at the MDI reservoir at intervals of 10 s for the first minute, every 30 s for the successive two minutes and, finally, every one minute until the complete infiltration of approximately 0.08 L of ethanol, corresponding to a cumulative infiltration height of 50 mm. Infiltration of water was much slower than infiltration of ethanol and, therefore, measurement intervals were increased up to 15 min. The influence of temperature on SWR measurements was considered negligible given that field tests within an experimental condition (i.e., given site, soil layer and vegetation habitat) were completed in no more than 1-2 days during which the differences in temperature were small and, in any cases, influenced the different SWR indices in a comparable way.

Soil sorptivity was estimated as the slope of the regression line between the early-time cumulative infiltration, I (L), and square root of time, t (T) (Philip, 1957). According to Tillman et al. (1989), the repellency index, RI, is the adjusted ratio of ethanol sorptivity, S_e (L $T^{-0.5}$), to water sorptivity, S_w (L $T^{-0.5}$) (i.e., RI = 1.95 S_e / S_w). However, measurements of S_e and S_w cannot be performed sequentially at the same point since the initial conditions change between the two fluids whereas pairwise measurements of S_e and S_w may result in possible misestimating of RI due to soil heterogeneity. In this study, the approach proposed by Pekárová et al. (2015) was followed that considers 100 estimates of RI obtained from all possible combinations of 10 S_e by 10 S_w measurements at each sampling site. By this approach, the statistics of RI are derived from the empirical frequency distribution which accounts for overall spatial variability of SWR. The RI estimated according to Pekárová et al. (2015) is also referred to as combined repellency index. For comparative purposed, RI was also calculated from the mean S_e and S_w values at each of seven experimental conditions. Using water infiltration data, the water repellency cessation time (WRCT) was estimated as the intersection between the two regression lines representing the early-time (hydrophobic) and late-time (wettable) soil conditions in a I vs. $t^{0.5}$ graph (Lichner et al., 2013b). The same graph allowed to calculate a modified repellency index RI_m as the ratio of the sorptivities in the two stages of the infiltration process (Sepehrnia et al., 2016).

The analysis of the statistical distribution of a given set of data was carried out by the Lilliefors (1967) test at P = 0.05. Only the normal and the log-normal distributions were considered because soil physical properties were often found to be adequately described by these distributions (Warrick, 1998). The mean and the coefficient of variation (CV) of a given dataset were calculated according to the statistical distribution better describing the experimental data (Lee et al., 1985). Outliers in dataset were detected as values falling above or below 1.5 times the interquartile range (Helsel and Hirsh, 2002) and excluded from the following statistical analyses. Comparisons between mean values were conducted by a t-test (P = 0.05), either homoscedastic or not according to an F-test (P = 0.05).

C.3.3. Results and discussion

For both forest sites (CF and JF), summer sampling yielded significantly lower and more variable soil water contents in the surface duff than in the underlying mineral soil (Table 2). A significant increase of soil moisture of the duff but not of the underlying mineral soil was observed between the two sampling dates at Ciavolo. As a consequence of rainfall that occurred in autumn, water content on the latter date was more uniformly distributed, both

horizontally (CV = 5.8–8.0%), and vertically given that CFO2 and CFM2 were characterized by equal mean θ_0 values. Reduced transpiration and lack of canopy interception were considered responsible for the higher soil moisture content observed in the glade of Ciavolo on the second date (ratio between mean θ_0 values in CGM2 and CFM2 equal to 1.7).

As expected, the pine duff at both sites (Ciavolo and Javea) was characterized by significantly lower bulk density and higher organic matter content than the underlying mineral soil (Table 2). In particular, the ratio between the bulk density of the duff and that of the mineral soil varied in the range 0.51–0.68, whereas the same ratio for OM ranged between 3.1 and 5.5. In general, the differences between the properties of the two sampled layers were more pronounced at Javea than at Ciavolo (Table 2). At this second site, the mean values of ρ_b and OM in the duff did not change in the spell between the two sampling dates (CFO1 and CFO2), whereas a significant reduction by a factor of 0.93 and 0.84, respectively, was found for the subsoil (CFM1 and CFM2) (Table 2).

At the second sampling date, the two mineral soils of Ciavolo (CFM2 and CGM2) showed significant different values of ρ_b and OM. However, the variability of point measurements of bulk density and organic matter for the mineral soils of Ciavolo was generally limited (ρ_b = 1.01–1.29 kg m^{-3}; OM = 3.8–5.0%) and within the range encountered for similar soil types (Bagarello et al., 2014). The WDPT tests conducted at the glade site of Ciavolo (CGM2) showed no occurrence of water repellency given that the water drops placed on the soil surface always infiltrated in less than 5 s (WDPT < 5 s). The very fast infiltration time precluded the estimation of statistics for WDPT in this site and, therefore, these data were excluded from the following analysis. The hypothesis of WDPT data distributed according to a log-normal distribution was never rejected except for the duff layer of Javea (JFO1) for which neither the normal or the log-normal distributions described the WDPT data. The normal distribution was rejected in two additional cases and, when both the normal and log-normal distributions were not rejected, the Lilliefors statistic was generally lower for the log-transformed data. Therefore, the log-normal distribution was assumed for WDPT data and results summarized by calculating the geometric mean, GM, and the associated CV (Lee et al., 1985).

In both forest sites, the surface duff exhibited a marked SWR (Table 3), whereas the subsurface layer was hydrophobic only at the Ciavolo site where WDPT ranged from a minimum of 100 up to 4425 s (Table 3). According to the classification by Dekker and Ritsema (1994), the pine duff was classified as severely water repellent. The WDPT of the

duff was from 2 to 5.3 times that of the mineral soil layer at Ciavolo, depending on sampling date, and 370 times higher at Javea. In the spell between the two sampling campaigns conducted at Ciavolo, the WDPT decreased by a not significant 14% in the duff layer and increased by a factor of 2.5 in the mineral subsoil (Table 3).

Table 2 Statistics of initial soil water content (θ_0), bulk density (ρ_b), and organic matter content (OM) for different sampling depths and dates at the experimental sites of Ciavolo (C) (Italy) and Javea (J) (Spain) where F. forest, G: glade, O: decomposed organic floor layer (duff), M: mineral soil; 1: first sampling; 2: second sampling, *N*: sample size.

	Ciavolo					Javea	
	CFO1	CFO2	CFM1	CFM2	CGM2	JFO1	JFM1
Initial water content, θ_0 ($cm^3\ cm^{-3}$)							
N	10	10	9	10	10	10	8
min	0.104	0.149	0.149	0.155	0.245	0.033	0.054
max	0.160	0.199	0.180	0.182	0.312	0.114	0.139
mean	0.128 (a),(c)	0.175 (a),d	0.166 b,(c)	0.169 b,d,(e)	0.281 (e)	0.066 (f)	0.098 (f)
CV (%)	16.9	8.01	6.33	5.80	7.51	36.9	29.2
Bulk density, ρ_b ($kg\ m^{-3}$)							
N	10	10	9	10	10	10	8
min	0.450	0.641	1.108	1.011	1.120	0.181	0.817
max	1.077	0.891	1.242	1.219	1.291	0.864	1.276
mean	0.725 a,(c)	0.749 a,(d)	1.172 (b),(c)	1.089 (b),(d),(e)	1.192 (e)	0.548 (f)	1.082 (f)
CV (%)	32.4	9.5	4.14	5.70	4.73	45.5	14.9
Organic matter content, OM (%)							
N	10	10	10	10	10	10	10
min	19.10	21.31	4.60	3.80	4.43	22.7	8.22
max	21.66	21.74	4.80	4.04	5.00	28.7	8.87
mean	20.03 a,(c)	21.48 a,(d)	4.66 (b),(c)	3.93 (b),(d),(e)	4.71 (e)	26.6 (f)	8.54 (f)
CV (%)	7.04	1.07	2.41	3.11	6.02	12.6	3.83

Mean values followed by the same letter enclosed in brackets are significantly different according to a two-tailed t test (P = 0.05). Mean values followed by the same letter not enclosed in brackets are not significantly different.

The observed decrease of WDPT was probably a consequence of the well document decrease of SWR as the initial water content increases (i.e., Fer et al., 2016; de Jonge et al., 1999; Dekker and Ritsema, 1994; Lichner et al., 2013a;). For the mineral layer, the hydrophobicity increased notwithstanding the soil water content did not change and the organic matter content decreased (Table 2) thus suggesting that amphiphilic hydrophobic compounds were probably leached from the surface duff as consequence of rainfall that occurred in autumn (Vogelmann et al., 2013). This interpretation was supported by the large difference in WDPT observed for the mineral clay-loam soil layer under the pine forest and the spontaneous grass. Indeed, WDPT < 5 s was observed in 100% of cases in the soil of the glade site (CGM2)

whereas, in the mineral soil of forest site (CFM2), the minimum value of WDPT was equal to 100 s.

Table 3 Statistics of water drop penetration time, WDPT, water repellency cessation time, WRCT, repellency index, RI, and modified repellency index, RI_m, for different sampling depths and dates at the experimental sites of Ciavolo (C) (Italy) and Javea (J) (Spain) where F: forest, G: glade, O: decomposed organic floor layer (duff), M: mineral soil; 1: first sampling; 2: second sampling, *N*: sample size.

	Ciavolo					Javea	
	CFO1	CFO2	CFM1	CFM2	CGM2	JFO1	JFM1
Water drop penetration time, WDPT (s)							
N	30	30	29	30	30	30	29
min	868	150	113	100		480	1
max	3534	6890	855	4425		7517	18
geometric mean	1689 a,(c)	1454 a,(d)	300 (b),(c)	745 (b),(d)	<5	2139 (e)	5 (e)
CV (%)	48.4	182.0	53.6	136.7		116.1	106.1
Water repellency cessation time, WRCT (s)							
N	10	9	10	10	10	10	10
min	9736	4653	2446	1701	479	2496	169
max	20204	13678	8502	8772	861	11250	761
geometric mean	13933 (a),(c)	8908 (a),(d)	4344 b,(c)	3534 b,(d),(e)	631 (e)	6268 (f)	386 (f)
CV (%)	25.4	35.3	45.0	56.4	21.5	64,2	54,2
Repellency index, RI (–)							
N	100	100	100	100	100	100	100
min	11.9	10.3	1.9	3.3	1.4	5.7	0.4
max	224.0	129.6	27.7	31.2	4.7	79.5	4.3
geometric mean	55.1 (a),(c)	32.5 (a),(d)	6.1 (b),(c)	9.7 (b),(d),(e)	2.7 (e)	22.4 (f)	1.3 (f)
CV (%)	68.8	70.5	69.7	54.6	26.1	63.7	64.8
Mean repellency index, RI (–), according to Tillman et al. (1989)							
	57.2	28.0	6.5	9.9	2.7	22.5	1.2
Modified repellency index, RI_m (–)							
N	8	10	10	8	10	10	9
min	16.8	6.3	6.9	10.4	4.6	2.8	1.7
max	60.3	57.3	23.2	17.8	7.9	14.2	3.6
GM	29.7 a,(c)	21.3 a,(d)	13.5 b,(c)	13.4 b,(d),(e)	5.8 (e)	5.6 (f)	2.1 (f)
CV (%)	48.2	76.1	43.3	15.8	16.3	53.1	24.1

Mean values followed by the same letter enclosed in brackets are significantly different according to a two-tailed t test (P = 0.05). Mean values followed by the same letter not enclosed in brackets are not significantly different.

A different result was obtained for the mineral subsoil of Javea (JFM1) that showed wettable conditions (WDPT ≤ 5 s) in 37% of cases, thus confirming that the dynamic of hydrophobic compounds in the subsoil is mostly unknown and needs further analysis (Buczko et al., 2002; Buczko et al., 2005; Jungerius and Dejong, 1989).

Large variability of results is rather common for WDPT measurements. García et al. (2005) found 57% of wettable field-moist samples (N = 89) at depths 0–0.025 m under the *Pinus pinea* trees in southern Spain, which is consistent with the findings of Lichner et al. (2013a) for a *Pinus sylvestris* forest in Slovakia (N = 39). These authors reported relative frequencies of strongly, severely and extremely water repellent conditions equal to 23, 18 and 5%, respectively.

McKissock et al. (1998) found that WDPT was directly correlated to OM. This investigation also showed a statistically significant positive relationship (R^2 = 0.830) between mean WDPT and OM values (N = 7) (Figure 2). This means that the amount of soil OM has a strong influence on the persistence of SWR. However, the chemical characteristics of OM influence to a greater extent SWR and soil wettability can be better interpreted if organic composition is considered (Buczko et al., 2005; Ellerbrock et al., 2005; Vogelmann et al., 2013). In fact, the relatively small amount of hydrophobic compounds could not be necessarily proportional to the amount of total OM (Doerr et al., 2000). A linear increasing relationship was found between WDPT and the potential wettability index that is the proportion of hydrophobic to hydrophilic functional groups (Fer et al., 2016; Leue et al., 2015). A similar result was found by Ellerbrock et al. (2005) despite SWR was not directly correlated with OM. Analysis of OM composition was not conducted in this study but these findings could explain the very different behavior observed in terms of WDPT for the clay-loam soils of CFM2 and CGM2 sites that were characterized by approximately the same amount of OM (Figure 2).

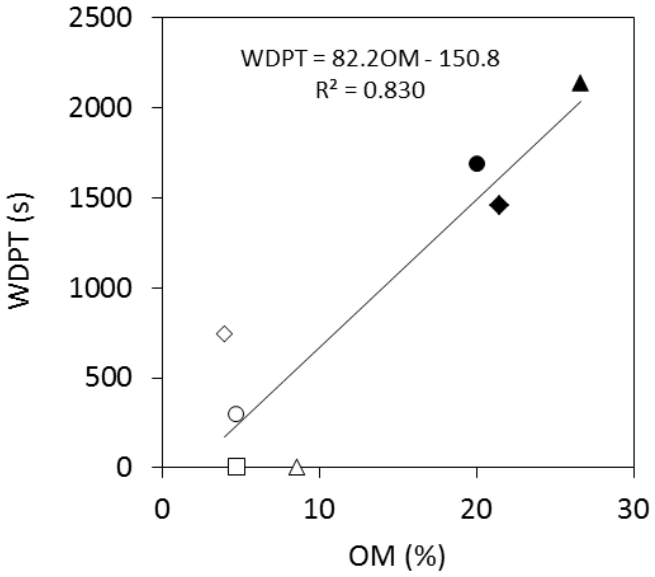

Fig. 2 Relationship between the organic matter (OM) content and the water drop penetration time (WDPT) for the different vegetation covers, sampling depths and initial soil water contents of the experimental sites of Ciavolo (Italy) and Javea (Spain) (● CFO1; ◆ CFO2; ○ CFM1; ◇ CFM2; □ CGM2; ▲ JFO1; △ JFM1).

Minidisk infiltration tests conducted with ethanol as infiltrating liquid were in line with the infiltration theory that prescribes a more or less prolonged transient phase in which infiltration rate, i (L T^{-1}) decreases, followed by a steady state infiltration phase in which infiltration rate is practically constant. This behaviour is shown in figure 3a in which normalized infiltration rate (i.e., i / i_{max}) is plotted as function of normalized time (t / t_{max}). In the initial stage of water infiltration, hydrophobicity prevented water entry into the soil thus resulting in a low infiltration rate (Figure 3b). Following wetting of hydrophobic compounds, infiltration rate increased at larger duration of the run. As highlighted by bold lines in figure 3b, an increase of infiltration rate at late time was also detected for the mineral soils of Ciavolo glade (CGM2) and Javea (JFM1) that were classified as wettable according to the WDPT tests. The occurrence of hydrophobicity was even more evident when the cumulative water infiltration data were plotted as function of the square root of time. All water infiltration tests exhibited a clear "hockey-stick-like" shape that allowed calculation of WRCT as the intersection point of two straight lines, representing the initial and the late stages of I vs. $t^{0.5}$ relationships (Lichner et al., 2013b) (Figure 4). An upward concave shape of the I vs. $t^{0.5}$ plot is predicted by the infiltration theory also for wettable soils and could complicate the assessment of SWR. However, transition in this case is gradual and occurs relatively soon for MDI experiments as consequence of passage from the initial stage of infiltration, in which flow is dominated by vertical capillarity, to a stage in which infiltration is dominated by both vertical gravity and lateral capillarity (Vandervaere et al., 2000).

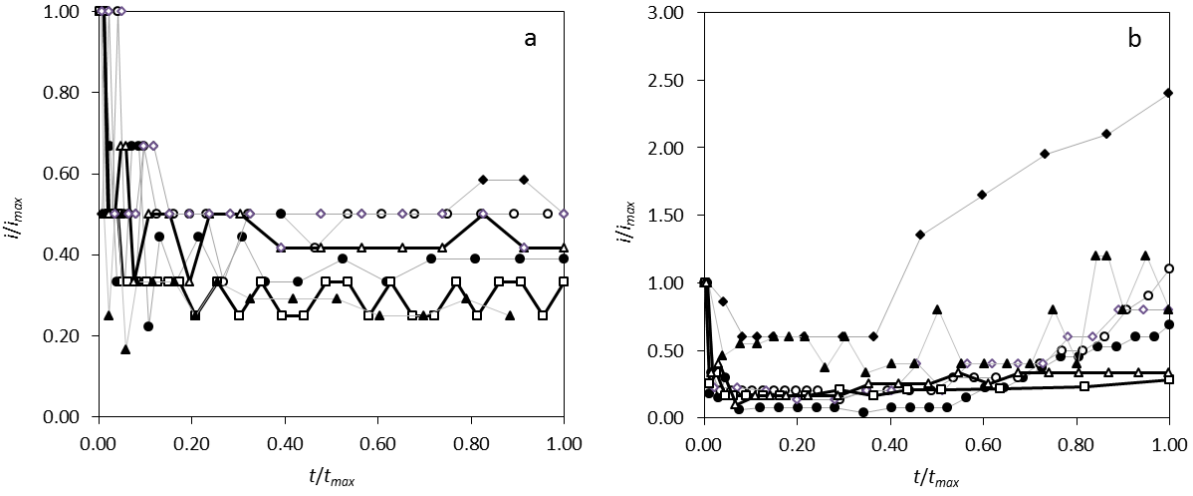

Fig. 3 Examples of normalized infiltration rate, i/i_{max} (-), vs. normalized time, t/t_{max} (-),data collected during minidisk infiltrometer tests conducted at the experimental sites with: a) ethanol and b) water as infiltrating liquids (● CFO1; ◆ CFO2; ○ CFM1; ◇ CFM2; □ CGM2; ▲ JFO1; △ JFM1; infiltration data in bold lines were collected in sites that were classified as wettable according to WDPT test).

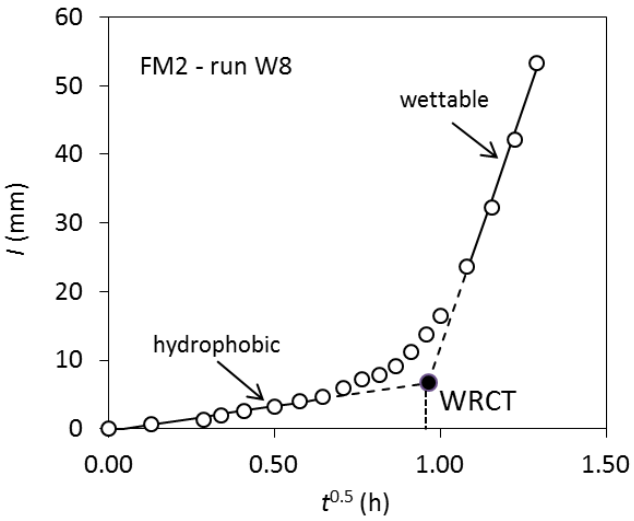

Fig. 4 Example of the estimation of the water repellency cessation time (WRCT) for a MDI experiment conducted with water in the mineral sublayer of the Ciavolo pine forest.

For each sampling condition, WRCT data were better described by a log-normal than a normal distribution. The GM of WRCT measured in the duff (CFO1, CFO2 and JFO1) was up to 16 times that of the corresponding underlying mineral soils (CFM1, CFM2 and JFM1) (Table 3) but differences by a factor of 5.6–6.9 were found between the mineral soils of the forest (CFM1 and CFM2) and the glade (CGM2) thus confirming that pine stands influence the hydrophobic characteristics of deeper soil layer at Ciavolo. The log-transformed values of WRCT, determined under different conditions of vegetation, sampling depth and initial soil water content at the experimental sites (N = 7), were significantly correlated (R^2 = 0.925) to the corresponding log(WDPT) values (Figure 5). The regression line was characterized by an intercept greater than zero and a slope lower than one (Figure 5) and the discrepancies between WRCT and WDPT were more pronounced for low values of hydrophobicity and decreased as SWR increased. In other terms, a higher ability of WRCT to detect weak SWR phenomena was observed, as compared to the more traditional WDPT test. Therefore, the WRCT, determined from a single water infiltration experiment conducted by the MDI, seems potentially more suitable to assess "sub-critical" repellency that occurs when the water-solid contact angle is less than 90° but not zero (Tillman et al., 1989). Under these circumstances, water infiltration rate is reduced but not prevented at all, as in the case of severe hydrophobicity.

For all ethanol and water infiltration tests, S_e and S_w estimation was successfully conducted given that it was always possible to select at least three initial data denoting a linear I vs. $t^{0.5}$ relationship. As common for most soil hydrodynamic properties (e.g., Warrick, 1998), the log-normal distribution better described the empirical frequency distribution of RI at each experimental site due to the high level of heterogeneity and positive skewness of the data. Statistics for RI confirmed the influence of pine vegetation on SWR already shown by the other indices (Table 3). Mean RI values in the duff of the forest sites (CFO1, CFO2 and JFO1) were from 3.3 to 17 times higher than the corresponding RI values measured in the subsoil (CFM1, CFM2 and JFM1). Furthermore, the ratio between the mean RI in the forest

and the glade soils of Ciavolo ranged from 2.2 to 20 according to the different sampling depths and dates (Table 3). The differences in RI values between the forest and the glade sites of Ciavolo are in agreement with those detected by Lichner et al. (2012) in a sandy soil at Sekule (southwestern Slovakia). They found that the mean RI values in the duff under *Pinus sylvestris* trees were from 3.6 to 11.9 times higher than the mean RI values estimated in the glade (covered with the biological soil crust) and grassland soils.

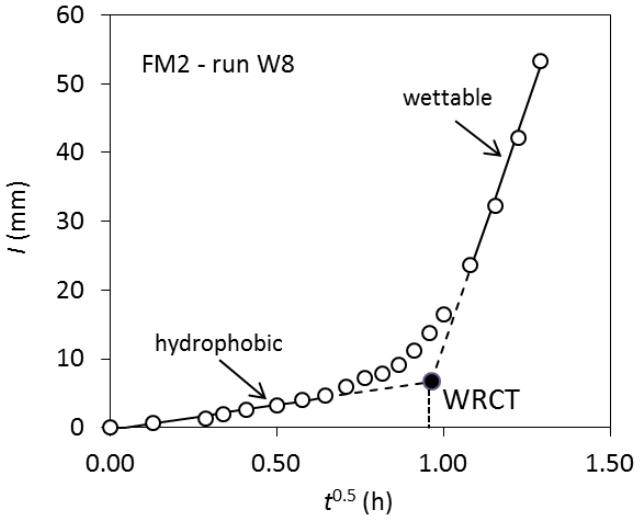

Fig. 5 Relationship between water drop penetration time (WDPT) and water repellency cessation time (WRCT) for different vegetation covers, sampling depths and initial soil water contents of the experimental sites of Ciavolo (Italy) and Javea (Spain) (● CFO1; ◆ CFO2; ○ CFM1; ◇ CFM2; □ CGM2; ▲ JFO1; △ JFM1).

In agreement with the vertical dynamics of hydrophobic compounds suggested by the WDPT tests, RI at Ciavolo decreased in the duff and increased in mineral subsoil in the spell between the two samplings (Table 3). Only one sampling campaign was conducted at Javea and analysis of temporal evolution of SWR is not possible. However, the wettable or weak hydrophobic conditions detected for the mineral subsoil by WDPT, WRCT and RI indices suggest absence of leaching phenomena in this site. Indeed, minidisk infiltration tests conducted with ethanol yielded steady-state infiltration rates in the surface organic layer of Javea (JFO1) that were 3.8-5.8 times lower than those in the corresponding layer at Ciavolo (CFO1 and CFO2). Given that steady-state infiltration rate is a close estimate of soil hydraulic conductivity and that infiltration process with ethanol is not influenced by hydrophobicity, it was concluded that the different extent of vertical SWR observed in the two sites was a consequence of the different transmission properties of the organic layer overlaying the mineral soil.

The geometric mean values of RI were practically coincident with the mean RI values calculated according to Tillman et al. (1989) as adjusted ratio of the mean of S_e and S_w at each of seven experimental conditions (Table 3). In other terms, conducting pairwise infiltration experiments with ethanol and water to determine mean values of S_e and S_w yields a mean RI value equal to that obtained applying the combination procedure suggested by Pekarova et al. (2015) with the advantage that this last procedure allows a straightforward quantification of SWR variability.

The sharp increase in the slope of the cumulative water infiltration data plotted in the form I vs. $t^{0.5}$ (Figure 4) suggested to propose a modified repellency index, RI_m, defined as the ratio of the sorptivities estimated at the late and early stages of a single water infiltration test conducted by MDI. The statistics of RI_m, reported in Table 3, confirmed the differences between the surface duff and the underlying mineral soil for both Ciavolo and Javea sites and between the mineral soils in the forest (CFM2) and the glade (CGM2) but not between the first and the second sampling date at the forest site of Ciavolo.

Independently of the sampled layer and the initial soil water content, the spatial variability of the repellency indices deduced from MDI experiments were comparable (Table 3) and generally lower in the glade site than in the forest ones. Estimation of SWR by WDPT measurements yielded in some cases larger spatial variability. The soil surface area sampled in a drop scale infiltration test is of the order of 0.14 cm^2 whereas the MDI samples a 100 times larger surface area. Therefore, the observed differences in CVs can be considered a consequence of the different spatial support of the two considered field tests (Moody and Schlossberg, 2010).

The repellency indices obtained by the infiltration tests conducted by MDI were generally correlated among them and with the WDPT index (Table 4).

Table 4 - Correlation matrix of repellency indices for the different vegetation covers, sampling depths and initial soil water contents of the experimental sites of Ciavolo (Italy) and Javea (Spain).

	log(WDPT)	log(WRCT)	log(RI)	log(RI_m)
log(WDPT)	1			
log(WRCT)	**+0.9617**	1		
log(RI)	**+0.7957**	**+0.8515**	1	
log(RI_m)	+0.6847	**+0.8095**	**+0.8102**	1

Values in bold are significantly different from zero according to the Student t-test (P = 0.05)

In particular, both the original repellency index, RI, and the modified repellency index, RI_m, showed a closer correspondence with WRCT than WDPT, thus confirming that the water repellency assessment conducted by infiltration-based tests (i.e., WRCT, RI, and RI_m) yields comparable results. In particular, a significant linear regression line was found between log(WRCT) and log(RI_m) and between log(RI) and log(RI_m) (Figure 6) suggesting that the modified repellency index RI_m, obtained from a single infiltration experiment conducted with water as infiltrating fluid, could be considered suitable for assessing the hydrologic effects of SWR by overcoming the experimental drawback of conducting two infiltration runs with

different liquids (water and ethanol) in different sampling points. Despite WRCT and RI_m require the same experimental information, the ratio between two slopes of the *I* vs. $t^{0.5}$ graph appears inherently more robust and less subjective than the estimation of a single point characterizing the transition from hydrophobic to wettable conditions.

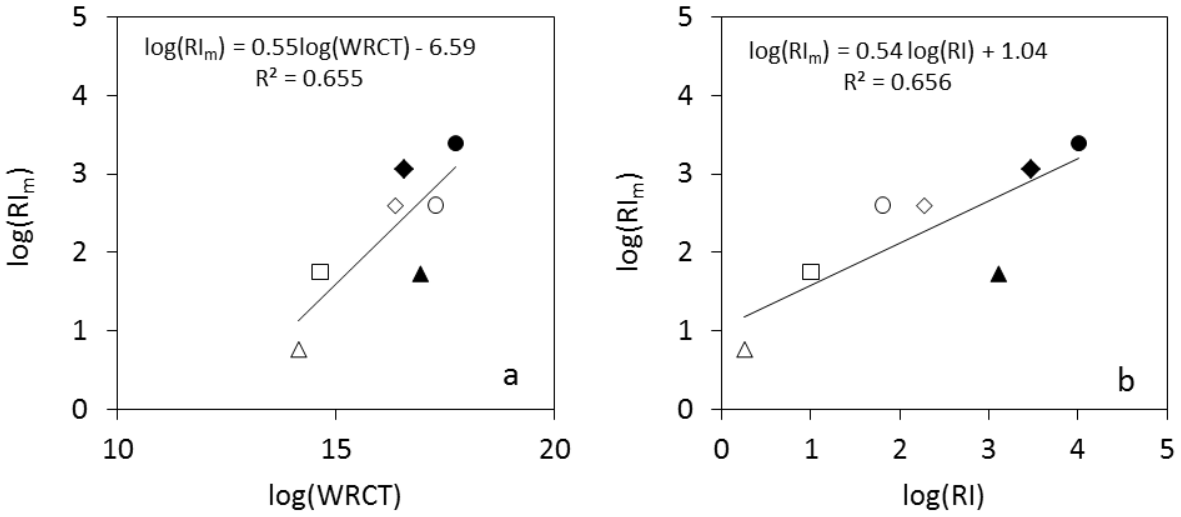

Fig. 6 Regression lines between the log-transformed values of (a) water repellency cessation time (WRCT) and modified repellency index (RI_m), (b) repellency index (RI) and modified repellency index (RI_m) for different vegetation covers, sampling depths and initial soil water contents at the experimental sites of Ciavolo (Italy) and Javea (Spain) (● CFO1; ◆ CFO2; ○ CFM1; ◇ CFM2; □ CGM2; ▲ JFO1; △ JFM1).

C.3.4. Conclusions

All the water repellency indices (WDPT, WRCT, RI and RI_m) unanimously detected severe SWR of the surface soil layer of the pine forests of Ciavolo and Javea due to the high amount of organic matter (OM > 20%). However, for the clay loam soil of Ciavolo, higher hydrophobicity was observed in the mineral subsoil under the pine trees than in an adjacent glade area despite the OM content of the two investigated sites was comparable. Furthermore, SWR of the mineral subsoil increased in conjunction with autumnal rainfalls. It was hypothesized that leaching of hydrophobic compounds, such as resins and waxes from decomposing pine needles in the overlying duff, determined the observed SWR evolution. The same vertical distribution of hydrophobic compounds was not observed in the forest site of Javea where the mineral subsoil was wettable or weakly hydrophobic. In this case, WDPT, WRCT, RI and RI_m indices were comparable to those determined in the glade area of Ciavolo. Due to lower hydraulic conductivity properties of the duff in Javea site, percolation of hydrophobic compounds to the subsoil was slowed or prevented at all, thus resulting in a

sharply stratified condition with the uppermost part of the soil profile characterized by severe or extreme SWR and the immediately underlying soil being practically wettable.

The considered indices were generally correlated one another and lead to SWR estimations generally concurrent even if some discrepancies in prediction were observed. In particular, at low hydrophobicity levels, the SWR indices gathered from the MDI tests signaled SWR conditions that were not detected by the traditional WDPT index. This result confirms that the traditional WDPT test is able to discriminate between hydrophobic and wettable soil conditions but is less suitable to account for sub-critical SWR. On the other hand, infiltration experiments conducted by the MDI can disclose sub-critical conditions, that is the conditions in which infiltration is reduced but not prevented at all and may negatively affect hydrological process. Furthermore, the soil volume sampled by the MDI is more representative of small scale variability of SWR that cannot be detected by the droplet test.

The WRCT and modified repellency index RI_m, requiring only a single MDI experiment conducted with water, yielded SWR estimates in reasonable agreement with those obtained with the RI test. The two indices, being able to account for subcritical SWR, offer a way to quantify with a single number the complex site-specific soil wetting properties. Further investigations are necessary to test the validity of WRCT and RI_m on different soil-vegetation associations also with the aim to define classification criteria for these repellency indices. However, they appear potentially usable for SWR assessment in alternative to the more cumbersome RI approach.

Acknowledgements

This study was supported by grants from the Università degli Studi di Palermo (project FFR 2012 and Dottorato di Ricerca in Scienze Agrarie, Forestali e Ambientali, ciclo XXIX, D50002D13+1012), the Slovak Scientific Grant Agency VEGA (project No. 2/0054/14), Ministerio de Economía and Competitividad of Spanish Government (project CGL2013-47862-C2-1-R), Botánica Mediterránea S.L., and Montgó Natural Park. Field data in Italy and Spain were collected by V. Alagna. All authors analyzed the data and contributed to write the manuscript.

References

Alagna, V., Bagarello, V., Di Prima, S., Iovino, M., 2016. Determining hydraulic properties of a loam soil by alternative infiltrometer techniques. Hydrol. Processes, 30, 2, 263–275.

Bagarello, V., Castellini, M., Di Prima, S., Iovino, M., 2014. Soil hydraulic properties determined by infiltration experiments and different heights of water pouring. Geoderma, 213, 492–501.

Beatty, S.M., Smith, J.E., 2013. Dynamic soil water repellency and infiltration in post-wildfire soils. Geoderma 192, 160-172.

Buczko, U., Bens, O., Fischer, H., Hüttl, R.F., 2002. Water repellency in sandy luvisols under different forest transformation stages in northeast Germany. Geoderma, 109, 1–2, 1–18.

Buczko, U., Bens, O., Hüttl, R.F., 2005. Variability of soil water repellency in sandy forest soils with different stand structure under Scots pine (Pinus sylvestris) and beech (Fagus sylvatica). Geoderma, 126, 3–4, 317–336.

Cerdà, A. 1996. Seasonal variability of infiltration rates under contrasting slope conditions in southeast Spain. Geoderma, 69, 217–232.

Cerdà, A., Doerr, S.H., 2007. Soil wettability, runoff and erodibility of major dry-Mediterranean land use types on calcareous soils. Hydrol. Processes, 21, 17, 2325–2336.

DeBano, L.F., 2000. Water repellency in soils: a historical overview. J. Hydrol., 231–232, 4–32.

de Jonge, L.W., Jacobsen, O.H., Moldrup, P., 1999. Soil water repellency: effects of water content, temperature, and particle size. Soil Sci. Soc. Am. J. 63(3), 437-442.

Dekker, L.W., Ritsema, C.J., 1994. How water moves in a water repellent sandy soil. 1. Potential and actual water repellency. Water Resour. Res., 30, 9, 2507–2517.

Doerr, S.H., 1998. On standardizing the 'Water Drop Penetration Time' and the 'Molarity of an Ethanol Droplet' techniques to classify soil hydrophobicity: A case study using medium textured soils. Earth Surf. Proc. Land., 23, 7, 663–668.

Doerr, S.H., Shakesby, R.A., Walsh, R.P.D., 1996. Soil hydrophobicity variations with depth and particle size fraction in burned and unburned Eucalyptus globulus and Pinus pinaster forest terrain in the Águeda Basin, Portugal. Catena, 27, 1, 25–47.

Doerr, S.H., Shakesby, R.A., Walsh, R.P.D., 2000. Soil water repellency: its causes, characteristics and hydro-geomorphological significance. Earth-Sci. Rev., 51, 1–4, 33–65.

Ebel, B.A., Moody, J.A., Martin, D.A. 2012. Hydrological conditions controlling runoff generation immediately after wildfire. Water Resour. Res., 48, W03529.

Ellerbrock, R.H., Gerke, H.H., Bachmann, J., Goebel, M.-O., 2005. Composition of organic matter fractions for explaining wettability of three forest soils. Soil Sci Soc Am J 69(1), 57-66.

Fer, M., Leue, M., Kodesova, R., Gerke, H.H., Ellerbrock, R.H., 2016. Droplet infiltration dynamics and soil wettability related to soil organic matter of soil aggregate coatings and interiors. Journal of Hydrology and Hydromechanics 64(2), 111-120.

García, F.J.M., Dekker, L.W., Oostindie, K., Ritsema, C.J., 2005. Water repellency under natural conditions in sandy soils of southern Spain. Soil Research, 43, 3, 291–296.

Iovino, M., Castellini, M., Bagarello, V., Giordano, G., 2016. Using static and dynamic indicators to evaluate soil physical quality in a sicilian area. Land Degradation & Development 27(2), 200-210.

Hallett, P.D., Baumgartl, T., Young, I.M., 2001. Subcritical water repellency of aggregates from a range of soil management practices. Soil Sci. Soc. Am. J., 65, 1, 184–190.

Hallin, I., Douglas, P., Doerr, S.H., Bryant, R., 2013. The role of drop volume and number on soil water repellency determination. Soil Sci. Soc. Am. J., 77, 5, 1732–1743.

Helsel, D.R., Hirsch, R. M. 2002. Statistical methods in water resources. Techniques of Water resources investigations, Book 4, chapter A3. U.S. Geological Survey. 522 p. Publication available at: http://water.usgs.gov/pubs/twri/twri4a3/

Hunter, A.E., Chau, H.W., Si, B.C., 2011. Impact of tension infiltrometer disc size on measured soil water repellency index. Can. J. Soil Sci., 91, 1, 77–81.

Jungerius, P.D., Dejong, J.H., 1989. Variability of water repellence in the dunes along the Dutch coast. Catena, 16, 4–5, 491–497.

Lee, D.M., Reynolds, W.D., Elrick, D.E., Clothier, B.E., 1985. A comparison of three field methods for measuring saturated hydraulic conductivity. Can. J. Soil Sci., 65, 3, 563–573.

Letey, J., Carrillo, M.L.K., Pang, X.P., 2000. Approaches to characterize the degree of water repellency. J. Hydrol., 231–232, 61–65.

Leue, M., Gerke, H.H., Godow, S.C., 2015. Droplet infiltration and organic matter composition of intact crack and biopore surfaces from clay-illuvial horizons. Journal of Plant Nutrition and Soil Science 178(2), 250-260.

Lichner, L., Holko, L., Zhukova, N., Schacht, K., Rajkai, K., Fodor, N., Sándor, R. 2012. Plants and biological soil crust influence the hydrophysical parameters and water flow in an aeolian sandy soil. J. Hydrol. Hydromech., 60, 4, 309–318.

Lichner, L., Capuliak, J., Zhukova, N., Holko, L., Czachor, H., Kollar, J., 2013a. Pines influence hydrophysical parameters and water flow in a sandy soil. Biologia, 68, 6, 1104–1108.

Lichner, L., Hallett, P.D., Drongová, Z., Czachor, H., Kovacik, L., Mataix-Solera, J., Homolák, M., 2013b. Algae influence the hydrophysical parameters of a sandy soil. Catena, 108, 58–68.

Lilliefors HW. 1967. On the Kolmogorov-Smirnov test for normality with mean and variance unknown. J. Am. Stat. Assoc., 62, 318, 399–402.

Ma'shum, M., Farmer, V., 1985. Origin and assessment of water repellency of a sandy South Australian soil. Soil Research 23(4), 623-626.

McKissock, I., Gilkes, R.J., Harper, R.J., Carter, D.J., 1998. Relationships of water repellency to soil properties for different spatial scales of study. Soil Research, 36, 3, 495–508.

Moody, D.R., Schlossberg, M.J., 2010. Soil water repellency index prediction using the molarity of ethanol droplet test. Vadose Zone J., 9, 4, 1046–1051.

Nelson, D.W, Sommers, L.E. (1996). Methods of Soil Analysis. Part 3. Chemical Methods. Soil Science Society of America Book Series no.5, pp. 961–1010.

Nyman, P., Sheridan, G., Lane, P.N.J. 2010. Synergistic effects of water repellency and macropore flow on the hydraulic conductivity of a burned forest soil, south-east Australia. Hydrol. Processes, 24, 2871–2887.

Pekarova, P., Pekar, J., Lichner, L., 2015. A new method for estimating soil water repellency index. Biologia, 70, 11, 1450–1455.

Philip, J.R. 1957. The theory of infiltration: 4. Sorptivity and algebraic infiltration equations. Soil Sci., 84, 257–264.

Rodríguez-Alleres, M., Benito, E., de Blas, E., 2007. Extent and persistence of water repellency in north-western Spanish soils. Hydrol. Processes, 21, 17, 2291–2299.

Sepehrnia, N., Hajabbasi, M.A., Afyuni, M., Lichner Ľ., 2016. Extent and persistence of water repellency in two Iranian soils. Biologia, 71, 1137–1143.

Soil Survey Staff, 2014. Keys to Soil Taxonomy, 12th ed. NRCS, Washington, DC.

Tillman, R.W., Scotter, D.R., Wallis, M.G., Clothier, B.E., 1989. Water-repellency and its measurement by using intrinsic sorptivity. Aust. J. Soil Res., 27, 4, 637–644.

Tschapek, M., 1984. Criteria for Determining the hydrophilicity-hydrophobicity of Soils. Zeitschrift für Pflanzenernährung und Bodenkunde 147(2), 137-149.

Vandervaere ,J.P., Vauclin, M., Elrick, D.E., 2000. Transient flow from tension infiltrometers: II. Four methods to determine sorptivity and conductivity. Soil Sci. Soc. Am. J., 64:1272-1284.

Van't Woudt, B.D., 1959. Particle coatings affecting the wettability of soils. Journal of Geophysical Research 64(2), 263-267.

Vogelmann, E.S., Reichert, J.M., Prevedello, J., Consensa, C.O.B., Oliveira, A.É., Awe, G.O., Mataix-Solera, J., 2013. Threshold water content beyond which hydrophobic soils become hydrophilic: The role of soil texture and organic matter content. Geoderma, 209–210, 177–187.

Warrick, A.W., 1998. Appendix 1: Spatial variability. In: Hillel, D. (Ed.), Environmental Soil Physics. Academic Press, San Diego, pp. 655–675.

Watson, C.L., Letey, J., 1970. Indices for characterizing soil-water repellency based upon contact angle-surface tension relationships. Soil Sci. Soc. Am. J., 34, 6, 841–844.

C.4. Alternative analysis of transient infiltration experiment to estimate soil water repellency*

Alagna V.[1], Iovino M.[1]*, Bagarello V.[1], Mataix-Solera J.[2], Lichner Ľ.[3]

[1] Dipartimento di Scienze Agrarie e Forestali, Università degli Studi di Palermo, Palermo, Italy

[2] Departamento de Agroquímica y Medio Ambiente, Universidad Miguel Hernández, Elche, Spain

[3] Institute of Hydrology, Slovak Academy of Sciences, Bratislava, Slovak Republic

*Corresponding author. E-mail: massimo.iovino@unipa.it, tel +39 091 23897070, fax +39 091 484035

Abstract

The adjusted ratio between ethanol and water sorptivity measured by infiltration experiments conducted by the minidisk infiltrometer (MDI) is largely applied to assess soil water repellency (SWR). Compared to the droplet tests, it is more indicated to detect sub-critical SWR as it explores larger soil volume and directly accounts for the effect hydrophocity on soil infiltration. However, estimation of sorptivity by the commonly applied horizontal infiltration equation may be overestimated as it neglects the effects of gravity and lateral capillarity on the asymmetric infiltration process. The two-term infiltration model proposed by Haverkamp et al. (1994), that is valid for early to intermediate infiltration times, is potentially more able to yielded unbiased estimations of sorptivity. In this investigation, different techniques to estimate the soil sorptivity from MDI experiments conducted with ethanol, S_e, and water, S_w, were compared including the S1 and SL approaches that make use of the horizontal infiltration equation and the CL and DL approaches that are based on the linearization of the two-term infiltration equation. A new repellency index was proposed as the ratio between the slopes of the linearized data for the wettable and hydrophobic stages of water infiltration. The dataset included 85 MDI test conducted in three sites in Italy and Spain under different experimental conditions resulting from four vegetation habitats (forest of *Pinus pinaster* and *Pinus halepensis*, burned pine forest, annual grasses), two soil horizons (organic and mineral), three post-fire treatments, and dry or wet initial soil water contents. The approaches S1 and SL, based on the analysis of early-time infiltration data only, yielded a systematic overestimation of S_e and the S1 approach was inapplicable in 42% of experiments conducted with water thus preventing determination of repellency index (RI = 1.95 S_e/S_w). The biases in S_e and S_w estimations conducted by the SL approach yielded an overestimation of RI by a factor of 1.33 and 1.17 as compared to the values estimated with the CL and DL approaches. Moreover, these discrepancies were more pronounced in less water repellent soils

thus making the reliability of SL approach questionable for sub-critical SWR assessment. For the experimental conditions considered, the proposed repellency index, RI_s, was significantly correlated with the *RI* and Water Drop Penetration Time (WDPT) indices thus showing the potential reliability of soil hydrophobicity assessment by this index. Compared to *RI* that requires two infiltration experiments conducted with ethanol and water, RI_s offers a way to quantify with a single water experiment the complex site-specific soil wetting properties. Furthermore, it includes information on both sorptivity and conductivity measured in the wettable and repellent stages of the infiltration process and can be therefore considered more directly linked to the hydrological processes affected by soil water repellency.

Keywords: Two-term infiltration model, Soil water repellency, Minidisk infiltrometer, Repellency index

* This is a pre-refereeing draft submitted to Hydrological Processes in 2016.

C.4.1. Introduction

Soil water repellency reduces affinity of soils to water resulting in detrimental implication for plants growth as well as for hydrological processes. These include reduced matrix infiltration, development of fingered flow, irregular wetting fronts, and overall increased runoff generation and soil erosion (DeBano, 2000; Doerr et al., 2000). Soil water repellency stems from re-orientation of amphiphilic compounds during heating or drying which results in a non-zero contact angle between water and soil. In severe cases, when the contact angle exceeds 90°, water infiltration is prevented (Letey et al., 2000). However, it has increasingly been recognized that infiltration rates and pattern can be affected by "sub-critical" repellency that occurs when the water-solid contact angle is less than 90° but not zero (Tillman et al., 1989). Under these circumstances, water infiltration rate is reduced but not prevented at all as in the case of severe hydrophobicity (Hunter et al., 2011). During the last decade, it has become clear that soil water repellency is much more widespread than formerly thought, having been reported for a wide variety of soils, land uses and climatic conditions (Bachmann et al., 2007; Buczko et al., 2005; Buczko et al., 2006; Butzen et al., 2015; Lichner et al., 2011).

Due to its dynamic nature, soil water repellency is described in terms of both its persistence and degree. The water drop penetration time (WDPT) test (Doerr, 1998; Letey et al., 2000; Watson and Letey, 1970) has been diffusely applied to characterize the persistence

of soil water repellency. However, WDPT is a measure of the time required for the contact angle to change from its original value, which was greater than 90°, to a value approaching 90° and thus it is not necessarily an index of the water repellency (Cerdà and Doerr, 2007; Letey et al., 2000). Given the wettability of a hydrophobic soil surface can be increased by lowering the surface tension of the liquid, the degree of SWR can be assessed by using different mixtures of water and ethanol. With the Molarity of an Ethanol Droplet (MED) test, the degree of soil water repellency is associated to the concentration (or liquid–air surface tension) of the aqueous ethanol solutions that enters the soil almost instantaneously (Letey et al., 2000). However, it was argued that this method lacks the precision required to distinguish intermediate degrees of water repellency so that it is not adequate to characterize sub-critical repellency (Moody and Schlossberg, 2010).

Alternative approaches characterize SWR by comparing the soil-ethanol and soil-water sorptivities in an adjusted ratio (Tillman et al., 1989). Compared with drop scale infiltration tests (WDPT and MED), repellency indices based on infiltration tests are inherently scaled to account for soil physical properties other than hydrophobicity (e.g., the volume, connectivity and the geometry of pores) that directly influence the hydrological processes. Furthermore, the soil surface area sampled in a drop scale infiltration test is of the order of 0.14 cm^2 and measurements of water repellency can be significantly influenced by spatial variability (Moody and Schlossberg, 2010). Tension infiltration experiments are preferred to ponded ones to exclude the contribution of macropores that may overwhelm soil hydrophobicity (Cerdà, 1996; Ebel et al., 2012; Nyman et al., 2010). Miniaturized tension infiltrometers were proposed to determine water repellency at the aggregate scale (Hallett and Young, 1999) but, for field use, standard infiltrometers are more suited. Hunter et al. (2011) compared the influence of tension infiltrometer disk size suggesting that the minidisk infiltrometer (MDI) (Decagon Devices Inc., Pullman, USA), having a 4.5 cm diameter disk, is appropriate for field assessment of SWR. In a recent investigation, the MDI proved to be a practical alternative to the classical tension infiltrometer to estimate hydrodynamic properties of a loam soil (Alagna et al., 2016).

Soil sorptivity, S_0 (L $T^{-0.5}$), is commonly estimated from the Philip (1957) horizontal infiltration equation, but the assessment of the linear part of cumulative infiltration, I (L), vs. square root of time, t (T), relationship describing the early stage of the infiltration process could be problematic in water repellent soils (Carrick et al., 2011; Di Prima et al., 2016). Sorptivity was estimated as the infiltration rate out of a MDI during a fixed time interval, generally 1-5 min (Hunter et al., 2011; Lewis et al., 2006; Robichaud et al., 2008), as it is

considered fast enough to be an operational procedure for teams working in the field. However, the early-time linear regression of the I vs. $\sqrt{t}$ data neglects the effects of gravity and lateral capillary flux at the periphery of the source thus resulting in S_0 overestimations (Angulo-Jaramillo et al., 2016). An unbiased estimation of soil sorptivity is possible by fitting the two-term cumulative infiltration equation proposed by Haverkamp et al. (1994) to the infiltration data collected from early to intermediate infiltration time. In this case, validity of Philip's equation is not needed (Bagarello and Iovino, 2003; Vandervaere et al., 2000a). Haverkamp et al. (1994) model has been largely applied to estimate the hydrodynamic properties of a variety of soils using infiltration data collected under both tension and ponded conditions (Bagarello et al., 2014; Dohnal et al., 2010; Gonzalez-Sosa et al., 2010). However, to the best of our knowledge the two-term infiltration model has not been applied to assess SWR.

Determination of the repellency index needs two sorptivity values, one for water and one for ethanol, to be determined. As consequence of the influence of the antecedent soil water content on both ethanol and water sorptivity (Tillman et al., 1989), the two experiments cannot be conducted at exactly the same site. Due to spatial variability of SWR, as well as of other soil physical characteristics, a large number of replicated runs should be carried out to obtain a reliable estimate of the repellency index, for a given area, as the ratio of the averages of sorptivity found with ethanol and water. The possibility to derive a repellency index from a unique water infiltration experiment conducted by the MDI at a single site is thus intriguing also considering the potential advantages that stem from the simplicity of the technique (easy portability, small volumes of water, short duration of field experiment). An attempt to assess SWR by a single experiment was made by Lichner et al. (2013) who derived the water repellency cessation time (WRCT) as the time corresponding to the intersection of the two straight lines representing the cumulative infiltration vs. square root of time relationship for hydrophobic and near wettable conditions. Alagna et al. (2016) found that the WRCT was significantly correlated to WDPT under different soil and vegetation conditions. Therefore, they considered the WRCT essentially a measure of SWR persistence even if a higher ability to detect sub-critical repellency condition as compared to the traditional WDPT test was observed.

This investigation aimed at establishing the best applicative procedure to assess water repellency index from water/ethanol sorptivity measurements conducted by the MDI. In particular, different techniques to estimate the soil sorptivity using water, S_w, and ethanol, S_e, were compared including i) infiltration rate in a fixed time interval, ii) analysis of early-time

infiltration data and iii) linearization of the axisymmetric transient infiltration equation. The influence of the different sorptivity estimation techniques on the classical water repellency index calculated according to Tillman et al. (1989) was investigated in three Mediterranean sites under different soil/vegetation managements. Finally, a new single-test repellency index was proposed and evaluated against existing approaches.

Theory

Haverkamp et al. (1994) proposed the following three-dimensional infiltration equation for disk infiltrometers, valid for short to medium times:

$$I = S_0\sqrt{t} + \left[\frac{2-\beta}{3}K_0 + \frac{\gamma S_0^2}{r(\theta_0 - \theta_i)}\right]t \qquad (1)$$

where I (L) is the cumulative infiltration, t (T) is the time, θ_0 (L^3L^{-3}) is the volumetric soil water content corresponding to the imposed pressure head at the soil surface h_0 (L), θ_i (L^3L^{-3}) is the initial soil water content, $S_0 = S(h_0)$ ($L\ T^{-1/2}$) is the soil sorptivity, $K_0 = K(h_0)$ ($L\ T^{-1}$) is the soil hydraulic conductivity, r (L) is the radius of the circular source, β and γ are coefficients that are commonly set at 0.6 and 0.75, respectively. The first term of the right-hand side of eq.(1) accounts for vertical capillary flow and dominates infiltration during its early stage. The second term corresponds to the gravity-driven vertical flow and the third one represents the lateral capillary component at the edge of the circular infiltration surface (Smettem et al., 1994).

Eq. (1) can be linearized by dividing both sides by $\sqrt{t}$ (Cumulative Linearization, CL, method) or by differentiating the cumulative infiltration data with respect to the square root of time (Differentiated Linearization, DL, method) (Vandervaere et al., 2000a). In both cases, the soil sorptivity can be estimated as the intercept of the regression line fitted to the linearized experimental data. With this approach, the effects of gravity and lateral expansion are explicitly accounted for and soil sorptivity can be obtained using the complete experimental information collected for short to medium time (Angulo-Jaramillo et al., 2016). Vandervaere et al. (2000b) proposed DL method to account for the water stored in the contact material during the early stages of infiltration. However, if no contact material is used, CL method and DL method should result in similar S_0 estimates. A test of the expected equivalence of the two methods was conducted by Bagarello and Iovino (2004) who found that the two linearization methods were not perfectly equivalent in estimating S_0.

When the experimental cumulative infiltration data are plotted in the form of $I/\sqrt{t}$ vs. $\sqrt{t}$ or $dI/d\sqrt{t}$ vs. $\sqrt{t}$, the validity of eq.(1) can be easily checked and discontinuities in the infiltration process can easily be detected given they result in deviation from the monotonically increasing linear behaviour (Vandervaere et al., 2000a). Water repellency is one of most common circumstances producing deviation from the classical infiltration theory (Di Prima et al., 2016; Ebel and Moody, 2013; Imeson et al., 1992). Despite the SWR influence on the infiltration process depends on a variety of factors, including organic matter content and composition and initial soil water content, it has been recognized that, after an initial stage, infiltration rate increases as consequence of soil wetting (Beatty and Smith, 2013; Carrick et al., 2011). Comparing the soil hydrodynamic properties collected during the initial hydrophobic and subsequent wetting stages of an infiltration process can allow to quantify SWR. In particular, provided eq.(1) can separately applied to both stages, the intensity of repellency can be defined as the ratio between the slopes of the linearized cumulative infiltration relationships fitting the wetting and the hydrophobic stages of the infiltration process:

$$RI_s = \frac{\left[\frac{2-\beta}{3}K_w + \frac{\gamma S_w^2}{r\Delta\theta}\right]}{\left[\frac{2-\beta}{3}K_r + \frac{\gamma S_r^2}{r\Delta\theta}\right]} \qquad (2)$$

in which the subscript *w* refers to the wettable stage of infiltration and the subscript *r* to the repellent one.

Compared to the classical repellency index that makes use of two sorptivity measurements conducted with ethanol and water at two different sites, the repellency index defined by eq.(2) needs only one infiltration experiment conducted at a single site with water and, furthermore, it accounts for the effects induced by water repellency on the two hydrodynamic properties (sorptivity and hydraulic conductivity) that directly influence hydrological processes.

C.4.2. Materials and methods

Infiltration data were collected in the two Mediterranean managed pine forests of Ciavolo and Javea already sampled by Alagna et al. (2016) and in a fire-affected forest site in which different post-fire management strategies were implemented. Characteristics of sampling sites

are summarized in table 1 and detailed information on the two pine forest sites can be found in Alagna et al. (2016).

Table 1 Characteristics of the considered experimental sites.

Site	Coordinates UTM	Elevation and slope	Land use	Soil type	Soil texture (USDA)
Ciavolo, Marsala (Italy)	37°45'40.6" N, 12°34'09.0" E	105 m a.s.l. 4.4%	*Pinus pinaster* (30 years old), Spontaneous annual grasses	*Typic Rhodoxeralf*	Clay-loam
Javea, Alicante (Spain)	38°48'10.6"N 0°11'23.4"E	98 m a.s.l.	*Pinus halepensis* (40 years old)	*Lithic Rhodoxeralf*	Silty-clay
Javea, Alicante (Spain)	38°48'15.0"N 0°09'18.8"E	213 m a.s.l 5%	Burned pine forest under different post-fire treatments	*Lithic Rhodoxeralf*	Sandy-loam

The fire-affected site is located in the mountainous area of Javea, close to Alicante, Spain, in an artificially-terraced hillslope with southeast exposure (figure 1). Before fire occurrence, a *Pinus halepensis* vegetation stands, around forty years old, populated the site. The fire occurred in September 2014 resulting in a complete loss of forest trees. Starting from December 2014, two alternative post-fire management strategies were implemented in which: i) burned trees were cut at the ground level and removed (C treatment) and, ii) the soil was mulched with chopped pine residues (R treatment). For comparative purposes, a control thesis (no treatment, N) was also considered in which no operation was performed and the burned vegetation was left in situ. According to USDA classification, the soil is sandy loam (clay, *cl* = 11.1%, silt, *si* = 34.8%, sand, *sa* = 54.1%) with negligible differences among the three experimental sites. Field experiments at the three sites was performed on 15-17 June 2015 after a

Fig. 1 View of the experimental site in the fire-affected forest of Javea (Spain)

prolonged dry period that resulted in a very low soil moisture condition at the time of sampling (mean initial soil water content, θ_i = 0.033 cm^3cm^{-3}) (table 2). The mean daily temperature at the time of sampling was 20.8° C.

Table 2 Means and coefficients of variation (CV) of organic matter content, OM, soil bulk density, ρ_b, and initial water content, θ_i, for the experimental conditions considered resulting from different land use (P = *Pinus pinaster* forest, H = *Pinus halepensis* forest; B = burn pine forest, G = glade), soil (O = organic soil, M = mineral soil), post-fire treatment (N = no treatment, C = cut and removal of burnt trees, R = soil with chopped burnt residues), and initial soil water content (D = dry condition, W = wet condition).

Experimental condition	θ_i (cm^3cm^{-3})		ρ_b (g cm^{-3})		OM (%)	
	mean	CV (%)	mean	CV (%)	mean	CV (%)
P-O-D	0.128	16.9	0.725	32.4	20.0	7.04
P-O-W	0.175	8.01	0.749	9.50	21.5	1.07
P-M-D	0.166	6.33	1.172	4.14	4.66	2.41
P-M-W	0.169	5.80	1.089	5.70	3.93	3.11
G-M-W	0.281	7.51	1.192	4.73	4.71	6.02
B-M-N	0.046	39.9	1.025	12.6	7.70	14.6
B-M-R	0.034	15.3	1.011	8.0	7.15	9.55
B-M-C	0.020	19.3	0.876	19.4	6.73	13.6
H-O-D	0.066	36.9	0.548	45.5	26.6	12.6
H-M-D	0.098	29.2	1.082	14.9	8.54	3.83

In the two pine forests of Ciavolo and Javea, both the decomposed organic floor layer (duff) and the underlying mineral soil layer were sampled. At Ciavolo, sampling was repeated two times (before and after autumnal rainfall) to explore different initial moisture conditions and, furthermore, the mineral soil of a grass vegetated glade, approximately 50 m far from the pine site, was sampled for comparative purposes. At the burned site of Javea, only the soil mineral layer was sampled after removing ash and/or mulching residues.

For each experimental site and time of sampling, from five to ten infiltration tests were conducted by a standard MDI with a 45 mm diameter disk and an imposed pressure head at the soil surface h_0 = –2 cm. Both a 95% ethanol and deionized water were used, placing the disk of the MDI directly on the soil surface previously levelled using a small amount of 2-mm sieved soil collected near the infiltration point. A stand and a clamp were used to maintain the MDI upright. Approximately 50 mm of ethanol or water was allowed to infiltrate in each MDI test. Overall, 85 infiltration tests with ethanol and 85 infiltration tests with water were conducted at the experimental sites. Cumulative infiltration of ethanol was visually recorded at the MDI reservoir at intervals of 10 s for the first minute, every 30 s for the successive two minutes and, finally, every one minute until the complete infiltration of approximately 0.08 L

of ethanol, corresponding to a cumulative infiltration I = 50 mm. Infiltration of water was much slower than infiltration of ethanol and, therefore, measurement intervals were increased up to 15 min. For the 15 runs conducted with water at the fire-affected site of Javea, infiltration runs were stopped after 1.5 h.

Soil sorptivity using water, S_w, and ethanol, S_e, were estimated according to different approaches: 1) infiltration rate calculated for the first minute of infiltration (S1 approach); 2) slope of the straight line describing the I vs. $\sqrt{t}$ relationship during the early stage of infiltration process according to Philip (1957) (SL approach); 3) intercept of the regression line fitting the linearized infiltration data in the form of $I/\sqrt{t}$ vs. $\sqrt{t}$ (CL approach); and 4) intercept of the regression line fitting the linearized infiltration data in the form of $dI/d\sqrt{t}$ vs. $\sqrt{t}$ (DL approach).

According to Tillman et al. (1989), the repellency index was calculated as:

$$RI = 1.95\frac{S_e}{S_w} \quad (3)$$

in which the constant 1.95 accounts for the different surface tensions and viscosities of the two infiltrating liquids. To exclude influence of soil spatial variability on *RI* estimation, the procedure proposed by Pekarova et al. (2015) was followed that considers all the possible combinations of estimated S_e and S_w values within an experimental site to obtain *RI* (Alagna et al., 2016).

Comparisons between repellency indices calculated according to the different procedures were conducted considering the ten experimental conditions resulting from four land uses (i.e., *Pinus pinaster* forest in Ciavolo (P), *Pinus halepensis* forest in Javea (H), burned pine forest in Javea (B), glade area in Ciavolo (G)), two sampled soils (i.e., organic (O) or mineral (M)), three post-fire treatment (no treatment (N), cutting and removing burned trees (C), mulching with burned tree residues (R)), and two initial soil moisture conditions (i.e., dry (D) or wet (W)). Average values of organic matter content, bulk density and initial water content determined for the experimental conditions examined are reported in table 2.

C.4.3. Results and Discussion

MDI tests with ethanol

Plot of cumulative infiltration of ethanol was in line with the infiltration theory given that a transient phase, in which infiltration rate decreases, was followed by a steady state infiltration phase in which infiltration rate is practically constant (figure 2a). In most cases, I vs. t

relationships appeared linear, with no concavity or a concavity limited to the very early stage of infiltration . This linear trend indicated that gravity and also lateral capillary influenced the axisymmetric flow out of the disk source from the beginning of the infiltration process (Bagarello et al., 2004; Di Prima et al., 2016; Dohnal et al., 2010; Vandervaere et al., 2000a; Vandervaere et al., 2000b).

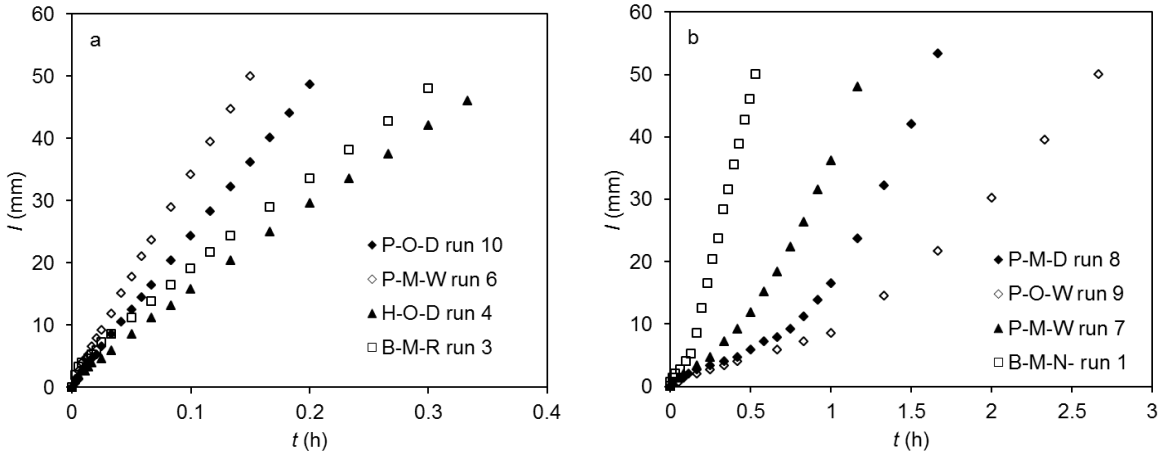

Fig. 2 Example of cumulative infiltration curves obtained in selected sites using ethanol (a) and water (b) as infiltrating fluid.

Steady state infiltration rate, i_s (L T^{-1}), as determined by the least-squares regression slope of the linear portion of the *I* vs. *t* curve (Bagarello et al., 1999), ranged between 45.1 and 1065 mm h^{-1} (CV = 80.9%) and the minimum and maximum i_s values were obtained for the organic soil, respectively at the pine forest sites of Javea and Ciavolo (H-O-D and P-O-D), thus showing the large variability of conditions that may be encountered under the same type of vegetation. However, the mean steady state infiltration rate was generally higher in the clay-loam soil of Ciavolo than in the sandy-loam and silt-clay soil of Javea (table 3).

Limiting the analysis to the mineral soils (i.e., excluding the tests conducted on organic soils), the steady state infiltration rate decreased in the order: Ciavolo clay-loam > Javea sandy-loam > Javea silty-clay. Since ethanol has an effective contact angle of zero with soil surface, it was presumed that all pores corresponding to the applied pressure head were filled with ethanol. In particular, due to different surface tension and density of ethanol, the effective applied pressure head at the soil surface is −5 cm (Jarvis et al., 2008) and, therefore, the maximum diameter of pores conducting ethanol is 0.6 mm. Under the same applied tension (h_0 = −2 cm), the maximum water filled pore diameter is 1.5 mm. Therefore, if infiltrating liquid is water a larger infiltration rete is expected in the sandy-loam due to the

higher frequency of relatively larger pores. When infiltrating liquid is ethanol, the smaller conductive pores are more represented in clay-loam thus justifying the higher values of i_s observed in this soil.

Table 3 Results of MDI tests conducted with ethanol for the different experimental conditions considered.

Experimental condition	N	t_s (h)	i_s (mm h^{-1})	Sorptivity, S_e (mm h$^{-0.5}$)			
				S1	SL	CL	DL
P-O-D	10	0.021	624.1	104.4	79.9	34.8	38.1
P-O-W	10	0.051	402.4	33.0	26.9	9.5	8.0
P-M-D	10	0.119	219.2	51.4	44.3	13.6	15.5
P-M-W	10	0.055	293.1	48.4	36.1	13.7	17.3
G-M-W	10	0.102	175.4	33.0	33.8	15.4	12.2
B-M-N	5	0.103	106.7	33.0	27.2	20.4	24.9
B-M-R	5	0.087	166.6	46.1	41.6	29.2	30.1
B-M-C	5	0.120	122.8	41.2	36.6	29.1	28.9
H-O-D	10	0.137	107.2	25.5	23.6	14.2	11.5
H-M-D	10	0.108	100.7	27.8	24.0	16.9	16.2
All data	N	85	85	85	85	84	84
	Min	0.01	45.1	10.2	10.9	0.4	0.7
	Max	0.27	1065	163.0	128.4	61.7	68.4
	Mean	0.09	249.4	45.1a	37.8b	18.6c	19.0c
	CV	72.1	80.9	67.5	60.4	71.3	74.2

Mean values followed by the same letter are not statistically different according to a paired t-test (P = 0.05)

The time required to achieve steady-state flow, t_s (T), (Bagarello et al., 1999), was larger than the fixed time to estimate sorptivity according to S1 approach (t = 1 min) in 95.3% of cases. Therefore, steady-state flow was generally reached in more than 1 min and a transient phase potentially applicable to estimate sorptivity by both the S1 and SL approaches was observed. As matter of fact, plots of I vs. $t^{0.5}$ showed an initial linear part including at least four points thus allowing reliable estimates of soil sorptivity according to SL approach. Mean values of sorptivity estimated according to S1 and SL approaches for the different experimental conditions spanned over a similar range of values (table 3) and the S_e values estimated by the two approaches for each MDI test (N = 85) were highly correlated (figure 3a). However, a bias from the identity line was observed at higher sorptivity values underlining that the influence of lateral capillarity, and probably of gravity, comes into play even for time lower than 1 min. According to a paired t-test, the two approaches were not equivalent in estimating ethanol sorptivity (table 3). This result makes questionable the choice to calculate S_e using only infiltration data collected in the early stage of the infiltration process.

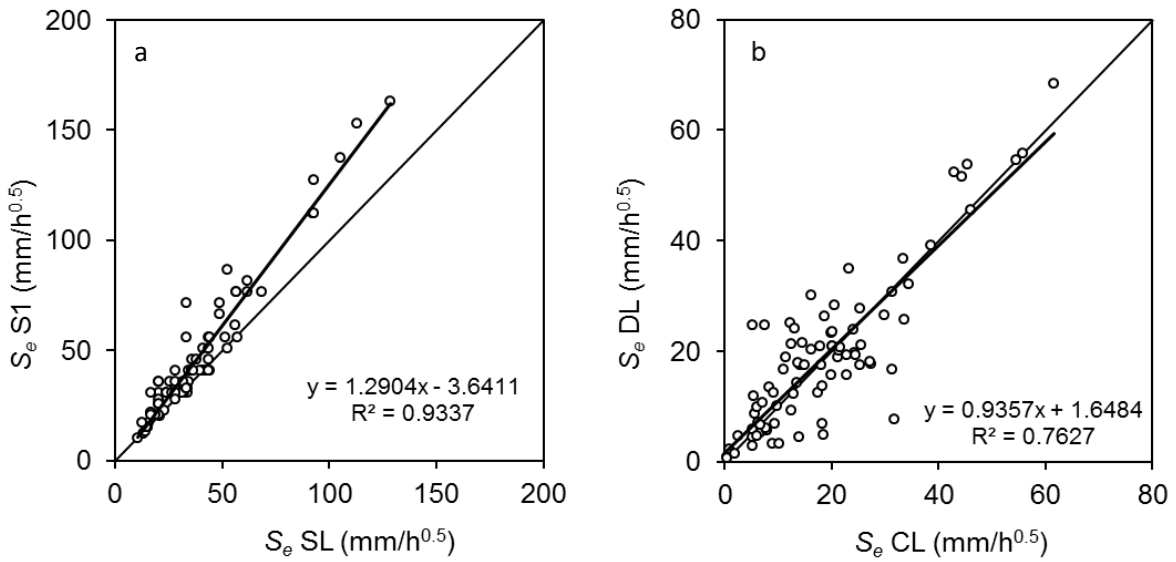

Fig. 3 Comparison between ethanol sorptivity values, S_e, estimated according to different approaches: a) SL vs. S1, b) CL vs. DL.

The CL and DL approaches were also applicable given that a linear relationship between $I/\sqrt{t}$ and $\sqrt{t}$ data and between $dI/d\sqrt{t}$ and $\sqrt{t}$ data was recognized for the entire duration of the infiltration test in most cases (77% and 79%, respectively). Reliability of the CL and DL approaches was confirmed by highly significant values of coefficients of determination for the $I/\sqrt{t}$ vs. $\sqrt{t}$ and $dI/d\sqrt{t}$ vs. $\sqrt{t}$ linear regressions. In particular, R^2 values for each infiltration test were always higher than 0.629 for CL approach (mean R^2 = 0.977) and 0.513 (mean R^2 =0. 859) for DL approach. Mean S_e values estimated by the CL and DL approaches were not significantly different (table 3) and the regression line between the single S_e estimates obtained by the two approaches (N = 85) was not different from the identity line (figure 3b). However, mean S_e values obtained by the experimental information collected from early to intermediate infiltration time (CL and DL approaches) were lower than those obtained using only the early time information (table 3). Therefore, the four considered approaches for estimating ethanol sorptivity were not equivalent and a systematic overestimation of S_e was observed for the approaches (S1 and SL) that make the use of early-time infiltration data only. Equivalent estimates of S_e can be obtained by CL and DL approaches thus confirming that lateral capillarity, and probably of gravity, influence ethanol infiltration from the very short times.

MDI tests with water

Plots of cumulative water infiltration vs. time typically exhibited a upward convex shape that is indicative of water repellency occurrence (figure 2b). In particular, the increase in

infiltration rate is indicative of a reduction in SWR as infiltration proceeds (Beatty and Smith, 2013; Carrick et al., 2011; Di Prima et al., 2016; Ebel and Moody, 2013; Imeson et al., 1992). Prolonged contact with water can lead to the loss of SWR as consequence of the displacement of amphiphilic compounds from the soil particle surface operated by the attraction of water to the polar ends of these molecules (Doerr et al., 2000). The WDPT test (Woudt, 1959), for example, is a measure of the duration of this process which depends on a variety biotic and abiotic factors and it leads to a wettable soil and, thus, to an increase in infiltration rate.

Due to hydrophobicity, the duration of infiltration runs was much longer than with ethanol ranging up to 8.7 h. For 14 runs out of 70, the runs were stopped before the MDI reservoir had completely emptied but, in any cases, providing that test duration was at least 3 h. One infiltration experiment, conducted in the organic soil of Ciavolo (P-O-D), was stopped after 9 h when only 15.8 mm of water had infiltrated. Mean values of infiltration rate $\bar{\imath}$, i.e. the ratio between the final cumulative volume and the corresponding duration, were lower for organic soils (P-O-D, P-O-W, H-O-D) than mineral soils (table 4). The highest $\bar{\imath}$ values were obtained in the non-vegetated site of Ciavolo (G-M-W) ($\bar{\imath}$ = 101.7 mm h^{-1}) and in the mineral subsoil of the pine forest in Javea (H-M-D) ($\bar{\imath}$ = 126.6 mm h^{-1}).

The very slow infiltration in the early stages of the process made the estimation of soil water sorptivity, S_w, more problematic. Indeed, in 36 infiltration tests, (42% of cases), water flow out of the MDI did not start during the first 1 min of infiltration thus making it impossible to estimate S_w by the S1 approach. Wetting of soil surface, as detected by the rising of the first air bubble within the MDI reservoir, was particularly slow in the organic soil of the pinus forests (P-O-D, P-O-W, H-O-D, N = 30), where the average time for the infiltration starting was 705 s (maximum value = 3000 s). For the remaining 49 runs, the S_w values calculated by the S1 approach ranged from 5.1 to 76.4 mm $h^{-0.5}$, with a mean value S_w = 18.0 mm $h^{-0.5}$ (CV = 93.8%). According to a paired t-test (P = 0.05), sorptivity estimated by the S1 approach was higher that the sorptivity estimated by the remaining three approaches (SL, CL and DL) (Table 4).

Despite the difficulties in detecting the starting of the wetting process, analysis of water infiltration data confirmed the results obtained with ethanol as infiltrating fluid. A criterion based on a fixed short time (1 min in this case) tended to overestimate both ethanol and water sorptivity whereas, in extremely water repellent soils, is not able for appreciating the initial stages of infiltration. Therefore, its application as a general criterion for assessing repellency index is questionable. Maybe, the poor applicability of S1 approach in strongly hydrophobic soil could be overcome by selecting a shorter time interval for ethanol

infiltration and a larger time interval for water infiltration but this choice would probably hinder the benefit of rapidity and simplicity for which this approach has been proposed (Lewis et al., 2006; Robichaud et al., 2008). Due to this drawback, the S1 approach was excluded from the subsequent analysis on the assessment of soil water repellency index.

Table 4 Results of MDI tests conducted with water for the different experimental conditions considered.

Experimental condition	N	t_{tot} (h)	$\bar{\imath}$ (mm h^{-1})	Sorptivity, S_w (mm h$^{-0.5}$)			
				S1	SL	CL	DL
P-O-D	10	7.10	7.0	5.4	2.7	1.7	1.5
P-O-W	10	4.18	12.6	6.9	8.1	4.9	3.5
P-M-D	10	2.47	24.8	6.8	3.1	1.6	1.1
P-M-W	10	2.14	26.8	7.9	7.1	6.2	5.4
G-M-W	10	0.53	101.7	22.9	24.1	14.9	12.8
B-M-N	5	0.86	44.4	10.0	9.0	6.6	4.2
B-M-R	5	1.78	19.0	5.1	6.9	5.2	5.7
B-M-C	5	1.38	17.5	9.4	9.0	6.8	5.8
H-O-D	10	4.34	3.8	n.a.	2.0	0.8	1.3
H-M-D	10	0.41	126.6	42.8	37.9	33.7	33.0
All data	N	85	85	49	85	80	82
	Min	0.2	2.6	5.1	0.9	0.2	0.2
	Max	9.0	55.2	76.4	63.9	60.1	61.5
	Mean	2.7	39.8	18.0a	11.5b	9.0b	8.0b
	CV	86.1	41.6	93.8	115.6	133.1	147.3

Mean values followed by the same letter are not statistically different according to a paired t-test (P = 0.05).

The SL, CL and DL approaches yielded statistically equivalent estimates of S_w (table 4) even if an overestimation of sorptivity is still detected when only early time infiltration data are used (SL approach) (figure 4). For water infiltration runs, gravity and lateral capillarity probably came into play at a later stage of the infiltration process as compared to the ethanol infiltration tests and, therefore, the use of SL approach did not yield as large overestimation of S_w as the ones yieded by ethanol. The S_w values estimated by the linearization approaches (i.e., CL and DL) were not significantly different (table 3) and the regression line between the single S_w estimates was not different from the identity line (figure 4). However, it should be mentioned that in five and three cases out of 85, respectively, the CL and DL approaches could be not applied as it was not possible to identify a monotonic increasing trend in the $I/\sqrt{t}$ vs. $\sqrt{t}$ or $dI/d\sqrt{t}$ vs. $\sqrt{t}$ data or the intercept of the regression line was negative.

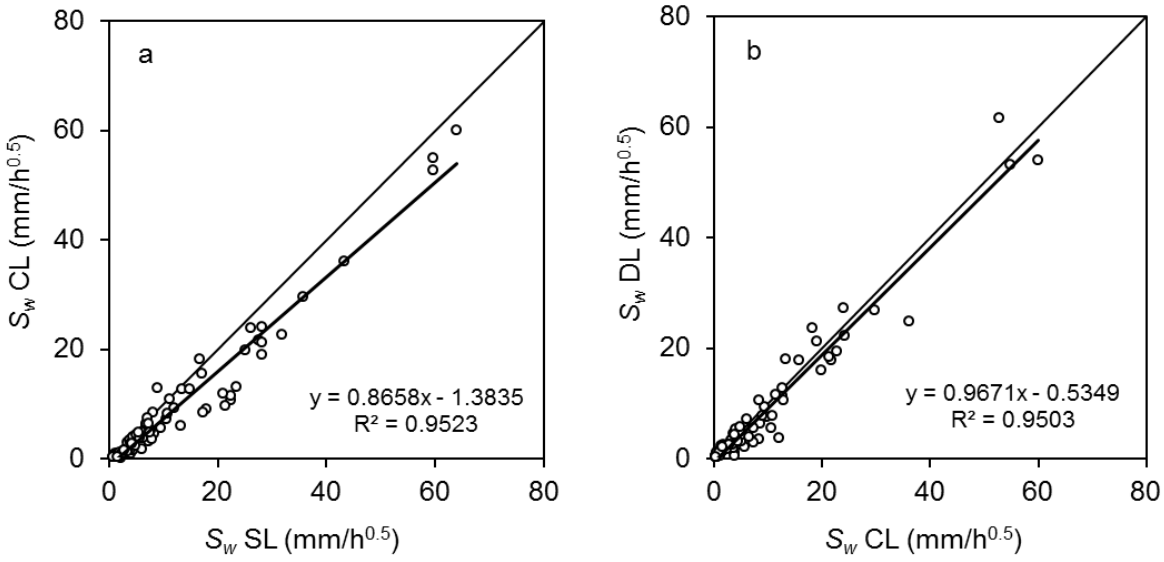

Fig. 4 Comparison between water sorptivity values, S_w, estimated according to different approaches: a) SL vs. CL, b) CL vs. DL.

Estimation of water repellency index

Independently of the estimation approach (SL, CL or DL), mean S_e values for each experimental conditions (table 3) were higher than the corresponding S_w values (table 4), the only exception being for the mineral soil of the pine forest of Javea (H-M-D). This last site was the only one that clearly showed not-repellent conditions among the 10 experimental cases considered. Estimation of the repellency index according to the classical procedure by Tillman et al. (1989) (RI = 1.95 S_e/S_w) depended on the approach followed to estimate S_e and S_w (table 5). According to a Tukey HSD test (P = 0.05) discrepancies between the RI estimated under the different experimental conditions tended to be less pronounced in hydrophobic soils whereas in less water repellent soils the SL approach tended to overestimate RI. The mean overestimation of RI calculated with the SL approach was by a factor of 1.33 and 1.17 as compared to the CL and DL approaches, respectively (table 5). In eight out of ten experimental conditions, the RI estimated by CL and DL approaches were not statistically different. This was an expected result given that the S_e and S_w values estimated by the two approaches were not statistically different (table 3 and 4) and the scatterplots of S_e and S_w were close to the 1:1 line (figure 3 and 4). In 50% of cases, the SL approach yielded RI values differing from those calculated by CL and DL ones. It was concluded that the use of SL approach for estimating ethanol and water sorptivities may result in RI overestimation particularly under sub-critical water repellency conditions.

The two approaches based on the linearization of the cumulative infiltration data collected in the range from early to intermediate times, yielded more similar estimates of RI

and can therefore be considered more reliable for field estimation of soil water repellency. However, a negative aspect of using linearization approach is that *S* estimation may be affected by a subjective selection of the linear part of the $I/\sqrt{t}$ vs. $\sqrt{t}$ and $dI/d\sqrt{t}$ vs. $\sqrt{t}$ plots to be used for fitting of eq. (1) (Vandervaere et al., 2000a; Vandervaere et al., 2000b) Bagarello and Iovino, 2004). In general, selection of data describing a linearly increasing relationship was easier in CL than in DL plot due to the scattering effect associated to the finite difference calculation of the term $dI/d\sqrt{t}$ (figure 5).

Table 5 Mean values of *RI* index calculated according to eq.(3) using ethanol and water sorptivities estimated with different approaches.

Experimental condition	SL	CL	DL
P-O-D	55.1a	45.4a	52.3a
P-O-W	32.5a	19.5b	28.5ab
P-M-D	6.1a	1.9b	3.6a
P-M-W	9.7a	3.6b	4.6b
G-M-W	2.7a	2.0b	1.7b
B-M-N	6.6a	6.6a	12.8b
B-M-R	11.1a	10.4a	10.5a
B-M-C	8.0a	8.3ab	10.5b
H-O-D	22.4a	18.9a	19.3a
H-M-D	1.3a	1.0b	1.0b

Mean values followed by the same letter are not statistically different according to HSD Tukey test ($P = 0.05$)

The *RI* value for H-M-D was lower than 1.95 (table 5) which was considered by Tillman et al. (1989) as the value discriminating between not-repellent and repellent conditions. It is worth noting that *RI* values were always higher in the organic surface soils than in the underlying mineral ones with values ranging up to *RI* = 55 under dry conditions. However, high *RI* were also observed in the mineral subsoil of the pine forest of Ciavolo (P-M-D and P-M-W) and also in the mineral soil of the burned site of Javea mulched with chopped pine residues (B-M-R) (table 5). As highlighted by Alagna et al. (2016), leaching of hydrophobic compound from the overlying organic duff or mulching layer could be responsible for this findings.

The total cumulative water infiltration data linearized in the form of both CL or DL approach, always showed an increasing trend that was characterized by a practically unique slope in no-repellent soils (figure 5b and 5d), whereas showed a typical "hokey-stick-like" shape in water repellent soils (figure 5a and 5c). In this last case, the experimental plot was characterized by an initial increasing linear part followed, after a knee, by a more or less pronounced change in slope. Identification of the slopes of the two parts of the linearized

plots was easy in 94% of cases for the CL approach and in 80% of cases when the DL one was followed. In one case only the two approaches were not applicable. In the remaining cases (i.e., 6% of cases for CL and 20% for DL), the estimation of one of the two slopes was characterized by a minimum number of points (i.e., three points) or a non-significant low coefficient of correlation was found. Nevertheless, a meaningful trend was always visually detectable and, therefore, these estimations were maintained in the dataset.

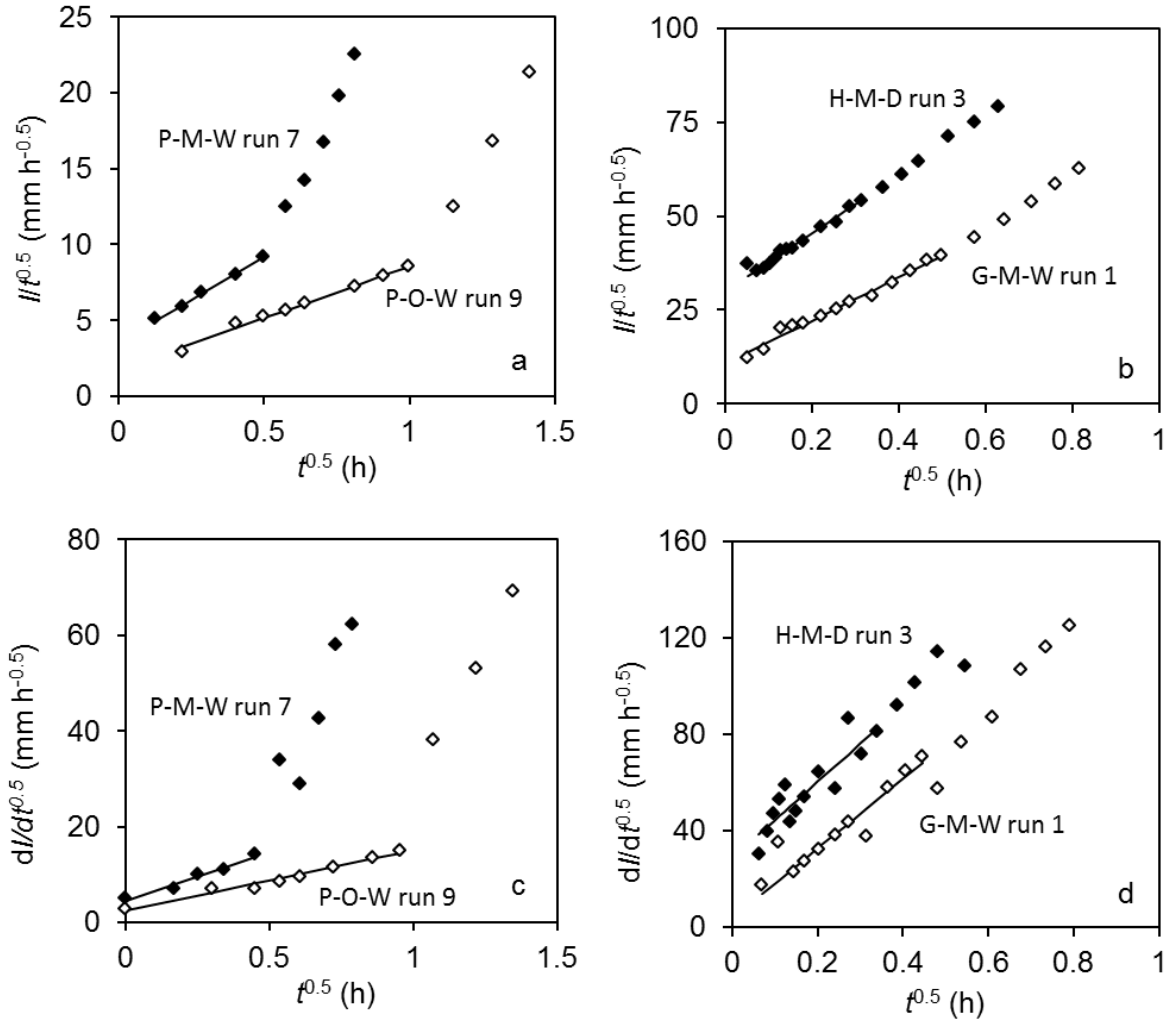

Fig. 5 Examples of application of cumulative linearization CL approach (a and b) and differentiated linearization DL approach (c and d) to water infiltration experiments in hydrophobic (a and c) and non-hydrophobic (b and d) soils.

The mean RI_s values calculated for each experimental conditions by the CL and DL approaches were not statistically different in eight out of ten experimental conditions (table 6) and the regression line between mean RI_s calculated according to the two linearization procedures was not different from the identity line (figure 6). Depending of the considered experimental conditions, the RI_s values ranged from 1.2 to 37.9 (CL approach) and from 1.7

to 39.3 (DL approach) (table 6). The clear increasing trend of RI_s at increasing soil hydrophobicity was confirmed by the significant correlations found with the classical *RI* index calculated according to eq.(3) and the WDPT index (table 7). In particular, the proposed RI_s index detected repellency condition for the mineral soil of the glade at Ciavolo (G-M-W) (RI_s = 2.3-2.7) that was classified as not repellent according to the traditional WDPT test (mean drop persistence time < 5 s) (Alagna et al., 2016).

Table 6 Statistics of the proposed repellency index RI_s (eq. 2) calculated according to CL and DL approaches for the different experimental conditions considered.

Experimental condition	CL approach					DL approach				
	N	min	max	mean	CV	N	min	max	mean	CV
P-O-D	10	1.8	107.8	37.9	92.4	10	1.3	99.1	39.3	80.9
P-O-W	10	5.5	47.3	18.9	63.9	10	2.7	59.6	21.1	96.1
P-M-D	10	2.9	11.4	7.1	38.6	10	3.9	27.4	12.1	55.1
P-M-W	10	2.9	24.3	10.2	64.7	10	3.7	22.4	11.7	61.7
G-M-W	10	1.3	3.2	2.3	22.4	10	1.4	4.0	2.7	27.4
B-M-N	4	1.3	3.2	2.3	22.4	4	1.4	4.0	2.7	27.4
B-M-R	5	1.0	1.4	1.2	12.8	5	1.0	2.0	1.7	24.6
B-M-C	5	1.4	3.0	1.8	38.2	5	1.4	7.8	3.5	75.1
H-O-D	10	2.0	10.3	3.6	68.8	10	0.7	8.5	4.0	59.9
H-M-D	10	1.1	5.2	2.4	61.6	10	0.9	3.1	1.9	37.9

Table 7 Coefficients of determination for linear regressions between the repellency index, RI_s (eq. 2), calculated according to both the CL and DL approaches and the repellency index, *RI* (eq. 3) and the Water Drop Penetration Time, WDPT, for the experimental conditions considered (N = 10)

	R^2	P
RI_s CL approach vs. *RI* SL approach	0.841867	**
RI_s CL vs. *RI* CL	0.752825	**
RI_s CL vs. *RI* DL	0.804692	**
RI_s CL vs. WDPT	0.377799	*
RI_s DL approach vs. *RI* SL approach	0.843154	**
RI_s DL vs. *RI* CL	0.730205	**
RI_s DL vs. *RI* DL	0.763418	**
RI_s DL vs. WDPT	0.459049	*

* significant at P = 0.05; ** significant at P = 0.01

This result was in line with *RI* values calculated by eq.(3) that ranged between 1.7 and 2.7 (table 5), thus confirming that the RI_s index was able to detect subcritical soil water repellency conditions that were not assessed by the more commonly used WDPT test. On the other hand, inconsistency between WDPT and *RI* or RI_s were observed for the organic layer of Javea forest site (H-O-D) that showed the most water repellent conditions according to the WDPT test (t = 2139 s) but not according to the *RI* and RI_s tests (figure 7). However, when the point

corresponding to this experimental condition was excluded from the regression analysis, the coefficient of determination for WDPT vs. RI_s data increased up to R^2=0.8803 (P = 0.01) for the CL approach and R^2=0.8943 (P = 0.01) for the DL one.

It was concluded that information gathered from a single water infiltration experiment conducted by the MDI for a relatively long time intervals is potentially exploitable to assess the soil water repellency. Similar conclusions were drawn by Lichner et al. (2013) who proposed to assess the soil hydrophobicity by the water repellency cessation time (WRCT) that was estimated as the intersection between the two regression lines representing the early-time (hydrophobic) and late-time (wettable) conditions when the cumulative infiltration data are plotted in a I vs. $\sqrt{t}$ plot. For the reduced dataset collected only at the forested sites of Ciavolo and Javea, Alagna et al. (2016) found WRCT to be significantly correlated to the widely applied WDPT index. Furthermore, they also tested a modified repellency index, RI_m, defined as the ratio of the slopes of the I vs. $\sqrt{t}$ plot at the late and early stages of the infiltration process. Both the WRCT and the RI_m proposed by Alagna et al. (2016) are obtained from the I vs. $\sqrt{t}$ plot of cumulative water infiltration data. However, this approach neglects influence of gravity and lateral capillarity that comes into play after the very early-time stage of the infiltration process. Therefore, plots of I vs. $\sqrt{t}$ exhibit an upward convex shape that is not due to the increase of water infiltration rate as consequence of soil wetting but is due to the progressively increasing importance of gravity and lateral capillarity

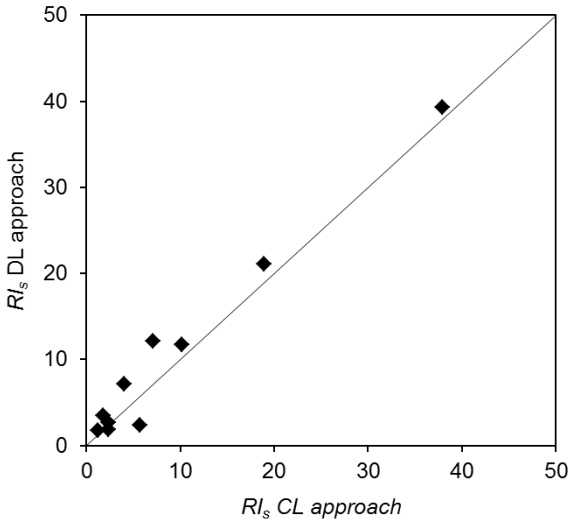

Fig. 6 Comparison between the mean repellency index RI_s estimated by the CL and DL approaches for the different experimental conditions considered (N = 10).

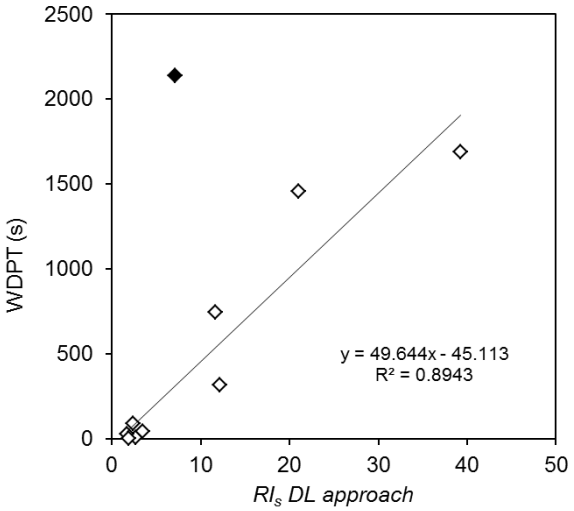

Fig. 7 Relationship between the repellency index RI_s calculated by the DL approach and the Water Drop Penetration Time (WDPT) for the different experimental conditions considered (N = 10). Filled dot refers to the data collected in the organic layer of Javea forest site (H-O-D).

flow. Using cumulative infiltration data in the form of I vs. $\sqrt{t}$ graph may thus misestimate the repellency phenomena. This hypothesis is confirmed by examination of ethanol infiltration plots that showed that an increase in I vs. $\sqrt{t}$ slope even when both CL and DL plots are clearly linear (figure 8). According to the ratio between the two slopes in a I vs. $\sqrt{t}$ plot an artefact water repellency could be estimated that is not possible in fact. On the other hand, the repellency index calculated according to eq.(1) includes information on both sorptivity and conductivity measured in the wettable and repellent stages of the infiltration process and can be therefore considered more directly linked to the hydrological processes affected by soil water repellency.

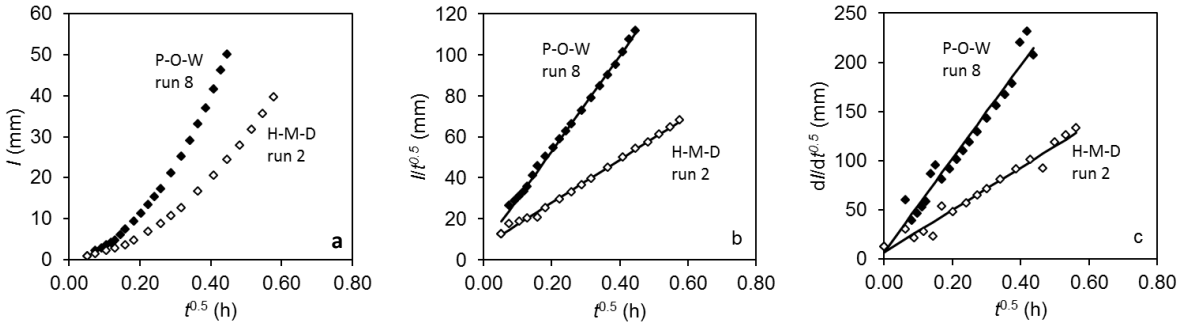

Fig. 8 Examples of cumulative ethanol infiltration curves plotted according to different representations: a) linearization of the early time infiltration data in the form I vs. $t^{0.5}$; b) linearization of the complete infiltration curve according to CL approach; c) linearization of the complete infiltration curve according to DL approach.

C.4.4. Conclusions

The adjusted ratio between ethanol and water sorptivities, estimated by a tension infiltration experiment, was proposed a valuable tool to assess the sub-critical soil water repellency. However, the commonly applied horizontal infiltration equation that makes use only of the initial stage of the axisymmetric flow out of a MDI may results in overestimations of sorptivity due to the neglected effects of gravity and lateral capillarity on infiltration. The two-term infiltration model proposed by Haverkamp et al. (1994), that is valid for early to intermediate infiltration times, is potentially more able to yielded unbiased estimations of sorptivity. For variable experimental conditions resulting from different soil texture, vegetation habitats, sampled horizons and initial soil water contents, the approaches based on the linearization of the two-term infiltration model (CL and DL) yielded similar estimates of S_e and S_w. A systematic overestimation of S_e was observed for the approaches (S1 and SL) that make the use of early-time infiltration data only, whereas the S1 approach was inapplicable in 42% of experiments conducted with water thus preventing estimation of

Tillman et al. (1989) repellency index, *RI*, by this approach. The biases in S_e and S_w estimations conducted by the SL approach yielded an overestimation of *RI* by a factor of 1.33 and 1.17 as compared to the values estimated with the CL and DL approaches. Moreover, these discrepancies were more pronounced in less water repellent soils thus raising doubts about the strength of this approach in sub-critical water repellency conditions.

For the experimental conditions considered, the mean values of the new repellency index, RI_s, defined as the ratio of the slopes of the linearized data in the wettable and hydrophobic stages of infiltration were significantly correlated with the mean *RI* and WDPT indices thus showing the potential reliability of soil hydrophobicity assessment by this index. Compared to the *RI* index, RI_s is estimated from a single water infiltration experiment conducted by the MDI thus overcoming drawbacks of conducting paired water and ethanol infiltration experiments in two different sites (i.e., small scale spatial variability, variable temperature effect on the physical characteristics of the two infiltrating liquids). As for previously proposed repellency indices (i.e., WRCT, RI_m), the new RI_s offers a way to quantify with a single number the complex site-specific soil wetting properties. However, it appears physically more sound in that includes information on both sorptivity and hydraulic conductivity measured in the wettable and repellent stages of the infiltration process thus being more directly linked to the hydrological processes affected by soil water repellency.

Further investigations are necessary to test the validity of the new index on different sub-critical water repellent conditions also with the aim to define classification criteria more quantitatively associated to the actual water-solid contact angle.

References

Alagna, V., Bagarello, V., Di Prima, S., Iovino, M., 2016a. Determining hydraulic properties of a loam soil by alternative infiltrometer techniques. Hydrological Processes 30(2), 263-275.

Alagna, V., Iovino, M., Bagarello, V., Mataix-Solera, J., Lichner, L., 2016b. Application of minidisk infiltrometer to estimate water repellency in Mediterranean pine forest soils. Submitted to Journal of Hydrology and Hydromechanics.

Angulo-Jaramillo, R., Bagarello, V., Iovino, M., Lassabatere, L., 2016. Unsaturated Soil Hydraulic Properties, Infiltration Measurements for Soil Hydraulic Characterization. Springer International Publishing, Cham, pp. 181-287.

Bachmann, J., Deurer, M., Arye, G., 2007. Modeling Water Movement in Heterogeneous Water-Repellent Soil: 1. Development of a Contact Angle–Dependent Water-Retention Model All rights reserved. No part of this periodical may be reproduced or transmitted in any form or by any means, electronic or mechanical, including photocopying, recording, or any information storage and retrieval system, without permission in writing from the publisher. Vadose Zone J 6(3), 436-445.

Bagarello, V., Di Prima, S., Iovino, M., Provenzano, G., 2014. Estimating field-saturated soil hydraulic conductivity by a simplified Beerkan infiltration experiment. Hydrological Processes 28(3), 1095-1103.

Bagarello, V., Ferraris, S., Iovino, M., 2004. An Evaluation of the Single-test Tension Infiltrometer Method for determining the Hydraulic Conductivity of Lateral Capillarity Domain Soils. Biosyst Eng 87(2), 247-255.

Bagarello, V., Iovino, M., 2003. Field Testing Parameter Sensitivity of the Two-Term Infiltration Equation Using Differentiated Linearization. Vadose Zone J 2(3), 358-367.

Bagarello, V., Iovino, M., 2004. Indagine di laboratorio su una metodologia innovativa per la determinazione della conducibilità idraulica del suolo con l'infiltrometro a depressione. Rivista di Ingegneria Agraria, 2:81-92 (in italian with english abstract).

Bagarello, V., Iovino, M., Reynolds, W.D., 1999. Measuring hydraulic conductivity in a cracking clay soil using the Guelph Permeameter. T Asae 42(4), 957-964.

Beatty, S.M., Smith, J.E., 2013. Dynamic soil water repellency and infiltration in post-wildfire soils. Geoderma 192, 160-172.

Buczko, U., Bens, O., Hüttl, R.F., 2005. Variability of soil water repellency in sandy forest soils with different stand structure under Scots pine (Pinus sylvestris) and beech (Fagus sylvatica). Geoderma 126(3–4), 317-336.

Buczko, U., Bens, O., Hüttl, R.F., 2006. Water infiltration and hydrophobicity in forest soils of a pine–beech transformation chronosequence. J Hydrol 331(3–4), 383-395.

Butzen, V., Seeger, M., Marruedo, A., de Jonge, L., Wengel, R., Ries, J.B., Casper, M.C., 2015. Water repellency under coniferous and deciduous forest — Experimental assessment and impact on overland flow. Catena 133, 255-265.

Carrick, S., Buchan, G., Almond, P., Smith, N., 2011. Atypical early-time infiltration into a structured soil near field capacity: The dynamic interplay between sorptivity, hydrophobicity, and air encapsulation. Geoderma 160(3–4), 579-589.

Cerdà, A., 1996. Seasonal variability of infiltration rates under contrasting slope conditions in southeast Spain. Geoderma 69(3–4), 217-232.

Cerdà, A., Doerr, S.H., 2007. Soil wettability, runoff and erodibility of major dry-Mediterranean land use types on calcareous soils. Hydrological Processes 21(17), 2325-2336.

DeBano, L.F., 2000. Water repellency in soils: a historical overview. J Hydrol 231–232(0), 4-32.

Di Prima, S., Lassabatere, L., Bagarello, V., Iovino, M., Angulo-Jaramillo, R., 2016. Testing a new automated single ring infiltrometer for Beerkan infiltration experiments. Geoderma 262, 20-34.

Doerr, S.H., 1998. On standardizing the 'Water Drop Penetration Time' and the 'Molarity of an Ethanol Droplet' techniques to classify soil hydrophobicity: A case study using medium textured soils. Earth Surf Proc Land 23(7), 663-668.

Doerr, S.H., Shakesby, R.A., Walsh, R.P.D., 2000. Soil water repellency: its causes, characteristics and hydro-geomorphological significance. Earth-Science Reviews 51(1–4), 33-65.

Dohnal, M., Dusek, J., Vogel, T., 2010. Improving Hydraulic Conductivity Estimates from Minidisk Infiltrometer Measurements for Soils with Wide Pore-Size Distributions. Soil Sci Soc Am J 74(3), 804.

Ebel, B.A., Moody, J.A., 2013. Rethinking infiltration in wildfire-affected soils. Hydrological Processes 27(10), 1510-1514.

Ebel, B.A., Moody, J.A., Martin, D.A., 2012. Hydrologic conditions controlling runoff generation immediately after wildfire. Water Resour Res 48(3), n/a-n/a.

Gonzalez-Sosa, E., Braud, I., Dehotin, J., Lassabatere, L., Angulo-Jaramillo, R., Lagouy, M., Branger, F., Jacqueminet, C., Kermadi, S., Michel, K., 2010. Impact of land use on the hydraulic properties of the topsoil in a small French catchment. Hydrological Processes 24(17), 2382-2399.

Hallett, P.D., Young, I.M., 1999. Changes to water repellence of soil aggregates caused by substrate-induced microbial activity. Eur J Soil Sci 50(1), 35-40.

Haverkamp, R., Ross, P.J., Smettem, K.R.J., Parlange, J.Y., 1994. 3-Dimensional Analysis of Infiltration from the Disc Infiltrometer .2. Physically-Based Infiltration Equation. Water Resour Res 30(11), 2931-2935.

Hunter, A.E., Chau, H.W., Si, B.C., 2011. Impact of tension infiltrometer disc size on measured soil water repellency index. Can J Soil Sci 91(1), 77-81.

Imeson, A.C., Verstraten, J.M., van Mulligen, E.J., Sevink, J., 1992. The effects of fire and water repellency on infiltration and runoff under Mediterranean type forest. Catena 19(3–4), 345-361.

Jarvis, N., Etana, A., Stagnitti, F., 2008. Water repellency, near-saturated infiltration and preferential solute transport in a macroporous clay soil. Geoderma 143(3–4), 223-230.

Letey, J., Carrillo, M.L.K., Pang, X.P., 2000. Approaches to characterize the degree of water repellency. J Hydrol 231–232(0), 61-65.

Lewis, S.A., Wu, J.Q., Robichaud, P.R., 2006. Assessing burn severity and comparing soil water repellency, Hayman Fire, Colorado. Hydrological Processes 20(1), 1-16.

Lichner, L., Eldridge, D.J., Schacht, K., Zhukova, N., Holko, L., Sir, M., Pecho, J., 2011. Grass Cover Influences Hydrophysical Parameters and Heterogeneity of Water Flow in a Sandy Soil. Pedosphere 21(6), 719-729.

Lichner, L., Hallett, P.D., Drongová, Z., Czachor, H., Kovacik, L., Mataix-Solera, J., Homolák, M., 2013. Algae influence the hydrophysical parameters of a sandy soil. Catena 108(0), 58-68.

Moody, D.R., Schlossberg, M.J., 2010. Soil Water Repellency Index Prediction Using the Molarity of Ethanol Droplet Test gsvadzone 9(4), 1046-1051.

Nyman, P., Sheridan, G., Lane, P.N.J., 2010. Synergistic effects of water repellency and macropore flow on the hydraulic conductivity of a burned forest soil, south-east Australia. Hydrological Processes 24(20), 2871-2887.

Pekarova, P., Pekar, J., Lichner, L., 2015. A new method for estimating soil water repellency index. Biologia 70(11), 1450-1455.

Philip, J.R., 1957. THE THEORY OF INFILTRATION: 1. THE INFILTRATION EQUATION AND ITS SOLUTION. Soil Sci 83(5), 345-358.

Robichaud, P.R., Lewis, S.A., E., A.L., 2008. New procedure for sampling infiltration to assess post-fire soil water repellency. In: F.S. U.S. Department of Agriculture, Rocky Mountain Research Station (Ed.), Fort Collins, CO, pp. 14.

Smettem, K.R.J., Parlange, J.Y., Ross, P.J., Haverkamp, R., 1994. 3-Dimensional Analysis of Infiltration from the Disc Infiltrometer .1. A Capillary-Based Theory. Water Resour Res 30(11), 2925-2929.

Tillman, R.W., Scotter, D.R., Wallis, M.G., Clothier, B.E., 1989. Water-Repellency and Its Measurement by Using Intrinsic Sorptivity. Aust J Soil Res 27(4), 637-644.

Vandervaere, J.-P., Vauclin, M., Elrick, D.E., 2000a. Transient Flow from Tension Infiltrometers I. The Two-Parameter Equation. Soil Sci. Soc. Am. J. 64(4), 1263-1272.

Vandervaere, J.-P., Vauclin, M., Elrick, D.E., 2000b. Transient Flow from Tension Infiltrometers II. Four Methods to Determine Sorptivity and Conductivity. Soil Sci. Soc. Am. J. 64(4), 1272-1284.

Watson, C.L., Letey, J., 1970. Indices for Characterizing Soil-Water Repellency Based upon Contact Angle-Surface Tension Relationships1. Soil Sci. Soc. Am. J. 34(6), 841-844.

Woudt, B.D.v.t., 1959. Particle coatings affecting the wettability of soils. Journal of Geophysical Research 64(2), 263-267.

C.5. Impact of reforestations with exotic and native species on water repellency of forest soils

V. Alagna, M. Iovino*, V. Bagarello

Department of Agricultural and Forest Sciences, University of Palermo, Viale delle Scienze, 90128 Palermo, Italy
* Corresponding author. E-mail: massimo.iovino@unipa.it, tel +39 091 23897070, fax +39 091 484035

Abstract

Forest duff layer is usually water repellent due to the hydrophobic organic compounds resulting from leaf exudates and degradation of tree tissues. Transition from hydrophobic to wettable conditions, or vice versa, is largely controlled by water content and, thus, by overall climatic conditions. Influence of initial duff moisture on the occurrence of water repellency was investigated by the water drop penetration time (WDPT) and the ethanol percentage (EP) tests on four Sicilian forest soils. Sampling was conducted in the duff layers of exotic species used in the past for reforestation (*Pinus pinaster*, P, and *Eucaliptus camaldulensis*, E), and of native forests species of *Quercus ilex* (L) and *Quercus pubescens* (R). Potential water repellency, accounting for hyper-dry soil conditions, and actual water repellency, accounting for the effect of rainfall on the initial moisture contents, were assess. The E duff was characterized by the highest potential water repellency (WDPT = 4610 s, EP = 23.8%) whereas the P duff was the least repellent one (WDPT = 2099 s, EP = 22.0%). The largest difference between actual and potential water repellency was observed for the R duff. The water repellency vs. initial moisture relationship was different for WDPT and EP. In the former case, a decreasing relationship was observed with a transition between hydrophobic and wettable conditions in the range $0.14 < \theta < 0.19$ cm^3cm^{-3}. The EP vs. θ relationships showed a maximum in the range $0.10 < \theta < 0.15$ cm^3cm^{-3}. Leaching of organic compounds by simulated rainfall was always effective in reducing water repellency even if the WDPT reductions were one or two orders of magnitude larger than EP ones. Wettable conditions were generally more easily restored in the duff of exotic species (P and E) than in native ones (L and R), probably as consequence of the relatively higher content of soluble hydrophobic compounds that are easily leached from the particles surface.

Keywords: Exotic and native tree species, Duff, Soil water repellency, WDPT, EP, Leaching

C.5.1. Introduction

Forest provides a variety of ecosystem services including productivity, carbon storage, water retention and provision of clean water (Millennium Ecosystem Assessment, 2005). As a complex biological system, forest influences the extent and rate of water exchanges between hydrosphere, lithosphere and atmosphere thus regulating the hydrological cycle. The plant roots and microorganisms in the rizosphere increase soil porosity improving oxygen exchange, water retention capacity and rainfall infiltration (Daisy et al., 2006). Moreover, the surface litter layer formed by decomposed vegetal material represents a natural mulching that protects the soil from rainsplash and erosion (Pinchak et al., 1985; Gholami et al., 2013; Walsh and Voight 1977; Sayer, 2006).

Exudates by leaves and organic substances, resulting from degradation of tree tissues, contain amphiphilic organic molecules that coat soil particles and may be responsible of water repellency (Doerr et al., 2000). The interaction between amphiphilic organic molecules and soil particles is largely governed by water content (Doerr et al., 2000; Ellies et al., 2005). Drying increases water repellency given that hydrophobic ends of organic compounds remain exposed, whereas wetting results in a re-orientation of organic molecules that expose their hydrophilic ends so that soil surface becomes wettable (Doerr, 1998; Lichner et al., 2007). Severe water repellency is expected following prolonged dry, warm summers that are typical of Mediterranean region with a transition from water repellent (hydrophobic) to wettable (hydrophilic) conditions during the autumn/winter months (Buczko et al., 2005; Lichner et al., 2013; Rodríguez-Alleres et al., 2007).

The transition from wettable to hydrophobic status (and vice versa) was generally associated to a critical water content (CWC) even if several studies reported it as a range between two water contents rather than a single water content (de Jonge et al., 1999; Dekker and Ritsema, 1994; Dekker et al., 2001). The lower water content of the range defines the condition below which the medium is water repellent, the higher one represents the water content above which the medium is wettable. Several studies aimed at determining CWC in agricultural soils but investigations conducted in forest soils are limited (Hunter, 2011). Compared to agricultural soils, in a forest soil organic matter tends to accumulate in the floor layer. This layer plays a crucial role in hydrological processes (Keith et al., 2010) influencing partition of rainwater in infiltration and runoff (Guevara-Escobar et al., 2007). However, most studies focused on the underlying mineral horizons (e.g. Poulenard et al., 2001; Zehetner and Miller, 2006) and very few on forest floor (Neris et al., 2013). Different forest species lead to a diversification of the organic matter accumulated in the organic floor layer thus influencing

the nature of hydrophobic organic compounds. In particular, high degree of water repellency were generally associated to evergreen trees and, in particular, to conifer trees (Doerr et al., 2009; Agee, 1979).

Organic coating of soil particles determines a contact angle between water and soil greater than 90°. When a droplet of water is put on the surface of these soils, it does not penetrate as long as re-orientation of organic molecules changes the liquid-solid contact angle to a values less than 90° (Van't Woudt, 1959; Richardson, 1984). The water drop penetration time (WDPT) test is a measure of time required for the contact angle to change (Wessel, 1988) and, therefore, it can be considered a measure of the persistence of water repellency. Without a specific physical meaning, an arbitrary threshold of 5 s was taken to distinguish the soils in hydrophobic or hydrophilic (Richardson, 1984). According to Bisdom et al. (1993) the following classes of persistence of water repellency can be distinguished: slightly ($5 < WDPT \leq 60$ s), strongly ($60 < WDPT \leq 600$ s), severely ($600 < WDPT \leq 3600$ s), and extremely ($WDPT > 3600$ s) water repellent soil. Given the contact angle depends on the surface tension of the liquid, this last property be used as an index of water repellency (Watson and Letey, 1970). The surface tension of water can be lowered by adding a non-polar liquid such as, for instance, ethanol. As matter of fact, the surface tension of an aqueous ethanol solution depends in a nonlinear way from the volumetric ethanol content (Butler and Wightman, 1932; Vazquez et al., 1995) and the ethanol percentage (EP) (Watson and Letey, 1970; King, 1981) or molarity of ethanol droplet (MED) (King, 1981; Roy and McGill, 2002) was proposed as a measure of the degree or severity of soil water repellency. A droplet of ethanol solution applied on the soil surface will penetrate rapidly if its surface tension determines a liquid-solid contact angle lower than 90°. Once again, arbitrarily, it was chosen a threshold of 5 seconds as a infiltration reference time (Letey et al., 1975; Richardson, 1984). Therefore, the degree of water repellency can be expressed as the lowest ethanol percentage (EP) that allows penetration of the droplet in less than 5 s. Doerr (1998) distinguished seven classes of water repellency severity: very hydrophilic (0% EP), hydrophilic ($0 < EP \leq 3$ %), slightly hydrophobic ($3 < EP \leq 5$%), moderately hydrophobic ($5 < EP \leq 8.5$%), strongly hydrophobic ($8.5 < EP \leq 13$%), very strongly hydrophobic ($13 < EP \leq 24$%), and extremely hydrophobic ($24 < EP \leq 36$%).

Both the tests are simple and operatively fast but the results have different physical significance given that the WDPT test determines the persistence of water repellency, whereas the EP test indicates the apparent surface tension of the solid surface, that is the severity of water repellency (Dekker and Ritsema, 1994; Doerr et al., 2000).

Dekker and Ritsema (1994) called “potential” the soil water repellency measured on oven-dried soil samples to be distinguished from the “actual” soil water repellency that is determined for the specific field-moistened conditions. Measurement of the potential water repellency allows to compare different soil types excluding the effect of initial soil moisture. Comparison between potential and actual water repellency provides information on the hydrophobic behavior of soils. Actual water repellency measured on differently moistened samples allows to determine the CWC values signaling the transition from hydrophobic to wettable conditions.

In Sicily, reforestation strategies have been undertaken to prevent soil degradation (La Mantia, 2002). However, in order to achieve timely and effective soil cover, fast-growing exotic evergreens species (mostly, pinus and eucalyptus) were preferred to native species. Ecosystem services provided by reforestation have been considered in terms of water yield, water quality and soil carbon storage, the potential negative impact on soil hydrophobicity has not been specifically assessed.

The main objective of this investigation was to compare the degree of soil water repellency induced by reforestations with both exotic and native trees. The WDPT and EP tests were applied on organic floor samples of four forest species (*Quercus ilex*, *Quercus pubescens*, *Pinus pinaster* and *Eucaliptus camaldulensis*) to explore the influence of initial water content on soil water repellency. The influence of leaching of hydrophobic compounds operated by rainfall was also investigated.

C.5.2. Materials and methods

Soil sampling and sample preparation

Soil samples were collected in the surface organic floor (O2 horizon) of four forest sites located in the northern of Sicily (Figure 1). The main characteristics of sampling sites are listed in Table 1. In all cases, forest floor consisted of an approximately 5 cm thick duff formed by decomposed leaves (Neris et al., 2013). Two sampling sites were located in the small artificial woodland of Ciavolo, approximately 40 ha, where two exotic species, *Pinus pinaster* (P) and *Eucaliptus camaldulensis* (E), were planted 30-35 years ago to re-naturalize a degraded site. The soil is a *Typic Rhodoxeralf* (Soil Survey Staff, 2014) with clay loam texture. Pinus plantation occupy most of the forested surface with an almost full canopy density whereas eucalyptus trees are assembled in spots including not more than a dozen of stands.

Fig. 1 Sampling sites

Other two sampling sites were established in native forests located at Tortorici and Palermo. In Tortorici forest site, the sampling area was located under a *Quercus pubescens* (R) population, 40 years old, fully covering the soil. Undergrowth includes sparse *Ruscus aculeatus* and *Hedera helix* bush. The soil is medium textured and classified as *Typic Xerumbrepts*. The fourth sampling site is located in a grove in Parco d'Orleans, close to the University of Palermo. The soil is sandy clay with moderate gravel content. The plantation includes 30 years old *Quercus ilex* (L) trees fully covering the soil. Average annual rainfall is 500, 600 and 750 mm respectively in Marsala, Tortorici and Palermo.

Table 1 Main characteristics of sampling sites and duff samples used

Forest soil	Site	Location	Elevation (m a.s.l.)	Vegetation stand	Age of trees	OM (%)[a]
L	Palermo	38°6'30.8"N 13°21'7.78" E	33	*Quercus ilex*	30	33.68 (1.1)
R	Tortorici	38°02'21.97"N 14°51'01.46"E	832	*Quercus pubescens*	40	33.13 (2.0)
P	Marsala	37°45'21.60"N 12°33'55.51"E	107	*Pinus pinaster*	30-35	46.27 (1.0)
E	Marsala	37°45'21.46"N 12°33'57.22"E	117	*Eucaliptus camaldulensis*	30-35	49.28 (2.8)

[a] Values based on the average of three replicates. Coefficient of variation (%) are reported in brackets

At each site, five samples, each approximately 3 kg by mass, were randomly collected in the upper 5 cm of the soil profile within an area of 5x5 m^2 after removing uncompounded

vegetal material. The samples were then pooled into a single sample, put into an air tight plastic bag and carried to the laboratory for analyses. Sampling was carried out in late spring after a dry period of at least 30 days that was considered sufficient for re-establishment of hydrophobicity (Crockford et al., 1991; Dekker et al., 2001). The samples were air-dried for 15 days in the laboratory at room temperature (~25 °C) and then carefully sieved through a 2-mm mesh sieve. The coarser material and large plant residues were discarded and the remaining fine-earth fraction was gently mixed until it appeared to be homogeneous. Three subsamples of each soil were oven-dried at 40, 70 and 105°C (±1 °C) for one week, then equilibrated at room temperature for approximately 24 h in chemical dryers and**,** finally, sieved according to the same procedure followed for air-dried samples.

For each forest soil, a mass of approximately 500 g of sieved air-dried substrate was leveled in a perforated funnel (diameter 0.25 m) and leached with 28 L of tap water. A nylon cloth prevented loss of soil with effluent water. The total cumulative infiltration height was equal to 570 mm roughly corresponding to the average rainfall of the northern part of Sicily. Water was supplied under suction by a standard tension infiltrometer (Perroux and White, 1988) with a 0.24 m diameter porous plate set at a pressure head of -2 cm. Tension infiltration was preferred to ponded one in order to prevent irregular wetting patterns due to hydrophobicity that may result in non-uniform leaching of the soil (Wang et al., 2000; Letey, 2001). Following the leaching process, the substrates were air-dried for 15 days and then sieved through a 2-mm mesh sieve.

Samples of air-dried, oven-dried and leached soils were placed into aluminum containers having dimensions of 19.7 x 14.7 cm^2 and accurately leveled. Sample height was measured by a micrometer in nine points distributed on sample surface (Figure 2) and the average value was assumed to calculate the bulk volume of sample, V (L^3). Water content at the time of sample preparation was determined by thermogravimetric method on small samples (15 g by mass) and the mass of the solid fraction of the sample, M_s (M) determined as $M_s = M_i/(1 + U_i)$ in which M_i (M) is the mass of air-dried soil packed in the container and U_i (M M^{-1}) is the gravimetric soil water content of air-dried sample. Sample bulk density, ρ_b (M L^{-3}) was calculated as M_s/V and the initial volumetric water content, θ_i (L^3L^{-3}), determined accordingly. Porosity, ϕ (L^3L^{-3}), was determined assuming a specific weight of 2.05 g cm^{-3} as usual for organic substrates (Huntington et al., 1989).

To explore the influence of water content on soil water repellency, the air-dried samples of leached and non-leached soils were wetted to fixed saturation ratios θ/ϕ equal to

0.05, 0.10, 0.15, 0.20, 0.25 and 0.30. Water volumes needed to achieve the selected θ/ϕ values were calculated from the mass of soil and the porosity of each sample and applied to each tray by a spray bottle. Once moistened, the sample were sealed with a plastic film and left in incubation for 24 hours to allow water redistribution. Then, the samples were weighted again and the effective volumetric water content, θ, determined to account for water loss during the wetting process or by evaporation during incubation.

Laboratory measurements

Chemical analyses were carried out on air-dried substrates including total organic matter content (OM) estimation by loss on ignition method (LOI) (Christensen and Malmros, 1982). Soil water repellency was evaluated by the water drop penetration time (WDPT) test (Wessel, 1988) and the ethanol percentage (EP) test (Watson and Letey, 1970). Both tests involve the use of a medical drop to displace the drops on the soil surface. Therefore, a preliminary analysis of different droppers was conducted in order to select the one that allowed the smallest CV of drop size. Uniformity of drops was checked weighting 60 drops by an analytical scale (±0.0001g). The selected dropper was characterized by a mean droplet size of 60 µL (CV = 8.61%) slightly smaller than the one (80-200 µL) used by Hallin et al. (2013).

The water drop penetration time (WDPT) test involved placing 30 drops of distilled water onto the smoothed sample surface from a height of 10 mm to avoid excessive kinetic energy of the drop and recording the times required for their complete penetration. The use of 30 drops allows to estimate the mean WDPT value with an error of ±10% at 95% confidence according to Hallin et al. (2013). The drops were placed systematically in three rows according a 1.5 x 1.5 cm^2 grid inside the tray, starting at the top left corner and finishing in the bottom right as reported in Figure 2.

The ethanol percentage test was carried out using nine fixed mixtures of 95% denatured ethanol and deionized water (Letey et al., 2000). Ethanol concentrations (by volume) of 5%, 7%, 10%, 13%, 15%, 20%, 25%, 30%, 35% were

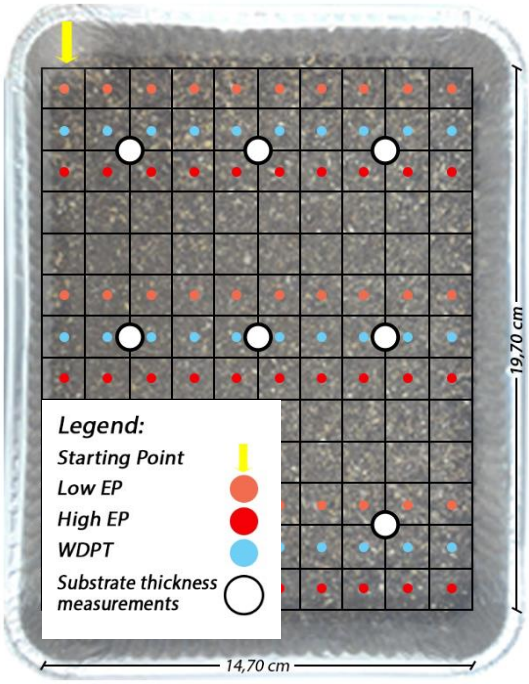

Fig. 2 Sampling grid used for WDPT and EP tests

used. A preliminarily test was performed on different samples of each substrate subject to the different treatments (air-dried or oven-dried leached or non-leached) to select the two concentrations, among the nine available, that infiltrated respectively in less and more than the threshold time (5 s). This allowed to limit the number of drops applied to the sample surface to 60 (i.e. 30 drops with lower concentration and 30 with higher concentration) thus reducing the surface occupation.

The drops were placed on the soil sample surface according to surface grid similar to one used for WDPT test (Figure 2) and the time for their infiltration was recorded. Then, the EP value corresponding to the threshold time was obtained by interpolation of the infiltration times of the two drops placed in pairwise locations. The soil water repellency was characterized by the lowest ethanol percentage (EP) that allowed penetration of the droplet in 5 s.

All the tests were carried out under controlled laboratory conditions of temperature (20 ±1°C) and air relative humidity (55 ±3%).

Analysis of data

A first objective of this investigation was to compare the "actual" and "potential" water repellency induced on forest soils by native and exotic forest species. At this aim, WDPT and EP data collected on the air dried samples were compared to those determined on the samples oven-dried at 105°C. A second objective was to explore the transition from hydrophobic to wettable conditions. At this aims, the WDPT and EP data collected at the different soil water content were analysed and the occurrence of critical water content value (or a critical water content range) discriminating the two extreme condition investigated. Finally, the effect of leaching of hydrophobic compounds was investigated by comparing the WDPT and EP data collected on leached and non-leached soil samples at different water contents.

All the three objectives have applicative implications given that the first accounts for the effect of hyper-dry soil conditions that may occur during very intense heat pulse in Mediterranean summers.

The second is relative to the transition stages that occurs during spring or autumn when soil dries or wets. The third investigate the ability of very heavy winter rains to reduce soil water repellency.

The normality of the distributions for both the untransformed and the ln-transformed WDPT and EP data was tested by the Lilliefors (1967) test at $P = 0.05$. The mean and the coefficient of variation (CV) of a given data set were calculated according to the statistical

distribution better describing the experimental data (Lee et al., 1985). Comparison between mean values were tested by a Tukey Honestly Significant Difference (HSD) test (P = 0.05).

C.5.3. Results and discussion

The duff material considered in this investigation was generally characterized by high levels of organic matter content, OM, (Table 1). The mean value of organic matter content of the native species (L and R) was around 33% whereas for exotic species it ranged between 46% and 49%. Variability of OM content was lower than 3%.

The volumetric water content of the air-dried samples ranged from 0.031 to 0.072 cm^3cm^{-3} depending on the considered species. Specifically, the L duff was characterized by a higher air-dried moisture θ_0= 0.072 cm^3cm^{-3} than the other duff layers (R=0.041; P=0.031 and E=0.050 θ_0 cm^3cm^{-3}).

Actual and potential soil water repellency

Under the different tested conditions, the log-normal distribution was never rejected for WDPT data, therefore the results were summarized by calculating the geometric mean, GM, and the associated CV (Lee et al., 1985).

The geometric mean of actual WDPT values ranged between 363.4 and 1767 s, confirming that all the forest soils taken into account in this investigation were at least strongly water repellent (Table 2) according to the classification proposed by Bisdom et al. (1993). The duff of E and L species were classified as severely water repellent (600 < WDPT $\leq$ 3600 s). The WDPT test showed that the most repellent duff was that of *Eucaliptus camaldulensis* (WDPT = 1767 s) whereas the less repellent was that of *Quercus pubescens* (WDPT = 363.4 s). The WDPT measurements were characterized by low variability, with coefficients of variation varying between 23 and 37% (Table 2). The mean actual WDPT values of the four duff layers were significant different. The duff of E species was 3.84 times more repellent than the P one. For the native species, L species conferred more water repellency than R one and the differences were equal to a factor of three. According to the actual water repellency induced on the duff layers the tree species can be classified in the following order: E>L>P>R. It is worth noting that notwithstanding the duff of E species was the most repellent substrate, its water content was not the lowest (Table 2). The substrates showing the lowest water content values (P and R) were also characterized by the lowest

values of actual water repellency, given that the mean values of WDPT were 460.7 and 363.4 s for P and R duff layers, respectively.

Table 2 Statistics of water drop penetration time (WDPT) test and ethanol percentage (EP) test conducted to assess potential and actual water repellency of the duff of the different forest tree species (L = *Quercus ilex*, R = *Quercus pubescens*, P = *Pinus pinaster*, E = *Eucaliptus camaldulensis*)

Statistics and variable	WDPT (s)		EP (%)	
	Potential Oven-dried	Actual Air-dried	Potential Oven-dried	Actual Air-dried
		L		
θ_0 (cm^3 cm^{-3})	0.000	0.072	0.000	0.072
Min	1973	632	20.83	22.86
Max	4092	1530	23.91	25.00
Mean or GM	2824.8	1103.9	22.44	23.86
	a A	a B	a A	a B
CV %	22.3	22.8	4.03	2.44
		R		
θ_0 (cm^3 cm^{-3})	0.000	0.041	0.000	0.041
Min	3420	176	20.51	17.65
Max	5858	675	24.39	20.00
Mean or GM	4610.0	363.4	22.14	18.98
	b A	b B	a A	b B
CV %	11.8	34.5	4.27	2.70
		P		
θ_0 (cm^3 cm^{-3})	0.000	0.031	0.000	0.031
Min	505	275	20.00	21.34
Max	5963	1095	24.23	26.70
Mean or GM	2099.0	460.7	21.96	24.24
	c A	c B	a A	a c B
CV %	75.3	30.3	4.96	5.20
		E		
θ_0 (cm^3 cm^{-3})	0.000	0.050	0.000	0.050
Min	1300	778	21.70	22.96
Max	7720	3048	26.51	26.95
Mean or GM	4668.4	1767.0	23.78	24.50
	b A	d B	b A	c B
CV %	47.6	37.1	5.08	3.51

Mean or geometric mean (GM) values in a column followed by the same lower case letter are not statistically different according to a Tukey HDS test (P = 0.05). For a given tests (WDPT or EP), values in a row followed by the same upper case letter era not statistically different according to a two-tailed t-test (P = 0.05).

Oven-drying the duff samples determined an marked increase of WDPT values (Table 2). All substrates were classified as severely water repellent (Bisdom et al., 1993) with mean values of potential WDPT ranging from 2099 to 4668 s. The potential water repellency was 2.6 times higher than the actual one in the duff layer of L and E species and up to 12.7 times higher for R duff (Table 2). Transition from actual to potential water repellency determined an increase of coefficients of variation for P and E substrates. According to a Tukey test

(P=0.05) means of potential WDPT were statistical not significantly different only between R and E forest tree species. However, the most hydrophobic substrate once again was E one (Table2). In particular, the potential persistence of SWR changed and can be summarized as follows: E=R>L>P. These results were in line with those found by other authors who have reported an increase of water repellency when switching from actual to potential (Dekker and Ritsema, 1994; Buczko et al., 2002, 2005).

Given that the oven-dried procedure has homogenized the duff layer under the same water content, the observed differences between the four forest soils should probably be found in a different composition of the hydrophobic compounds contained in OM as suggested by Wallis and Horne (1992). In fact, the amount of OM cannot justify the results because, for instance, R duff was among the most repellent despite its organic matter content is the lowest (33%) whereas P duff was the less repellent but its OM content is among the highest (46%). However, as suggested by other authors, another reason for these differences can be due to wetting and drying history prior to the sampling (Dekker et al., 1998; de Jonge et al., 1999; Doerr and Thomas, 2000; Buczko et al., 2002).

For the different tested conditions, the hypothesis of EP values distributed according to a normal distribution was never rejected and, therefore, the dataset was characterized by the arithmetic mean and the associated coefficients of variation (CV).

The mean actual EP values ranged between 19 and 24.5% and the coefficients of variation were very low (CV= 2.4-5.2%) (Table 2). According to Doerr (1998) the duff of L and R species was classified as very strongly hydrophobic whereas the duff of P and E species was extremely hydrophobic. The R substrate was characterized by a mean values of EP significantly lower than the others (Table 2) whereas E, P, L were statistically similar (i.e., E=P=L>R). Also the ethanol percentage test revealed that *Eucaliptus camaldulensis* induced the highest severity of water repellency between the forest tree species investigated. The severity of actual water repellency of P substrate was equal to L and E ones despite its water contents was more than 1.6 times lower. This result highlighted that the EP test was to a less extent influenced by the water content of the substrate and confirmed by the measurements of potential EP (Table 2). Indeed, the mean potential EP values ranged in an interval (from 22 to 23.8%) included in the interval of actual EP and in three cases out of four the potential EP was lower than actual EP. The percentages of reduction in the degree of potential repellency were equal to 3, 6 and 9% for the substrates of E, L and P respectively, while the R substrate showed an increase of 16% in EP. The coefficients of variation, while remaining still low, increased for potential EP as compared to actual EP except for the P duff (Table 2). In terms

of degree of potential water repellency, the forest tree species were classified in a different order respect to the actual repellency (E>L=R=P). The statistical comparisons did not showed significant differences between the substrates of L, R and P notwithstanding the P duff had on organic matter content lower than the other two. On the other side, potential EP of E duff was larger than the others even if its OM content was similar to that of P duff. Therefore, it was confirmed that the observed differences cannot be attributed to the OM content but probably depend on the different hydrophobic compounds contained in the substrates.

Transition from hydrophobic to wettable conditions

The results of WDPT tests conducted to determine the actual water repellency at different water contents are shown in Figure 3a. In general, the four duff layers investigated followed the same trend as mean ln(WDPT) values decreased at increasing water contents. In particular, for low values of moisture, the actual WDPT was almost constant and independent of water content until it reached a critical moisture threshold value above which the WDPT values decreased to the condition of wettability (WDPT $\leq$ 5 s) (Figure 3a).

The coefficients of variation were small in both the hydrophobic and wettable condition but generally increased in the transition interval (Figure 3a). The substrates exhibited the maximum values of hydrophobicity for water contents lower than a critical value that ranged between 0.08 and 0.14 cm^3 cm^{-3}. In order to identify the critical water content values discriminating the transition from hydrophobic to wettable condition, the differences between the mean values of ln(WDPT) corresponding to the different initial θ values were analyzed by a Tukey test (P = 0.05). For low water contents of the sequence WDPT values were generally not significant, but were so for water contents greater than the critical value. The critical water contents (CWCH) below which the soils were hydrophobic are reported in Table 3. For values of θ> CWC, the hydrophobicity of the substrates showed a transition zone in which the persistence of water repellency decreased linearly from the value corresponding to CWCH to a value CWCW above which the substrate were wettable (WDPT $\leq$ 5 s). The values of CWCW were determined as intersection of the regression line ln(WDPT) in the transition zone vs. θ with the line WDPT= 5 s (Figure 3a). The critical water content values that identify the wettability, CWCW, are reported in Table 3. The substrates of exotic trees (P and E) had CWCW values lower than those of the native species. The E duff was more water repellent at low θ values it maintained water repellency in a wide θ range ($\theta < 0.137$ cm^3 cm^{-3}).

Table 3 Critical water contents that define the condition of hydrophobicity (CWCH) and wettability (CWCW) for the persistence of water repellency (WDPT) and the degree of water repellency (EP)

	L	R	P	E
CWCH ($cm^3\ cm^{-3}$)	0.117	0.074	0.106	0.137
CWCW ($cm^3\ cm^{-3}$)	0.279	0.218	0.187	0.197
CWCM ($cm^3\ cm^{-3}$)	0.108	0.154	0.100	0.140
CWCO ($cm^3\ cm^{-3}$)	0.294	0.252	0.184	0.209

Furthermore, water repellency for this substrate decreased more rapidly at increasing the moisture content (Figure 3a). In the L duff the transition from extremely repellent to wettable conditions was more gradual and the water content needed to increase up to 0.28 cm^3cm^{-3} for a complete wettability.

The results of EP tests conducted at the different water contents for the four duff samples are shown in Figure 3b. As a general trend, EP increased for water content values in the range $0 < \theta < 0.15$ cm^3cm^{-3} and then decreased for higher θ values (Figure 3b). The maximum degree of actual water repellency was obtained for a critical water content, CWCM, equal to 0.100 cm^3cm^{-3} for P and L duff layers and 0.14-0.15 cm^3cm^{-3} for E and R ones (Table 3). Beyond these values, the severity of actual water repellency sharply vanished (Figure 3b) up to reach condition of EP=0 for a critical water content, CWCO, varying between 0.18 and 0.29 $cm^3\ cm^{-3}$ depending on the considered duff (Table 3). The severity of water repellency of exotic species (P and E) vanished before than the native tree species (L and R) confirming the findings obtained by WDPT test (Table 3).

Significant differences between EP values measured at different water contents were generally found (Figure 3b) probably as a consequence of the lower variability of EP data. This last result could also be a consequence of the lower reliability of WDPT test compared to EP one. Especially in conditions of high hydrophobicity, the identification of the complete infiltration of a water droplet applied on the soil surface can be subjective and, therefore, affected by operator's error. Instead, the EP test required a simple assessment of the status of drop mixture (completely infiltrated or not) at a given time (t = 5 s) and, therefore, the evaluation of this index is less affected by intrinsic errors.

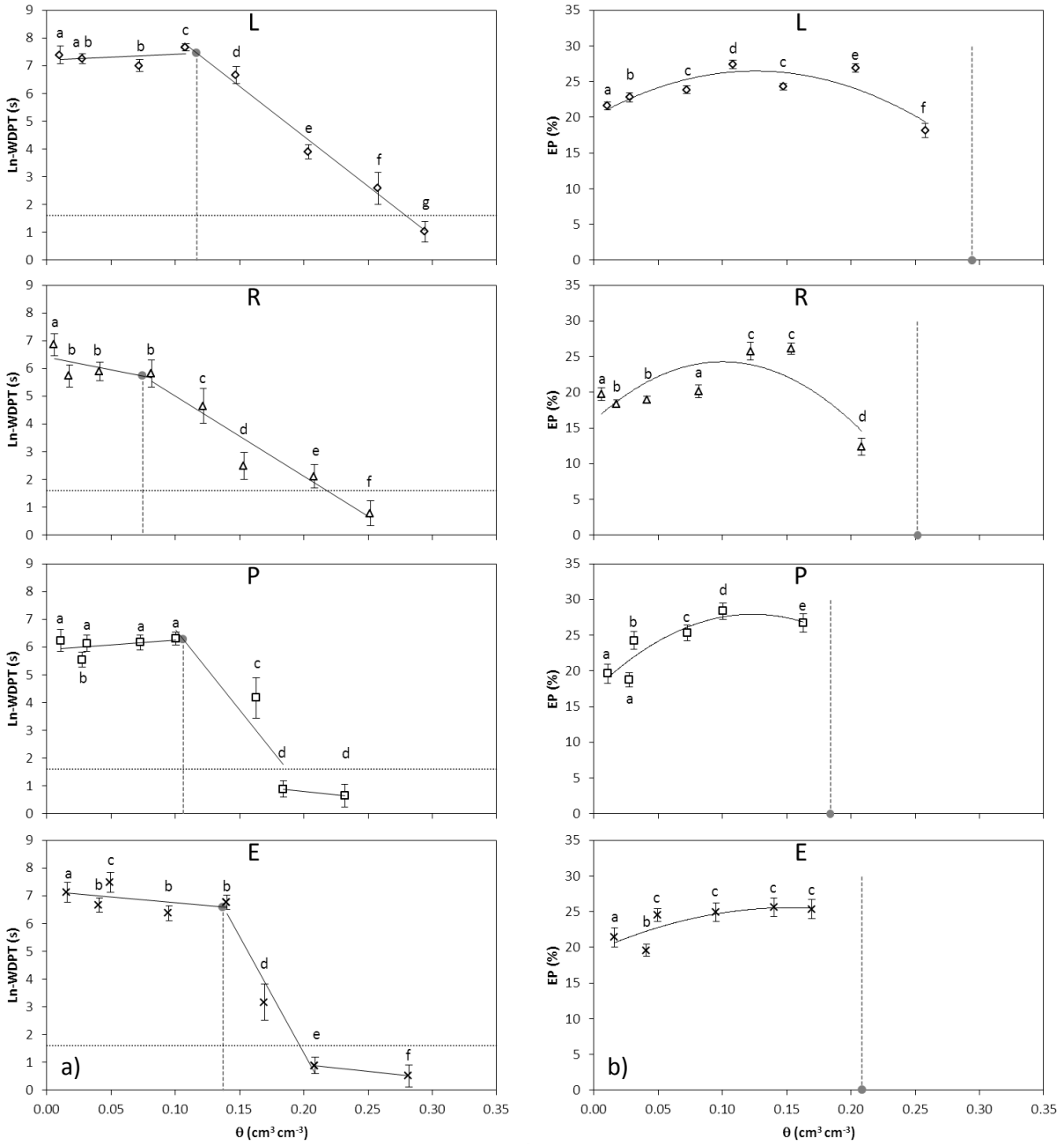

Fig. 3 Measured WDPT (a) and EP (b) values for different initial soil water contents. Data points in a plot associated to the same letter were not statistically different according to a Tukey HDS test (P = 0.05).

Effect of leaching on water repellency

Following leaching, the persistence of water repellency in the duff samples always decreased (Figure 4). The geometric means of WDPT were never higher than 355 s and generally much lower than those observed on the non-leached substrates. Among the investigated duff layers, the leaching process was less effective in the R duff which remained strongly water repellent for low values of initial water content. Reduction was variable between the different duff samples and, for a given duff depended on initial moisture (Figure 4). In the E duff leaching

was effective in reducing WDPT values by a factor of 50 to 500. For the other duff layers reductions were less affected by the initial water content and ranged from 2 to 30 times. It should be emphasized that, unlike the non-leached samples, the WDPT vs. θ relationship was characterized by a maximum at same intermediate water contents in the range from 0.075 cm^3cm^{-3} to 0.12 cm^3cm^{-3} (Figure 4). Leaching induced a more limited reduction in EP of the duff samples (Figure 5). In particular, reductions in the ratio between EP in non-leached and leached duff samples varied between 1.1 and 4 with a mean value of 1.7 (Figure 5). For the leached substrates, too, EP was characterized by a maximum in the range from 0.08 to 0.13 cm^3cm^{-3} depending on the duff sample (Figure 5). On basis of these results it can be concluded that the leaching process of soluble organic compounds operated by natural rainfall can attenuate the intensity of water repellency in the organic floor of forest soils.

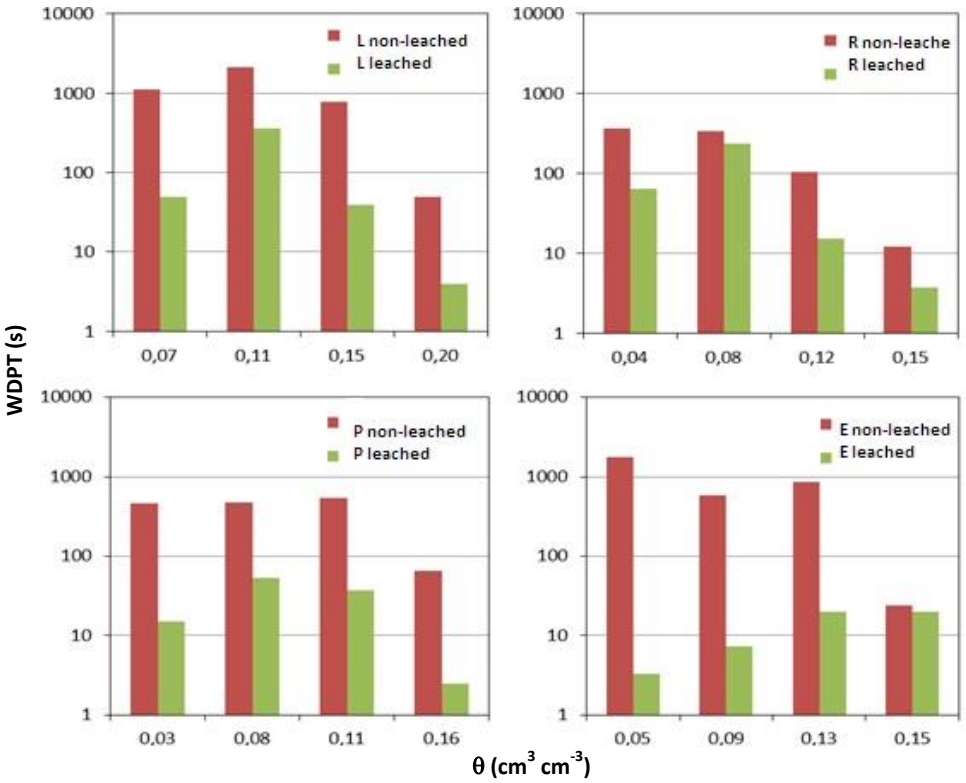

Fig. 4 Measured WDPT values at different initial soil water contents before and after leaching of the duff samples.

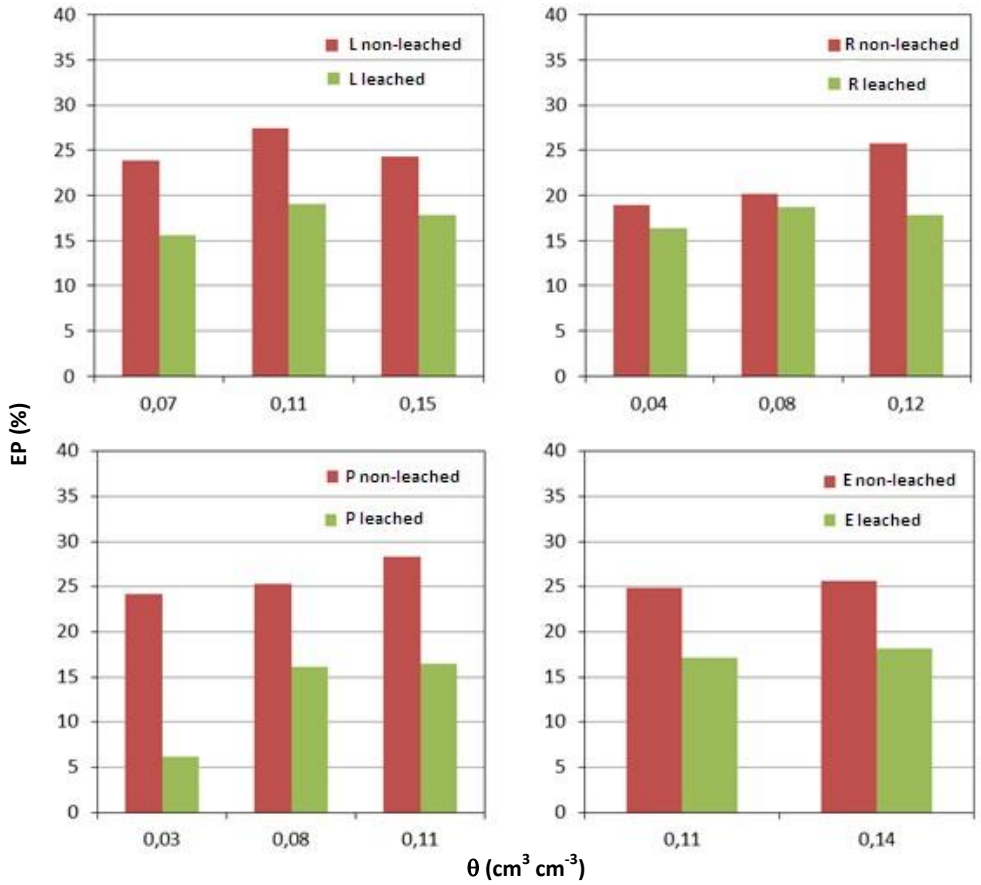

Fig. 5 Measured EP values at different initial soil water contents before and after leaching of the duff samples.

C.5.4. Conclusions

Water repellency of four Sicilian forest floor layers (duff) was investigated by two common droplet tests: i) water drop penetration time (WDPT) test that determine the persistence and ii) ethanol percentage (EP) test that measures the severity of water repellency. To account for diversification in organic matter quantity and quality determined by the different forest species, both native (*Quercus ilex*, L, and *Quercus pubescens*, R) and exotic (*Pinus pinaster*, P, and *Eucaliptus camaldulensis*, E) tree species were considered. Actual and potential WDPT values of the E duff were the highest among the four considered (respectively, 1767 and 4668 s). However, ranking of actual and potential WDPT values for the remaining substrates showed discrepancies, particularly for the R duff that exhibited the lowest actual WDPT but a very high potential WDPT (i.e., WDPT = 4610 s). The EP test confirmed that E duff was the most water repellent substrate and R duff the one showing the largest increase between actual and potential water repellency. These findings should be considered when investigating the effects of hyper-dry conditions that may verify in Sicilian forests during the very prolonged hot summer typical of Mediterranean climate. The observed differences were not explained by

the OM content of the different duff layers, thus concluding that composition rather than total amount of OM influenced the hydrophobic behavior of the considered forest floors.

Initial water content influenced both persistence and intensity of water repellency. All the duff layers showed high WDPT values for low initial water content ($\theta < 0.14$ cm^3cm^{-3}) and become wettable for $\theta < 0.19$ cm^3cm^{-3}. A more or less prolonged transition interval was detected that was delimitated by two critical water contents discriminating, from low to high θ values, the hydrophobicity and wettability thresholds. The relationship between EP and θ always showed a maximum in the range of initial water content around 0.10-0.15 cm^3 cm^{-3}. For higher θ values EP sharply decline to zero in particular for the exotic species (P and E).

Leaching of organic compounds by simulated rainfall was always effective in reducing both the persistence and the intensity of water repellency. However, the extend of the observed reductions of WDPT in leached duff samples ranged from a minimum factor of 50 up to a factor of 500, whereas the corresponding reductions for EP never exceeded a factor of 4. Winter rainfalls were more efficient in restoring wettable conditions in the floor of the exotic species (P and E) than in native ones (L and R). This result could be attributed to a relatively higher content of soluble hydrophobic compounds that are easily dislocated from the particles surface by added water. The more efficient leaching mechanism observed in these substrates indirectly confirms this hypothesis.

References

Agee, J.K., 1979. The influence of prescribed fires on water-repellency of mixed-conifer forest floor. In: Linn, R.M. (Ed.), Proceedings of the First Conference on Scientific Research in the National Parks, vol. II. New Orleans, L.A., USDI National Park Service Transactions and Proceedings Series No. 5, pp. 695–701.

Bisdom, E.B.A., Dekker, L.W., Schoute, J.F.T. 1993. Water repellency of sieve fractions from sandy soils and relationships with organic material and soil structure. Geoderma, 56, 105–118.

Buczko, U., Bens, O., Fischer, H., Hüttl, R.F. 2002. Water repellency in sandy luvisols under different forest transformation stages in northeast Germany. Geoderma, 109, 1– 18.

Buczko, U., Bens, O., Hüttl, R.F. 2005. Variability of soil water repellency in sandy forest soils with different stand structure under Scots pine (Pinus sylvestris) and beech (Fagus sylvatica). Geoderma, 126(3–4), 317-–336.

Butler, J.A.V., Wightman, A. 1932. Adsorption at the surface of solutions: Part I. The surface composition of water–alcohol solutions. J. Chem. Soc. Part II, 2089– 2097.

Christensen, B.T., Malmros, P.A. 1982. Loss-on-ignition and carbon content in a beech forest soil profile. Holarct. Ecol., 5, 376–380.

Crockford, S., Topadilis, S., Richardson, D.P. 1991. Water repellency in a dry sclerophyll forest-measurements and processes. Hydrol. Process. 5, 405– 420.

Daisy, Núñez, Laura, Nahuelhual, Carlos, Oyarzún. 2006. Forests and water: The value of native temperate forests in supplying water for human consumption. Ecological Economics, 58, 606–616.

de Jonge, L.W., Jacobsen, O.H., Moldrup, P. 1999. Soil water repellency: Effects of water content, temperature, and particle size. Soil Sci. Soc. Am. J., 63, 437–442

Dekker, L.W., Ritsema, C.J. 1994. How water moves in a water repellent sandy soil: potential and actual water repellency. Water Resources Research, 30 (9), 2507–2517.

Dekker, L.W., Ritsema, C.J., Oostindie, K., Boersma, O.H. 1998. Effect of drying temperature on the severity of soil water repellency. Soil Sci., 163, 780–796.

Dekker, L.W., Doerr, S.H., Oostindie, K., Ziogas, A.K., Ritsema, C.J. 2001. Water repellency and critical soil water content in a dune sand. Soil Sci. Soc. Am. J., 65, 1667-1674

Doerr, S.H. 1998. On standardizing the 'Water Drop penetration Time' and the 'Molarity of an Ethanol Droplet' techniques to classify soil hydrophobicity: a case study using medium textured soils. Earth Surface Processes and Landforms, 23, 663-668.

Doerr, S.H., Thomas, A.D. 2000. The role of soil moisture in controlling water repellency: new evidence from forest soils in Portugal. J. Hydrol., 231– 232, 134– 147.

Doerr, S. H., Woods, S. W., Martin, D. A., Casimiro, M. 2009. 'Natural background'soil water repellency in conifer forests of the north-western USA: Its prediction and relationship to wildfire occurrence. Journal of Hydrology, 371(1), 12-21.

Doerr, S.H., Shakesby, R.A., Walsh, R.P.D. 2000. Soil water repellency: its causes, characteristics and hydro-geomorphological significance. Earth-Science Reviews, 51(1–4), 33–65.

Ellies, A., Ramírez, C., Mac Donald, R. 2005. Organic matter and wetting capacity distribution in aggregates of Chilean soils. Catena, 59, 69-78

Gholami, L., Sadeghi, S.H., Homaee, M. 2013. Straw mulching effect on splash erosion, runoff, and sediment yield from eroded plots. Soil Sci. Soc. Am. J., 77, pp. 268–278

Guevara-Escobar, A., González-Sosa, E., Ramos-Salinas, M., Hernández-Delgado, G.D. 2007. Experimental analysis of drainage and water storage of litter layers. Hydrology and Earth System Sciences, 11, 1703–1716

Hallin, I., Douglas, P., Doerr, S. H., Bryant, R. 2013. The role of drop volume and number on soil water repellency determination. Soil Science Society of America Journal, 77(5), 1732-1743.

Hunter, A. 2011. Investigation of water repellency and critical water content in undisturbed and reclaimed soils from the Athabasca oil sands region of Alberta, Canada, M.Sc. Thesis, Department of Soil Science, University of Saskatchewan.

Huntington, T.G., Johnson, C.E., Johnson, A.H., Siccama, T.G., Ryan, D.F. 1989. Carbon, organic matter, and bulk density relationships in a forested Spodosol. Soil Science, 148(5), 380-386.

Keith, D.M., Johnson, E.A., Valeo, C. 2010. A hillslope forest floor (duff) water budget and the transition to local control. Hydrological Processes, 24, 2738–2751.

King, P.M. 1981. Comparison of methods for measuring severity of water repellence of sandy soils and assessment of some factors that affect its measurements. Aust. J. Soil Res., 19, 275– 285

La Mantia, T. 2002. L'arboricoltura da legno nel paesaggio siciliano. Rimboschimenti e piantagioni nelle trasformazioni del paesaggio. (vol. 15, pp. 135-153). Quaderni IAED, n.15.

Lee, D.M., Reynolds, W.D., Elrick, D.E., Clothier, B.E. 1985. A comparison of three field methods for measuring saturated hydraulic conductivity. Canadian Journal of Soil Science, 65, 563–573.

Letey, J. 2001. Causes and consequences of fire-induced soil water repellency. Hydrological Processes, 15, 2867-2875.

Letey, J., Carrillo, M.L.K., Pang, X.P., 2000. Approaches to characterize the degree of water repellency. J. Hydrol., 231–232, 61– 65.

Letey, J., Osborn J.F., Valoras, N. 1975. Soil water repellency and the use of nonionic surfactants, Contrib. 154,85pp., Calif. Water Resour. Center, Davis.

Lichner, L., Hallett, P.D., Feeney, D., Dugová, O., Šír, M., Tesař, M. 2007. Field measurement of the impact of hydrophobicity on soil water transport under different vegetation over time. Biologia, 62, 537– 541.

Lichner, L., Capuliak, J., Zhukova, N., Holko, L., Czachor, H., Kollar, J. 2013. Pines influence hydrophysical parameters and water flow in a sandy soil. Biologia, 68(6), 1104–1108.

Lilliefors, HW. 1967. On the Kolmogorov-Smirnov test for normality with mean and variance unknown. Journal of the American Statistical Association, 62(318), 399-402.

Millennium Ecosystem Assessment. 2005. Ecosystems and Human Well-being: Synthesis. Island Press, Washington, DC.

Neris, J., Tejedor, M., Rodríguez, M., Fuentes, J., Jiménez, C. 2013. Effect of forest floor characteristics on water repellency, infiltration, runoff and soil loss in Andisols of Tenerife (Canary Islands, Spain). Catena, 108, 50-57.

Perroux, K.M., White, I. 1988. Designs for disc permeameters. Soil Science Society of America Journal, 52, 1205-1215.

Pinchak B.A., Schuman G.E., Depuit E.J. 1985. Topsoil and mulch effects on plant species community responses of revegetated mined land. J. Range Manag., 38 (1985), pp. 262–265.

Poulenard, J., Podwojewski, P., Janeau, J.L., Collinet , J. 2001. Runoff and soil erosion under rainfall simulation of Andisols from the Ecuadorian Páramo: Effect of tillage and burning. Catena 45, 185–207.

Richardson, J.L. 1984. Field observation and measurement of water repellency for soil surveyors. Soil Surv. Horiz., 25, 32-36.

Rodríguez-Alleres, M., Benito, E., de Blas, E. 2007. Extent and persistence of water repellency in north-western Spanish soils. Hydrological Processes 21(17), 2291-2299.

Roy, J.L., McGill, W.B. 2002. Assessing soil water repellency using the molarity of ethanol droplet (MED) test. Soil Sci, 167, 83–97.

Sayer, E.J. 2006. Using experimental manipulation to assess the roles of leaf litter in the functioning of forest ecosystems. Biol Rev 81, 1–31. Doi:10.1017/S1464793105006846.

Van't Woudt, B.D. 1959. Particle coatings affecting the wettability of soils. J. Geophys. Res., 64, 263– 267.

Vazquez, G., Alvarez, E., Navaza, J.M. 1995. Surface tension of alcohol water+ water from 20 to 50. degree. C. Journal of chemical and engineering data, 40(3), 611-614.

Wallis, M.G., Horne, D.J. 1992. Soil water repellency. Advances in Soil Science, 20, 91-146.

Walsh, R.P.D., Voight, P.J. 1977. Vegetation litter: an underestimated variable in hydrology and geomorphology. J. Bio 4, 253–277. doi: 1 0.2307/3038060

Wang, Z., Wu, Q.J., Wu, L., Ritsema, C.J., Dekker, L.W., Feyen, J. 2000. Effects of soil water repellency on infiltration rate and flow instability. Journal of Hydrology, 231-232, 265-276.

Watson, C.L., Letey, J. 1970. Indices for characterising soil water repellency based upon contact angle–surface tension relationships. Soil Sci. Soc. Am. Proc., 34, 841– 844.

Wessel, A.T. 1988. On using the effective contact angle and the water drop penetration time for classification of water repellency in dune soils. Earth Surf. Proc. Landforms, 13, 555–562.

Zehetner, F., Miller, W.P. 2006. Erodibility and runoff-infiltration characteristics of volcanic ash soils along an altitudinal climosequence in the Ecuadorian Andes. Catena, 65, 201 – 213

Conclusions

Water infiltration influences surface runoff and soil erosion, profile recharge rate and solute transport and, therefore, it is essential to agricultural production. Infiltration can be affected by two widespread phenomena, hydrophobicity and sealing (or crusting), both linked to the organic matter content which are responsible of decrease in infiltration rate. Water repellency or hydrophobicity is a consequence of soil particles coating with hydrophobic compounds in soils with abundant organic matter as the forest soils. Surface seals or crust develop in soil poor of organic matter as consequence of the weak aggregate stability. Both phenomena are conditioned by climate conditions given that water repellency depends on soil water content and it is extremely severe under very dry conditions. On the other hand, the aggregate breakdown and seal formation is to a great extent dependent on the kinetic energy of rainfall. Despite both hydrophobicity and sealing affect the very surface layer of the soil profile, their effects on the hydrological process could be particularly negative. In recent years, the occurrence of these phenomena has been largely studied in Mediterranean regions where the weather conditions are frequently extreme with hot and dry spells in summer time and high intensity rainfalls in autumn which can cause flooding and soil erosion.

The use of field infiltration experiments are mandatory to assess the hydrological impact of soil water repellency and surface sealing. The main objective of the thesis was to estimate, through the use of infiltration measurements, how water infiltration processes are affected by the occurrence of crusting and hydrophobicity in Mediterranean area by measuring the soil hydraulic properties influenced by these phenomena. The results provide an advancement on knowledge gained so far. A preliminary step to achieve this objective consisted in comparing different infiltrometric techniques (Part A) with the aim to choose the most suitable methods to evaluate both the effects of surface sealing (Part B) and water repellency (Part C) on soil hydraulic properties and relate infiltration processes. The most important outcomes of the thesis are summarized below.

a) Field infiltration experiments for soil hydraulic characterization

Investigation reported in chapter A.2 aimed at comparing different ponded and tension infiltration techniques to determine the hydraulic properties of a loam soil. In particular, the BEST procedure that has recently received a wide interest by the scientific community was compared to other field-based techniques of well-established use (the pressure infiltrometer, PI, the tension infiltrometer, TI, the minidisk infiltrometer, MDI, the simplified falling head,

SFH, technique and the bottomless bucket, BB, method). It was concluded that BEST yields statistically similar estimates of K_s to those obtained with the other methods considered. The results differed at most by a factor of three, thus confirming the ability of the method to predict the soil hydraulic properties. Moreover, it was proved that the MDI is a practical alternative to the classical tension infiltrometer to estimate soil hydrodynamic properties. Indeed, the mean values of saturated hydraulic conductivity obtained by the two methods differed by a non-significant factor of 1.20. This preliminary investigation allowed to explore the peculiarities of the field infiltration techniques and, consequently, allowed to identify the most appropriate methods to be applied in the field for assessing the effects of surface sealing and water repellency on the infiltration process.

b) Effect of sealing process and surface crust on water infiltration

The simplified method proposed in chapter B.2 to determine the hydraulic resistance of the soil surface crust, which uses a combination of two infiltrometer techniques (MDI and BEST), allowed to overcome some of the drawbacks of the existing measurement methods. In particular, it is particularly simple and, for the sandy loam and the clay soils investigated, it was able to discriminate between different levels of crust hydraulic resistance. The use of extemporaneous measurements carried out by a simple infiltrometer technique under ponded condition and application of the BEST procedure were able to evaluate the influence of sealing on infiltration process (chapter B.3). In fact, the occurrence of natural rainfalls between the sampling campaigns determined the development of a surface crust that resulted in a reduction of hydraulic conductivity which was detected by the beerkan experiments carried out along and between the rows of a vineyard. However, measurement and prediction of infiltration in crusted soils can be difficult due to the intrinsic characteristics of crust as well as the extremely dynamic nature of the processes involved in its formation. Therefore, the indirect method proposed in chapter B.4 aimed at investigating the development of the surface sealing during a beerkan infiltration experiment conducted by pouring water from different heights (0.03 and 1.5 m). The hydraulic conductivity showed a reduction from 13 to 27 times when water was poured by high height because soil surface was perturbate by the high energy level of water which mimicking the effects of rain caused the development of sealing process. The perturbation determined by the high height can be considered a viable approach to characterize the effect of water application procedure on estimation of soil hydraulic properties.

c) Effect of water repellency on infiltration processes

The use of the common droplet tests (WDPT and EP) does not convey useful information to understand the influence of water repellency on water infiltration processes. As also shown in chapters C.2 and C.3, these tests were not able to identify conditions of sub-critical water repellency, that is the most common situation in natural soils in which infiltration is slowed but not prevented at all as in the case of severe hydrophobic conditions. Application of the repellency index, RI, proposed by Tillman et al. (1989) that makes use of an intrinsic soil property like the sorptivity, appears more suitable from the hydrological point of view. Moreover, it allows to identify sub-critical water repellency. In chapters C.2 and C.3, the MDI was used to estimate RI on different forest soils with the aim to investigate its vantages and disadvantages. One of the drawbacks of the RI index is due to the use of ethanol to measure soil sorptivity. In this case, the two infiltration experiments with water and ethanol, cannot be conducted at exactly the same sampled area due to the influence of the antecedent soil water content. Two new indices, RI_m and RI_s, are proposed in chapters C3 and C4 respectively, that are obtained by a single MDI experiment carried out with water. These indices were found to be correlated with the traditional WDPT test and to the more cumbersome RI index. Therefore, they can be proposed as alternative procedures for soil water repellency assessment. In particular, the RI_s index, estimated as the ratio between the slopes of the linearized transient infiltration model proposed by Haverkamp et al. (1994) in the wettable and hydrophobic stages of infiltration, includes information on both sorptivity and conductivity obtained from the total experimental data collected by MDI and, therefore, could be considered more directly linked to the hydrological processes affected by soil water repellency.

In conclusion, the field infiltration experiments applied in this investigation and the new procedures and indices proposed were able to evaluate the effects of sealing and hydrophobicity on infiltration process and, consequently, they are potentially suitable to assess their impact on hydrological behavior of the ecosystems affected by these phenomena. However, these procedures and new indices proposed need to be further tested on other soil types and in different areas to confirm their reliability before they can be considered as a generally applicable techniques.